The role of isothiocyanates as epigenetic modulators in malignant melanoma

M Mitsiogianni

PhD

2020

The role of isothiocyanates as epigenetic modulators in malignant melanoma

Melina Mitsiogianni

A thesis submitted in partial fulfilment of the requirements of the University of Northumbria at Newcastle for the degree of Doctor of Philosophy

Research undertaken in the Faculty of Health and Life Sciences

July 2020

Declaration

Declaration I declare that the work contained in this thesis has not been submitted for any other award and that it is all my own work. I also confirm that this work fully acknowledges opinions, ideas and contributions from the work of others. I declare that the Word Count of this Thesis is 46959 words.

Name: Melina Mitsiogianni

Signature:

Date: 16/7/2020

Abstract

Malignant melanoma is one of the most aggressive types of human skin cancer, characterized by high mortality due to its resistance to current therapies. Thus, there is an imperative need to develop more effective therapeutic approaches. To this end, isothiocyanates (ITCs), the biologically active plant secondary metabolites of glucosinolates, have been shown to act as promising anti-melanoma agents, mediating various biological effects, including modulation of detoxifying enzymes, induction of oxidative stress, apoptosis as well as modulation of the epigenome among others. This study aimed to characterize the effect of 5 ITCs [Sulforaphane (SFN); Iberin (IBN); Allyl- (AITC); Benzyl- (BITC) and Phenethyl-Isothiocyanate (PEITC)] on lysine acetylation and methylation marks as a potential epigenetic-induced anti-melanoma modality. An *in vitro* model of malignant melanoma was utilized, consisting of (i) human (A375) and (ii) murine (B16-F10) malignant melanoma cells; human metastatic melanoma cells derived from (iii) brain (VMM1) and (iv) lymph node (Hs 294T); (v) non-melanoma epidermoid carcinoma (A431) cells and (vi) immortalized keratinocyte (HaCaT) cells. All cell lines were subjected to treatments with varying doses and time frames for each of the 5 ITCs and various cytotoxicity end points were determined [cell viability (by Resazurin assay), levels of reactive oxygen species (ROS), total glutathione (GSH), cell cycle distribution and apoptosis (by flow cytometry)]. Furthermore, western immunoblotting was used to determine the expression of specific histone acetyltransferases (HAT), deacetylases (HDAC) and methyltransferases (HMT) together with acetylation and methylation marks on histones. Overall, we demonstrate that all five ITCs were able to reduce cell viability, decrease GSH levels, and promote G2/M cell cycle arrest and apoptosis. Moreover, utilizing a real-time PCR microarray based gene expression profiling platfrom, we found several genes implicated in apoptosis-related processes. Finally, all 5 ITCs showed to influence histone acetylation and methylation patterns by modulating several key enzymes (HDACs, HATs and HMTs) that mediate these epigenetic processes and consequently the acetylation and methylation status of specific lysine residues on histones 3 and 4, in human malignant melanoma cells.

Acknowledgements

Firstly, I would like to thank my supervisor, Prof. Mihalis Panagiotidis, for his continuous help and support throughout this three-year PhD project. I am extremely grateful for his assistance in every possible aspect, from providing guidance and advice to personal encouragement, for the completion of this project. His motivation and enthusiasm was of great help during the more challenging parts of the project.

I would also like to thank the Multi-Disciplinary Research Theme in "Bio-economy" at Northumbria University for awarding me a PhD studentship as part of this project. I am also very thankful to the technical staff at Northumbria University for their continued help throughout the project.

Furthermore, I would like to thank my friends and colleagues in the lab for their help and support, creating a pleasant and supportive atmosphere to work in. Special thanks go to Dr. Theodora Mantso, Dr. Sotiris Kyriakou and Elena Eftychiou for their emotional support as well as technical assistance throughout the project.

Finally, my greatest thanks go to my family for continuously supporting me whenever needed and always being there for me. Their continous encouragement and emotional support have been a source of reassurance throughout difficulties over the years. Special thanks also go to my friend Sophia Rizou for her emotional support as well as to my friends Margarita, Christina, Nikos, Vassilis, Stylianos, Rafaella, Panagiotis and Vera for their support and enthusiasm in keeping spirits and motivation high.

Overview of the Outcomes of this Study

Published scientific and research papers from this project

- Mitsiogianni, M., Koutsidis, G., Mavroudis, N., Trafalis, D. T., Botaitis, S., Franco, R., Zoumpourlis, V., Amery, T., Galanis, A., Pappa, A., & Panayiotidis, M. I. (2019). The Role of Isothiocyanates as Cancer Chemo-Preventive, Chemo-Therapeutic and Anti-Melanoma Agents. *Antioxidants* (Basel), 8(4).

- Mitsiogianni, M., Amery, T., Franco, R., Zoumpourlis, V., Pappa, A., & Panayiotidis, M. I. (2018). From chemo-prevention to epigenetic regulation: The role of isothiocyanates in skin cancer prevention. *Pharmacology & Therapeutics*, 190, 187-201

- Mitsiogianni, M., Mantso, T., Trafalis, D. T., Vasantha Rupasinghe, H. P., Zoumpourlis, V., Franco, R., Botaitis, S., Pappa, A., & Panayiotidis, M. I. (2019). Allyl isothiocyanate regulates lysine acetylation and methylation marks in an experimental model of malignant melanoma. *European Journal of Nutrition*.

- Mitsiogianni, M., Trafalis, D. T., Franco, R., Zoumpourlis, V., Pappa, A., & Panayiotidis, M. I. (2020). Sulforaphane and iberin are potent epigenetic modulators of histone acetylation and methylation in malignant melanoma. *European Journal of Nutrition.*

Published scientific and research papers from side projects

- George, V. C., Ansari, S. A., Chelakkot, V. S., Chelakkot, A. L., Chekkalot, C., Menon, V., Ramadn, W., Ethiraj, K. R., El-Awady, R., Mantso, T., Mitsiogianni, M., Panagiotidis, M. I., Dellaire, G., & Rupashinge, H. P. V. (2019). DNA-dependent protein kinase: Epigenetic alterations and the role in genomic stability of cancer. *Mutation Research*, 780, 92-105.

- Dimitriou, N. M., Tsekenis, G., Balanikas, E.C., Pavlopoulou, A., Mitsiogianni, M., Mantso, T., Pashos, G., Boudouvis A. G., Lykakis, I. N., Tsigaridas, G., Panayiotidis, M. I., Yannopapas, V., & Georgakilas A. G. (2017). Gold nanoparticles, radiations and the immune system: Current insights into the physical mechanisms and the biological interactions of this new alliance towards cancer therapy. *Pharmacology &* Therapeutics, 178,1-17.

- Kyriakou, S., Mitsiogianni, M., Mantso, T., Cheung, W., Todryk, S., Veuger, S., Pappa, A., Tetard, D., & Panayiotidis, M. I. (2020). Anticancer activity of a novel methylated analogue of L-mimosine against an in vitro model of human malignant melanoma. *Investigational New Drugs*, 38(3),621-633.

- Mantso, T., Sfakianos, A.P., Atkinson, A., Anestopoulos, I., Mitsiogianni, M., Botaitis, S., Perente, S., Simopoulos, C., Vasileiadis, S., Franco, R., Pappa, A., & Panayiotidis, M. I. (2016). Development of a Novel Experimental In Vitro Model of Isothiocyanate-induced Apoptosis in Human Malignant Melanoma Cells. *Anticancer Research*, 36(12),6303-6309.

Conference posters

From this project

- Mitsiogianni M, Pappa A, Panayiotidis M. Isothiocyanates as potent epigenetic regulators in human malignant melanoma chemoprevention. 25th Biennial Congress of the European Association for Cancer Research, 2018, Amsterdam, Netherlands

From side projects

- Kyriakou S, Mitsiogianni M, Mantso T, Cheung W, Todryk S, Veuger S, Pappa A, Tetard D, Panayiotidis MI. Novel insights into the role of a methylated analogue of L-mimosine in an in vitro model of malignant melanoma. 28th International Conference on Chelation-A Landmark on Chelation Sience and Medicine, 7th International Conference on Oncology and Anticancer Research, 10th International Conference RAHMS: Recent Advances in Health and Medical Sciences, 2019, Paphos, Cyprus

Scientific work to be published

- Mitsiogianni, M., Trafalis, D. T., Franco, R., Zoumpourlis, V., Gorgoulis, V. G., Pappa, A., & Panagiotidis, M. I. BITC and PEITC as epigenetic regulators by modulating lysine acetylation and methylation marks in an in vitro malignant melanoma model.

  Mitsiogianni, M., Kyriakou, S., Trafalis, D. T., Franco, R., Pappa, A., & Panayiotidis M. I. A Comparative Study of Isothiocyanate-Induced Cytotoxicity in A Well Characterized In Vitro Model of Malignant Melanoma.

Table of Contents

List of figures

List of tables

Chapter 1

Introduction

1.1 General Introduction: Epigenetics, Cancer and Nutrition

1.1.1 Overview of Epigenetic Mechanisms

"Epigenetics" refers to hereditary and reversible modulations in gene transcriptional activity independently from the DNA sequence itself (Javaid & Choi, 2017; Probst et al., 2009). These modifications occur at an early stage in life (during cell differentiation) and contribute to the different phenotypes and functions of the cellular subtypes in various tissues and organs. The epigenome is the main modulator of gene expression that contributes to such cellular diversity via modifications that take place at the level of both DNA and proteins (Margueron & Reinberg, 2010). Such alterations include the addition of methyl- and acetyl-groups, on DNA bases. These kind of modifications also occur on specific amino acids on histone tails. Other well known alterations that take place on the tails of histone proteins include phosphorylation, sumoylation, ubiquitinationpoly (ADP-ribosylation) (Probst et al., 2009).

Among them, the best characterized epigenetic alterations include DNA methylation at cytosine residues, posttranslational modifications on the amino (N)-terminal tails of histones and alterations in non-coding RNA profiles, especially in micro-RNAs (mi-RNAs) activity (Bonasio et al., 2010; Golbabapour et al., 2011; Margueron & Reinberg, 2010). All these modifications function together to regulate the transcriptional activity and thus are crucial for various cellular processes including those for normal development and preservation of tissue-specific gene expression (Avner & Heard, 2001; Ferguson-Smith & Surani, 2001; Hemberger, 2007; Li et al., 1993; Maltepe et al., 2010; Panning & Jaenisch, 1998).

At DNA level, the most important and well-studied modification is methylation which, in turn, involves the addition of methyl-groups in cytosine bases resulting in the production of 5-methylcytosine (5mC) residues. It mainly occurs at specific regions that are rich in CpG dinucleotides called CpG islands (Kulis & Esteller, 2010; Tsai & Baylin, 2011). Generally, methylation of CpG dinucleotides (primarily found on transcriptional start sites such as in the case of gene promoters) lead to the transcriptional inactivation of genes, since the presence of methyl groups blocks the access of these regions to transcription factors (Moore et al., 2013; Siegfried & Simon, 2010) (Fig. 1.1).

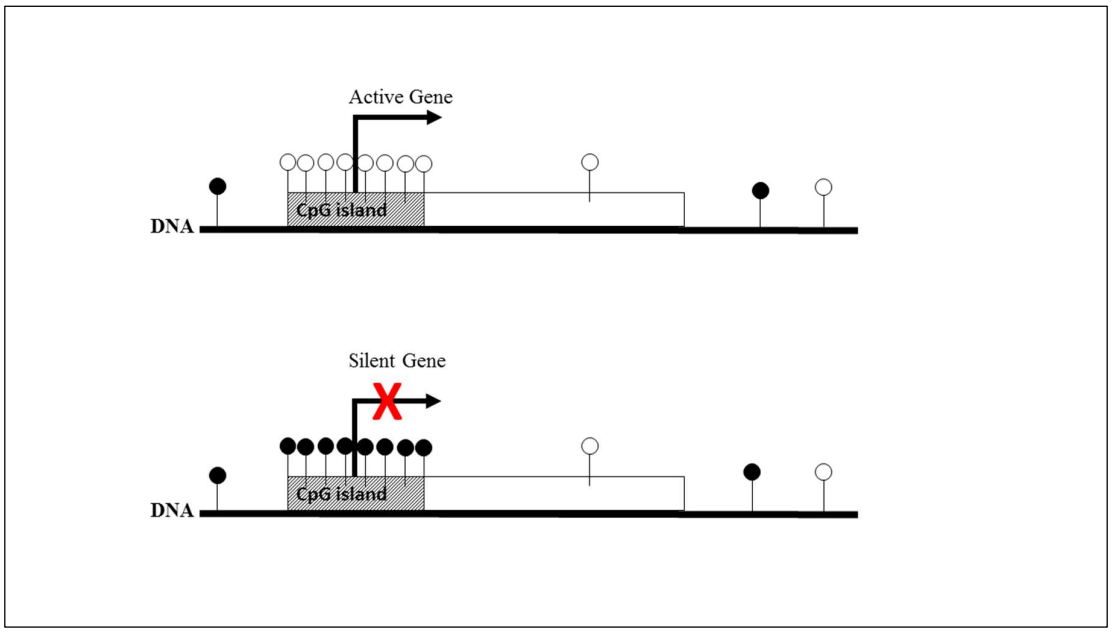

Figure 1.1: Methylation of CpG dinucleotides and role in gene transcription. CpG islands are regions rich in guanine and cytosine residues that are spread across the genome. They are frequently located in the promoter regions of the genes and they can be methylated by enzymes called DNA methyltransferases (DNMTs). Generally CpG islands are hypo-methylated thus allowing the binding of transcription factors and subsequently gene transcription. The addition of methyl groups on the other hand, block the access on cellular molecules and downstream genes remain silenced. Black circles stands for methylated CpG islands, while white circles for unmethylated ones.

The transfer of the methyl-groups into the C residues is catalyzed by a group of enzymes, called DNA methyltransferases (DNMTs). The most important of these enzymes are *DNMT1* (DNA methyltransferase 1), *DNMT3A* (DNA methyltransferase 3A) and *DNMT3B* (DNA methyltransferase 3B). *DNMT3A* and *DNMT3B* are *de novo* methyltransferases that preferentially catalyse the addition of methyl groups on non-methylated cytosines. *DNMT1* is a maintenance methyltransferase that recognizes hemi-methylated DNA and mainly provides sustenance for the mitotic inheritance of methylated DNA bases (Moore et al., 2013). Apart from their role in establishing and maintaining methylation marks on CpG dinucleotides, DNMTs are also implicated in chromatin conformational changes since they mediate the recruitment of molecules such as methyl binding domain proteins (MBDs), histone modifying enzymes and other effector proteins. This shows that there is a cross-talk among the epigenetic components that act on the DNA bases and those acting on histone

proteins (Fuks et al., 2003; Klose & Bird, 2006; Moore et al., 2013; Siegfried & Simon, 2010).

A range of modifications including methylation, acetylation, phosphorylation, ubiquitination, poly (ADP-ribosylation) and sumoylation take place at the N-terminal tails of these proteins around which the DNA is wrapped, thus forming the nucleosomes (Fig. 1.2) (Berger, 2007; Lawrence et al., 2016; Rice & Allis, 2001). Specifically, nucleosomes are made by an octamer, composed of two copies each of the four core histone proteins (H2A, H2B, H3 and H4), rounded by 147 base pairs long DNA sequence. Sequential units of nucleosomes are the basic components of a higher organization, known as chromatin (Javaid & Choi, 2017; Margueron & Reinberg, 2010), a structure characterized by a complex and multilayer regulatory network linked to unique cellular responses, such as the regulation of gene expression and the protection of genomic integrity and stability (being involved in functions, including DNA replication, transcription, recombination and repair) (Berger, 2007; Martin & Zhang, 2005). Both DNA and histone proteins undergo various modifications either directly affect nucleosome positioning (and the state of chromatin compression) or influence the binding of proteins that interact with DNA and histones (which have undergone specific conformational alterations) thereby, affecting gene expression (Dawson & Kouzarides, 2012; Lawrence et al., 2016). Generally, when chromatin is condensed and compact, (termed “heterochromatin”), gene expression is silenced. In contrast, when the chromatin is in an “open” state (known as “euchromatin”) then cellular components are able to bind to gene promoters and consequently initiate the transcriptional process (Woodcock & Ghosh, 2010). Nucleosome position and spacing are modulated by ATP-dependent chromatin regulators which hydrolyze ATP in order to alter the position of the nucleosomes or promote nucleosome exchange for the incorporation of histone variants (Becker & Horz, 2002; Kim et al., 2009; Li et al., 2007).

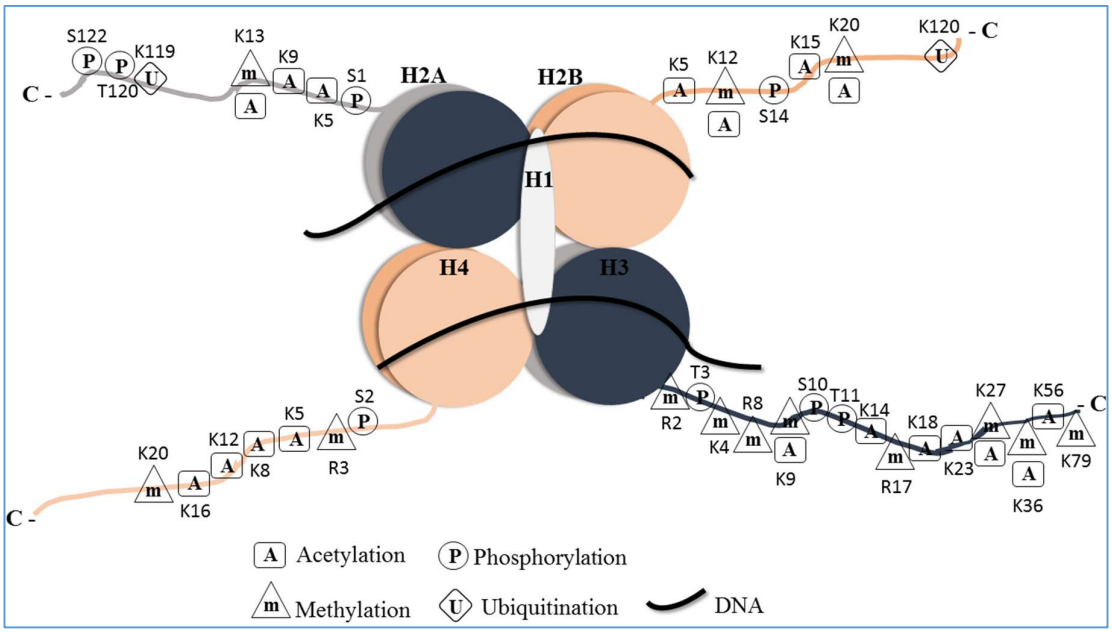

Figure 1.2: Posttranslational modifications on the N-terminal tail of histone proteins. The DNA in the nucleus is wrapped around an octamer consisting of two copies of each of the 4 core histone proteins (H2A, H2B, H3, H4) forming a complex known as nucleosome. The amino (N) terminal tail of the histones undergo various post-translational modifications such as methylation, acetylation, phosphorylation and ubiquitination all of which can regulate the nucleosome structure. In addition, specific sites in specific amino acids [K: Lysine, R: Arginine, T: Threonine, S: Serine] are shown where these modifications take place on particular histone tails.

Among the various modifications on histone proteins, the best characterized ones are methylation and acetylation. The key enzymes that catalyze these modifications are histone methyltransferases (HMTs) and histone acetyltransferases (HATs) respectively (Wang et al., 2009). Histone acetylation mainly occurs in lysines and is generally considered to result in gene activation (Wang et al., 2009). There are three major families of HATs: i) the GNAT (*Gcn5*-related N-acetyltransferases), ii) the MYST [the acronym derives from the four founding members of this HAT family: mammalian MOZ (males absent on the first), yeast Y bf2/Sas3 and Sas2, and mammalian Tip60 (TAT-interacting protein 60)] and iii) the CBP/p300 (cAMP response element binding protein). Each family has a different specificity towards their histone and amino acid targets and are generally categorized into Type A and Type B both of which are located in the nucleus and cytoplasm, respectively. Histones on nucleosomes found within the nucleus are acetylated by Type A HATs while Type B HATs

have a housekeeping role by acetylating newly synthesized histones found in the cytoplasm (Biswas & Rao, 2017; Javaid & Choi, 2017).

Histone methylation takes place on arginine and lysine amino acids and is associated with either reactivation or silencing of genes, based on the specific site and extent of the modification itself (Li et al., 2007; Yan & Boyd, 2006). The methylation of histone proteins is catalyzed by three distinct families of enzymes: i) the SET-domain containing protein family (Su(var)3-9, Enhacer-of-zeste and Trithorax), ii) the non-SET domain protein family and iii) the protein arginine methyltransferases (PRMT1) family (Biswas & Rao, 2017; Greer & Shi, 2012).

Finally, non-coding RNAs (ncRNAs) are functional RNA molecules which do not translate into proteins and are important regulators of the expression of gene targets at the transcriptional and post-transcriptional level. There are two main groups of ncRNAs, namely short (<30 nucleotides) and long (>200 nucleotides) ncRNAs. The short ones are further divided into three major classes: i) micro-RNAs (mi-RNAs), ii) short interfering RNAs (siRNAs), and ii) P-element-induced wimpy testis (piwi)-interacting RNAs (piRNAs) (Srijyothi et al., 2018; Zhang et al., 2019). Both groups are involved in epigenetic processes including heterochromatin formation, histone modifications, targeting of DNA methylation and gene silencing (Peschansky & Wahlestedt, 2014).

Among them, mi-RNAs (21-26 nucleotides in length) are the most studied and well characterized. They are transcribed, by RNA polymerase II, as non-coding primary miRNA (pri-miRNA) transcripts and are processed into precursor miRNA (pre-miRNA) under the activity of a microprocessor complex. This complex consists of Drosha and the DiGeorge syndrome critical region in gene 8 (*DGCR8*) which are found into the nucleus where the pre-miRNAs produced are transported into the cytoplasm where they are finally transformed into mature and functional miRNA by Dicer (Srijyothi et al., 2018). mi-RNAs are key regulators of gene expression through binding to the 3' untranslated region (UTR) of their target messenger RNAs (mRNAs), as a complex with Argonaute (AGO) family proteins, forming the so called miRNA-induced silencing complex (miRISC). According to the degree of complementarity between mi-RNA on miRISC and mRNA target, mi-RNAs either suppress the translation or induce the cleavage or degradation of the latter (Fig. 1.3) (O'Brien et al., 2018; Shukla et al., 2011; Valencia-Sanchez et al., 2006). In addition to their regulatory function in gene transcriptional activity, they play pivotal roles in various biological processes including cell death, proliferation, differentiation and development (Wahid et al.,

2010). Advances in this field, have shown that these molecules are also implicated in the regulation of the epigenetic machinery by controlling DNA methylation and histone modifications. For instance, it has been reported that these molecules can target and modulate the activity of genes that transcribe epigenetic modifying enzymes such as DNMTs and histone deacetylases (HDACs). DNA methylation and histone modifications have been associated with the regulation of mi-RNAs expression, suggesting that there is a feedback loop that control the activity of the epigenetic network (Chuang & Jones, 2007; Moutinho & Esteller, 2017; Yao et al., 2019).

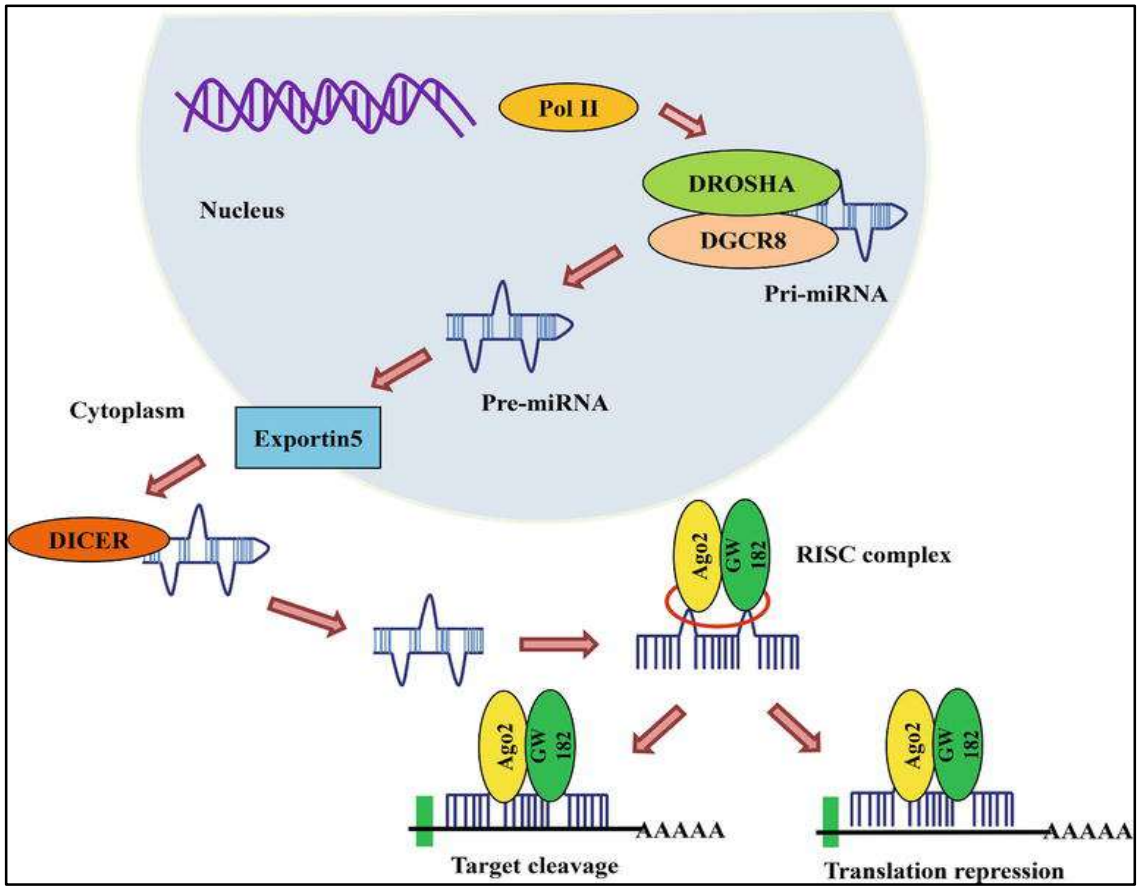

Figure 1.3: mi-RNA biosynthetic process. mi-RNAs are functional, short, non-coding RNAs (21-26 nucleotides) that are important in gene transcriptional regulation. They are transcribed by RNA polymerase II into primary mi-RNAs (pri-miRNA) and are further processed into precursor mi-RNAs (pre-miRNA) under the activity of Drosha and DGR8. Pre-miRNAs are then exported to the cytoplasm by exportin 5, where under Dicer activity are transformed into mature mi-RNA. The mi-RNAs produced are loaded into the Argonaut (AGO) family of proteins and form a miRNA-induced silencing complex (mi-RISC) which target the 3' untranslated region of complementary messenger RNAs (mRNAs). If the

complementarity is complete the mRNA target is cleaved, while incomplete complementarity result in translational suppression (Srijyothi et al., 2018).

All the above mentioned modifications act in a coordinative manner in order to regulate the genetic information. It is obvious that there is a crosstalk among the components of the epigenetic machinery thereby creating a highly organized and complex network for the regulation of gene expression (Biswas & Rao, 2017; Chuang & Jones, 2007; Kondo, 2009; Murr, 2010). Abnormalities in normal cellular epigenetic patterns are associated with the disruption of the normal function of genes thus resulting in a wide range of pathologies, including malignant transformation (Egger et al., 2004; Ziech et al., 2010).

1.1.2 Epigenetics in Cancer

Until relatively recently, carcinogenesis was considered to be a primarily genetic condition, it is now known that epigenetic dysregulation alongside with multiple genetic lesions are responsible for inducing cellular transformation (Dawson & Kouzarides, 2012; Taby & Issa, 2010). The rapid evolution of the cancer epigenetics field led to important observations regarding the alterations that occur in the epigenetic landscape of transformed cells in comparison to normal cells. Global changes and reprogramming of the epigenetic machinery have been reported to be part of the initiation, progression and metastatic stages of carcinogenesis (Nebbioso et al., 2018; Sandoval & Esteller, 2012; Taby & Issa, 2010).

The involvement of the epigenome in malignant transformation was, first, introduced by the identification of alterations in the pattern of DNA methylation patterns in various human cancers (Feinberg & Vogelstein, 1983). For instance, hypo-methylation of CpG islands across the genome is considered as a hallmark of cancer. Tumorigenesis is generally characterized by global hypo-methylation at multiple genomic regions as well as hyper-methylation at specific sites [mostly in the promoter and/or the first exon region as well as in satellite sequences, transposable elements and repetitive genomic sequences [e.g. long interspersed element (LINE), short interspersed nuclear element**s** **(**SINEs), Alu elements, centromeric repeats etc.] (Kulis & Esteller, 2010; Sharma et al., 2010). Global loss of methylation is usually associated with the induction of various proto-oncogenes and transposomal translocation, resulting in genomic and chromosomal instability (Berdasco & Esteller, 2010; Eden et al., 2003; Sharma et al., 2010). In contrast, hyper-methylation of specific promoter regions leads to repressive chromatin structures that block access to transcription factors and result in transcriptional silencing of tumour suppressor genes (Gokul & Khosla, 2013). A number of tumour suppressor genes have been shown to be

epigenetically inactivated due to hyper-methylation of their promoter. These genes are of particular importance for the maintenance of cell homeostasis, since they are involved in various physiological processes including DNA repair, cell cycle regulation and metastasis. Thus, their down-regulation is a critical step in carcinogenesis (Moison et al., 2014). The first one to be reported was the Retinoblastoma gene (RB), associated with sporadic and hereditary retinoblastomas (Greger et al., 1989). Furthermore, hyper-methylation indirectly affects gene transcription by recruiting molecules that bind to methylated regions, such as HDACs and methylated-binding proteins, causing changes in the organization of chromatin. (Costello & Plass, 2001; Gokul & Khosla, 2013).

Apart from DNA methylation, abnormalities in the pattern of epigenetic marks on histone proteins are also implicated in tumorigenesis (Sawan & Herceg, 2010). Histone alterations are dynamic and co-ordinately regulated and reversed under the activity of opposing enzymes. An imbalance in the function of these enzymes disrupts gene transcription, leading to aberrant gene activation and consequently to tumorigenesis (Hassler & Egger, 2012). Malignant cells are characterized by global modulations in both acetylated and methylated histone marks. The evolution of the cancer epigenetic field led to the identification of specific histone alterations that are currently considered as a distinctive feature of cancer. For instance, genome-wide hypo-acetylation of lysine 16 accompanied with the loss of tri-methylation at lysine 20 of histone H4 were the first epigenetic marks documented to be differentially distributed in various cancer types (Füllgrabe et al., 2011). Moreover, alterations in the methylation pattern of H3K4, H3K9 and H3K27 have been reported during cancer development (Chakravarthi et al., 2016). In line, the enzymes responsible for the formation of these epigenetic marks are also deregulated in cancer. HDACs (responsible for the removal of acetyl groups from histone tails) have been observed to be over-expressed in tumour cells (Kanwal & Gupta, 2012). Similarly, HMTs are also abnormally expressed in tumour cells (Albert & Helin, 2010). A characteristic example is the *Ezh2* (Enhancer of zeste homolog 2) gene which is documented to be highly expressed in various malignancies. Ezh2 catalyses the methylation of lysine 27 at histone H3 (H3K27me), a mark commonly observed in carcinomas being associated with repression of various genes, including genes involved in the Wnt/β catenin signalling pathway, in chemo-resistance, through regulation of DNA damage mechanisms [e.g. *BRCA-1*, recombinase *RAD51,* X-ray repair cross complementing 2 and 3 *(XRCC2* and *XRCC3*) etc.] as well as in cellular proliferation and differentiation [e.g. Runt-related transcription factor 3 (*RUNX3*), Cyclin dependent kinase inhibitor 1C (*CDKN1C*), Kruppel like Factor 2 (*KLF2*) etc.], in invasion, metastatic spreading [*e.g.*, E-

cadherin, Forkhead box C1 (*FOXC1*), Disabled homolog 2-Interacting Protein (*DAB2IP*), Raf Kinase Inhibitory Protein (*RKIP*), Microseminoprotein Beta (*MSMB*), tissue inhibitors of metalloproteinases (TIMPs) etc.] and neovascularization [e.g. *vasohibin1* (*VASH1*), *KLF2*, *MSMB*, TIMPs etc.]. In addition, a number of anti-metastatic microRNAs (including miR-101, let-7c, miR-200b, miR-139-5p, and miR-125b) have been also reported to be epigenetically silenced by Ezh2 (Crea et al., 2012; Deb et al., 2013; McCabe et al., 2012).

Other important constituents of the epigenetic network implicated in driving the behavior of tumor growth are mi-RNAs. Their genomic localization, transcriptional regulation and processing are all factors reported to be involved in carcinogenesis (Farazi et al., 2011; Malumbres, 2013; Ohtsuka et al., 2015). The first report of their involvement in human tumorigenesis came from studies where miR-15a and miR-16-1 were shown to be down-regulated in chronic lymphocytic leukaemia patients (Calin et al., 2002). Since then, various studies have reported multiple mi-RNAs being differentially expressed in cancer cells compared to normal ones (Lu et al., 2005; Mar-Aguilar et al., 2013; Ratert et al., 2013; Tian et al., 2018; Volinia et al., 2006; Zhou et al., 2014). For example, in a mi-RNA expression profile analysis, the mir-17-92 cluster was found to be significantly over-expressed in human lung cancers and was also shown to be associated with increased cell proliferation (Hayashita et al., 2005). Other mi-RNAs that were shown to be implicated in carcinogenesis are mir-27a, mir-96, and mir-182 which were markedly expressed in breast cancer cells resulted in repression of tumor-related Forkhead box protein O1 (*FOXO1*) involved in the regulation of apoptotic response, cell cycle checkpoints, and cellular metabolism (Guttilla & White, 2009). Interestingly, their expression seems to be regulated by other epigenetic modulators, especially DNA methylation as well as specific histone alterations (Baer et al., 2013; Malumbres, 2013). Typical examples are mir-9, mir-148, mir-124, mir-137, mir-34, mir-127 and mir-512 that were frequently documented to be suppressed in a number of malignancies associated with CpG hyper-methylation (Liu et al., 2013; Sato et al., 2011). Generally, oncogenic mi-RNAs are usually over-expressed in malignancies whereas tumour suppressors ones are found to be silenced. However, mi-RNA implication in tumorigenesis is more complex, since there are mi-RNAs having a dual role in the tumorigenic process (acting either as tumour suppressors or oncogenes) based on their targets (Jansson & Lund, 2012; Li et al., 2010). Characteristic example is that of the mir-148 family which was reported to be upregulated in multiple myeloma and hepatocellular carcinoma while found to be suppressed in breast and gastric cancers (Chen et al., 2013; Friedrich et al., 2017).

Due to the reversible nature of the epigenetic modifications, the scientific community has focused in the identification of agents that could restore the epigenetic pattern observed in cancers back to a "normal" landscape. Thus, epigenetic modulators are currently considered as potential and promising targets for therapeutic interventions. Recent advances in the epigenetic therapy field have already led to the development of a number of small molecule inhibitors against epigenetic regulators, whereas several others (such as azacitidine, decitabine, vorinostat, romidepsin, panobinostat and belinostat) have recently been approved by the Food and Drug Administration (FDA) and are used in the clinical setting for the treatment of various human cancers (Boumber & Issa, 2011; Dawson & Kouzarides, 2012; Nebbioso et al., 2018; Qi et al., 2016). These are basically DNMT and HDAC inhibitors and constitute the first generation of epigenetic drugs. Research is currently focused in producing a 'second generation' of inhibitors that target other epigenetic enzymes, such as HMTs, HATs, histone demethylases (HDMs) as well as methyl- and acetyl-binding proteins (Boumber & Issa, 2011; Qi et al., 2016). In this direction, among the various molecules that are tested, phytochemicals have emerged as particularly attractive, because of their potential to target epigenetic components and the expectation that these plant-derived molecules will have fewer side effects than conventional chemotherapeutics (Ullah et al., 2014)

1.1.3 Nutrition, Cancer and Epigenetics

The onset of cancer depends not only on the interplay of genetic and epigenetic lesions but also on environmental factors such as nutrition (Bishop, 2015). Nutrition is an important factor influencing health and it is mainly implicated in the prevention of chronic disease development including carcinogenesis (Russo, 2007; Slawson et al., 2013). According to the estimations of the World Cancer Research Fund (WCRF) and the American Institute for Cancer Research (AICR), around 30-40% of cancer incidence worldwide could be avoided by adopting healthy eating habits, weight control and physical activity (Donaldson, 2004; Gonzalez, 2006; Wiseman, 2019). Since then, the protective effect from the consumption of plant-derived products has been well established in numerous epidemiological studies. Numerous case-control and cohort studies have shown a link between fruit and vegetable consumption and reduced risk for various cancers like lung, colorectal, prostate, breast and gastric (Gonzalez, 2006). However the data obtained from these type of studies are controversial and also lack an understanding of the underlined mechanism(s) by which dietary factors influence cancer risk (Sapienza & Issa, 2016; Willett, 2010). New technologies and approaches enabled the exploration of the complex interaction of nutrition with genetic and epigenetic factors. This led to the emergence of the field of nutritional

epigenetics (Mayne et al., 2016). The current notion on a relationship between diet and cancer arises from the association between specific dietary consumption patterns and an individual's risk for developing cancer (Bishop & Ferguson, 2015; Sapienza & Issa, 2016).

In this respect, natural products are known to offer various health benefits by exerting pleiotropic protective mechanisms and thus have gained scientific interest (Di Domenico et al., 2012; Ziech et al., 2012). The potential of these molecules in disease prevention is mainly attributed to their capacity to prevent, reverse and/or suppress the multi-stage tumorigenic process and thus stimulate an interest in the context of chemoprevention (Kang et al., 2011; Weng & Yen, 2012).

In particular, attention has been focused on compounds derived from fruits and vegetables specifically citrus fruits, dark green and cruciferous vegetables, etc. The association between higher consumption of these foods and reduced cancer risk has been suggested to result from their high content of particular phytochemicals, such as lignans, curcumin, anthocyanin, quercetin, gingerol, limonene, indole-3-carbinol, genistein, apigenin, saponins, resveratrol, coumarins, epigallocatechin gallate, lutein, isothiocyanates and many others. These bioactive constituents are documented to exhibit a variety of biological properties including anti-inflammatory, anti-infectious, anti-oxidant and anti-cancer (Fitsiou et al., 2016; Issa et al., 2006; Johnson, 2007; Li et al., 2014; Nohynek et al., 2006). In addition, emerging evidence shows that these nutraceuticals influence gene expression by modulating epigenetic regulators implicated in CpG island methylation, histone protein modifications and mi-RNA induction (Rupasinghe et al., 2016; Supic et al., 2013). Such phytochemicals correspond to a wide range of biologically-active secondary metabolites and are classified (according to their functional and chemical activities) into phenolics, carotenoids, alkaloids, nitrogen-containing and organosulfur compounds (Liu, 2004).

1.2 Cruciferous Vegetables, Glucosinolates and Isothiocyanates

Cruciferous vegetables belong to the *Brassica* family (e.g. broccoli, watercress, Brussels sprouts, cabbage, horseradish, cauliflower, mustard, etc.) and are rich sources of an important group of phytochemicals called glucosinolates (GLs) (Verkerk et al., 2009). GLs are characterized by a common structure consisted of a β-thioglucosilated moiety which is linked to a sulfonated aldoxime and a variable aglucone side chain (R). This R chain derives from eight selected amino acids: alanine, leucine, isoleucine, valine, phenylalanine, tyrosine, tryptophan and methionine (and possibly glutamic acid) (Agerbirk & Olsen, 2012; Kliebenstein et al., 2005). The precursor amino acids used at the early biosynthetic stages

generally determine the classification of GLs into aromatic, heterocyclic (indoles), aliphatic, multiple glycosylated, benzoate and sulfur-containing GLs (Clarke, 2010; Fahey et al., 2001).

The type and content of GLs in plants differ within as well as between the *Brassicaceae* family members. Various environmental factors are responsible for the content and type of GLs, including climate, cultivation, genotype, region, even the part and developmental stage of the plant (Charron et al., 2005; Kliebenstein et al., 2001; Velasco et al., 2007; Śmiechowska et al., 2010). About 200 different GL structures have been identified (Clarke, 2010) which, upon hydrolysis, give rise to multiple bioactive secondary metabolites including ITCs. The type and corresponding breakdown products of GLs are determined to a large extent by the eight amino acid precursors of their side chain. For example, ITCs are produced by the hydrolysis of aliphatic or aromatic GLs that are usually derived from methionine and phenylalanine residues respectively (Cancer, 2004). These are the main mediators of the multiple health benefits derived from the consumption of cruciferous vegetables (Dinkova-Kostova & Kostov, 2012; Wagner et al., 2013).

In particular, ITCs are highly reactive electrophiles that all share an R-N=C=S core structure. The R in the structure represents a variable side chain, which consists of allyl or alkyl groups and reversibly interacts with the thiol group of cystine residues, forming dithiocarbamates (Zhang, 2012b). Examples of well-characterized cancer chemopreventive ITCs include sulphoraphane (SFN), iberin (IBN), allyl-ITC (AITC), benzyl-ITC (BITC) and phenethyl-ITC (PEITC) all of which represent the most frequent ones found in commonly eaten cruciferous vegetables (Fig. 1.4) (Cancer, 2004).

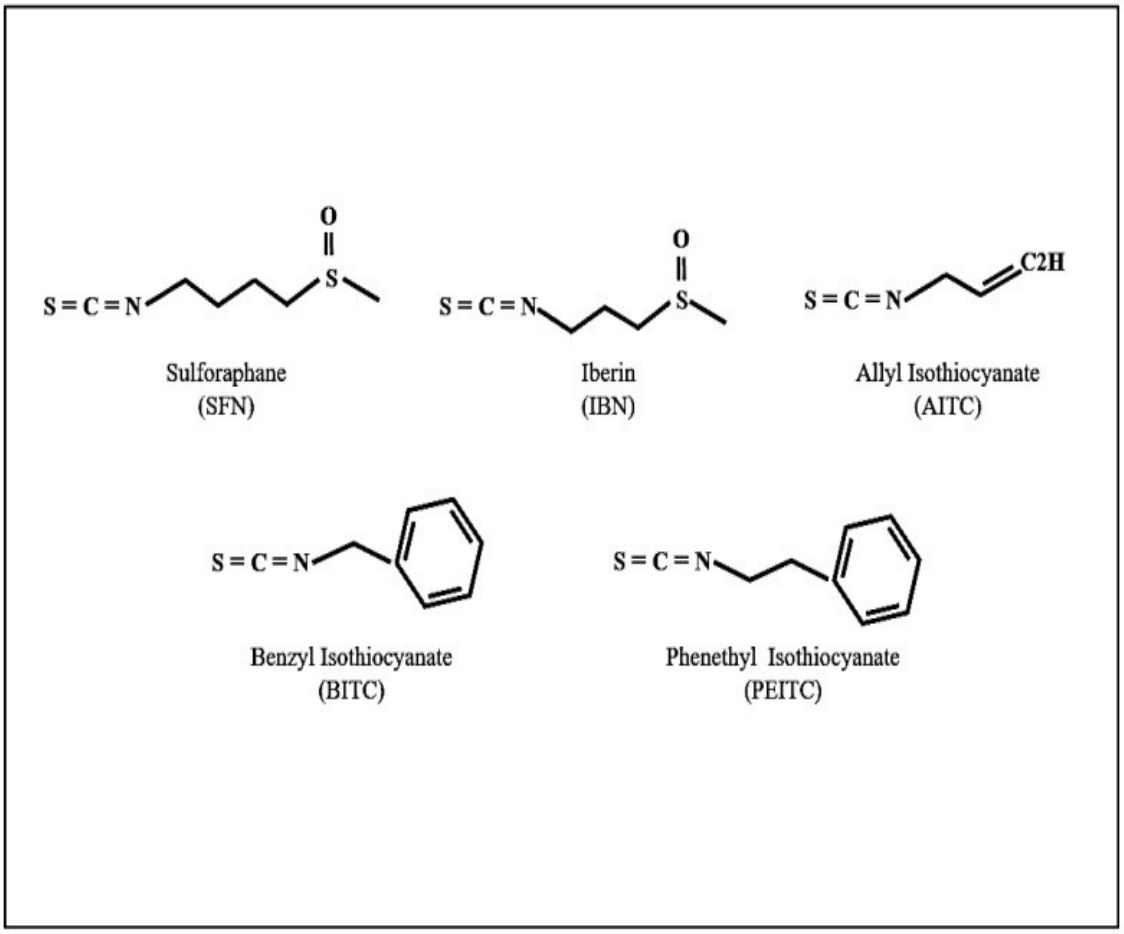

Figure 1.4: The structure of major ITCs Adapted from (Mitsiogianni et al., 2019)

1.2.1 GLs Biosynthesis and Metabolism

Studies utilizing the model species *Arapidopsis Thaliana* led to the identification of genes involved in the GLs biosynthetic process. This pathway occurs in three stages: i) side chain elongation; ii) formation of the glycone moiety and iii) secondary modifications in the side chain (Grubb & Abel, 2006; Halkier & Du, 1997; Wittstock & Halkier, 2002). Briefly, during the first step, the side chain elongation starts with the transamination of the α-amino acid to form an α-keto acid which then undergoes condensation with acetyl coenzyme A (Graser et al., 2000). After isomerization, oxidation takes place which is followed by decarboxylation to form a 2-oxo acid with an additional methylene group. This cycle can be repeated a number of times resulting to the addition of a carbon atom each time (Graser et al., 2000; Sønderby et al., 2010) (Fig. 1.5a). The second step in the process, is the formation of the core structure of GLs. Oxidation of the amino acid precursor by cytochrome P450 enzymes give rise to an N-hydroxyl amino acid, in the presence of *NADPH*. This reaction results in the formation of unstable intermediates and it is poorly characterised (Mithen et

al., 2000). In general, oxime is converted to an aci-nitrol compound which can accept thiol groups (Grubb & Abel, 2006; Wang et al., 2011; Wittstock & Halkier, 2002). At first, it was proposed that the donor of the thiol group was cysteine (Cys) but recently glutathione (GSH) has been shown to act as such donor. This is followed by the cleavage of cysteine by a C-S lyase to form thiohydroximate (Geu-Flores et al., 2011; Sønderby et al., 2010). Then, S-thioglucosilation of the thiohydroximate, by *UDPG*: thiohydroximate glucosyltransferase, generates desulfoglycosinolate (Mithen et al., 2000). Finally, the complete glucosinolate is yielded after the sulfation of desulfoglucosinolate by 3′phosphoadenosine 5′-phosphosulfate (PAPS) which serves as the sulphate donor for the reaction (Koprivova & Kopriva, 2016; Mugford et al., 2009) (Fig, 1.5b).

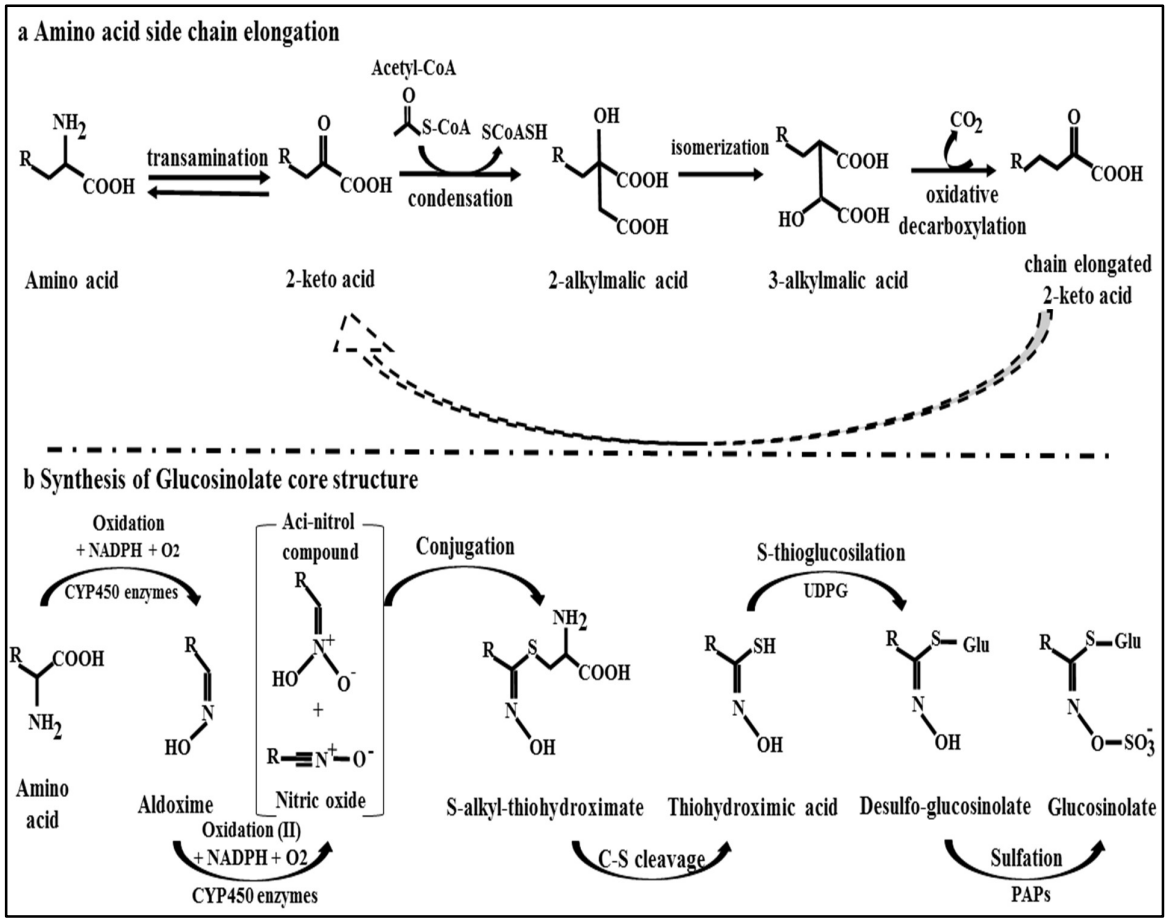

Figure 1.5: Biosynthetic process of Glucosinolates (GLs). The biosynthetic pathway involves two main stages: a) side chain elongation and b) formation of the core structure of GL. a) During the first stage, an amino acid precursor undergoes transamination leading to the formation of a 2-keto acid, which then, through a condensation process, produce a 2-alkylmalic acid. Next, isomerization takes place followed by oxidative decarboxylation to

produce a 2-keto acid with an additional methylene group. b) The second step of GLs biosynthesis, starts with the oxidation of the amino acid, in the presence of cytochrome P450 enzymes and NADPH, resulting in the formation of an unstable intermediate (aldoxime). The oxidation of this aldoxime, give rise to an aci-nitrol compound which is then conjugated with a nitric oxide, forming an S-alkyl-thiohydroximate. Next, S-alkyl-thiohydroximate is cleaved by a C-S lyase to form a thiohydroximate, followed by S-thioglucosilation to generate a desulfoglycosinolate. Final step in the process is the sulfation of the desulfoglucosinolate and the complete glucosinolate is produced. In this figure, R stands for the specific functional side chain of each amino acid, UDPG for *UDPG*: thiohydroximate glucosyltransferase and PAPs for 3′phosphoadenosine 5′-phosphosulfate.

The third and final step involves secondary modifications like hydroxylation, methoxylation, desaturation, sulphation and glucosylation, all of which are responsible for forming the wide range of known GLs. Other factors that contribute to such diversity are the presence of different types of side chains (simple and branched alkyl, ω-methylthioalkyl, aryl or heterocyclic) and differences in amino acid elongation (Wittstock & Halkier, 2002).

1.2.2 GL Metabolism- Mustard Oil Bomb

Myrosinase was first discovered by Bussy in 1839 as a protein essential for the release of essential oil from mustard seed. Later, it was reported that myrosinase is the enzyme responsible for the hydrolysis of GLs (Andréasson & Jørgensen, 2003). There are a number of genes (a gene family comprising at least three differentially expressed subfamilies of myrosinase genes) responsible for the transcription of distinct isoforms of myrosinase. Different isoforms of this enzyme have been found with diverse activities while their distribution appears to be organ- and species-specific. Finally, differences in activity levels have been also observed among different plant species (del Carmen Martinez-Ballesta & Carvajal, 2015; Thangstad et al., 2004).

Hydrolysis of GLs starts with the disruption of plant integrity, after chewing or cutting it. Then, myrosinase is released and comes in contact with its substrates. In doing so, it acts as a β-thioglucosidase and breaks down the sulfur group of the glucosidic bond (Agerbirk & Olsen, 2012; Angelino & Jeffery, 2014). Within the plant, myrosinase is generally considered to be physically isolated from GLs, located in idioblastic cells. However, their compartmentalization inside the plants is still not yet fully understood (Andréasson et al., 2001).

Studies on the compartmentalization of myrosinase were conducted in *Arapidopsis thaliana* indicating that while GL-containing cells, known as S-cells, were found between the phloem and the endoderm of the plant, myrosinase itself was found to be in close proximity with the phloem parenchyma of myrosin cells (Andréasson et al., 2001; del Carmen Martinez-Ballesta & Carvajal, 2015; Koroleva et al., 2000). This physical isolation of GLs allows the degradation of GLs, by myrosinase, to take place only when the plant is stressed.

Once the myrosinase-glucosinolate system (also known as mustard oil bomb) is activated, an aglycone unstable intermediate metabolite is formed, called thiohydroximate-O-sulfonate. Next, a non-enzymatic reaction occurs followed by a simultaneous rearrangement of the core structure of GLs, resulting in the production of biologically and chemically distinct compounds including thiocyanates, isothiocyanates, nitriles and indoles (Fig. 1.6) (Barba et al., 2016; Bones & Rossiter, 2006; Grubb & Abel, 2006). A subsequent lossen rearrangement usually promotes ITCs formation (Agerbirk & Olsen, 2012; Bones & Rossiter, 2006; Mithen et al., 2000; Thornalley, 2004). The outcome of this process, is largely based on many factors like temperature, availability of ferrous ions and epithiospecifier proteins (ESP), pH, presence of proteins that interact with myrosinase as well as the type of GLs. For example, at pH 7.0, ITCs are preferentially formed whereas at more acidic conditions (or when ESPs are present) the synthesis of nitriles is promoted (Barba et al., 2016; Halkier & Du, 1997; Kissen et al., 2009).

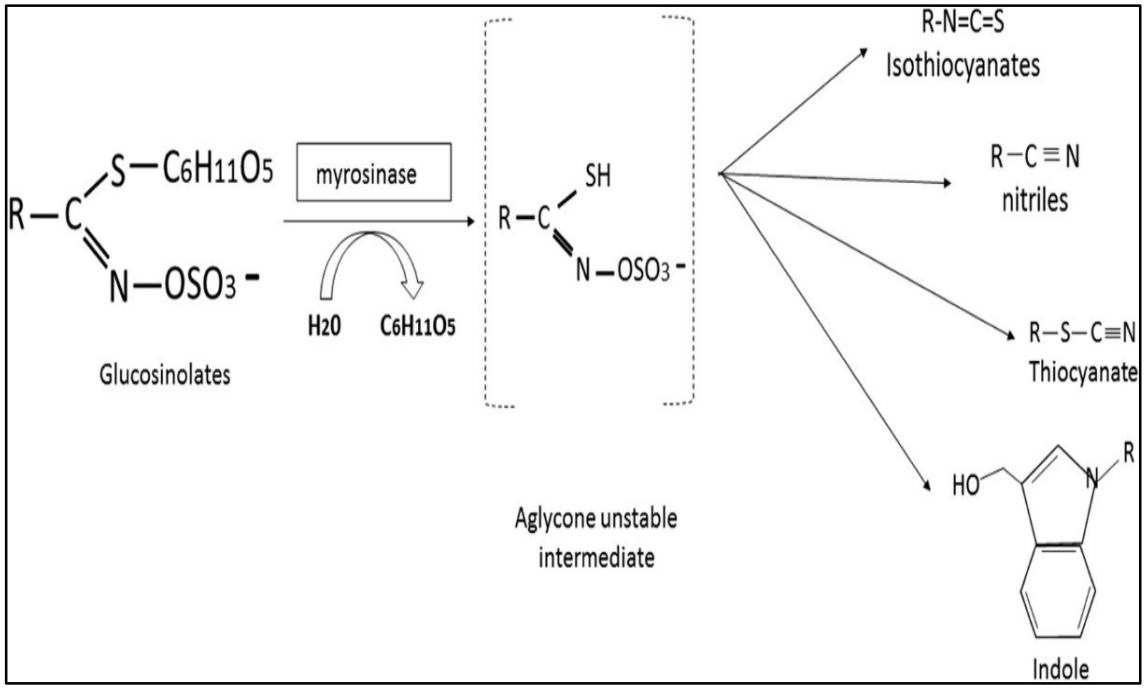

Figure 1.6: Hydrolysis of GLs by myrosinase. Upon tissue disruption, myrosinase is released and interacts with its GL substrates by catalyzing their hydrolysis. As a result, the formation of an aglycone unstable intermediate product is formed and subsequently a non-enzymatic reaction occurs followed by a simultaneous rearrangement of their core structure, leading to the production of diverse metabolites including ITCs, thiocyanates, nitriles and indoles. Adapted from (Mitsiogianni et al., 2018)

1.2.3 ITC Metabolism

As already mentioned above, GLs are converted into a range of compounds, including ITCs, which are readily absorbed in the gastro-intestinal (GI) tract. ITCs are electrophiles and thus are eliminated from the body via the mercapturic acid pathway (Angelino & Jeffery, 2014; Grzywa et al., 2016). Briefly, ITCs are produced in the gut and then are diffused into the blood circulation through the GI. Once inside the cells, ITCs bind reversibly, but with high affinity, to glutathione (GSH) and a GSH-ITC conjugation product is formed catalysed by glutathione S transferases (GSTs). The conjugates are further metabolized in the liver (where the GSH moiety is enzymatically modified) forming cysteinyl-glycine (Cys-Gly) and cysteine (Cys) conjugates by the action of gamma glutamyltranspeptidase (GTP) and cysteinylglycinase (CGase) enzymes, respectively. Then, the metabolites are transferred in the kidney where the final N-acetylcysteine-(NAC-) conjugates (mercapturic acids) are produced by the activity of N-acetyltransferase (NAT). Finally, the mercapturic acids are actively secreted into the urine (Angelino & Jeffery, 2014; Barba et al., 2016; Palliyaguru et

al., 2018; Zhang, 2012b) (Fig. 1.7). The overall metabolic process largely depends on GST isoenzyme polymorphisms, often present, since binding of ITC-GSH by GSTs is the first step in this process (Nakamura et al., 2018). ITCs circulate through the body, as different conjugates, thereby exerting their health-promoting benefits (Angelino & Jeffery, 2014; Grzywa et al., 2016; Palliyaguru et al., 2018).

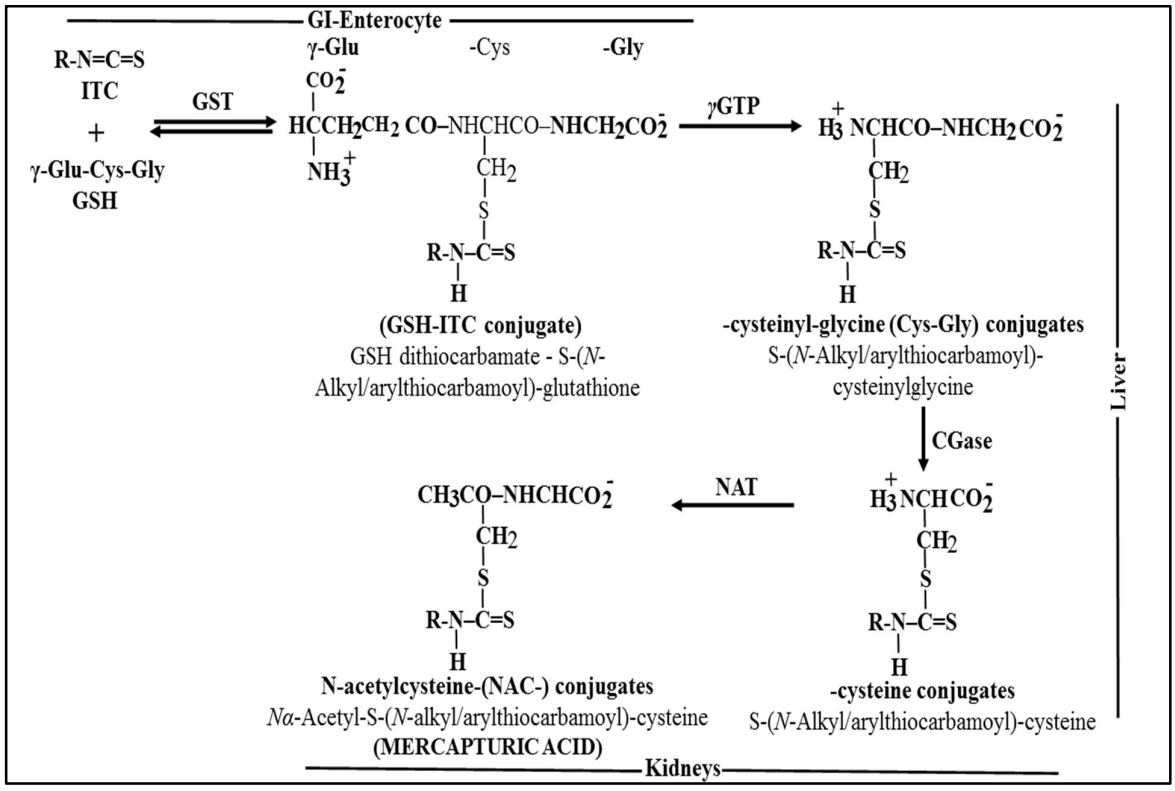

Figure 1.7: ITCs metabolism through the mercapturic acid pathway. After consumption of cruciferous vegetables, ITCs are produced in the gut and are further eliminated from the body through the mercapturic acid pathway. Briefly, once produced, they are absorbed in the gastro-intestinal (GI) track and they are diffused in the cells, where they bind with high affinity and reversibly with glutathione (GSH), under the activity of glutathione S transferase (GST), forming GSH-ITC conjugates. These conjugates are then transferred, through the blood circulation in the liver where the GSH moiety is further modified, yielding cysteinyl-glycine (Cys-Gly) and cysteine (Cys) conjugates, modifications catalyzed by gamma glutamyltranspeptidase (GTP) and cysteinylglycinase (CGase) enzymes, respectively. Cysteine-conjugates are then transferred in the kidneys, where the mercapturic acids [N-acetylcysteine-(NAC-) conjugates] are formed by the action of N-acetyltransferase (NAT) and are finally eliminated from the body through the urine.

The amount of ITCs produced and absorbed in the body is dependent on various factors such as from the total GL content in the plant all the way to how *Brassica* vegetables were processed (Palliyaguru et al., 2018). In general, food processing is crucial and could result in lower levels of ITCs mainly due to i) endogenous myrosinase inactivation, ii) release of GLs in the heating media and the iii) unstable nature of GLs that are degraded after exposure to higher cooking temperatures. Thermal-induced degradation of GLs, affects the formation of the final product depending on the temperature applied as well as the pH and the presence of ferrous ions. For example, at 100ºC upwards the formation of the more thermo-stable nitriles is favoured (Hanschen et al., 2012). Many other factors also determine the amount of GLs (and therefore their concentration and intake) including cultivation, storage and post-harvest processing (Ciska et al., 2000; Deng et al., 2015; Song & Thornalley, 2007). However, it is noteworthy that lower levels of ITCs can be formed through hydrolysis of GLs, by bacterial myrosinases, in the colon. When the vegetables are consumed, after cooking, the endogenous myrosinase is destroyed and ITCs formation is basically promoted by the microbiome in the intestinal track, a rather "poor" process that leads to a much lower yield of ITCs (Angelino et al., 2015) (Fig, 1.8).

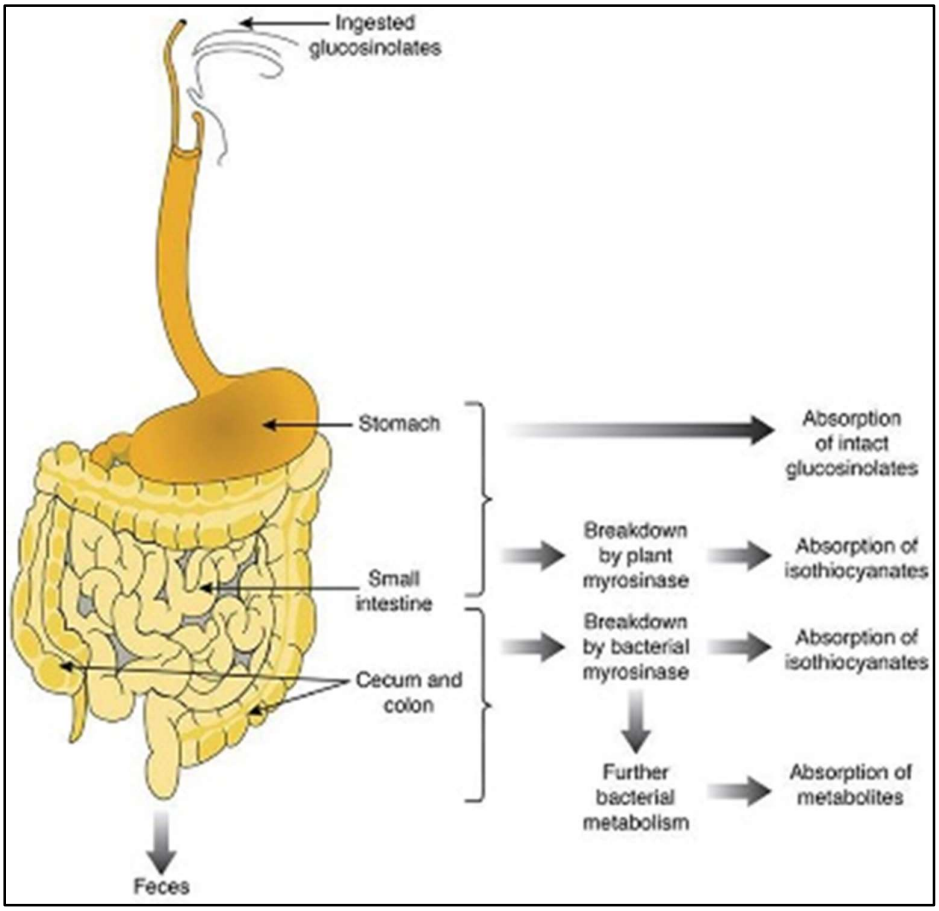

Figure 1.8: Schematic presentation of the fate of GLs and their metabolites in the human gut Adapted from (Barba et al., 2016).

The intake of cruciferous vegetable is generally estimated by measuring the levels of mercapturic acids (i.e. selective biomarkers of total ITCs consumption) that are excreted in urine (Barba et al., 2016; Nakamura et al., 2018). Finally, experimentally, the gold-standard methodology for ITC quantification is the cyclocondensation assay which calculates the total yield of ITCs in plant extracts, plasma and urine, without differentiating into the diverse types of ITCs present. The assay is based in the interaction of 1,2-benzenedithiole with the carbon moiety in the -N=C=S structure, shared by all ITCs, leading to the formation of 1,3-benzodithiole-2-thione, which can be spectroscopically measured, and is proportional to ITCs quantity (Egner et al., 2008; Nakamura et al., 2018; Zhang, 2012a). Individual ITCs are measured using more sensitive analytical methodologies such as high-performance liquid chromatography (HPLC), gas chromatography (GC) and mass spectrometry (MS) (Nakamura et al., 2018).

1.3 Biological Activities of ITCs: Anti-microbial, Anti-oxidant and Anti-inflammatory Functions

ITCs exert a plurality of biological functions, ranging from defence against pathogens to cancer prevention (Grubb & Abel, 2006). Among them, their anti-microbial, anti-oxidant, anti-inflammatory and anti-cancer properties are of particular importance and consequently have been extensively studied (Fig, 1.9).

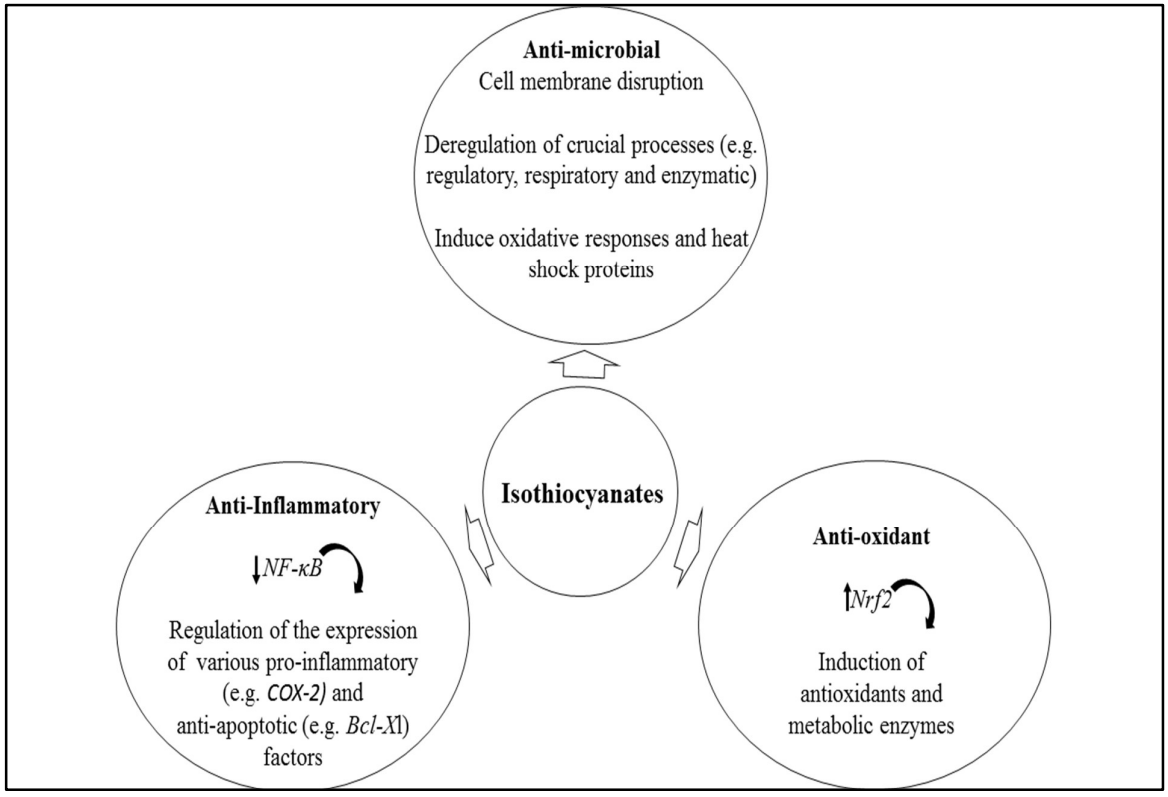

Figure 1.9: Biological activities exerted by ITCs. ITCs exert a wide range of biological properties, including anti-microbial, anti-inflammatory and anti-oxidant properties. ITCs reported to exert a protective effect against bacteria and fungi via multiple mechanisms including disruption of cell membrane, deregulation of key functional processes and induction of heat shock proteins and oxidative stress. They are also able to modulate the activity of various enzymes involved in anti-oxidant and metabolic processes through activation of the nuclear factor erythroid-derived 2-like 2 (*Nrf2*) pathway, which is crucial for the overall ITC antioxidant capacity. Moreover, the capacity of these nutraceuticals to abrogate inflammatory responses is another key aspect of their protective role. ITCs educe the activity of the nuclear factor-kappa B (*NF-κB*) pathway and consequently down-regulate the expression of pro-inflammatory [such as cyclooxygenase 2 (*COX-2*) and inducible nitric

oxide synthase (*iNOS*)] and anti-apoptotic proteins (such as *Bcl-Xl, Bcl-2, Bcl-3*), which are mediated by this pathway.

1.3.1 Anti-microbial activity

Many studies have reported an anti-microbial potency of ITCs against bacteria (Borges et al., 2014; Freitas et al., 2013; Kaiser et al., 2017; Ko et al., 2016; Kurepina et al., 2013; Lin et al., 2000) as well as fungi (Drobnica et al., 1967; Kurepina et al., 2013; Manyes et al., 2015). These studies strongly suggest the potential use of ITCs as natural antibiotic agents, natural additives in foods and/or natural pesticides. Many mechanisms have been reported to contribute to their anti-microbial properties including i) disruption of cell membrane, ii) deregulation of regulatory, respiratory and enzymatic processes and iii) induction of heat shock proteins and oxidative stress (Dufour et al., 2015). The potency of ITCs against pathogens seem to depend on their chemical structure (e.g. presence of sulfinyl group, length of the side chain, lipophilic and electrophilic activities, etc.) as well as the bacterial strains since some of them appear to be more resistant than others (Dias et al., 2014; Wilson et al., 2013).

1.3.2 Anti-oxidant activity

This is another important function of ITCs which has been extensively reviewed. They have been shown to directly interact and modulate the activity of various anti-oxidant enzymes in addition to acting indirectly through activation of the nuclear factor erythroid-derived 2-like 2 (*Nrf2*) pathway. More specifically, exposure to ITCs induces the activation of *Nrf2* which is then conjugated with the Kelch-like ECH-associated protein 1 (*Keap1*). This is orchestrated in a series of events where ITCs first interact with the sulfhydryl residues of *Keap 1* and then *Nrf2* is released into the cytoplasm followed by transfer to the nucleus. In there, *Nrf2* induces the transcription of phase II detoxifying enzymes [e.g. glutathione S-transferases (GSTs), *NAD(P)H* quinine oxidoreductase 1 (*NQO-1*), heme oxygenase 1 (*HO-1*), glutamate cysteine ligase (*GCL*) and gamma glutamylcysteine synthetase (*γGCS*)] by binding to the antioxidant response element (ARE) on their promoters (Fuentes et al., 2015; de Figueiredo et al., 2015). ITCs can also increase *Nrf2* activity indirectly through the induction of other signalling cascades that mediate *Nrf2* phosphorylation thereby inducing ARE transcriptional activity (Cheung & Kong, 2010). Several pathways have been shown to mediate ITC-induced activation of *Nrf2* including extracellular-signal-regulated kinase (*ERK*), c-Jun N-terminal kinase (*JNK*) and Protein kinase B (*PKB*, also known as *Akt*) in various cancer cells (Cheung & Kong, 2010; Ernst et al., 2011; Jakubíková et al., 2005; Xu

et al., 2006). The significant role of the *Nrf2* factor in contributing to the overall ITC antioxidant capacity is demonstrated in the McWalter study where treatment with ITCs enhanced the activation of detoxifying enzymes in wild type mice and murine cell lines but not in *Nrf2* deficient ones (McWalter et al., 2004). In line to these observations, elevated levels of antioxidants and metabolizing enzymes was reported to be mediated by *Nrf2* activity in HePG2 cells as well after exposure to Wasabi-derived SFN and SFN analogues (Trio et al., 2017).

On another note, it should be mentioned that although transient and regulated activation of Nrf2 can exert a protective effect, in healthy individuals, constitutive activation of the pathway could be detrimental in fully-developed cancers (Catanzaro et al., 2017). Ectopic expression of the *Nrf2* pathway could be potentially of an advantage to cancer cells. Persistent *Nrf2* activity can create an environment that promotes cell growth and survival and also can impair the metabolic processes of some anti-cancer drugs thus leading to chemo-resistance (Furfaro et al., 2016; Jaramillo & Zhang, 2013; No et al., 2014).

1.3.3 Anti-inflammatory activity

As far as the anti-inflammatory properties of ITCs are concerned, they were thought to be mainly mediated by the down-regulation of the nuclear factor-kappa B (*NF-κB*) pathway which, in turn, regulates the expression of pro-inflammatory factors [e.g. cyclooxygenase 2 (*COX-2*) and inducible nitric oxide synthase (*iNOS*)] as well as anti-apoptotic proteins (e.g. *Bcl-Xl, Bcl-2, Bcl-3*) (Del Prete et al., 2011; Shan et al., 2012; Surh & Na, 2008). Briefly, *NF-κB* activation is triggered by various pro-inflammatory stimuli such as cytokines, growth factors and DNA-damaging agents resulting in the inactivation of I-κB through regulation of kinases and phosphatases upstream of the pathway (Lin-Feng & Greene, 2004). Once *NF-κB* is free, it translocates to the nucleus and binds in the promoter of target genes thereby inducing their transcription (Ghosh & Karin, 2002; Surh & Na, 2008). It has been shown that ITCs can inhibit the phosphorylation of IκBα and IκB kinases which remain in complex with *NF-κB* thus deterring its transfer to the nucleus. The inhibitory effect of ITCs in *NF-κB* expression is also associated with the induction of various signalling cascades. For instance, exposure of endothelial cells to SFN i) down-regulates the toll-like receptor (TLR)-4 signalling pathway by affecting downstream effectors such as p38 mitogen-activated protein kinase (*MAPK*) and *JNK* and ii) suppresses *NF-κB*-mediated expression of adhesion molecules to prevent inflammatory insult to endothelial cells (Shan et al., 2012). It has been also proposed that ITCs can inhibit the inflammatory process through the *Nrf2* signalling

pathway which has been shown to interact with the *NF-κB* signalling pathway (although the exact mechanism is not yet fully understood) (Cuadrado et al., 2014; Li et al., 2016; Li et al., 2008). Recently, studies proposed the involvement of the epigenome (Qu et al., 2015; Yang et al., 2016) and the macrophage migration inhibitory factor (MIF) pathway (Crichlow et al., 2012; Spencer et al., 2015), as novel targets of ITC-induced anti-inflammatory responses. MIF is a pro-inflammatory cytokine implicated in pro-tumorigenic, pro-angiogenic, and anti-apoptotic processes and thus it contributes in the development of various inflammatory diseases (e.g. rheumatoid arthritis and atherosclerosis) as well as in diverse stages of tumorigenesis, including proliferation and angiogenesis (Crichlow et al., 2012; Spencer et al., 2015; Tyndall et al., 2012). Finally, another novel anti-inflammatory role of ITC has been proposed recently. Specifically, SFN-treatment have been shown to inhibit the formation of multiple inflammasomes in an *Nrf2*-independent manner, suggesting that SFN can serve as an effective anti-inflammatory factor against inflammasome-originated diseases (Greaney et al., 2016).

1.4 ITCs in Cancer: Chemo-preventive Properties

ITCs ability to act as chemo-preventive agents has been well-documented in a number of studies. More specifically, in various epidemiological studies have reported that a diet rich in cruciferous vegetables can gradually decrease the risk of tumour development (Ambrosone et al., 2004; Cohen et al., 2000; Jain et al., 1999; Romagnolo & Selmin, 2012; Tang et al., 2010; J. Wang et al., 2014; Yang et al., 2010). However, contradicting data have emerged over the last years, with studies supporting a weak correlation between cruciferous vegetable consumption and cancer risk (Fowke et al., 2011; Wu et al., 2014). To this end, low consumption of cruciferous vegetables was not significantly associated with lung cancer susceptibility among smoking women (209 incident lung cancer cases and 787 individually matched non-smoking controls), although a meta-analysis reported a correlation between urinary levels of ITCs, *GSTM1* genotype, and risk for lung cancer (Fowke et al., 2011). Although, these observations are ambiguous, most of the scientific outcomes strongly support an inverse relationship between intake of ITCs (through dietary consumption of cruciferous vegetables) and the overall susceptibility to cancer development.

Such a protective effect is considered to depend on an individual's genetic variation in GST genes coding for enzymes that catalyse the conjugation of ITCs, with GSH, a metabolic process crucial for the elimination of ITCs and the deactivation of xenobiotics (Brennan et al., 2005; Seow et al., 2002; Zhao et al., 2007). Thus, reduced activity of these enzymes

result in longer exposure of tissues to ITCs and in a significantly lower risk for disease development. For instance, individuals that acquired two null variants of the *GSTM1* and *GSTT1* alleles found to be more resistant against cancer development due to longer ITC exposure (Higdon et al., 2007; Seow et al., 2005; Zhao et al., 2001). In contrast to these observations, there are studies that currently support the correlation between GSTs-null polymorphism with an increased cancer risk (Cai et al., 2014; Yang et al., 2015; Zhao et al., 2015) while others suggest that there is no correlation between cancer susceptibility and GSTs polymorphisms (Tan et al., 2013; Vogtmann et al., 2014). It is obvious that the influence of GST genotype on cancer susceptibility is still not well defined, due to many contradictory and inconsistent data in this field of research.

1.5 ITCs in Cancer Therapy: Anti-cancer Activities

A number of *in vitro* and *in vivo* studies have documented the ability of ITCs to act as anti-tumorigenic agents in various cancer types, including breast (Jensen et al., 2019; Pledgie-Tracy et al., 2007; Xiao et al., 2008; Xiao et al., 2006; Xie et al., 2017), prostate (Cho et al., 2016; Khurana et al., 2017; Zhang et al., 2016), brain glioblastoma (Chou et al., 2015), colon (Liu et al., 2017; Pappa et al., 2006) and skin (Abel et al., 2013; Kerr et al., 2018; Mantso et al., 2016). The potential of these compounds to act as cytotoxic agents is attributed to a wide range of mechanisms including i) modulations of phase I and phase II detoxifying enzymes, ii) suppression of cell growth via induction of cell cycle arrest and cell death, iii) repression of metastatic and angiogenetic processes and iv) modifications of the epigenetic mechanisms. The overall proposed mechanism of ITC-induced cytotoxicity is summarized in Fig. 1.10.

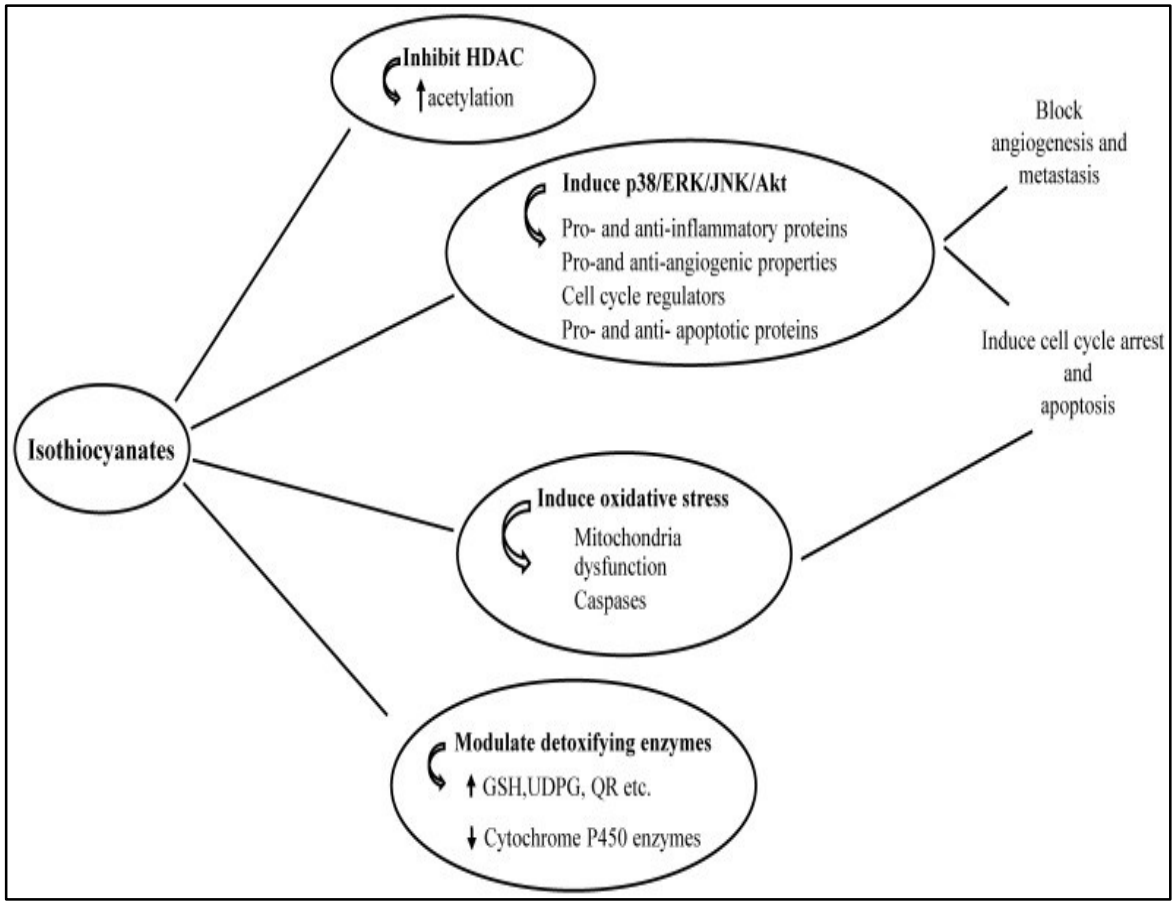

Figure 1.10: Cellular pathways targeted by ITCs. The effect of ITCs in cell proliferation and survival is mediated via modulation of multiple pathways, including various signaling transduction cascades (e.g. PI3K/AKT, MAPKKs, etc.), increased oxidative stress (ROS) and enhanced mitochondrial dysfunction, resulting in modulation of phase I and II enzymatic activity, induction of growth arrest and apoptosis, inhibition of metastatic processes and impaired activity of the epigenetic machinery. Adapted from (Mitsiogianni et al., 2019)

1.5.1 Inhibition of Phase I and Induction of Phase II Enzymes

Phase I and II enzymes are essential regulators of the xenobiotic-metabolizing system by interacting with numerous chemicals such as toxins, xenobiotics and carcinogens and thus mediate their metabolism and excretion from the body. Phase I enzymes [which belong to the cytochrome P450 (CYP450) family] are enzymes that either promote the deactivation or in some cases the activation of pro-carcinogens, to their active form. On the other hand, phase II enzymes (e.g. glutathione S-transferases, GSTs, *UDP*-glucuronosyl transferase, *NADPH* quinine reductases and glutamate cysteine ligase) exert a predominantly protective role by interacting with carcinogens thereby influencing their solubility and elimination from the body. Thus, ITCs have been shown to interact with both phase I and II enzymes to

modulate carcinogen metabolism. In general, these compounds decrease phase I enzymes, to prevent the activation of carcinogens, while upregulate phase II enzymes in order to increase the detoxification process and inhibit ROS-induced damage (Keum et al., 2004; Talalay & Fahey, 2001).

The effect of ITCs (mainly SFN, AITC, BITC, PEITC and IBN) in the activity levels of the detoxifying enzymes has been reported in a range of cancers, including acute myeloid leukaemia (Gao et al., 2010), bladder (Munday, 2002), breast (Wang et al., 2005), liver (Basten et al., 2002) and skin (Dinkova-Kostova et al., 2006). The Nrf2 pathway, as already mentioned above, is a key mediator of the ITC-triggered detoxification process including phase II detoxifying enzymes (Boddupalli et al., 2012; Hu et al., 2006). For example, SFN has been shown to deactivate *CYP2B*, *CYP3A2* and *CYP1A2* as well as triggering the expression of quinone and glutathione reductase phase II enzymes in rats (Yoxall et al., 2005). PEITC also found to decrease nicotinamide N-methyltransferase (NNMT) levels in rats by increasing the *UDP*-glucuronosyltransferase *UGT1A6* expression and modulating *CYP2B15* activity (Telang & Morris, 2010). In another study, both BITC and PEITC prevented the metabolic process of nicotine and tobacco-specific nitrosamine 4-(methylnitrosamino)-1-(3-pyridyl)-1-butanone (NNK) through a *NADPH*-dependent inhibition of *CYP2A6* and *CYP2A13* activation, respectively (von Weymarn et al., 2006). In addition, SFN enhanced the activation of several GSTs (A3, A4, M1, P1 and T1) involved in the inactivation of aflatoxin B1-8,9-epoxide (AFBO) in murine AML 12 cells (Gao et al., 2010). In line with these observations, treatment of lung adenocarcinoma (A549) cells and primary normal human bronchial epithelial (NHBE) cells with both broccoli sprout extracts as well as SFN, BITC and PEITC, upregulated *GSTP1* (Glutathione S-transferase P) and *NQO1* (*NAD(P)H* dehydrogenase [quinone] 1) enzymes (Tan et al., 2010).

1.5.2 Cell Cycle Arrest and Apoptotic Induction

It is now well-established from both *in vivo* (Bhattacharya et al., 2010; Boreddy et al., 2011; Cho et al., 2016; Srivastava et al., 2003) and *in vitro* (Chen et al., 2012; Cheng et al., 2016; Parnaud et al., 2004; Stan et al., 2014; Tsai et al., 2012; Xiao et al., 2006) studies that ITC-induced cytotoxicity is mediated by cell cycle growth arrest and apoptotic induction.

Generally, ITCs have been reported to perturb the cell cycle by modulating the expression levels of various molecules that regulate its progression (Chen et al., 2012; Cheng et al., 2016; Fimognari et al., 2004; Herman-Antosiewicz et al., 2007; Jun-Hee et al., 2009; Matsui et al., 2007; Parnaud et al., 2004). Briefly, the cell cycle is composed of four distinct phases,

namely G1, S, G2 and M. There is also a resting phase (G0) where cells progress from rest to proliferation and back to G0 phase. Cellular progression from one phase to the next is very organized, in a series of steps, and highly controlled by the so-called cell cycle regulators [e.g. cyclins, cyclin-dependent kinases (CDKs) and CDK inhibitors (such as *p21* and *p27*)] most of which have been shown to be deregulated in cancer (Diaz-Moralli et al., 2013; Otto & Sicinski, 2017). In this respect, ITCs can inhibit cell cycle progression by modulating the activity of cell cycle regulators. More specifically, treatment of human colon carcinoma (HT29) cells with SFN increased the number of cells arrested in the G2/M phase by activating *p21* and *cdc2* kinases (Parnaud et al., 2004). Furthermore, human cervical cancer cells were also growth arrested at the G2/M phase, under SFN exposure, an effect associated with inhibition of *Cyclin B1* and disruption of *cyclin B1/CDC2* conjugate (Cheng et al., 2016). In addition, SFN induced cell cycle arrest (at G0/G1 phase) and apoptosis in T24 bladder cancer cells through enhanced expression of the CDK inhibitor *p27* (Shan et al., 2006). In another study, PEITC modulated the activities of *p53*, *p21*, *p17*, *CDK2* and *cyclin E* leading to growth inhibition of the human oral carcinoma (HSC-3) cells at the G0/G1 phase (Chen et al., 2012). Moreover, AITC and BITC have also been shown to increase the accumulation of cells at the G2/M phase by modulating the expression of various regulatory proteins (e.g. *Cyclin B1*, *Cdk1*, *Cdc25B* and *p21*), important in cell cycle progression, using human prostate (Xiao et al., 2003), pancreatic (Zhang et al., 2006) and leukemic cancer cell lines (Miyoshi et al., 2004). Finally, deregulation of cell cycle progression has been proposed to gradually result in the induction of apoptosis (Parnaud et al., 2004).

The role of ITCs in apoptotic induction has been extensively studied and reported (Mi et al., 2011; Rudolf et al., 2009; Wu et al., 2009). Apoptosis is a genetically programmed cell death and the whole process is complex and regulated by various proteins including, but not limited to, several caspases, proteins that belong to the B cell lymphoma 2-family (*Bcl2*) and the tumour-related *p53* gene. Deregulation of apoptosis results in cancer survival and thus, molecules that can modulate specific targets in critical cellular pathways are considered as promising therapeutic agents (Fernald & Kurokawa, 2013; Zörnig et al., 2001). In this context, modifications in the activity of pro-apoptotic (e.g. *Bax*, *Bid* and *Bak*) and anti-apoptotic (e.g. *Bcl2* and *Bcl-XL*) agents as well as several caspases have been implicated in ITC-mediated cell death. In a characteristic study, exposure of human pancreatic cancer cells to PEITC upregulated *Bak* expression, while downregulated expression of *Bcl2* and *Bcl-XL*, thus promoting apoptosis (Stan et al., 2014). In addition, treatment of Jurkat T-leukemia cells with SFN induced apoptosis by increasing *Bax* and *p53* expression levels (Fimognari

et al., 2002). Moreover, AITC-induced apoptosis of human renal carcinoma cells was also accompanied with increased levels of *Bax* and reduced levels of *Bcl2* (Jiang et al., 2016). Finally, in another study, treatment of human cervical cancer (HeLa) cells with PEITC and other structurally related ITCs triggered caspase-3 dependent apoptosis (Yu et al., 1998).

On another note, ITC-induced anti-proliferative effect is attributed to various regulatory cascades, including several signalling transduction pathways (e.g. PI3K/AKT, MAPKKs, c-jun and mTOR) (Cheung et al., 2008; Mondal et al., 2016; Tsai et al., 2012; Xu et al., 2006), increased reactive oxygen species (ROS) production (de Oliveira et al., 2014; Lee & Lee, 2011; Wu et al., 2011), inhibition of heat-shock proteins (Sarkar et al., 2012) and mitochondrial dysfunction (Chen et al., 2012; Rudolf et al., 2009; Sehrawat et al., 2016). Characteristic examples are those of AITC and BITC both of which were found to induce an oxidative response as well as induction of the *ERK* signalling pathway thus activating the intrinsic apoptotic pathway, accumulation at the G2/M phase, induction of mitochondrial depolarization and deregulation of mitochondrial-associated proteins in human breast adenocarcinoma cells (Tsai et al., 2012; Xiao et al., 2006). In favour to these observations, PEITC inhibited oral squamous carcinoma growth by causing cell cycle inhibition and apoptosis through stimulation of the mitochondria-dependent pathway, ROS production and calcium (Ca^{2+}) accumulation (Chen et al., 2012). Finally, studies have also shown the implication of the epigenetic machinery in ITC-induced cytotoxicity (Ma et al., 2006; Myzak et al., 2005; Myzak et al., 2004; Rajendran et al., 2011).

1.5.3 Autophagy

This is an important process for cell homeostasis, by which cells remove defective and redundant cellular components. In general, at "housekeeping levels", the induction of autophagy promotes cell survival and maintenance. However, under conditions such as reduced apoptosis and/or increased levels of autophagy, the autophagic machinery can also induce cell death either through self-cannibalization or by promoting apoptosis (Levine, 2007; Parzych & Klionsky, 2014). In carcinogenesis, it acts either as a tumour suppressor mechanism, by scavenging mutated proteins and faulty organelles, or as a mechanism that favours cancer cell survival and proliferation (Amaravadi et al., 2016; White, 2012). Alternatively, ectopic autophagic activation in cancer cells could act as a pro-death signal and/or activate T cell-dependent immune responses to inhibit cancer cell growth. It is obvious that autophagy implication in malignancy is complicated and ambiguous (Pietrocola et al., 2016; Yang et al., 2011). The notion that ITCs can act as autophagic inducers is a

rather new idea. Evidence currently supports this notion, however this autophagic induction seems to be controversial by having either a protective role (Chen et al., 2018; Hee Kim et al., 2016; Herman-Antosiewicz et al., 2006; Horwacik et al., 2015; Lee & Lee, 2017; Lin et al., 2012; Lin et al., 2017; Pawlik et al., 2017; Wang et al., 2018; Zhang et al., 2017) or promoting cell death (Bommareddy et al., 2009; Liu et al., 2018; Milczarek et al., 2018; Xiao et al., 2012; Yang et al., 2018), depending on tumour type, stage and genetic context. For instance, exposure of human lung cancer cells to BITC resulted in endoplasmatic reticulum (ER) stress-mediated induction of autophagy which was shown to have a protective effect against BITC-induced inhibition of cell growth. The suppressive effect of BITC in cell growth was increased when cells were pre-treated with an inhibitor of the autophagic process, strongly supporting the cyto-protective role of the autophagic activation (Zhang et al., 2017). In contrast, in human prostate cancer cells, PEITC promoted cell death through Atg5-induced activation of autophagy and apoptosis (Bommareddy et al., 2009).

1.5.4 Anti-metastatic and Anti-angiogenic Properties

ITCs also protect against cancer progression by supressing angiogenic and metastatic processes. New capillary formation is critical for cancer progression by promoting tumour growth, invasion and metastasis, supporting the high demands of tumours for oxygen and nutrients (Moserle & Casanovas, 2013). Metastasis, it is a complex process mainly regulated by genes essential in modifying the interplay between cells and extracellular matrix (Rudek et al., 2002). In this respect, ITCs were shown to modulate various agents implicated in metastasis and angiogenesis, including metalloproteinases (MMPs), plasminogen activators (PAs) and vascular endothelial growth factor (*VEGF*) (Boreddy, Sahu, et al., 2011; Gupta et al., 2013; Jackson et al., 2007; Kim et al., 2015; Thejass & Kuttan, 2007a; Wang et al., 2015; Zhu et al., 2014). To these ends, AITC and PITC diminished various pro-inflammatory cytokines [e.g. interleukin (*IL*)-*1β*, *IL-6*, tumour necrosis factor (TNF)-alpha] and *VEGF* while upregulated the tissue inhibitor of metalloproteinases (TIMP) in human umbilical vein endothelial (HUVECs) cells thus preventing tube formation, invasion and migration (Thejass & Kuttan, 2007a). Similarly, PEITC inhibited *VEGF* and prevented new vascularization *in vitro* (e.g. HUVECs and PC3 prostate cancer cells) and *ex vivo* (Xiao & Singh, 2007). BITC also effectively suppressed the formation of new capillaries and invasion of human glioma cells through inhibition of *MMPs-2* and *-9* and *VE*-cadherin while growth arrested cells at the G2/M phase via modulation of molecules that are involved in cell cycle progression (Zhu et al., 2014).

The anti-angiogenic and anti-metastatic capacity of ITCs have been also associated with modulation in the activity of major signalling pathways (e.g. *PI3K/Akt*, *p38/MAPK*, *NF-κB*, and *mTOR*) (Boreddy, Sahu, et al., 2011; Gupta et al., 2013; Lai et al., 2010; Lai et al., 2014; Milkiewicz et al., 2011; Wang et al., 2015; Xu et al., 2005). For example, exposure of human colon cancer cells to AITC (Lai et al., 2014) and BITC (Lai et al., 2010) inhibited cell growth and altered cell metastatic potential *via* reduction of matrix metalloproteinases (mainly MMP-2 and MMP-9), mediated by *PKC* and *MAPK* signalling pathways. In addition, post-translational modifications were shown to be involved in the anti-angiogenic effect of ITCs. Specifically, BITC, SFN and PEITC were shown to modulate the expression pattern of tumour suppressor (miR144, miR-122, miR-194) and oncogenic mi-RNAs (miR-181b, miR-9, miR-616-5p) thus inhibiting the formation of new capillaries as well as the invasion potential of human glioma (Zhu et al., 2014), non-small cell lung cancer (NSCLC) (Wang et al., 2017) and prostate cancer (Zhang et al., 2016) cells.

1.5.5 Epigenetic Modulation

ITCs can also exert their anti-tumorigenic activities by interfering with various components of the epigenetic network, including HDACs, DNMTs and mi-RNAs (Navarro et al., 2011).

In general, HDACs are associated with gene transcriptional silencing but ITCs have been identified as potent inhibitors of this family of enzymes. HDAC inhibitors are considered to be promising therapeutic agents against malignant transformation by inhibiting cancer cell growth, progression and invasion (Eckschlager et al., 2017; Ho et al., 2009). In particular ITCs, have been reported to inhibit HDAC activity and thus induce *Nrf2*-mediated activation of phase II detoxifying enzymes, cell cycle repression and apoptosis as well as modulate the angiogenic and metastatic potential (Batra et al., 2010; Rajendran et al., 2013; Su et al., 2014; Wang et al., 2008; Yuanfeng et al., 2015). More specifically, SFN found to act as efficient HDAC inhibitor and diminished the expression of specific HDACs, triggering growth arrest and apoptotic death in multiple cancer cell lines including those of murine melanoma, human glioma (Yuanfeng et al., 2015), prostate (Myzak et al., 2005), colon (Rajendran et al., 2013), lung (Jiang et al., 2016) and bladder (Abbaoui et al., 2017) origin. In particular, PEITC inhibited cell cycle progression of prostate cancer cells by increasing acetylation of H3 which was associated with increased expression of *p21* (Wang et al., 2008). In addition, BITC also reduced HDAC1/HDAC3 activity thus resulting in deactivation of NF-kB and cyclin D1 as well as growth inhibition (Batra et al., 2010). Finally, SFN showed to decrease prostate (Myzak et al., 2007) and bladder (Abbaoui et al., 2017) cancer cell proliferation by

blocking HDAC activation *in vivo*. Diminished activity of HDACs was also reported in the peripheral blood mononuclear cells of healthy individuals after broccoli sprouts consumption (at a single dose of 68g, approximately 105mg of SFN and equivalent to about 570g of mature broccoli) (Myzak et al., 2007).

Similarly, ITCs have been documented to modulate DNMT expression pattern thus leading to aberrant expression of genes important in malignant transformation (Kaufman-Szymczyk et al., 2015). In particular, ITCs have been demonstrated to exert an inhibitory effect on DNMTs (Hsu et al., 2011; Wong et al., 2014) usually accompanied with repression of histone deacetylation (Jiang et al., 2010; Kaufman-Szymczyk et al., 2015; Meeran et al., 2012; Meeran et al., 2010; Su et al., 2014; Zhang et al., 2013). To this end, it has been demonstrated that SFN-mediated impairment of DNMT1 activation was associated with HDAC inhibition leading to reduced histone deacetylation and re-activation of *p21* (Kaufman-Szymczyk et al., 2015). In line to these observations, human breast cancer cells exposed to SFN, induced apoptosis through reduction of DNMTs 1 and 3a expression and HDAC activity. Decreased levels of DNA methylation and histone deacetylation in these SFN-treated cells suppressed the induction of the human telomerase reverse transcriptase (hTERT), a gene commonly found up-regulated in various cancers (Meeran et al., 2010). Similar observations made in estrogen receptor (ER)-negative breast cancer cells treated with SFN, suggesting it's potential use as a therapeutic factor for the better management of ER-negative breast cancer patients (Meeran et al., 2012). Moreover, PEITC altered the activity of DNMTs and HDACs, in prostate cancer cells, influencing the reactivation of the tumour suppressor *RASSF1A* (Ras-association domain family 1 isoform A) and apoptotic induction (Boyanapalli et al., 2016).

Another significant aspect of ITCs interaction with the epigenome is their modulatory effect on specific miRNAs involved in cancer development and invasiveness. This is evident in a wide range of malignancies, including prostate (Xiao et al., 2012; Yu et al., 2013; Zhang et al., 2016), colon (Slaby et al., 2013), bladder (Shan et al., 2013) and glioblastoma (Lan et al., 2015). For instance, SFN and IBN upregulated the levels of tumour suppressors mir-23b, mir-27b while downregulated mir-155 in epithelial colon cell lines suggesting that miRNAs could be involved in the protective effect of ITCs (Slaby et al., 2013). SFN also found to inhibit tumour progression and migration of non-small cell lung cancer cells through down-regulation of mir-616-5p (Wang et al., 2017). In another study, prostate cancer cells under PEITC treatment, overexpressed mir-194 leading to decreased expression of MMPs thereby

blocking cellular invasion (Zhang et al., 2016). Finally, SFN also found to increase the expression of mir-200c, in human bladder cancer cells, which is then partly implicated in the inhibition of epithelial-to-mesenchymal transition (EMT) and of *COX-2* and *MMPs 2, 9* gene expression all of which are important for cellular migration (Shan et al., 2013).

1.6 Skin Cancer and ITCs: The Case of Melanoma

Skin cancer is considered as one of the most common types of cancer worldwide (Diepgen & Mahler, 2002; Nguyen & Ho, 2002). Its incidence is increasing rapidly over the years and its clinical picture generally appears as precancerous that over time can become malignant (Gordon, 2013).

The disease refers to three main types namely i) basal-cell skin cancer (BCC), ii) squamous-cell skin cancer (SCC) and iii) melanoma (Erb et al., 2008). Among them, BCC and SCC are generally known as non-melanoma skin cancers (NMSCs) and are the most common ones, with BCC accounting for about 80% of skin cancer incidence (Baxter et al., 2012; Madan et al., 2010). The classification in one of these types depends on the cells that are primarily affected. In particular, BCC is originated from keratinocytes of the basal layer or the hair follicles, SCC from keratinocytes at the top layer of epidermis, while melanoma originates from melanocytes, the cells known to produce melanin (Erb et al., 2008). In general, NMSCs (especially those diagnosed at an early stage) have a better prognosis, in contrast to malignant melanoma, which is a more aggressive and lethal type of cancer (Gordon, 2013).

1.6.1 Skin Cancer Aetiology and Pathophysiology

Skin cancer occurrence is multifactorial, including innate predisposition and inheritable traits (e.g. fair skin, sun sensitivity, red hair, freckles, presence of multiple naevi), environmental agents (e.g. exposure to UV radiation and/or chemical carcinogens such as tobacco) and geographical with white populations being at higher risk (Chang et al., 2010; Diepgen & Mahler, 2002; Martin-Gorgojo et al., 2017; Moan et al., 2015; Narayanan et al., 2010; Ting et al., 2007). In addition, various medical conditions (e.g. immunosuppression, chronic ulcers, human papillomavirus infection and genetic syndromes such as xeroderma pigmentosum, albinism, epidermodysplasia) are all considered risk factors (Devine et al., 2017; Diepgen & Mahler, 2002).

Among all these risk factors, UVR (Ultraviolet radiation) is considered to be the main cause of skin cancer occurrence (Pfeifer & Besaratinia, 2012). In general, UV light photons, that reach the double helix of DNA, contribute to genomic instability by causing DNA damage

in the skin cells and consequently the accumulation of mutations in genes important for skin homeostasis. In particular, UV radiation directly affects DNA by influencing cytosines to thymines or CC to TT substitutions. This mutational pattern is also known as "UV signature mutations" and it is frequently observed in skin cancer patients (Goto et al., 2015; Kim et al., 2013; Wikonkal & Brash, 1999). In addition, the UVA spectrum has also an indirect effect on the DNA sequence by causing photo-oxidative damage in bases, especially guanines leading to the formation of 8-oxo-7,8-dihydro-2′-deoxyguanosine (8-oxo-dG) adducts (Madan et al., 2010; Pfeifer & Besaratinia, 2012; Rünger, 2008; Sage et al., 2012; Seebode et al., 2016). UV-associated lesions result in the deregulation of genes involved in pathways important for cell growth and survival, such as the tumour suppressor *p53*, the Hedgehog pathway related protein patched homolog 1 (*PTCH1)* gene and the cyclin-dependent kinase inhibitor (*CDKN2*) (Brash, 2015; Freije et al., 2014; Luo et al., 2001). In addition, UVR is a potent modulator of skin immune responses (Schwarz et al., 2010; Welsh et al., 2011; Yu et al., 2014) and also strongly contributes to immunosuppression through induction of pro-inflammatory immunosuppressive cytokines (such as IL-10 and TNF-a) (Kanavy & Gerstenblith, 2011; Norval & Halliday, 2011). Subsequently, it causes further damage to the cells, genomic instability and suppression of repair pathways (Halliday, 2005; Meeran et al., 2008).

A number of genes and pathways have been shown to be deregulated in skin cancer thus potentially serving as important etiological, prognostic and therapeutic markers (Bosserhoff, 2006; Greinert, 2009; Hocker et al., 2008). For instance, aberrant activation of the sonic hedgehog signalling pathway has been associated with BCC occurrence (Athar et al., 2014) while SCC incidence is attributed mainly to the deregulation of *p53*-mediated pathways (Emmert et al., 2014) as well as to mutations in *RAS* and $p^{16INK4a}$ genes, although at a lower frequency (Emmert et al., 2014; Xie, 2008). Moreover, mutations in particular genes (e.g. *BRAF*, *NRAS*, *PTEN*) involved in cell cycle progression and apoptosis as well as deregulation of various signalling pathways (e.g. *p38/JNK/ERK/MAPK*, *PI3Kinase/Akt/mTOR*, *β*-catenin and *WNT*) account for the increased survival and proliferation of melanoma cells (Dahl & Guldberg, 2007; Hocker et al., 2008; Ko & Fisher, 2011; Shtivelman et al., 2014). Among them, the *RAS-ERK* pathway is of particular importance, as specific mutations on the *BRAF* gene (i.e. the*V600E* one) are the most common lesions observed in melanoma patients (Shtivelman et al., 2014). Finally, epigenetic abnormalities also contribute to skin carcinogenesis, with most studies being focused on their involvement in melanoma pathogenesis (Penta et al., 2018; Sigalotti et al., 2010).

1.6.2 Skin Cancer Epigenetics

Genome-wide hypo-methylation together with hyper-methylation of tumour suppressor genes have been associated with the onset and progression of skin cancer (Greenberg et al., 2014; Kamalika Saha et al., 2013). A number of tumour suppressor genes (e.g.*MLT-1* (Mucosa-associated lymphoid tissue lymphoma translocation protein 1), Snail (Zinc finger protein SNAI1), *MGMT* (O-6-methylguanine-DNA methyltransferase)], adhesion molecules like (*E*-Cadherin) (Fraga et al., 2004; Murao et al., 2006; J. Wu et al., 2014) and cell cycle regulators ($p16^{INK4a}$ and $p14^{ARF}$) (Brown et al., 2004; D'Arcangelo et al., 2017; J. Wu et al., 2014) have been found to be silenced due to extensive methylation on their promoters, thereby associated with early and advanced stages of both BCCs and SCCs. In addition, an increase in the activity of DNMTs has also been reported to accompany the increased methylation levels observed in NMSCs compared to normal skin (Nandakumar et al., 2011). In addition, in melanoma, promoter-hyper-methylation appears to be the mechanism of suppression for various critical genes including the *WNT* inhibitory factor 1 (*WIF1*), tissue factor pathway inhibitor 2 (*TFPI2*), ras association domain family 1 isoform A (*RASSF1A*), suppressor of cytokine signaling 1 (*SOCS1*) (Tanemura et al., 2009), O^6-methylguanine DNA methyltransferase (*MGMT*) (Kohonen-Corish et al., 2006), transcriptional activator estrogen receptor a (*ER-a*) (Mori et al., 2006) and *CDKN2A* (Straume et al., 2002). The latter, in particular, is associated with melanoma progression and poor prognosis of the disease as it is found to be hyper-methylated in 19% of melanoma patients (Straume et al., 2002). Excessive loss of methylation is also observed in skin carcinogenesis including melanoma (Schinke et al., 2010). Overexpression of the melanoma antigen, *MAGE*, is a typical example of hypo-methylation-induced activation of genes which is associated with down-regulation of *DNMT1* (Loriot et al., 2006; Tellez et al., 2009).

On the other hand, genome-wide hypo-acetylation is generally observed in melanoma resulting in silencing of tumour-associated gene expression (Sarkar et al., 2015; van den Hurk et al., 2012). Abnormal activation of HAT and HDAC enzymes, during melanogenesis, contribute to the down-regulation of pro-apoptotic proteins (e.g. *Bax*, *Bak*, *Bim*, caspases 8/9, *TNFRSF10A* and *TNFRSF10B*) as well as the up-regulation of anti-apoptotic proteins (e.g. *Bcl-2* and *Bcl-xl*) thereby favouring malignant cell survival (Penta et al., 2018; Sigalotti et al., 2010). Similarly, repression of the $p^{16\ INK4a}$ and *RASSF1A* tumour related genes in NMSC was mediated by reduced acetylation on H3 and H4 and the recruitment of chromatin remodelling proteins [e.g. methyl CpG binding protein 2 (*MeCP2*) and Methyl-CpG-binding domain protein 1 (*MBD1*)] (Nandakumar et al., 2011). In addition, in a skin cancer mouse

model, depletion of Sirt-2 deacetylase disturbed cell cycle through increased acetylation of Lys 16 on histone H4 (H4K16Ac) and PR-Set7 (Histone-lysine N-methyltransferase pr-set7) thus promoting malignant transformation (Serrano et al., 2013). In addition to histone acetylation, the methylation status of these proteins have also been implicated in malignant transformation. Recent evidence showed that enhanced expression of the Ezh2 (Enhancer of zeste homolog 2**)** methyltransferase (Zingg et al., 2015) and decreased activity of the SWItch/Sucrose Non-Fermentable (*SWI/SNF*) chromatin remodelling complex (Becker et al., 2009) enhance the metastatic potential of the disease.

mi-RNAs are also involved in skin tumorigenesis. Aberrant expression levels of Drosha and Dicer, the two main enzymes, involved in the mi-RNA maturation process in patients with NMSC reflect their importance in skin cell malignant transformation (Sand et al., 2010). Various mi-RNAs important in cell proliferation and other cellular processes including hedgehog, *MAPK/ERK, PI3K-Akt, WNT* and beta-catenin signalling cascades were found to be deregulated in skin tumours (Konicke et al., 2018; Sand et al., 2012). Among them, the oncogenic mir-21 [which supresses Phosphatase and tensin homolog (*PTEN*) and Programmed cell death protein 4 (*PCDC4*] tumour-suppressor genes and modulate the activity of *PI3K/AKT/mTOR* pathway, were shown to be upregulated in both BCC (Heffelfinger et al., 2012) and SCC (Darido et al., 2011). In addition, in a mi-RNA expression profile analysis study, apart from mir-21, other mi-RNAs were found to be deregulated in BCC including the let-7 family, mir-143, mir-182, mir-148a, mir-378 and mir-183. In particular, mir-183 is associated with disease invasiveness and metastatic potential while lower levels have been identified in infiltrative tumors (Heffelfinger et al., 2012). In SCC tumors, decreased expression of mir-124 and mir-214 was observed which was associated with increased activity of the *ERK* pathway resulting in aberrant cell proliferation, events associated with disease pathogenesis (Yamane et al., 2013). In addition, mir-199a-5p (that regulates cell adhesion and migration) is another mi-RNA with an aberrant expression in SCC tumours and furthermore associated with disease aggressiveness. (Kim et al., 2015; Wang et al., 2016). In addition, low levels of mir-200a (Bustos et al., 2017) and mir-375 (Mazar et al., 2011), result in increased malignant melanoma proliferation and migration. Moreover, high levels of mir-221 have been reported in melanoma patients, compared to healthy controls, resulting in cell cycle deregulation through repression of *c-Kit* and *p27* genes thereby favouring the malignant phenotype (Kanemaru et al., 2011). Many other mi-RNAs have been implicated in melanoma development, including mir-29c (T. Nguyen et al., 2011), mir-148 (Haflidadottir et al., 2010), mir-182 (Segura et al., 2009) and

mir-137 (Bemis et al., 2008) which regulate genes, like *MITF* (Microphthalmia-associated transcription factor), essential for melanoma cell proliferation and survival.

To conclude, taking into consideration the important role of the epigenetic machinery in skin carcinogenesis (summarized in Fig. 1.11) together with the fact that these modifications are reversible, it is understandable that the epigenetic components are promising targets for skin therapeutic interventions.

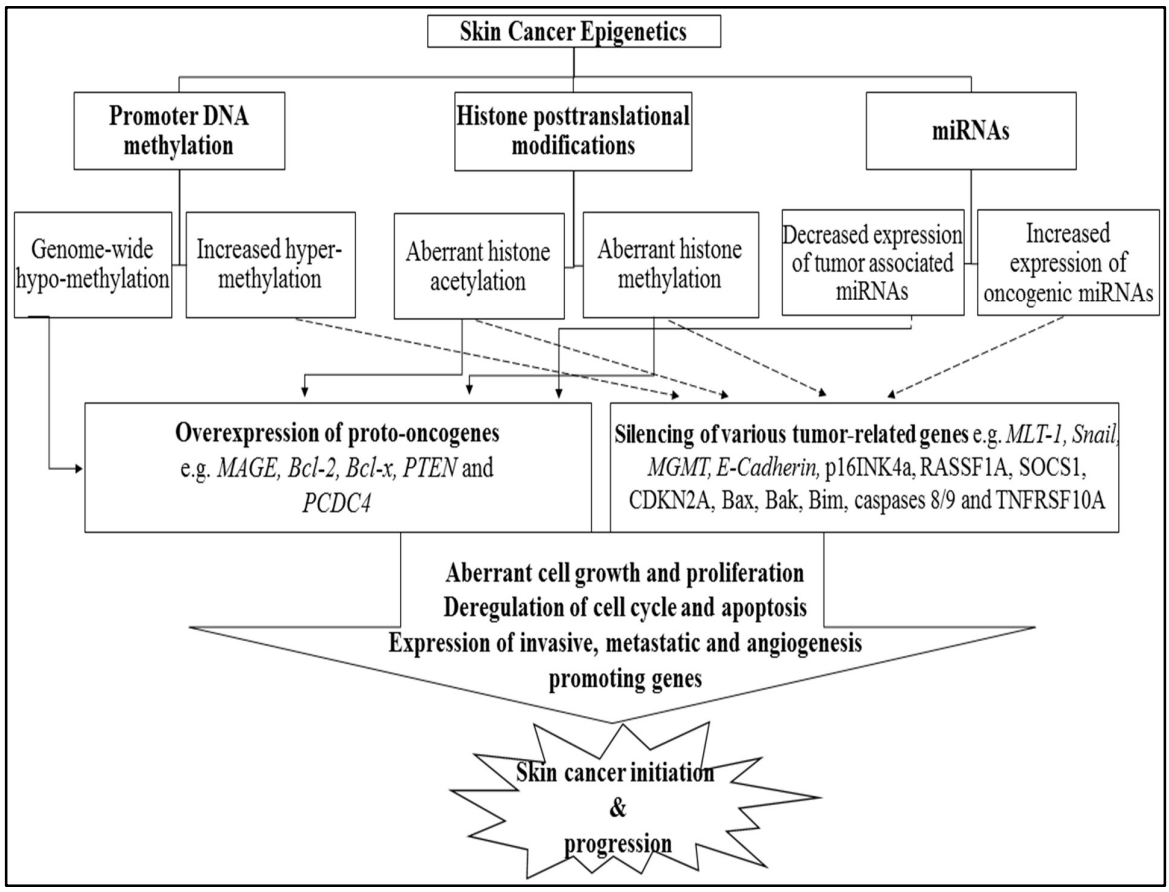

Figure 1.11: Epigenetic mechanisms involved in skin cancer carcinogenesis. A number of epigenetic mechanisms reported to be involved in skin carcinogenesis. In particular, genome-wide hypo-methylation as well as promoter hyper-methylation, have been associated with the onset and progression of skin cancer. Loss of methylation leads on the activation of various oncogenes (e.g. melanoma antigen, *Mage*) that promote tumour survival, while increased methylation on the promoter sites of various tumour suppressor genes [e.g.*MLT-1* (Mucosa-associated lymphoid tissue lymphoma translocation protein 1), Snail (Zinc finger protein SNAI1), adhesion molecules like (*E*-Cadherin), cell cycle regulators ($p16^{INK4a}$ and $p14^{ARF}$) etc.] is also usually reported in both melanoma and non-melanoma skin cancer, resulting in the downregulation of these genes. Moreover, abnormal

activation of histone acetylation as well as deacetylation enzymes, during skin tumorigenesis, also contribute to the deregulation of a number of genes important in malignant cell survival, such as pro-apoptotic proteins (e.g. *Bax*, *Bak*, *Bim*, caspases 8/9, *TNFRSF10A* and *TNFRSF10B*) as well as anti-apoptotic proteins (e.g. *Bcl-2* and *Bcl-xl*). Another important aspect in skin cancer epigenetics is the aberrant expression of various mi-RNAs that are important in cell proliferation and other cellular processes. All of these are usually found deregulated in skin tumours and thus gradually result in abnormalities of critical cell processes, including cell growth, proliferation, cell cycle, and apoptosis as well as metastatic processes that favour skin cancer cell survival.

1.6.3 ITCs in NMSC Chemoprevention and Therapy

Several lines of evidence support the protective role of ITCs against UV-induced (Dickinson et al., 2009; Dinkova-Kostova et al., 2010; Dinkova-Kostova et al., 2007; Dinkova-Kostova et al., 2006; Talalay et al., 2007) and chemically-induced (Gills et al., 2006; Xu et al., 2006) skin tumorigenesis, with the majority of them focusing on SFN. Topical treatment with SFN, on mouse skin, enhances the GSH biosynthetic process, increases GSH S-transferases (*GST4*) and protects against chemically-induced skin mutagenesis (Abel et al., 2013). Similarly, SFN blocked 12-O-tetradecanoylphorbol-13-acetate (TPA)-induced skin cancer progression in CD-1 mice by repressing TPA-mediated ornithine decarboxylase activity which is an obligatory step in TPA-induced promotion of carcinogenesis (Gills et al., 2006). The anti-photo-carcinogenic and anti-photoaging properties of 3-methoxybenzyl isothiocyanate (MBITC) have been recently documented in UVB-exposed 3D human skin reconstructed tissue where MBITC inhibited UVB-induced cell proliferation, MMPs expression, DNA damage and epidermal CPDs formation as well as prevented UVB-induced hyperplasia (Carpenter et al., 2018). In line with these observations, application of SFN (prior to irradiation) in the skin of BALB/c mice, exerted a protective effect against UVA-induced photo-aging, DNA oxidative and connective tissue damage via an *Nrf2*-dependent inhibition of *MMP-1* and *MAPK/AP-1* signaling cascades (Chaiprasongsuk et al., 2017). Moreover, SFN and PEITC induced the expression of cyto-protective proteins in HaCaT cells (Kleszczynski et al., 2013; Wagner et al., 2010) while pro-irradiation treatment (with these compounds) of an *ex vivo* human reconstituted skin tissue model diminished photo-oxidative damage and induced apoptosis through *Nrf2* activation (Kleszczynski et al., 2013). To this end, the importance of the *Nrf2* pathway in ITC-mediated protection against skin carcinogenesis is well-characterized in studies using *Nrf2* deficient mouse models. For instance, a recent study has shown that SFN exerted a protective effect against UV-induced

mutagenesis which was *Nrf2*-dependent(Saw et al., 2011). These results are in agreement with those of another study which has shown that the protective effect of SFN against 7,12-dimethylbenz(*a*)anthracene/12-O-tetradecanoylphorbol-13-acetate (DMBA)/(TPA)-induced skin tumorigenesis in C57BL/6 mice is also *Nrf2*-dependent (Xu et al., 2006). Activation of the *Nrf2* pathway, through epigenetic reprogramming, and the subsequent induction of target genes was also reported to be involved in SFN-mediated suppression of tumor transformation. Specifically, Nrf2 re-activation was attributed to promoter hypo-methylation through repression of DNMTs and HDACs activity. (Su et al., 2014). In addition, SFN has been shown to induce growth arrest and apoptosis in skin cancer (SCC-13) cells due to decreased tri-methylation of lysine 27 of H3 (H3K27me3), an effect associated with inhibition of the polycomb group (PcG) proteins due to enhanced proteosomal degradation (Balasubramanian et al., 2011). Similarly, in another set of experiments, SFN found to inhibit epidermal squamous carcinoma cell proliferation, invasion and migration *in vitro* and *in vivo* by targeting Protein arginine N-methyltransferase 5 (*PRMT5*) and methylosome protein 50 (*MEP50*). In particular, SFN reduces the expression of *PRMT5/MEP50* through proteosomal degradation thus suppressing the formation of di-methylated arginine 3 on H4 (H4R3me2), events important for SFN-mediated inhibition of metastasis in SCC tumors (Saha et al., 2017). It is noteworthy, that the mode of action of SFN is different in normal epidermal keratinocytes compared to cancer ones. For example, normal keratinocytes reported to be more resistant to SFN-induced inhibition of HDAC activity (and cellular proliferation) in comparison to the cancer cells (Dickinson et al., 2015). In agreement, another study has demonstrated the diverse nature of SFN's effectiveness in normal keratinocytes as compared to skin cancer cells. Specifically, it was shown that SFN protected primary normal keratinocytes from damage by slowing their growth while driving apoptosis in cancer cells. Furthermore, the mechanism by which SFN controls keratinocyte proliferation appears to be *p53* dependent (Chew et al., 2012). PEITC was also shown to prevent both TPA-and epidermal growth factor (EGF)-induced mouse epidermal JB6 cell transformation (through a *p53*-depend induction of apoptosis) (Huang et al., 1998).

1.6.4 ITCs in Melanoma Chemoprevention and Therapy

Growing evidence supports the protective role of ITCs against initiation, progression and metastasis of melanoma by utilizing various relevant *in vitro* models. Generally, such a protective effect is mediated by the induction of diverse signal transduction pathways, oxidative stress responses, disruption of mitochondrial functions, modulation of the activity of proliferative, apoptotic and inflammatory regulators, etc., summarized in Fig. 1.12. In

particular, SFN has been shown to cause morphological changes and DNA fragmentation in murine B16F-10 melanoma cells, indicative of apoptotic induction in these cells. SFN induced the intrinsic apoptotic pathway and significantly reduced melanoma cell viability by activating caspase 3, *Bax* and *p53* proteins while down-regulating the expression levels of anti-apoptotic *Bcl2* and various pro-inflammatory cytokines (Hamsa et al., 2011). Similarly, exposure of human melanoma (Bowes and SK-Mel-28) cells to SFN also decreased cell survival and proliferation through activation of mitochondrial mediated apoptosis associated with modulation in *p38* and *p53* activities, induction of oxidative-mediated DNA damage response and enhanced expression of pro-apoptotic *BAX* and *PUMA* (Rudolf et al., 2014). In agreement to these observations, BITC also found to increase apoptotic cell death in both murine and human *PAF-R* positive cells, mediated by elevated production of ROS and enhanced caspase3/7-like activity. Cells a expressing the platelet-activating factor receptor (*PAF-R*) are characterized by a higher metastatic potential and found to be more susceptible in BITC-induced apoptosis compared to *PAF-R* negative ones, suggesting that ITCs could be promising agents for better management of *PAF-R*-positive melanoma patients (Sahu, 2015). In another experimental setting it was the induction of multiple apoptotic pathways in human A375 malignant melanoma cells treated with SFN, BITC and PEITC were reported, as shown by the increased expression of several caspases indicative of the intrinsic, extrinsic and endoplasmic reticulum (ER)-based pathways (Mantso et al., 2016). In addition, PEITC increased ROS production that disrupted the mitochondrial membrane potential in A375.S2 cells, resulted in an increased number of cells at the G2/M phase, induced ER stress and mitochondrial-dependent apoptotic pathways (Huang et al., 2014). BITC reported to exert a similar effect in A375.S2 cells by inducing a ROS-mediated G2/M cell cycle growth arrest as well as apoptosis mediated by multiple signaling pathways (e.g. ER stress-, mitochondrial-dependent and death receptor-mediated pathways) through alterations in the expression of various cyclins and CDKs (e.g. cyclin A, CDK1, CDC25), proteins of the *BCL2* family and various caspases (Huang et al., 2012). In agreement, SFN, BITC and PEITC have also been shown to increase the number of A375 melanoma cells arrested at the G2/M phase by modulating the expression activity of several regulators of cell cycle progression (Mantso et al., 2019).

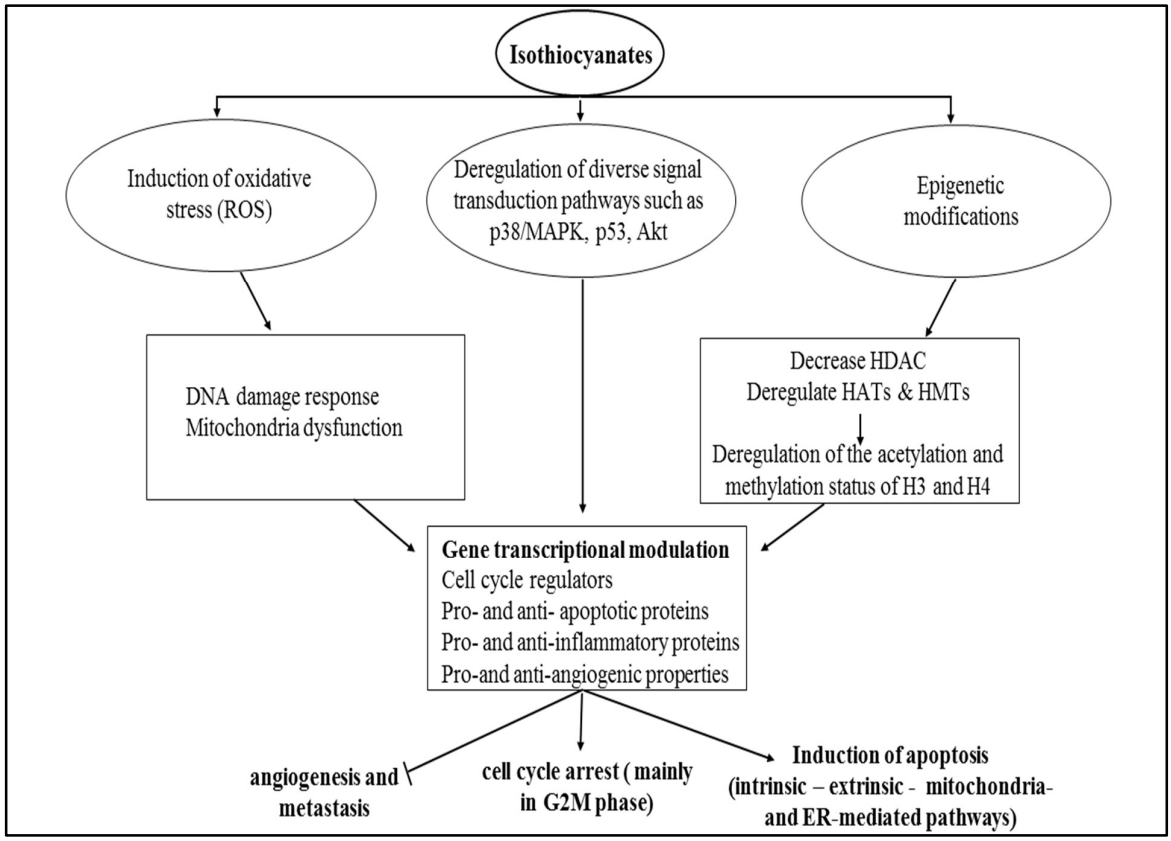

Figure 1.12: Cellular targets of ITCs anti-melanoma effect. The anti-melanoma effect of ITCs has been characterized in various studies both *in vitro* and *in vivo*. Briefly, ITCs have been reported to reduce melanoma cell proliferation and survival as well as to decrease tumor development in rodent models through modulations of multiple signaling pathways (e.g. p38/MAPK, p53 etc.), enhancement of oxidative responses (ROS) and deregulation of the epigenetic machinery, resulting in the induction of DNA damage, mitochondrial dysfunction and aberrant acetylation and methylation of core histones. Thus, upregulate the expression of various tumor-related genes, while downregulate the expression of oncogenes to promote cell cycle arrest, induce various apoptotic pathways (intrinsic, extrinsic, p53-, ER-, mitochondria mediated pathways) and block the metastatic, invasiveness and neo-angiogenic capacity of melanoma cells.

In addition, ITCs have also been shown to alter the angiogenic and metastatic potential of melanoma cells. In this respect, AITC and PITC inhibited the expression and secretion of pro-angiogenic factors (e.g. TNF-α and NO) that promote tumour specific vascularization both *in vitro* (B16F-10) and in *in vivo* (C57BL/6 mice) (Thejass & Kuttan, 2007). A similar anti-angiogenic effect was also reported in human umbilical vein endothelial cells (HUVECs) by AITC and PITC, through decreased expression of *VEGF* and various pro-

inflammatory cytokines, such as TNF-α and IL-1β (Thejass & Kuttan, 2007a). Moreover, the anti-metastatic potential of BITC and PEITC have been studied in murine B16F-10 (Lai et al., 2017) as well as in human A375.S2 (Y. S. Ma et al., 2017) cells and it was shown that both ITCs reduced viability, mobility and invasion of cells (through down-regulation of *MMP-2*), diminished expression of several proteins involved in the metastatic process and affected the *MAPK* signaling pathway. It should be mentioned though that the two ITCs differentially affected the expression of the proteins implicated in the metastatic potential of melanoma cells (Lai et al., 2017; Ma et al., 2017).

In the same context, a number of *in vivo* studies have also supported the anti-melanoma effect of ITCs. For instance, combinational treatment of C57BL/6 mice injected with B16F-10 cells and then treated with AITC, PEITC and SFN (1:1:1) resulted in reduced tumor growth, volume and weight(Bansal et al., 2015). In addition, intraperitoneal injection of both PEITC (Ni et al., 2014) and BITC (Ni et al., 2013) significantly declined the weight and size of tumours formed in A375.S2 BALB/c xenografts suggesting that both compounds can be effective in melanoma therapy. In another study, intraperitoneal administration of AITC and PITC, inhibited B16F-10-induced metastasis in the lungs of C57BL/6 mice (Manesh & Kuttan, 2003). Furthermore, intraperitoneally administration of SFN also prevented the migration of metastatic tumour cells in tumour bearing C57BL/6 mice by modulating a cell-mediated immune response and enhancing the activation of IFN-gamma and IL-2, while repressing pro-inflammatory cytokines such as IL-1β, TNF-alpha and granulocyte-macrophage colony-stimulating factor (GM-CSF) (Thejass & Kuttan, 2007b). Moreover, SFN inhibited melanoma proliferation, growth and mobility in B16F10 xenografts via decreased expression of MMP-9, an important regulator of tumour growth and invasion (Pradhan et al., 2010).

Additionally, ITCs (especially SFN) have been documented to contribute towards the concept of melanoma epigenetic therapy. In a recent study, exposure of A375 cells to AITC significantly diminished both HDAC and HAT activities and altered the expression of various enzymes (HDACs, HATs and HMTs) that regulate the acetylated and methylated status of H3 and H4, suggesting that AITC could act as epigenetic regulator capable of inhibiting melanoma progression (Mitsiogianni et al., 2019). In addition, another study has reported that SFN was able to inhibit the proliferation and growth of murine B16 and S91 melanoma cells, *in vitro*, by decreasing the activity of deacetylating enzymes while injection of albumin SFN-encapsulated microspheres intraperitoneally increased its anticancer

activity in melanoma tumour-bearing C57BL/6 mice (Do et al., 2010). Furthermore, ITCs reduced melanoma stem cells (MCS) viability, a subgroup of malignant melanoma cells characterized by high invasive and metastatic potential due to overexpression of the Ezh2 stem cell survival protein. Exposure of MCS cells to SFN decreased the expression of Ezh2 polycomb group protein and H3K27me3 formation thus reducing cell proliferation, invasion and migration in these cells. Finally, administration of SFN, in mice injected with A375-derived MCS cells, diminished tumour formation and growth, an effect which was associated with decreased expression levels of Ezh2 , H3K27me3, various MMPs together with enhanced expression of metalloproteinase inhibitor 3 (TIMP3) and apoptosis (Fisher et al., 2016).

Based on the knowledge acquired up to date, scientists focused on the formation of synthetic ITC analogues, having longer side chains or/and substitutions of sulphur group (e.g. by selenium), in order to produce structures with more potent anti-cancer efficacy. A number of these synthetic analogues have been developed and reported to be effective in repressing melanoma survival. It is also noteworthy that these analogues showed specificity towards cancer cells only as normal cells were found to be more resistant (Nguyen et al., 2011; Sharma et al., 2009; Sharma et al., 2008). For instance, naphthalimide is an example of a synthetic ITC analogue which has been found to exert a more potent cytotoxicity in both *in vivo* and *in vitro* experimental settings (Sk et al., 2011).

1.7: Working Hypothesis: Aims and Objectives

The hypothesis of the present study was that ITCs could act as potent epigenetic modulators, in malignant melanoma, thereby acting to promote apoptotic cell death. This, in turn, would suggest that ITCs could be promising candidates as "next generation" epigenetic therapeutic agents.

Considering that epigenetic modifications regulate differential gene expression, perhaps in this context they could serve as a common mechanism that reflects the plurality of anti-cancer properties exerted by ITCs, in terms of modulating the behavior of different genes in different cellular cascades. Specifically, in this study, we have aimed to characterize the effect of specific ITCs (abundant in the most commonly consumed *Brassica* vegetables) namely SFN, IBN, AITC, BITC and PEITC on specific acetylation and methylation marks on lysine molecules located on histone proteins H3 and H4 as well as on the expression patterns of several critical enzymes responsible for altering the epigenetic landscape. In this way, we will study the anti-melanoma properties of the above-mentioned ITCs as part of their well-described cytotoxic profile in an experimental *in vitro* model of human malignant melanoma.

Project objectives:

- ✓ To optimize the experimental conditions of an *in vitro* model of human malignant melanoma in order to test the cytotoxic effectiveness of ITCs.
- ✓ To assess the profile of the overall therapeutic potential of ITC-induced toxicity, characterizing diverse end points of cytotoxicity (viability, cell cycle growth arrest, apoptotic and necrotic cell death as well as ROS generation) in our *in vitro* model of human malignant melanoma.
- ✓ To assess ITCs ability to regulate the apoptotic process by identifying the expression pattern of several genes involved in distinct stages of apoptosis in human malignant melanoma cells.
- ✓ To characterize the epigenetic profile of each ITC treatment in the context of specific histone modifications in human malignant melanoma cells. In particular, to assess the expression of various enzymes capable of mediating lysine acetylation and methylation of histones 3 and 4.

Chapter 2

Materials & Methods

2.1 Cell Culture Methodologies

2.1.1 Cell Lines Utilized

For the purpose of this study we utilized an *in vitro* model of human malignant melanoma consisted of: (**i**) a human (A375) and (**ii**) a murine (B16 F10) primary malignant melanoma cell line; two human melanoma metastatic cell lines, (**iii**) one derived from brain (VMM-1) and (**iv**) one from lymph node metastasis (Hs 294T); (**v**) a human non-melanoma, epidermoid carcinoma (A431) cell line and (**vi**) a human normal immortalized keratinocyte (HaCaT) cell line (Table 2.1). All cell lines were authenticated using STR analysis on 2018.

At this point it should be mentioned that the A375 melanoma cell line was the main cell line utilized in all experimental settings throughout the project, while the rest of the cell lines were used on particular experimental designs, in the context of profiling the cytotoxic effects of ITCs to investigate their specificity towards primary, metastatic, non-melanoma skin cacinomas as well as normal cells.

Table 2.1: Description of all cell lines that constitute our *in vitro* malignant melanoma model

Cell Line	Supplier	Description
A375	Purchased from Sigma-Aldrich (St. Louis, MO, USA)	Human malignant melanoma, derived from the skin of a 54 year old female – Adherent, epithelial cells
B16 F10	Purchased from ATCC (Manassas, VA, USA)	Mouse melanoma, derived from mouse skin - Adherent, mixture of spindle-shaped and epithelial-like cells
VMM-1	Purchased from ATCC (Manassas, VA, USA)	Human brain metastatic malignant melanoma (Stage IV), derived from a metastatic tumor in the brain from a 62 years old male patient – Adherent, epithelial-like cells

Table 2.1: Description of all cell lines that constitute our *in vitro* malignant melanoma model (continued)

Hs 294T	Purchased from ATCC (Manassas, VA, USA)	Human lymph node metastatic malignant melanoma (Stage IV), derived from a metastatic tumor in the lymph nodes from a 56 years old male patient – Adherent, mixed stellate and polygonal
A431	Purchased from Sigma-Aldrich (St. Louis, MO, USA)	Human squamous carcinoma, derived from an epidermal carcinoma of the vulva taken from an 85 years old female – Adherent, epithelial cells
HaCaT	A kind gift from Dr Sharon Brody (Dermal Toxicology and Effects Group; Centre for Radiation, Chemical and Environmental Hazards; Public Health England, UK)	Human keratinocytes, in vitro spontaneously transformed keratinocytes from histologically normal skin – Adherent, monolayer cells

2.1.2 Cell Culture Materials and Reagents

Cells were incubated either in Dulbecco's Modified Eagle's (DMEM) medium or Roswell Park Memorial Institute (RPMI-1660) medium, purchased from Labtech International Ltd. (East Sussex, UK). Trypsin-EDTA, phosphate-buffered saline (PBS), Foetal Bovine Serum (FBS), L-Glutamine and Penicillin/Streptomycin were also obtained from Labtech International Ltd. (East Sussex, UK). Resazurin sodium salt, used to assess cell viability was purchased from Sigma-Aldrich (St. Louis, MO, USA). All chemicals were of analytical grade and supplied from Sigma-Aldrich (St. Louis, MO, USA), Applichem (Darmstadt, Germany), Invitrogen (Carlsbad, CA, USA) and Thermo Fisher Scientific (Waltham, MA, USA). Bovine Serum Albumin (BSA) was obtained by Affymetrix (Santa Clara, CA, USA)

and Dimethyl sulfoxide (DMSO) and ethanol (EtOH) by Sigma-Aldrich (St. Louis, MO, USA) (Table 2.2).

Table 2.2: List of materials used for cell culture

Reagents	Components
Complete Growth Media for A375, A431 and HaCaT cells	High Glucose DMEM (Dulbecco's Modified Eagle Medium) (Labtech Internationl Ltd, East Sussex, UK), supplemented with 10% fetal bovine resume heat-inactivated (Labtech), 2 mM *L*-Glutamine (Labtech), and 1% (v/v) penicillin/streptomycin mix.
Complete Growth Media for Hs 294T and B16 F10	High Glucose DMEM (Dulbecco's Modified Eagle Medium) (Labtech Internationl Ltd, East Sussex, UK), supplemented with 10% fetal bovine resume heat-inactivated (Labtech), 4 mM *L*-Glutamine (Labtech), and 1% (v/v) penicillin/streptomycin mix.
Complete Growth Media for VMM-1	High Glucose RPMI-1640 (Labtech International Ltd, East Sussex, UK), supplemented with 10% fetal bovine resume heat-inactivated (Labtech), 2 mM *L*-Glutamine (Labtech), and 1% (v/v) penicillin/streptomycin mix.
Phosphate Buffer Saline (PBS) [1X]	[NaCl]= 140 mM, [KCl]= 2.7 mM, [Na_2HPO_4]= 10 mM, [KH_2PO_4]= 1.7 mM, pH 7.4
Trypsin-EDTA Solution [1X]	1X Trypsin-EDTA 0.25% in PBS w/o Mg^{2+}, w/o Ca^{2+} (Labtech)
Cell Culture plates & flasks	Corning Inc., NY, USA
Stripettes	Corning Inc., NY, USA

2.1.3 Cells Cryopreservation and Recovery

All cell lines were cryopreserved to avoid contamination, aging, transformation and to minimize genetic change in continuous cell lines. Cultured cells were detached from the flasks by trypsinization. Once detached, cells were re-suspended in the desired growth medium, according to the cell type, and the number of viable cells was counted. Then, the suspension centrifuged at ~2000 rpm for about 2 min in order to pellet cells. The supernatant was then discarded carefully, without disturbing the pellet, which was then re-suspended in appropriate freezing medium [foetal bovine serum (FBS) containing 10% (v/v) DMSO] to a concentration of 5 x 10^6 to 1 x 10^6 cells/ml. Cells were next aliquoted into cryogenic storage vials and stored under vapour phase liquid nitrogen for long term storage.

Before usage, cells were thawed and re-suspended in 5 mL of the desired growth medium and centrifuged at 2000 *rpm* for 2 min, at room temperature (RT). The freezing media was then aspirated and the cell pellet was re-suspended in complete growth medium. Cell suspension was then transferred into a 25 cm^2 cell culture flask and maintained in a humidified atmosphere at 37 °C and 5% v/v CO_2. Cells were remained in culture for about 15-20 passages, after which new stocks were utilized.

All cell lines used in this study were authenticated with the Short-tandem repeat profiling (STR) method and tested for mycoplasma contamination prior to use.

2.1.4 Cells Propagation

All cell lines were cultured in 75 cm^2 flasks containing the desired complete growth medium (see Table 2.2 for appropriate growth media for each cell line) and maintained in a humidified atmosphere at 37ºC, in incubators providing 5% v/v CO_2. Cells were sub-cultured via trypsinization (2-3 times per week) after reaching 80-90% confluency. In particular, growth media was aspirated and cells were then washed with ~5 ml PBS. Next, 1X trypsin-EDTA was added into the flask (1 ml for A375, B16 F10, VMM-1 and Hs 294T cells or 2 mL for HaCaT and A431 cells) and cells were placed back in the incubator until they all detach from the flask's surface (5-10 min depending on the cell line). During trypsinization, cells were observed under the microscope to ensure that they had all been detached and next trypsin was de-activated by adding ~4-5 ml of growth medium into the flask. Finally, cells were sub-cultured at a ratio based on the replication rate of each cell line and the number of cells needed for further applications.

2.1.5 Counting and Plating of Cells

Cells were next transferred into a falcon tube and then centrifuged at 2,000 *rpm* for 2 min, at RT. Media was then aspirated, and cell pellet was thoroughly re-suspended in fresh media (5-12 ml according to the size of cell pellet). In order to determine the number of cells, 30 µl of this cell suspension was transferred into a micro-centrifuge tube and was mixed with an equal amount of trypan blue solution [0.4% (w/v); HyClone Inc, South Logan, USA]. Next, 10 µl of this mixture was loaded into a Neubauer counting chamber (i.e. haemocytometer) and the number of viable cells were then counted, under an inverted microscope.

Trypan blue was used to distinguish between viable and dead cells. The assay is based on the principle that live cells possess intact cell membranes and do not take up the dye (seen as bright/clear under microscope), while dead cells have damaged cell membranes and uptake trypan blue (stained blue).

The central area of the counting chamber is divided into 4 large squares. Each of these are further sub-divided into 16 smaller squares (Fig. 2.1). Only cells set within a large square and on the border lines on two sides (upper and right-hand boundary line) were counted. The number of cells counted in this set of 16 squares was recorded and the haemocytometer was moved to the next set until all 4 sets of 16 squares on the haemocytometer have been counted, and their values recorded.

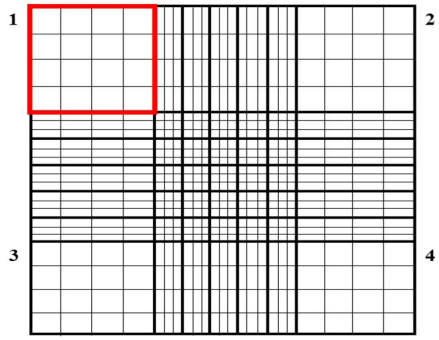

Figure 2.1: The central area of the haemocytometer's counting chamber. The red square indicates one of the 4 sets of 16 square used for cell counting.

The concentration of cells (number of cells/ ml) was then estimated using the following formula:

$$[\textbf{Concentration of live cells/ml}] = \frac{N}{4} \textbf{x DF x } 10^4$$

Where *N*= the average number of cells counted in the 4 squares of the counting chamber, *DF* (dilution factor) = 2 (1:1 dilution with trypan blue solution) and 10^4 = conversion factor to convert 10^4 µl to 1 ml (calculated according to the dimensions of the small square of the Neubauer chamber). After calculating the concentration of cells in the suspension, the desired number of cells is seeded into cell culture dishes, 96-well plates, etc., based on the requirements of the experimental protocols to be performed.

2.1.6 ITCs Exposure Protocols

An appropriate number of cells was plated and incubated at 37°C and 5% v/v CO_2, overnight. All cell lines were seeded in 100 µl of complete medium (depending on type of cell line) into 96-well plates (for cell viability assays) and kept in the incubator overnight, prior to exposure to each of the ITCs. The density of A375 cells was 8,000 and 4,000 cells/well; of B16F-10 cells was 6000 and 3000 cells/well; of VMM1 cells was 9000 and 5000 cells/well; of Hs 294T cells was 7000 and 4000 cells/well and for A431 and HaCaT cells 10,000 and 5,000 cells/well for 24 and 48 h, respectively. On the following day, cells were observed under the microscope to ensure that they reached confluency and exposed to a range of concentrations of each ITC (2.5-50 µM) for 24 and 48h, while control cells were incubated with complete medium only and/or with either 0.1% DMSO or 0.1% EtOH (in which ITCs were dissolved).

Table 3.3: List of ITCs administered in our experimental melanoma model

ITC	company	storage
SFN	Abcam, Cambridge, UK (ab141969)	Dissolved in DMSO at a concentration of 100 mM - Aliquots were stored at − 20 °C
IBN	Abcam, Cambridge, UK (ab141944)	Dissolved in EtOH at a concentration of 100 mM - Aliquots were stored at − 20 °C
AITC	Sigma-Aldrich, St. Louis, MO, USA (W203408)	Dissolved in DMSO at a concentration of 100 mM - Aliquots were stored at − 20 °C
BITC	Sigma-Aldrich, St. Louis, MO, USA (252492)	Dissolved in DMSO at a concentration of 100 mM - Aliquots were stored at − 20 °C
PEITC	Sigma-Aldrich, St. Louis, MO, USA (253731)	Dissolved in DMSO at a concentration of 100 mM - Aliquots were stored at − 20 °C

For other experimental protocols (flow cytometry, RNA and protein extraction, etc.), cells were seeded and allowed to adhere overnight in either 100 mm or 60 mm dishes, with cell densities being (100mm dish) for A375 cells, 1.4×10^6 and 0.7×10^6 per dish; for B16-F10, 2×10^6 and 1×10^6 per dish; for Hs 294T and VMM1, 1×10^6 and 0.8×10^6 per dish; for A431 and HaCaT, 1.8×10^6 and 1×10^6 per dish, for 24 and 48 h, respectively. Next day, cells were observed under the microscope to ensure that they reached confluency and exposed to 10 μM of each ITC, over different incubation periods.

Densities of cells seeded in 60 mm dishes were: A375 cells, 0.35×10^6 and 0.25×10^6 per dish; for Hs 294T cells, 0.45×10^6 and 0.35×10^6 per dish; for B16-F10 cells, 0.3×10^6 and 0.2×10^6 per dish and for VMM1 cells, 0.8×10^6 and 0.6×10^6 per dish for 24 and 48h, respectively.

2.1.7 Determination of Cell Viability: Resazurin Assay

The Resazurin assay was utilized, in this set of experiments, in order to determine cell viability. This assay is based on the ability of live cells to metabolize the non-fluorescent indicator dye resazurin into the highly fluorescent resorufin which is then detected by absorbance (at 570nm and 600nm as a reference wavelength) or fluorescence (excitation/emission maxima at 530-560/590 nm). The detection of the levels of absorbance or fluorescence scan is proportional to the number of viable cells.

All cell lines were seeded in 100 μl of complete medium into 96-well plates and kept in the incubator overnight. Next, cells were exposed to each ITC treatment at various concentrations, for 24–48h, as described in section *2.1.6 (ITCs Exposure Protocols*). At the indicated time points, resazurin (resazurin sodium salt dissolved in PBS at a final concentration of 1mg/ mL) was added in an amount equal to 1/10 of the volume in each well and incubated for 2-4h (depending on the metabolic capacity of each type of cancer cell line), at 37ºC. The plates were then centrifuged, and absorbance was recorded at 570 nm (using 600 nm as a reference wavelength) by utilizing a Spark 10 M multi-mode plate reader (Tecan, Männedorf, Switzerland). The levels of cell viability were estimated and expressed as percentage of control cells. Viable cells levels were estimated according to the optical density values recorded and cell viability was expressed as percentage of control cells. Five replicates (N=5) of each treatment condition were used in each experiment.

2.2 Flow Cytometry Protocols

The following experiments were performed by utilizing the FACS Canto II flow cytometer (BD Biosciences, San Jose, CA, USA). Details of the reagents used are shown on Table 2.4:

Table 2.4: Reagents and kits used for flow cytometry experiments

Reagent	Supplier
Dihydrorhodamine 123 (DHR123)	Sigma Aldrich, St. Louis, MO, USA (D1054)
CellEvent Caspase 3/7 Green Flow Cytometry Assay Kit	ThermoFisher Scientific Ltd, (C10427)
Intracellular GSG Assay Kit	Abcam, Cambridge, UK (Ab112132)
FxCycle PI/Rnase Staining Solution	ThermoFisher Scientific Ltd (F10797)
DAPI	Sigma Aldrich Ltd (10236276001)

2.2.1 Determination of Cell Cycle Phase Distribution

The FxCycle PI/RNase staining solution was used for the determination of cell population distributed among the phases of the cell cycle. The assay is based on the fact that DNA content differs in the diverse stages of the cell cycle: the Go/G1 phase contains one set of paired chromosomes per cell; the S phase is characterized by variable amount of DNA and the G2/M phase contains two sets of paired chromosomes per cell. The FxCycle PI/RNase solution contains propidium ioddide (PI), which binds to DNA and upon binding produces a fluorescent signal, allowing the determination of DNA content in cells (Excitation and Emission maxima at 535/617 nm).

To assess the DNA content of cells treated with each ITC, we used the FxCycle PI/RNase staining solution according to the manufacturer's instructions. Following exposure to 10 μM of each ITC for 24 and 48h (see section *2.1.6 ITCs Exposure Protocols),* cells were harvested and washed twice with PBS. Approximately, 0.5×10^6 cells were then fixed in cold 70% ethanol and stored at 4ºC for at least 1 hr (or longer), until being further processed. Fixed cells were then washed twice with PBS to remove ethanol and centrifuged at ~2000 *rpm* for 2min. Cell pellet was then re-suspended in FxCycle PI/RNase staining solution (0.5ml/1×10^6 cells) and incubated for 30 min at RT and protected from light. Analysis by flow cytometry yields frequency histograms showing population of cells distributed among the different cell cycle phases. Data from 10,000 events / sample were acquired.

2.2.2 Determination of Apoptosis

The CellEvent Caspase 3/7 Green flow cytometry assay kit was utilized for the detection of apoptosis through detection of the activated executioner caspases 3 and 7. The CellEvent Caspase 3/7 Reagent was utilized which is a tetrapeptide (DVED) conjugated with a nucleic

acid binding dye that is dissociated by the activated caspases 3/7, in apoptotic cells. Once the dye is free, it binds to the DNA and produces a fluorogenic signal (CellEvent Caspase 3/7 Detection Reagent; fluorescence excitation and emission maxima: ~511/533 nm). Using it together with 4', 6 – diamidino-2-phenylindole (DAPI), allows us to distinguish necrotic from apoptotic cells. DAPI is a fluorescent stain that can be diffused though the membranes of the dead cells only. Thus, the fluorescent intensity of Caspase 3/7 Reagent quantifies apoptotic cell population, whereas the fluorescent intensity of DAPI (excitation/emission 364/454) corresponds to the necrotic cell population.

To determine the extent of the apoptotic induction, under various experimental conditions, we used the CellEvent Caspase 3/7 Green flow cytometry assay kit according to the manufacturer's protocol. Post exposure of cells to 10 μM of each ITC, for 24 and 48h (see section *2.1.6 ITCs Exposure Protocols),* cells were harvested, washed twice with PBS and a single cell suspension of 1×10^6 cells/ml was prepared. Then, 0.5 μl of CellEvent Caspase 3/7 Green detection reagent was added to 0.5 ml (1μl/1 × 10^6 cells/ml – final concentration of reagent 500 nM) of each cell suspension. Samples were then incubated at 37ºC, for 30 min, and protected from light. During the final 5 min of incubation, DAPI (1 μM) was added to each sample to determine the percent of dead cells in the suspension. Flow cytometric analysis results in the identification of Caspase-3/7-positive, DAPI-positive and both Caspase-3/7- and DAPI-negative cells. For each experimental condition, we acquired data from 20,000 events / sample were acquired.

2.2.3 Determination of ROS Induction

Dihydrorhodamine 123 (DHR123) was used for the detection of intracellular ROS levels. The assay is based on the fact that in the presence of ROS (or other free intracellular radicals inside cells) will bind to DHR123 (an uncharged non-fluorescent dye) which is then oxidized and converted into the fluorescent rhodamine 123 (R123) dye that can then be detected (excitation/emission 488/530). We used this alongside with 4', 6 – diamidino-2-phenylindole (DAPI) in order to exclude the number of dead cells which do not produce ROS anyway.

Cells treated with each ITCs, for 24 and 48h (see section *2.1.6 ITCs Exposure Protocols*). At the indicated time points, cells were harvested and washed twice with PBS and a single cell suspension of 1×10^6 cells/mL was prepared. DHR 123 (dissolved in PBS at a concentration of 200 μM; stored at -20ºC) was then added in the suspension at a final concentration of 10 μM. Samples were next incubated for ~15 min at 37ºC. During the final

5 min of incubation, DAPI (1 μM) was added to each sample and incubated for further 5 min. Data from 10,000 events / sample were acquired while DAPI-positive cells were excluded from any further analysis.

2.2.4 Determination of GSH Levels

For the detection of intracellular levels of GSH, we used the GSH Detection Assay Kit according to the manufacturer's instructions. The kit detects the levels of reduced GSH (using a non-fluorescent Green Dye that emits fluorescence when reacts with intracellular thiol groups; excitation/emission= 490/520 nm). Specifically, we prepared a 200X Thiol Green detection reagent by mixing 500 μl DMSO with the Thiol Green Dye, contained in the kit. The reagent was aliquoted and stored at -20ºC.

Cells exposed to each of the ITCs for 24 and 48h (see section *2.1.6 ITCs Exposure Protocols*) and then were harvested. A single cell suspension of 1×10^6 cells/ml was prepared. Then, 2.5 μl of 200X Thiol Green detection reagent was added into 500ml in each cell suspension (5μl / 1×10^6 cells/ml) (containing serum media) and samples were incubated at 37ºC for 30 min. Then cells were centrifuged at 1000 *rpm* for 4 mins and cell pellets were re-suspended in 1ml of Assay Buffer. During the last 5min of incubation, DAPI (1 μM) was added to each sample, to determine the percent of dead cells in the suspension. Data of 10,000 events / sample were acquired.

2.3 Molecular Biology Methodologies

2.3.1 Extraction of RNA

Total RNA was extracted using the TRIzol Reagent according to the manufacturer's instructions. Following exposure of A375 cells to 10 μM of each ITC for 48h (see section *2.1.6 ITCs Exposure Protocols*), cells were collected via trypsinization, washed twice with PBS, suspended in 1ml (per $1\text{-}5\times10^6$ cells) TRIzol Reagent and stored in micro-centrifuge tubes at -20ºC, until being further processed.

Samples were allowed to thaw at RT for a few minutes and then 0.2ml of chloroform per 1ml of TRIzol was added. The tubes were shaken vigorously by hand for ~15sec, incubated for 5 min at RT and next, centrifuged at 12,000 x g for 15 min at 4ºC. After this step, the mixture was separated into 3 layers: a lower red phenol-chloroform phase, an interphase (containing DNA and proteins) and an upper colorless aqueous phase (containing the RNA). For RNA extraction, we transferred the aqueous phase of each sample, containing the RNA, into a fresh tube by angling the tube at 45° and pipette the solution out. For RNA precipitation, 0.5ml of 100% isopropanol, per 1ml of TRIzol reagent, was added to the

aqueous phase and samples were incubated for 10 min at RT. Then, samples were centrifuged at 12,000 x g for 10 min at 4ºC. Next, the supernatant was removed from the tubes while the RNA precipitate remained at the bottom of the tube. Pellets were then washed with 1ml of 75% ethanol per 1ml of TRIzol reagent used, vortexed briefly and centrifuged at 7,500 x g for 5 min at 4ºC. All remaining ethanol was discarded and pellets were allowed to air dry on the bench for ~5-10 min. Then, pellets were re-suspended in RNAase free water (~20-50μl, according to pellet size) and stored at -20ºC.

RNA quantity was determined by using the NanoDrop One/One^{C} (ThermoScientific, Waltham, MA, USA) which measures the absorbance at 260 and 280 nm thereby providing information on RNA concentration and sample quality respectively. In general, a sample with a 260/280 ratio of > 1.8 is considered to contain non-contaminated (pure) RNA.

RNA integrity and quality, were also assessed by running 2μg of each RNA sample on a 1% agarose gel. To prepare 1% agarose gel, we measured 1gr of agarose powder and mixed it with 100 ml of 1x Tris acetate EDTA (TAE) [for 1liter of 50X stock of TAE, we added 242 gr Tris-base, 57.1 ml acetate (100% v/v acetic acid), 100 ml of 0.5M sodium EDTA and dH2O up to one liter) in a flask. The mixture was then microwaved for 1-3 min (stopping every few seconds and swirling) until the agarose was completely dissolved. After the agarose solution was cooled down, for a few minutes, we added ethidium bromide (EtBr) to a final concentration of approximately 0.2-0.5 μg/ml (usually about 2-3 μl of stock solution per 100 ml gel) which then binds to DNA thus allowing to visualize the DNA under exposure to UV light. Then the agarose was poured into a gel tray with the well combs in place and left until it was completely solidified. Then, it was placed into an electrophoresis unit and 1X TAE was added until the gel was covered. Next, 2μg RNA samples were mixed with loading buffer (heated at ~70°C for ~5min) loaded and run the gel at ~100V. The gel was then visualized under UV light. Intact total RNA, run on a denaturing gel, showed as sharp 28S and 18S rRNA bands.

2.3.2 Synthesis of cDNA

Complimentary DNA was synthesized by using the SuperScript VILO cDNA synthesis kit (Invitrogen) according to the manufacturer's instructions. Briefly, 2.5μg RNA was diluted in RNAase free water to a total volume of 14μl. Then, 4 μl of 5X VILO Reaction Mix (random primers, MgCl2, dNTPs) and 2μl of 10X SuperScript Enzyme Mix (SuperScript III RT, RNaseOUT recombinant ribonuclease inhibitor and a proprietary helper protein) were added to the diluted RNA (total reaction volume = 20μl). The mixture was gently mixed and

incubated at 25ºC for 10 min. Next, the mixture was heated at 42ºC for 60 min to generate cDNA and then at 85ºC for another 5 min in order to inactivate the enzyme prior to be chilled at 4ºC. The resulting product was stored at -20ºC until further use.

2.3.3 Real-Time Polymerase Chain Reaction (qPCR)

The quantitative polymerase chain reaction was carried out by utilizing the TaqMan Array Human Apoptosis 96-well plates (Applied Biosystems, Carlsbad, CA, USA, 10480715). The predesigned 96-well plates contained a collection of dried-down TaqMan gene expression assays, which were composed of gene-specific primers and probe sets, for screening candidate genes involved at various stages of the apoptotic pathway. The use of Taqman probes significantly increases the specificity of the detection of qPCR and provides accurate quantification of the cDNA present. The TaqMan Array Human Apoptosis 96-well plates contains 92 assays for genes implicated at various stages of the apoptotic cascade along with 4 assays for candidate endogenous control genes (18S, GAPDH, GUSB and HPRT1) (Table 2.6).

TaqMan Universal master mix (2X) was thawed and 550µl were mixed with an equal amount (550 µl) of cDNA (diluted in DNase free water), up to a final volume of 1100µl (all volumes contained ~10% excess volume to have enough product to run a 96-well plate). cDNA input was 50ng per well. Then, the reaction mixture was gently vortexed and spinned down. Before loading the samples, the plate was centrifuged at 1,000 *rpm* for 1 min. Then 10µl of the cDNA-master mix solution into each well of the 96-well plate. The plate was covered with a clear adhesive film and was briefly centrifuged (1,000 *rpm* for 1 min) to ensure that the reaction mixture was collected at the bottom of the wells. The plates were run at the StepOne Plus Real-Time PCR system (Applied Biosystems, Carlsbad, CA, USA) and the thermal-cycling conditions was set according to manufacturer guidelines, indicated in the table below (Table 2.5).

Gene expression data were analyzed by the ΔΔCt method and were expressed as fold change compared to untreated controls, by using the DataAssist v3.01 software.

Table 2.5: Thermal cycling conditions for running the TaqMan Array 96-well plates

TaqMan Fast Universal Master Mix			
		PCR (40 cycles)	
Hold	**HOLD**	**MELT**	**ANNEAL/EXTEND**

Table 2.5: Thermal cycling conditions for running the TaqMan Array 96-well plates (continued)			
50 ºC	95ºC	95ºC	60ºC
2:00	0:20	0:03	0:30

Table 2.6: List of all apoptosis-related genes contained in the TaqMan Array Human Apoptosis 96-well plates

Gene Symbol – Assay ID		
1. 18S-Hs99999901_s1	34. FASLG-Hs00181225_m1	67. PRKCA-Hs00176973_m1
2. AIFM1-Hs00377585_m1	35. GAPDH-Hs99999905_m1	68. PRKCB-Hs00176998_m1
3. AKT1-Hs00178289_m1	36. GUSB-Hs99999908_m1	69. PRKCD-Hs01090047_m1
4. APAF1-Hs00559441_m1	37. HPRT1-Hs99999909_m1	70. PRKCE-Hs00178455_m1
5. ATM-Hs01112307_m1	38. HTRA2-Hs00234883_m1	71. PRKCZ-Hs00177051_m1
6. BAD-Hs00188930_m1	39. IGF1-Hs01547656_m1	72. REL-Hs00968436_m1
7. BAK1-Hs00940249_m1	40. IGF1R-Hs00609566_m1	73. RELA-Hs00153294_m1
8. BAX-Hs00180269_m1	41. IKBKB-Hs00233287_m1	74. RELB-Hs00232399_m1
9. BBC3-Hs00248075_m1	42. IKBKE-Hs01063858_m1	75. RIPK1-Hs00169407_m1
10. BCL2-Hs99999018_m1	43. IKBKG-Hs00415849_m1	76. RPS6KA1-Hs00177257_m1
11. BCL2L1-Hs00236329_m1	44. IL2-Hs00174114_m1	77. RPS6KA2-Hs00179731_m1
12. BCL2L11-Hs00197982_m1	45. IL6-Hs00985639_m1	78. RPS6KA3-Hs00177936_m1
13. BID-Hs00609632_m1	46. KDR-Hs00911700_m1	79. RPS6KA4-Hs00177670_m1
14. BIRC2-Hs01112284_m1	47. KIT-Hs00174029_m1	80. RPS6KA5-Hs00178054_m1
15. CASP3-Hs00234387_m1	48. MDM2-Hs99999008_m1	81. SLC25A4-Hs00154037_m1
16. CASP7-Hs00169152_m1	49. MET-Hs00179845_m1	82. SLC25A5-Hs00854499_g1
17. CASP8-Hs01018151_m1	50. NFKB1-Hs00765730_m1	83. SLC25A6-Hs00745067_s1
18. CASP9-Hs00154260_m1	51. NFKB2-Hs00174517_m1	84. TGFB1-Hs00998133_m1
19. CDKN2A-Hs00923894_m1	52. NFKBIA-Hs00153283_m1	85. TNF-Hs00174128_m1
20.CFLAR-Hs01116280_m1	53. NFKBIB-Hs00182115_m1	86. TNFRSF10A-Hs00269492_m1
21. CHEK2-Hs00200485_m1	54. NFKBIE-Hs00234431_m1	87. TNFRSF1A-Hs00533560_m1
22. CHUK-Hs00175141_m1	55. P53AIP1-Hs00223141_m1	88. TNFSF10-Hs00234356_m1
23. CYCS-Hs01588973_m1	56. PARP1-Hs00242302_m1	89. TNFSF12-Hs00611242_m1
24. DAPK3-Hs00154676_m1	57. PARP2-Hs00193931_m1	90. TP53-Hs01034249_m1
25. DAXX-Hs00154692_m1	58. PARP3-Hs00193946_m1	91. TRADD-Hs00182558_m1
26. DFFA-Hs00189336_m1	59. PARP4-Hs00173105_m1	92. TRAF2-Hs00184192_m1
27. DFFB-Hs00237077_m1	60. PIK3CA-Hs00180679_m1	93. TSPO-Hs00559362_m1
28. DIABLO-Hs00219876_m1	61. PIK3CB-Hs00927728_m1	94. VDAC1-Hs01019083_m1
29. EGFR-Hs01076078_m1	62. PIK3CD-Hs00192399_m1	95. VDAC2-Hs00762994_s1
30. ENDOG-Hs00172770_m1	63. PIK3R1-Hs00381459_m1	96. VDAC3-Hs00366592_m1
31. F2RL3-Hs00559732_m1	64. PIK3R2-Hs00178181_m1	
32. FADD-Hs00538709_m1	65. PMAIP1-Hs00560402_m1	
33. FAS-Hs00531110_m1	66. PPID-Hs00234593_m1	

2.4 Protein Methodologies

2.4.1 Protocols of Protein Extraction and Determination

2.4.1.1 Nuclear Extraction Protocol

Cells were trypsinized and washed twice with ice-cold PBS and then pellets were collected after centrifugation at 2,000 *rpm* for 2 min at 4ºC. Cell pellets were lysed in 2 volumes of lysis buffer (depending on size of pellet) (see Table 2.7) and were left on ice (while periodically vortexed) for ~15 min. Next, cell lysates were centrifuged at 3,000 *rpm* for 10 min at 4ºC. Then the supernatant was transferred into a fresh tube and the nuclei (at the bottom of the tube) were washed with lysis buffer by gently pipetting up and down. This step was repeated ~5 times while the nuclei were re-suspended in one volume of nuclear extraction buffer (see Table 2.7) avoiding clumping to occur. Next, lysates were vortexed in low speed and incubated on ice (while vortexed every minute) for ~30 min. Finally, lysates were centrifuged at full speed (15,000 *rpm*/25,200 *RCF*) for 5 min at 4ºC and then were transferred back in new tubes.

The protein content was determined by utilizing the Pierce BCA protein assay kit (Thermo Scientific, Waltham, MA, USA) according to the manufacturer's protocols. To this end, a standard curve was created by using Bovine Serum Albumin (BSA) as a standard. To do so, a set of BSA standards of known concentrations (0, 0.2, 0.5, 1, 2 μg/ μl) was prepared in a 96 well plate by mixing the appropriate volumes of dH_2O and BSA stock to a final volume of 20 μl. Samples were then added at a 1:10 dilution in duplicates. Next, we prepared our detection reagent by mixing 50 parts of BCA reagent A with 1 part of BCA reagent B (50:1), and then 200 μl of this solution was loaded in each well. The plate was then covered and incubated at 37ºC, for 30 min, and also protected from light. Finally, the plate was centrifuged at 2,000 *rpm*/448 *RCF* for ~2 min and the absorbance was then recorded at 562nm, using a Spark 10 M multi-mode plate reader. The unknown protein concentrations of the samples were calculated by generating a standard BSA curve.

Once protein concentration was determined, the exact volume of lysates was measured and was transferred to new micro-centrifuge tubes. Loading buffer (5X) was finally added in a ratio of 1 part of loading buffer in 4 parts of sample, which then were either immediately used or were stored at -20ºC (for several days) or -80ºC (long term storage), until future usage.

Table 2.7: List of constituents of protein extraction buffers

Lysis buffer	Nuclear extraction buffer
10mM HEPES pH 7.9	20mM HEPES pH 7.9
10mM KCl	420mM NaCl
0.1mM EDTA	0.1mM EDTA
1.5mM $MgCl_2$	1.5mM $MgCl_2$
0.2% NP40	25% glycerol
Prior to use, add: 1. 1mM DTT 2. Protease Inhibitor Tablets (Thermo Scientific) 3. Phosphatase Inhibitor Tablets (Thermo Scientific)	

2.4.1.2 Total Histone Extraction Protocol

Total histone extracts were obtained using the EPIXTRACT Total Histone Extraction Kit from Enzo Life Sciences, Inc (Farmingdale, NY, USA) according to manufacturer's protocol.

Following exposure of A375 cells to 10 μM of each ITC, for 48h (see section *2.1.6 ITCs Exposure Protocols*), cells were trypsinized and washed twice with ice-cold PBS while pellets were collected after centrifugation at 2,000 *rpm*/448 *RCF* for 2 min at 4ºC. Cell pellets were then re-suspended in 1X Pre-Lysis Buffer (1:10 dilution of 10X Pre-Lysis Buffer with dH_2O) at 1×10^7 cells/ml and incubated on ice for 10 min (while periodically vortexed gently). Cell lysates were next centrifuged at 10,000 rpm/ 11,200 RCF for 1 min at 4ºC. The supernatant was discarded and cell pellets were re-suspended in 3 volumes of Lysis Buffer (~200μl / 1×10^7 cells) and left on ice for 30 min. Afterwards lysates were centrifuged at 12,000 *rpm*/16,128 *RCF,* at 4ºC, and the supernatant was transferred into a new tube. Finally, 0.3 volumes (0.3ml/1ml of supernatant) of Balance-DTT Buffer were added to the supernatants. Balance-DTT Buffer was prepared by adding DTT solution to Balance Buffer at a 1:500 ratio.

Protein content was determined by utilizing the Pierce BCA protein assay kit (Thermo Scientific) according to the manufacturer's instructions [protocol described at section *2.4.1.1 Nuclear Extraction Protocol*)]. In this case, diluted samples (1:5) were added, in duplicates. After determining the protein concentration, the exact volume of lysates was measured and was transferred to new micro-centrifuge tubes. Loading buffer (5X) was finally added in a ratio of 1 part of loading buffer in 4 parts of sample, which then were either immediately

used or were stored at -20ºC (for several days) or -80ºC (long term storage), until future usage.

2.4.2 Determination of Total HDAC Activity

Total HDAC activity levels were determined using the Epigenase HDAC Activity/Inhibition Direct Assay kit, Epigentek (Farmingdale, NY, USA) according to the manufacturer's protocol. Briefly, for determination of HDAC activity, nuclear cell lysates were prepared (see section *2.4.1.1 Nuclear Extraction Protocol*) and 10 μg of extracts were incubated with an acetylated substrate for 90 min at 37°C.

For the enzymatic reaction, we prepared blank and sample wells in triplicates. In each blank well, 49 μl of reagent HO1 (HDAC Assay Buffer) was added with 1 μl of HO2 (HDAC Substrate). In sample wells, we added 45-48 μl of HO1, 1 μl HO2 and 1-4 μl (10 μg) of nuclear extracts (final volume in each well 50 μl). Then, strip-well microplates were tightly covered with clear adhesive film to avoid evaporation and incubated at 37°C for 90 min. Afterwards the reaction solution was removed and each well was washed three times with 150 μl of the diluted 1X Wash Buffer (10X Wash Buffer diluted to 1X with dH_2O). Next, 50 μl of the diluted HO4 (1:1000 dilution of HO4 Capture Antibody with 1X Wash Buffer) was added into each well, then the strip-slips were covered with Parafilm M and were incubated at room temperature for 60 min. Next HO4 solution was discarded, each well was then washed three times with 150 μl of the diluted 1X Wash Buffer and 50 μl of the diluted HO5 Detection Antibody Solution was added (HO5 diluted with 1X Wash Buffer at a ratio of 1:2,000). Strip-wells were then covered with Parafilm M and incubated, for 30min, at RT. After 30 min, HO5 solution was removed and each well was washed four times with 150 μl of the diluted 1X Wash Buffer. Finally, for signal detection, 100 μl of Developer Solution (DS) was added to each well and incubated at room temperature for 1-10min (~ 5 min in our case), protected from light. To stop the enzymatic reaction 100 μl of Stop solution (SS) was added and the optical density values were detected at 450 nm with an optional reference wavelength of 655 nm, using a Spark 10 M multi-mode plate reader (Tecan).

For a simple calculation of total HDAC activity the following formula was used:

$$[\textbf{HDAC Activity (OD/min/mg)}] = \frac{(\boldsymbol{Sample\ OD - Blank\ OD})}{(\textbf{Protein Amount (}\mu\textbf{g) x min})} \textbf{x 1000}$$

Where protein amount = the protein amount (μg) added in the reaction (herein 10μg) and min= incubation time with the HO2, HDAC substrate (herein 90min).

2.4.3 Determination of Total HAT Activity

HAT activity levels were determined using the EpiQuik HAT Activity/Inhibition Assay kit, Epigentek (Farmingdale, NY, USA) according to the manufacturer's protocol. Briefly, nuclear cell lysates were prepared (see section *2.4.1.1 Nuclear Extraction Protocol*) and 5 µg of extracts were incubated with a HAT substrate for 60 min at 37°C.

The first step in the process was the addition of 50 µl of diluted HT2 (HAT Substrate, 20 µg/ml) in each well. The strip-wells were then covered with Parafilm M and incubated at RT for 45 min. HT2 was diluted in 1X HT1 Wash Buffer (1:10 dilution of 10X HT1 with dH_2O) in a ratio 1:50. Afterwards HT2 was aspirated and each well was washed three times with 150 µl of the 1X HT1 Wash Buffer. Next, for each blank well, 30 µl of reagent HT5 (HAT Assay Buffer) was added, while for sample wells, we added 26 µl of HT5, 2 µl of diluted HT4 (1:20 dilution of HT4, Acetyl Co-A with HT5) and 2 µl (5 µg) of nuclear extracts (final volume in each well 30 µl). Then, strip-well microplates were tightly covered with clear adhesive film to avoid evaporation and incubated at 37°C for 60 min. Afterwards the reaction solution was removed and each well was washed three times with 150 µl of the diluted 1X HT1 Wash Buffer. Next, 50 µl of the diluted HT6 (1:100 dilution of HT6 Capture Antibody with 1X HT1 Wash Buffer) was added into each well, then the strip-slips were covered with Parafilm M and were incubated on an orbital shaker (50-100 *rpm*) at RT for 60 min. Then, HT6 solution was discarded, each well was then washed four times with 150 µl of the diluted 1X HT1 Wash Buffer and 50 µl of the diluted HT7 Detection Antibody was added (HT7 diluted with 1X HT1 Wash Buffer at a ratio of 1:1000). Strip-wells were then covered with Parafilm M and incubated at room temperature for 30min. After the passage of 30min, HT7 solution was removed and each well was washed four times with 150 µl of the diluted 1X HT1 Wash Buffer. Finally, 100 µl of HT8 (Developing Solution) was added to each well incubated at RT for ~ 5 min and protected from light. To stop the enzymatic reaction, 50 µl of HT9 (Stop Solution) was added and the optical density values were detected at 450 nm within 2-15 min, using a Spark 10M multi-mode plate reader (Tecan, Männedorf, Switzerland).

The HAT activity was calculated by utilizing the following formula:

$$[\textbf{HAT Activity (OD/min/mg)}] = \frac{(\boldsymbol{Sample\ OD - Blank\ OD})}{(\textbf{Protein Amount (µg) x min})} \textbf{x 1000}$$

Where protein amount = the protein amount (µg) added in the reaction (herein 5µg) and min= incubation time with the HT4, Acetyl Co-A (herein 60min).

2.4.4 Western Immunoblotting

Western immunoblotting was performed against various antibodies for specific HDAC, HAT and HMT enzymes (Histone Deacetylase (HDAC) sampler kit #9928; Lysine Acetyltransferase sampler kit #8686 and Lysine Methyltransferase sampler kit #8694) as well as acetylated and methylated marks on H3 and H4 (Acetyl-Histone H3 sampler kit #9927; Acetyl-Histone H4 sampler kit #8346; Tri-Methyl-Histone H3 sampler kit #9783; and Di-methyl-Histone H3 sampler kit #9847). All primary antibodies were obtained from Cell Signalling Technology, Danvers, MA, USA (Table 2.8).

Table 2.8: List of Antibodies used in Western Immunoblotting

Antibody	Dilution	Blocking Buffer	Isotope	Catalogue Number
Anti-HDAC1	1:1000	5% nonfat, dry milk in TBS-T*	Mouse	#5356
Anti-HDAC2	1:1000	5% nonfat, dry milk in TBS-T	Mouse	#5113
Anti-HDAC4	1:2000	5% BSA in TBS-T	Rabbit	#7628
Anti-HDAC6	1:1000	5% BSA in TBS-T	Rabbit	#7558
Anti-CBP	1:1000	5% BSA in TBS-T	Rabbit	#7389
Anti-AcCBP/p300	1:1000	5% BSA in TBS-T	Rabbit	#4771
Anti-PCAF	1:1000	5% BSA in TBS-T	Rabbit	#3378
Anti-GCN5L2	1:1000	5% BSA in TBS-T	Rabbit	#3305
Anti-G9a/EHMT2	1:1000	5% BSA in TBS-T	Rabbit	#3306
Anti-ESET	1:1000	5% BSA in TBS-T	Rabbit	#2196
Anti-RBBP5	1:1000	5% BSA in TBS-T	Rabbit	#13171
Anti-ASH2L	1:2000	5% BSA in TBS-T	Rabbit	#5019
Anti-SET 8	1:1000	5% BSA in TBS-T	Rabbit	#2996
Anti-SET 7-9	1:1000	5% BSA in TBS-T	Rabbit	#2813
Anti-AcH4K5	1:1000	5% BSA in TBS-T	Rabbit	#8647
Anti-AcH4K8	1:1000	5% BSA in TBS-T	Rabbit	#2594
Anti-AcH4K12	1:1000	5% BSA in TBS-T	Rabbit	#13944
Anti-AcH3K9	1:1000	5% BSA in TBS-T	Rabbit	#9649
Anti-AcH3K14	1:1000	5% BSA in TBS-T	Rabbit	#7627
Anti-AcH3K18	1:1000	5% BSA in TBS-T	Rabbit	#13998
Anti-AcH3K27	1:1000	5% BSA in TBS-T	Rabbit	#8173
Anti-AcH3K56	1:1000	5% BSA in TBS-T	Rabbit	#4243

Table 2.8: List of Antibodies used in Western Immunoblotting (continued)				
Anti-H3K4me2	1:1000	5% BSA in TBS-T	Rabbit	#9725
Anti-H3K9me2	1:1000	5% BSA in TBS-T	Rabbit	#4658
Anti-H3K27me2	1:1000	5% BSA in TBS-T	Rabbit	#9728
Anti-H3K36me2	1:1000	5% BSA in TBS-T	Rabbit	#2901
Anti-H3K79me2	1:1000	5% BSA in TBS-T	Rabbit	#5427
Anti- H3K4me3	1:1000	5% BSA in TBS-T	Rabbit	#9751
Anti-H3K9me3	1:1000	5% BSA in TBS-T	Rabbit	#13969
Anti- H3K27me3	1:1000	5% BSA in TBS-T	Rabbit	#9733
Anti-H3K36me3	1:1000	5% BSA in TBS-T	Rabbit	#4909
Anti- H3K79me3	1:1000	5% BSA in TBS-T	Rabbit	#4260
Anti-H3	1:2000	5% nonfat, dry milk in TBS-T	Rabbit	#4499
H4	1:1000	5% nonfat, dry milk in TBS-T	Mouse	#2935
TBP	1:1000	5% nonfat, dry milk in TBS-T	Rabit	#8515
Anti-rabbit, HRP-linked secondary antibody	1:2000	5% nonfat, dry milk in TBS-T	Goat	#7074
Anti-mouse, HRP-linked secondary antibody	1:2000	5% nonfat, dry milk in TBS-T	Horse	#7076

* TBS-T: Tris-buffered saline with 0.1% Tween ® 20 Detergent

Cell extracts were heated at 95ºC for 5 min (to denature proteins and reduce protein-protein interactions), were allowed to cool down for a few minutes and then vortexed and spinned down briefly. Proteins were then separated by using SDS polyacrylamide gels of different acrylamide concentration (10, 12, 10-20%, Novex Tris-Glycine pre-casted Gel, Invitrogen), according to the molecular weight of the protein of interest. Twenty (20) µg of nuclear and 10 µg of total histone protein extracts were then loaded onto a polyacrylamide gel and electrophoresis was carried out in SDS running buffer 1X (Table 2.9) at 80-120V for 3-4h, using mini gel tank and mini blot module (Invitrogen). A protein ladder (PageRuler plus Prestained Protein Ladder, 10-250kDa, ThermoScientific) was also loaded and separated in the SDS gel. After being separated, proteins were transferred electrophoretically onto PVDF membranes (either 0.45 or 0.2µm, according to the protein's molecular weight – PVDF membranes thickness of 100 µm with pore sizes of 0.25 or 0.45 µm were used. High and midium molecular weight proteins were blotted using a 0.45 µm pore size membrane, while 0.25 µm pore size membrane was used for low molecular weight proteins of <20k Da), by semi-dry transfer in Transfer Buffer (1X), utilizing the Trans-Blot Turbo Transfer System,

obtained from BioRad (Hercules, CA, USA) at pre-determined running conditions. Next, blots were blocked in 5% (w/v) non-fat milk powder in Tris-buffered saline with 0.1% Tween ® 20 Detergent (TBS-T) buffer (Table 2.9) for at least 1h at RT, under gentle agitation. After blocking, membranes were washed three times with TBS-T (~5min each time) and incubated overnight at 4°C, under agitation, with the appropriate primary antibodies, diluted in 5% milk or BSA, according to the manufacturer's instructions (see Table 2.8). The following day, membranes were washed three times in TBS-T buffer (~5min each time) and were then incubated with the appropriate horseradish peroxidase-conjugated secondary antibody for at least 1 hr at RT, under agitation. Then, membranes were washed three times in TBS-T and finally, labelled protein bands were visualized using the SuperSignal West Pico PLUS Chemiluminescent Substrate kit from Thermo Scientific (Waltham, MA, USA), according to the manufacturer's instructions. Protein bands were detected utilizing the G:BOX Chemi XX6/XX9 gel imaging system (Syngene, Cambridge, UK).

Table 2.9: List and composition of Buffers used for Western immunoblotting

Buffer	Components
SDS running buffer 10X	250 mM [Tris Base], 1.92M [Glycine], 1% [SDS], pH 8.3-8.5 Tris base : 30.3 g Glycine : 144 g SDS : 10 g dH_2O : up to 1 L
SDS running buffer 1X	25mM [Tris-base], 192mM [Glycine], 0.1% [SDS] 1:10 dilution of the SDS running buffer 10X with dH_2O
Transfer Buffer 10X	250 mM [Tris Base], 1.92M [Glycine], pH 8.3-8.5 Tris base : 30.3 g Glycine : 144 g dH2O : up to 1 L
Transfer Buffer 1X	25mM [Tris-base], 192mM [Glycine], 0.5% [SDS], 20% (v/v) [Methanol] TB 1X: 100ml (1:10 dilution) SDS: 5ml MeOH: 200ml dH2O : up to 1 L
Tris Buffered Saline (TBS) 10X	200 mM [Tris Base], 1.5M [NaCl], pH 7.5-7.6 Tris Base: 87.66 g NaCl: 24.22 g
Tris Buffered Saline 1X with 0.1% Tween-20 (TBST)	20 mM [Tris Base], 150 mM [NaCl], 0.1% [Tween 20] in dH_2O 1:10 dilution of the TBS buffer 10X with dH_2O and addition of 1ml Tween-20

2.5 Statistical analysis

In all sets of experiments (apart from viability assays), data were expressed as mean values ± standard deviation (SD). For viability assays, data were expressed as 95% confidence intervals (CI) . All calculations were performed on Microsoft Office Excel 2016 software and comparisons and normalizations were made between the untreated control and exposure (treated) groups.

Prior to any statistical analysis, the Shapiro Wilk (small sample sizes) normality test was performed to detect whether the sets of data are following the Gaussian (normal) distribution. Data passed the normality test [or lognormality test (values transformed into logarithms to create a Gaussian distribution)] and parametric tests were utilized accordingly.

Statistical significance for viability assays was assessed by one-way analysis of variance (one-way ANOVA) with Tukey's test for multiple comparisons (comparison between control and treated cells as well as between different treatment groups). CC50 values were calculated and expressed as 95% confidence intervals. GraphPad Prism 9.0.2 was used for statistical analysis and CC50 value calculations.

Statistical analysis for flow cytometry data was performed by one-way ANOVA with Tukey's test for multiple comparisons. Student's t-test was also used to compare the mean values for HDAC/HAT activity assays and western immunoblotting densitometry data (densitometry performed using Image J software V 1.4.3.67). IBM SPSS Statistics v.25 software was utilized for statistical analysis.

For all statistical analysis, a value of $p < 0.05$ was considered statistically significant and results with levels of significance were reported as *p≤ 0.05; ** p≤ 0.01; ***p≤0.001.

Chapter 3

Results

Results I – Cytotoxic effects of ITCs in an *in vitro* model of malignant melanoma

3.1 Profiling of ITCs-mediated Cytotoxic Effects Using an *in vitro* model of Malignant Melanoma

3.1.1 Cytotoxicity Profile: Determination of Cell Viability

To investigate the anti-melanoma effect of the five ITCs of interest (SFN, IBN, AITC, BITC and PEITC), in an *in vitro* experimental model of malignant melanoma consisting of human i) malignant melanoma (A375), ii) non-tumorigenic immortalized keratinocytes (HaCaT), iii) non-melanoma epidermoid carcinoma (A431), iv) melanoma derived from brain metastasis (VMM1), v) melanoma derived from lymph node metastasis Hs294T and vi) murine malignant melanoma (B16F10) cell lines. As keratinocytes and melanocytes are the main cells in the epidermis, this project aimed to determine the cytotoxic effect of these ITCs on human malignant melanoma (A375) cells in comparison to normal (HaCaT) keratinocytes and non-melanoma skin cancer (A431) cells. In addition, the cytotoxic potential of these ITCs not only in primary melanoma (A375) cells but also in metastatic-derived (VMM1 and Hs294T) ones was assessed. In order to address these objectives, the optimal experimental conditions capable of inducing cytotoxicity determined, in all the above-mentioned cell lines, by performing time-course (24 and 48hrs of exposure) and dose-response (2.5-50μM) kinetic experiments where cell viability was utilized as an endpoint of cytotoxicity, by using the resazurin assay.

Overall, it was shown that treatment with all 5 ITCs significantly decreased the viability of A375 (Figs. 3.1a, 3.2a, 3.3a, 3.4a, 3.5a), Hs294T (Figs. 3.1d, 3.2d, 3.3d, 3.4d, 3.5d) and B16F10 (Figs. 3.1f, 3.2f, 3.3f, 3.4f, 3.5f) cells in a concentration- and time-dependent manner in comparison to VMM1 (Figs. 3.1e, 3.2e, 3.3e, 3.4e, 3.5e), A431 (Figs. 3.1c, 3.2c, 3.3c, 3.4c, 3.5c) and HaCaT (Figs. 3.1b, 3.2b, 3.3b, 3.4b, 3.5b) cells. In the latter 3 cell lines, a noteworthy inhibition was evident, at concentrations of 25μM onwards. Reduced cell viability levels were reported, in our experiments, in as early as 24hrs of exposure in all 5 ITCs in A375, Hs 294T and B16F10 cells although this cytotoxic effect was even more profound after 48hrs of exposure.

In particular, regarding SFN, a reduction on viability levels of A375 (Fig. 3.1a) and B16F10 (Fig. 3.1f) cells was observed at 10 μM onwards. At this concentration the number of A375 viable cells was approximately 80% and 70%, at 24 and 48hrs of exposure respectively, while in B16F10 cells, 89% (at 24hrs) and 62% (at 48hrs). In Hs294T (Fig 3.1d), SFN treatment resulted in a more profound reduction in viability even at 5μM [by reaching 68% (at 24hrs) and 64% (at 48hrs)] suggesting that SFN was more cytotoxic in these cells.

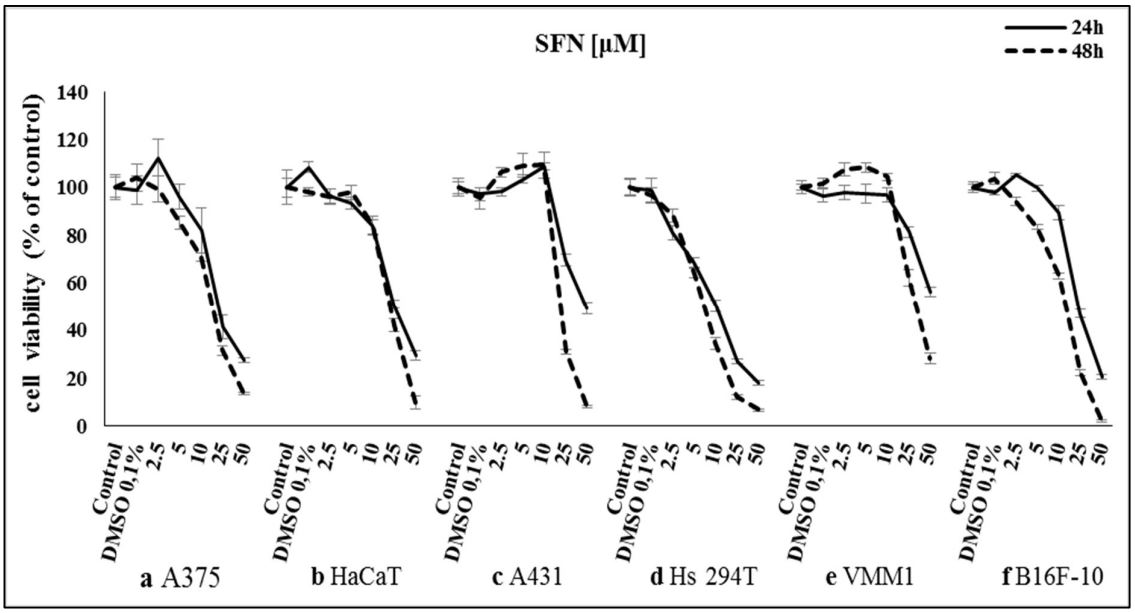

Figure 3.1: The effect of SFN in cell viability in an *in vitro* model of human malignant melanoma. Our *in vitro* model consisted of: **a**) malignant melanoma (A375), **b**) immortalized, normal keratinocyte (HaCaT), **c**) non-melanoma epidermoid carcinoma (A431), **d**) metastatic melanoma derived from lymph node (Hs294T), **e**) metastatic melanoma derived from brain (VMM1) and **f**) murine malignant melanoma (B16F10) cells. All cells were seeded into 96-well plates and next day they were exposed to a range of concentrations (2.5-50µM) of SFN for 24 and 48hrs. Cell viability was evaluated using the resazurin assay and was expressed as mean percentage of 0.1% v/v DMSO-treated (control) cells (as SFN was diluted in DMSO). Data shown are mean percentage of viable cells (n=5) expressed as 95%CI and are representative of three independent experiments. Statistical analysis performed using one-way ANOVA with Tukey's test for multiple comparisons and significance was set at *, $p<0.05$, **, $p<0.01$, ***, $p<0.001$, relative to corresponding (DMSO) controls.

As far as IBN, our data showed reduced viability levels as early as 24hrs of exposure, in both A375 (Fig 3.2a) and Hs294T (Fig 3.2d) cells at 10µM upwards. However, the reduction of cell viability was even greater at 48hrs of exposure and even at a concentration as low as 5µM. The viability of B16F10 cells (Fig 3.2f) was greatly reduced (at 10µM onwards) to 85% and 62% after 24 and 48hrs of exposure respectively.

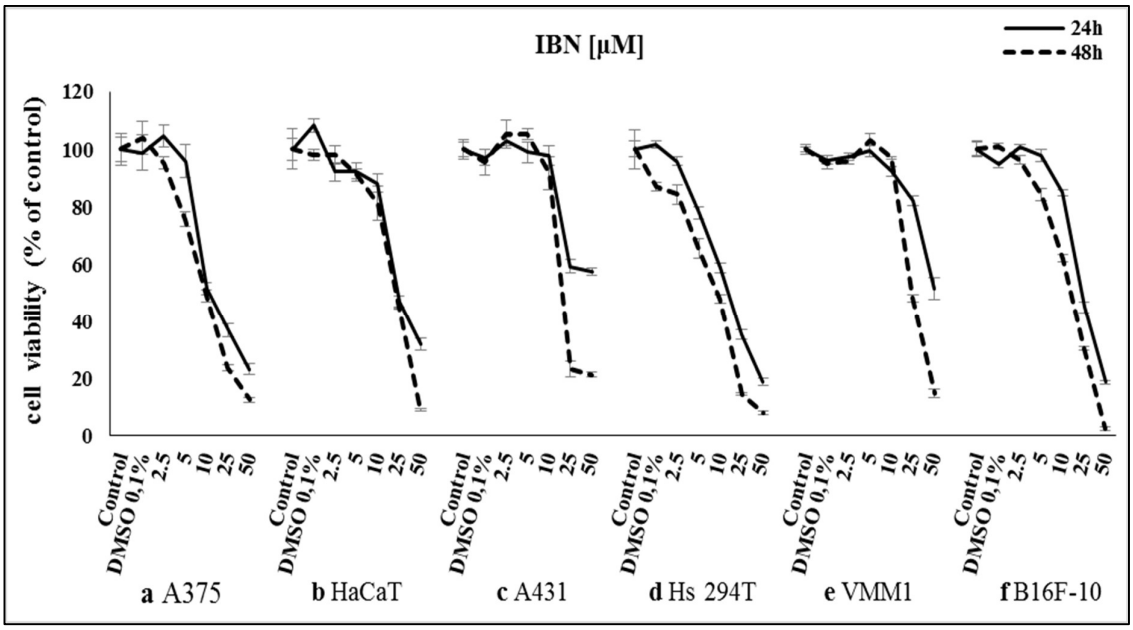

Figure 3.2: The effect of IBN in cell viability in an *in vitro* model of human malignant melanoma. Our *in vitro* model consisted of: **a**) malignant melanoma (A375), **b**) immortalized, normal keratinocyte (HaCaT), **c**) non-melanoma epidermoid carcinoma (A431), **d**) metastatic melanoma derived from lymph node (Hs294T), **e**) metastatic melanoma derived from brain (VMM1) and **f**) murine malignant melanoma (B16F10) cells. All cells were seeded into 96-well plates and next day they were exposed to a range of concentrations (2.5-50µM) of IBN for 24 and 48hrs. Cell viability was evaluated using the resazurin assay and was expressed as mean percentage of 0.1% v/v ETHO-treated (control) cells (as IBN was diluted in ETOH). Data shown are mean percentage of viable cells (n=5) expressed as 95%CI and are representative of three independent experiments. Statistical analysis performed using one-way ANOVA with Tukey's test for multiple comparisons and significance was set at *, $p<0.05$, **, $p<0.01$, ***, $p<0.001$, relative to corresponding (ETOH) controls.

Similarly, AITC was also found to reduce cell viability, at 10µM upwards, in A375 (Fig 3.3a), Hs294T (Fig 3.3d) and B16F10 (Fig 3.3f) cells. Specifically, at this concentration, AITC reduced the number of viable A375 cells to 80% and 70% after 24 and 48hrs of exposure respectively. Similarly, in Hs294T cells, cell viability was reduced to 85% and 75% while in B16F10 cells to 89% and 82% after 24 and 48hrs of exposure respectively.

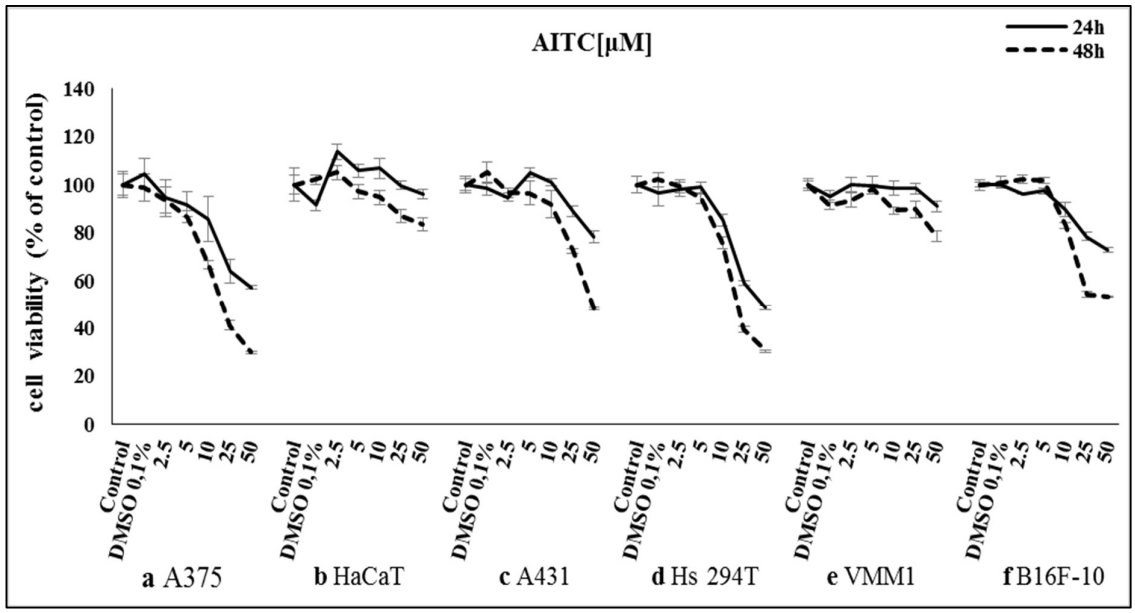

Figure 3.3: The effect of AITC in cell viability in an in vitro model of human malignant melanoma. Our *in vitro* model consisted of: **a**) malignant melanoma (A375), **b**) immortalized, normal keratinocyte (HaCaT), **c**) non-melanoma epidermoid carcinoma (A431), **d**) metastatic melanoma derived from lymph node (Hs294T), **e**) metastatic melanoma derived from brain (VMM1) and **f**) murine malignant melanoma (B16F10) cells. All cells were seeded into 96-well plates and next day they were exposed to a range of concentrations (2.5-50μM) of AITC for 24h and 48hrs. Cell viability was evaluated using the resazurin assay and was expressed as mean percentage of 0.1% v/v DMSO-treated (control) cells (as AITC was diluted in DMSO). Data shown are mean percentage of viable cells (n=5) expressed as 95%CI and are representative of three independent experiments. Statistical analysis performed using one-way ANOVA with Tukey's test for multiple comparisons. and significance was set at *, $p<0.05$, **, $p<0.01$, ***, $p<0.001$, relative to corresponding (DMSO) controls.

As far as BITC, a 30% reduction in cell viability was observed at 2.5 μM onwards in A375 cells at 48hrs of exposure (Fig 3.4a). At this condition, the viability of Hs294T (Fig 3.4d) and B16F10 (Fig 3.4f) cells was not significantly affected, while a noteworthy reduction was reported at 5μM onwards, after 48hrs of exposure, in both cell lines (61% and 76%, respectively.

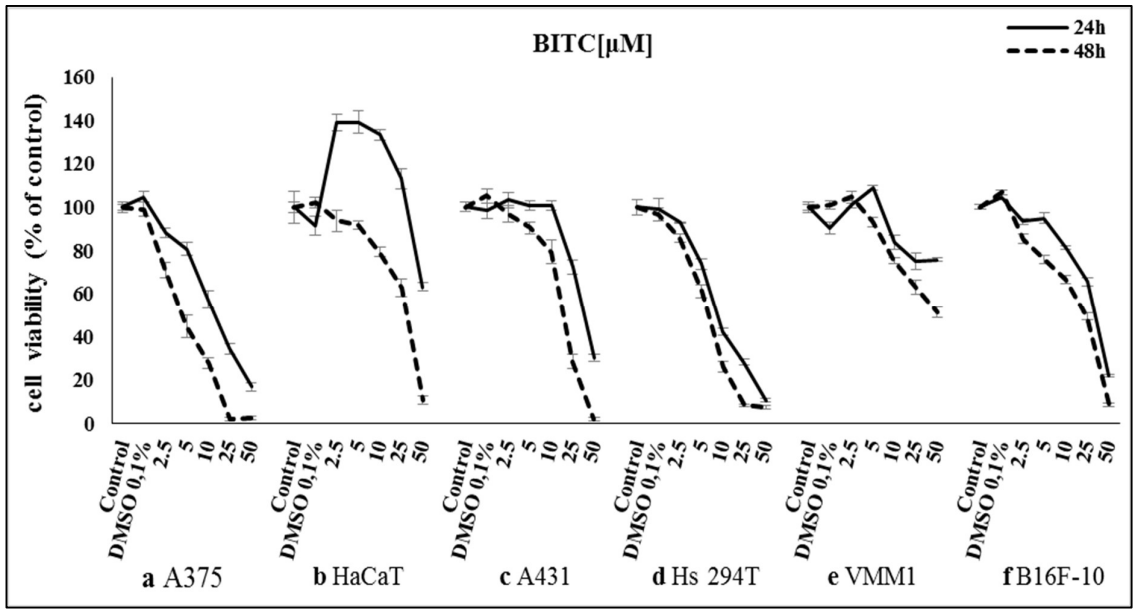

Figure 3.4: The effect of BITC in cell viability in an *in vitro* model of human malignant melanoma. Our *in vitro* model consisted of: **a**) malignant melanoma (A375), **b**) immortalized, normal, keratinocyte (HaCaT), **c**) non-melanoma epidermoid carcinoma (A431), **d**) metastatic melanoma derived from lymph node (Hs294T), **e**) metastatic melanoma derived from brain (VMM1) and **f**) murine malignant melanoma (B16F10) cells. All cells were seeded into 96-well plates and the next day they were exposed to a range of concentrations (2.5-50µM) of BITC for 24h and 48hrs. Cell viability was evaluated using the resazurin assay and was expressed as mean percentage of 0.1% v/v DMSO-treated (control) cells (as BITC was diluted in DMSO). Data shown are mean percentage of viable cells (n=5) expressed as 95%CI and are representative of three independent experiments. Statistical analysis performed using one-way ANOVA with Tukey's test for multiple comparisons and significance was set at *, $p<0.05$, **, $p<0.01$, ***, $p<0.001$, relative to corresponding (DMSO) controls.

Finally, PEITC reduced cell viability, in A375 (~61%) (Fig 3.5a) and B16F10 (~69%) (Fig 3.5f) cells at 25µM onwards, at 24hrs, whereas a greater reduction was observed at 10µM and 48hrs of exposure in both A375 (~53%) and B16F10 (~64%) cells. The reduction in cell viability levels was even further with Hs294T cells showing a 20% drop even at 5µM of PEITC after 48hrs of exposure (Fig 3.5d).

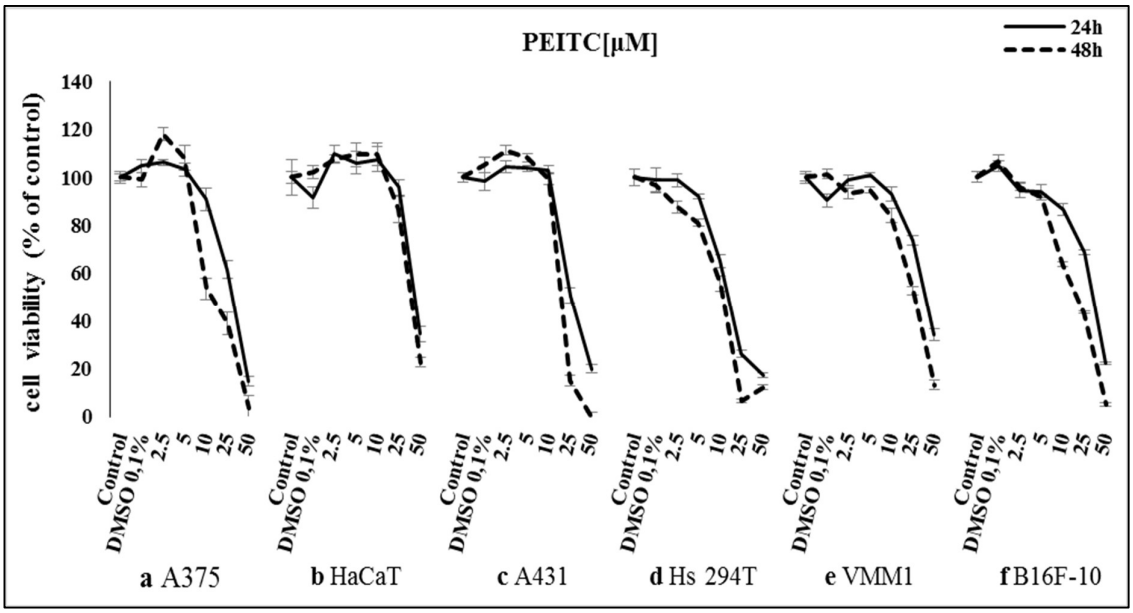

Figure 3.5: The effect of PEITC in cell viability in an *in vitro* model of human malignant melanoma. Our *in vitro* model consisted of: **a**) malignant melanoma (A375), **b**) immortalized, normal, keratinocyte (HaCaT), **c**) non-melanoma epidermoid carcinoma (A431), **d**) metastatic melanoma derived from lymph node (Hs294T), **e**) metastatic melanoma derived from brain (VMM1) and **f**) murine malignant melanoma (B16F10) cells. All cells were seeded into 96-well plates and the next day they were exposed to a range of concentrations (2.5-50μM) of PEITC for 24 and 48hrs. Cell viability was evaluated using the resazurin assay and was expressed as mean percentage of 0.1% v/v DMSO-treated (control) cells (as PEITC was diluted in DMSO). Data shown are mean percentage of viable cells (n=5) expressed as 95%CI and are representative of three independent experiments. Statistical analysis performed using one-way ANOVA with Tukey's test for multiple comparisons. and significance was set at *, $p<0.05$, **, $p<0.01$, ***, $p<0.001$, relative to corresponding (DMSO) controls.

On the contrary, no significant effect was observed on cell viability levels of A431 (Fig. 3.1c, 3.2c, 3.3c, 3.4c, 3.5c), VMM1 (Fig. 3.1e, 3.2e, 3.3e, 3.4e, 3.5e) and HaCaT (Fig. 3.1b, 3.2b, 3.3b, 3.4b, 3.5b) cells, under the same experimental conditions of ITC exposure, indicating a resistance against ITC-induced cytotoxicity. Specifically, the cytotoxic concentration, CC_{50} values (expressed with 95% confidence intervals),for each cell line, at 24 and 48hrs of ITC exposure, were calculated and summarized in Table 3.1. The overall statistical significance regarding the observed differences between the different treatment groups at 24 and 48hrs, was aslso assesses and summarized in Table 3.2. In general, a

significant reduction in cell viability was observed in all cell lines at concentrations of ITCs of 25μM upwards suggesting an induction of cytotoxicity exerted by these compounds. Taken altogether, our data suggest that A375, Hs294T and B16F10 cell lines are more sensitive to the cytotoxicity induced by all ITCs when compared to HaCaT, VMM1 and A431 ones. Furthermore, it appears that SFN, PEITC and IBN showed a higher cytotoxic potency against Hs294T cells while BITC and AITC were more potent against A375 cells. Overall, among all ITCs, BITC was shown to be the most potent whereas AITC the least potent one.

Based on the work described above, it was determined that a concentration of 10μM was the optimum one, in designing the next set of experiments, for further characterizing the cytotoxic profile of ITCs in our experimental *in vitro* melanoma model. This concentration (10μM) was chosen, as a significant reduction in viability levels was observed mainly in A375 melanoma cells, reflecting a selective specificity of ITCs towards the primary melanoma cell line. In higher concentrations, ITCs anticancer response is increased but demonstrated by a pattern of non-specificity towards both tumorigenic and non-tumorigenic cells.

Table 3.1: CC_{50} values of SFN, IBN, AITC, BITC and PEITC in A375, HaCaT, A431, VMM1, Hs294T and B16F10 cells, after 24 and 48hrs of exposure.

		A375	HaCaT	A431	VMM1	Hs294T	B16-F10
SFN	***$CC50_{24h}$ (μM)**	12.49 [10.45,14.92]	27.16 [25.54, 28.92]	46.02 [40.71, 53.26]	53.35 [50.82, 56.70]	8.501 [7.82, 9.238]	19.97 [19.25, 20.72]
	$CC50_{48h}$ (μM)	12.77 [11.71,13.94]	22.46 [17.20, 29.55]	22.92 [20.47, 28.96	31.96 [29.31, 34.92]	7.114 [6.73, 7.52]	12.63 [12.09, 13.20]
IBN	**$CC50_{24h}$ (μM)**	10.90 [9.40, 12.76]	21.51 [19.19, 24.11]	52.96 [44.11, 67.68]	42.43 [40.49, 44.60]	13.89 [12.81, 15.07]	23.24 [22.51, 24.00]
	$CC50_{48h}$ (μM)	8.65 [8.08, 9.27]	21.12 [16.56, 27.04]	19.12 [16.68, 21.91]	26.44 [24.87, 28.24]	8.525 [7.89, 9.20]	13.37 [12.40, 14.41]
AITC	**$CC50_{24h}$ (μM)**	12.40[9.72, 15.76]	ND	ND	ND	23.7 [19.60,27.82]	ND
	$CC50_{48h}$ (μM)	10.94 [9.88, 12.12]	ND	47.56 [45.09,50.45]	ND	22.49 [16.30,28,34]	15.065 [10.90,19.23]

Table 3.1: CC_{50} values of SFN, IBN, AITC, BITC and PEITC in A375, HaCaT, A431, VMM1, Hs294T and B16F10 cells, after 24 and 48hrs of exposure. (continued)							
BITC	**$CC50_{24h}$ (µM)**	10.71 [9.92, 11.56]	ND	36.43 [34.88, 38.05]	ND	7.602 [6.86, 8.44]	18.93 [17.60, 20.34]
	$CC50_{48h}$ (µM)	4.37 [4.04, 4.72]	26.49 [20.82, 33.92]	16.82 [15.81, 17.89]	45.37 [37.18, 58.70]	6.284 [5.89, 6.706]	12.15 [11.01, 13.36]
PEITC	**$CC50_{24h}$ (µM)**	19.13 [14.33, 25.3]	44.40 [41.23, 44.79]	26.89 [25.07, 28.91]	38.19 [36.61, 39.94]	12.76 [11.99, 13.60]	27.20 [26.02, 28.43]
	$CC50_{48h}$ (µM)	10.31 [8.843,12.18]	34.23 [28.03, 41.22]	19.78 [17.00, 21.75]	24.25 [22.50, 26.04]	10.24 [9.208, 11.36]	15.74 [14.95, 16.57]

*CC50 are expressed as 95% CI, calculated using GraphPad Prism.

Table 3.2: Statistical significance of the differences among SFN, IBN, AITC, BITC and PEITC in A375, HaCaT, A431, VMM1, Hs294T and B16F10 cells at 24 and 48hrs of exposure.

	24h		48h	
	P value	**Asterisk**	**P value**	**Asterisk**
A375	0.0318	*	<0.0001	***
HaCaT	0.2763	ns	0.0029	**
A431	0.8251	ns	0.0528	ns
Hs 294T	<0.0001	***	0.0052	**
VMM1	0.1504	ns	0.0057	**
B16F-10	0.0053	**	0.0007	***

Statistical significance was assessed by one-way ANOVA with Tukey's test for multiple comparisons. Using GraphPad Prism. Significance was set at *, $p<0.05$, **, $p<0.01$, ***, $p<0.001$.

3.1.2 Cytotoxicity Profile: Determination of Cell Cycle Growth Arrest

In this set of experiments, we have focused on determining the effect of 10µM of all 5 ITCs in affecting cell cycle progression in all cell lines at both 24 and 48hrs of exposure. To do so, the FxCycle PI/RNase staining solution was utilised in order to quantitate the content of DNA under each phase of the cell cycle and thereby analyse the distribution of cells in each phase of the cell cycle by flow cytometry (Figure S1 under supplementary material).

Overall, in A375 cells, an induction of the G2/M phase was observed by all ITCs but to a variable degree (Fig. 3.6). Specifically, exposure to BITC (Fig. 3.6d) caused the highest increase in the number of cells accumulated at the G2/M phase, which was intensified after 48hrs of treatment, followed by IBN (Fig. 3.6b) which also exhibited a similar effect. Additionally, SFN (Fig. 3.6a) and PEITC (Fig. 3.6e) also increased the number of cells at

the G2/M phase, when compared to untreated cells, but to a lower extent. This pattern was followed by a significant reduction in the number of cells at the G1 phase for all ITCs. Furthermore, the S phase remained relatively unaffected under treatment with BITC (Fig. 3.6d), IBN (Fig. 3.6b) and SFN (Fig. 3.6a) but not for PEITC (Fig. 3.6e). Interestingly, exposure to AITC although initially showed an induction at the G2/M growth arrest in A375 cells (alongside with reduced levels of the G1 phase), a shift of cell accumulation back to the G1 phase was observed, after 48hrs of exposure, with such levels reaching control ones (Fig. 3.6c). No significant differences were observed in the distribution of cells in S phase between AITC-treated and untreated (control) cells at both time points of exposure. Finally, our data showed a profound elevation in the number of dead cells, observed as an increase in the sub-G1phase, after 48hrs of exposure to all ITCs apart from AITC (Fig. 3.6).

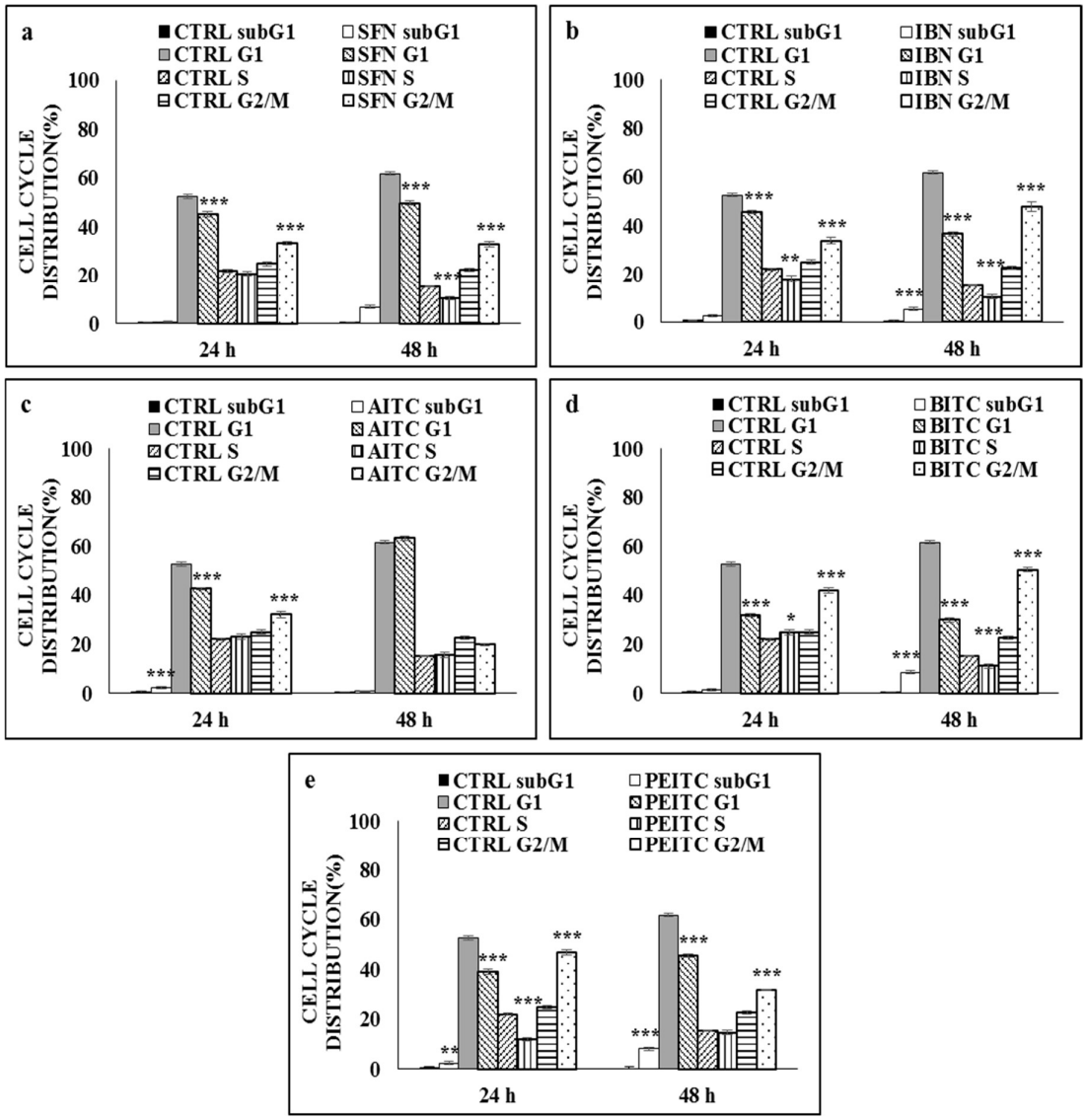

Figure 3.6: The effect of ITCs in cell cycle progression of A375 cells. Cells were exposed to 10μM of **a**) SFN, **b**) IBN, **c**) AITC, **d**) BITC and **e**) PEITC at 24 and 48hrs of exposure. The distribution of cells in sub-G1, G1, S and G2/M phases of the cell cycle were recorded by flow cytometry and quantified as percentage of cells (based on cellular DNA content) present in each phase of the cell cycle. Results are expressed as mean ± SD of three replicates. Data are representatives of three independent experiments. Statistical analysis performed by one-way ANOVA with Tukey's test for multiple comparisons. Asterisks indicate statistical significance at *, $p<0.05$, **, $p<0.01$, ***, $p<0.001$ when compared to their respective untreated control cells.

Similarly, in metastatic melanoma derived from lymph node (Hs294T) cells, both BITC (Fig. 3.7d) and PEITC (Fig. 3.7e), were capable of inducing a growth arrest at the G2/M phase, in

both time points of exposure, although the effect was not as potent as in A375 cells. In addition, AITC did not cause any significant effect in the distribution of Hs294T cells in any of the cell cycle phases when compared to untreated cells (Fig. 3.7c). Alternatively, BITC (Fig. 3.7d) was the most potent in blocking cell cycle progression followed by PEITC (Fig. 3.7e). Under these conditions, an increased accumulation of cells at the G2/M phase was accompanied by a reduced distribution of cells at the G1 phase, a pattern similar with that observed also under treatment with SFN and IBN (Figs. 3.7a & 3.7b respectively). It is noteworthy that the effect of SFN and IBN in growth arresting cells at the G2/M phase was greater at 24hrs of exposure as opposed to 48hrs where the percentage of cellular distribution reached control levels. In general, treatment with these two ITCs did not have a significant effect on levels of growth arrest as most cells were found at the G1 phase (Figs. 3.7a & 3.7b). In addition, our results showed that 24hrs of exposure to BITC (Fig. 3.7d) and PEITC (Fig. 3.7e) did cause a significant elevation of cells at the sub-G1 and S phases, compared to control cells; an effect which was maintained even at 48hrs of exposure to these ITCs.

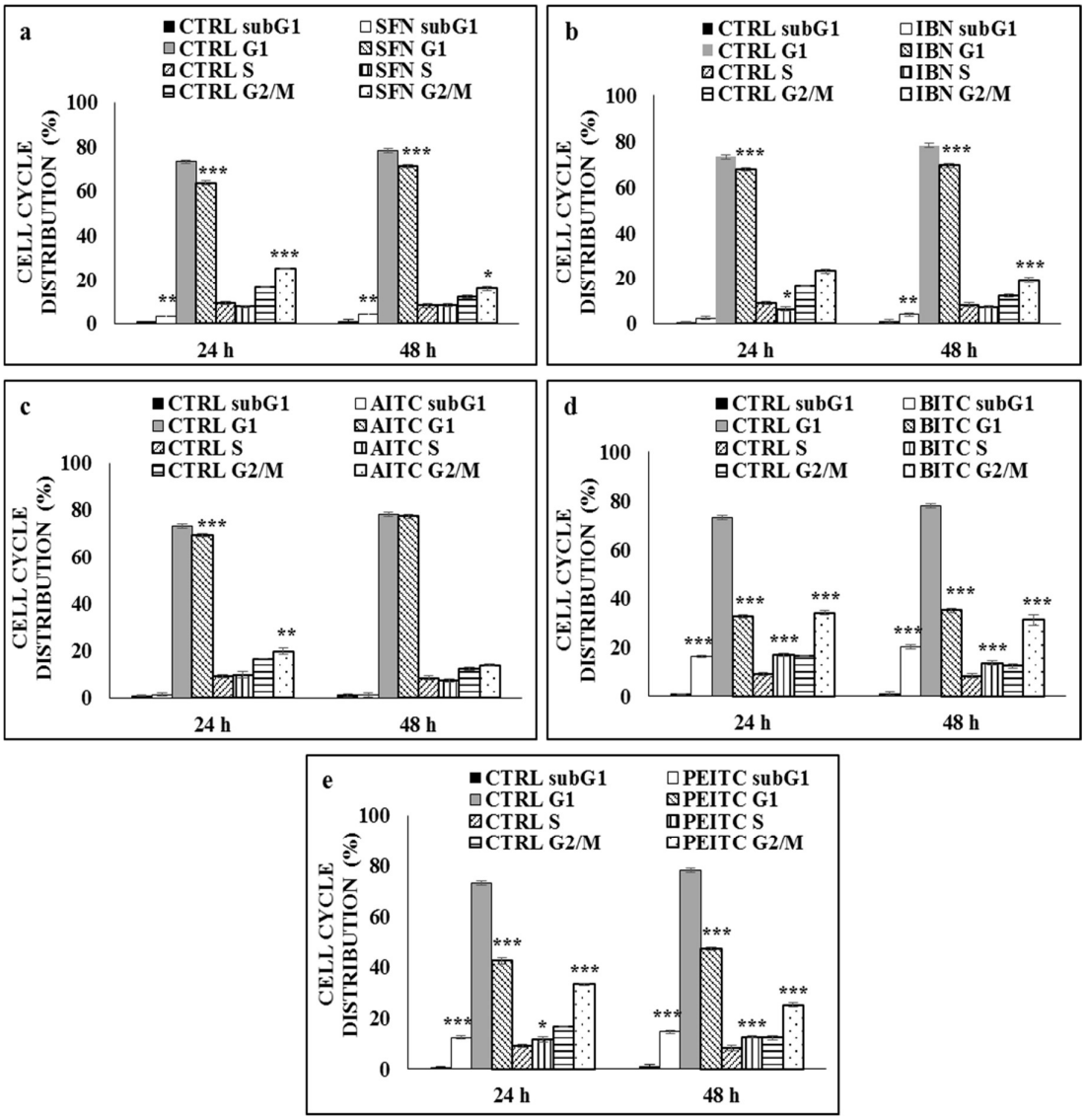

Figure 3.7: The effect of ITCs in cell cycle progression of Hs294T cells. Cells were exposed to10μM of **a**) SFN, **b**) IBN, **c**) AITC, **d**) BITC and **e**) PEITC at 24 and 48hrs of exposure. The distribution of cells in sub-G1, G1, S and G2/M phases of the cell cycle were recorded by flow cytometry and quantified as percentage of cells (based on cellular DNA content) present in each phase of the cell cycle. Results are expressed as mean ± SD of three replicates and are representatives of three independent experiments. Statistical analysis performed by one-way ANOVA with Tukey's test for multiple comparisons. Asterisks indicate statistical significance at *, $p<0.05$, **, $p<0.01$, ***, $p<0.001$ when compared to their respective untreated control cells.

With respect to metastatic melanoma derived from brain (VMM1) cells, it was shown that 24hrs of exposure to SFN (Fig. 3.8a) and IBN (Fig. 3.8b), resulted in a significant elevation

of cells at the G2/M phase, followed by a reduction of the G1 phase while the S phase remained relatively unaffected. On another note, 24hrs exposure to BITC (Fig. 3.8d) and PEITC (Fig. 3.8e) induced growth arrest at the S phase while at 48hrs of exposure, a shift towards the G2/M phase was reported (alongside with a further reduction of cells at the G1 phase). In addition, both BITC and PEITC significantly increased the number of cells at the sub-G1 phase, after 48hrs of exposure. Interestingly, a marked reduction of the G1 alongside with an increase in S phase were observed when VMM1 cells were exposed to AITC in both at both time points (Fig. 3.8c).

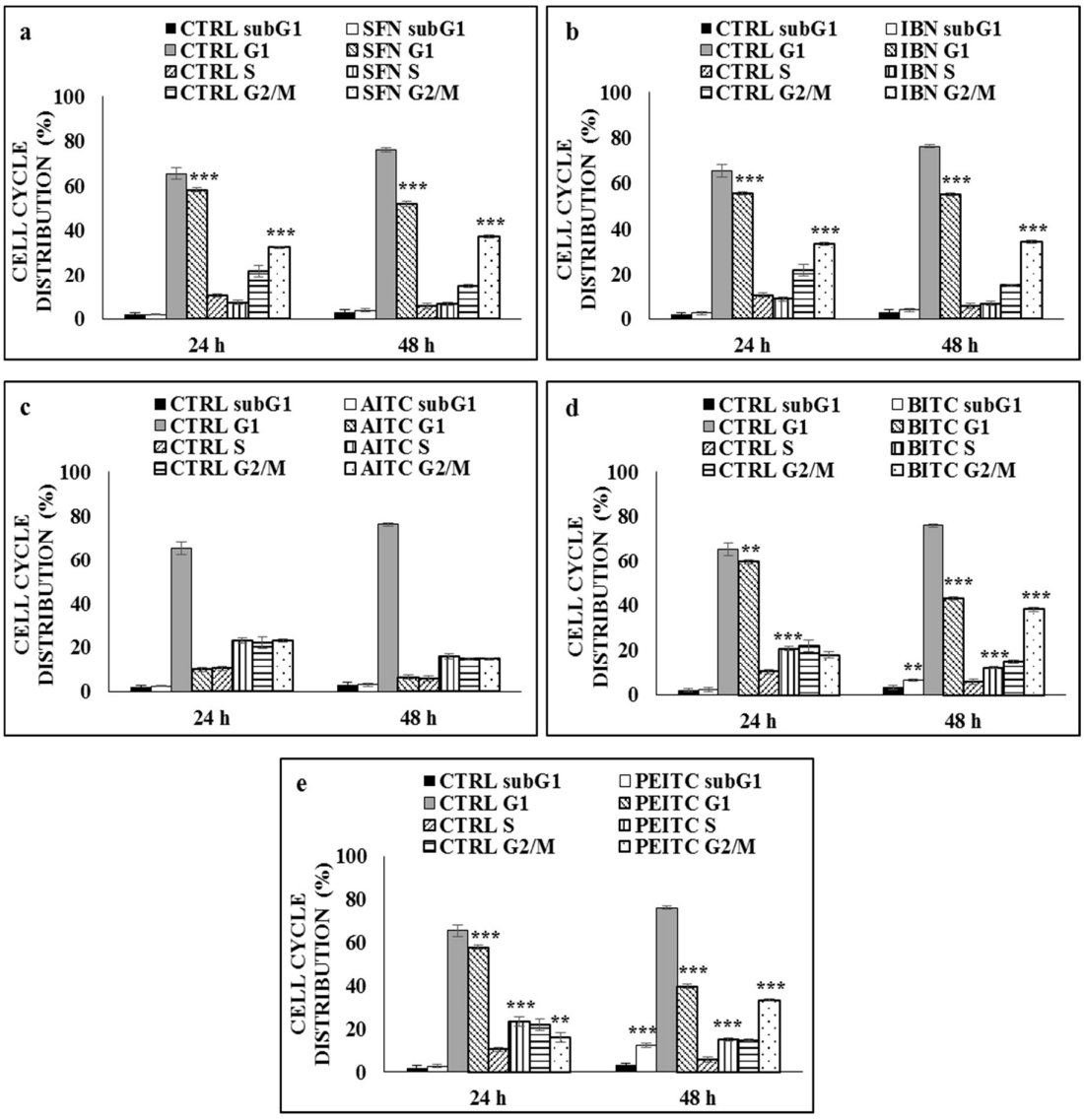

Figure 3.8: The effect of ITCs in cell cycle progression of VMM1 cells. Cells were exposed to10μM of **a**) SFN, **b**) IBN, **c**) AITC, **d**) BITC and **e**) PEITC at 24 and 48hrs of exposure. The distribution of cells in sub-G1, G1, S and G2/M phases of the cell cycle were

recorded by flow cytometry and quantified as percentage of cells (based on cellular DNA content) present in each phase of the cell cycle. Results are expressed as mean ± SD of three replicates and are representatives of three independent experiments. Statistical analysis performed by one-way ANOVA with Tukey's test for multiple comparisons. Asterisks indicate statistical significance at *, $p<0.05$, **, $p<0.01$, ***, $p<0.001$ when compared to their respective untreated control cells.

In non-melanoma epidermoid carcinoma (A431) cells, an elevation in G2/M phase was observed accompanied by a reduction in G1 phase after 24hrs of exposure to BITC and PEITC respectively (Figs. 3.9d & 3.9e), an effect which was maintained even at 48hrs of exposure to BITC, PEITC and SFN as well (although not as profound) (Fig. 3.9a). Moreover, PEITC (Fig. 3.9e) and IBN (Fig. 3.9b) reduced the number of cells accumulated in S phase, a pattern which was more profound at 24hrs of exposure while at 48hrs the number of cells was reported to be comparable to control levels. Interestingly, exposure to AITC caused no significant differences in the distribution of cells at all phases of cell cycle (Fig. 3.9c). Finally, the population of dead cells (showed as cellular distribution at the sub-G1 phase) was significantly enhanced after exposure to BITC, PEITC and slightly to IBN but not with SFN and AITC (Fig. 3.9).

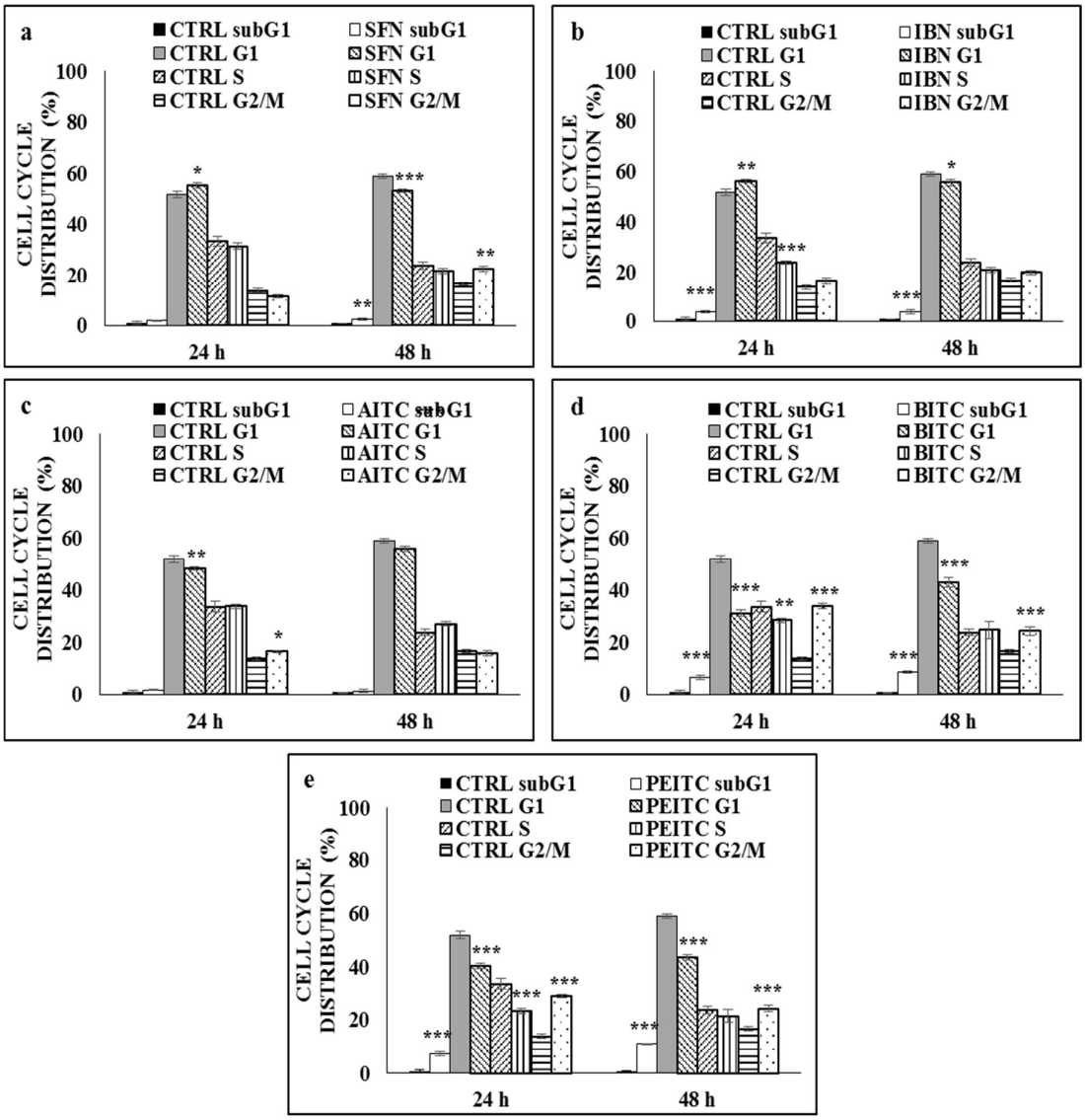

Figure 3.9: The effect of ITCs in cell cycle progression of A431 cells. Cells were exposed to10μM of **a**) SFN, **b**) IBN, **c**) AITC, **d**) BITC and **e**) PEITC at 24 and 48hrs of exposure. The distribution of cells in sub-G1, G1, S and G2/M phases of the cell cycle were recorded by flow cytometry and quantified as percentage of cells (based on cellular DNA content) present in each phase of the cell cycle. Results are expressed as mean ± SD of three replicates and are representatives of three independent experiments. Statistical analysis performed by one-way ANOVA with Tukey's test for multiple comparisons. Asterisks indicate statistical significance at *, $p<0.05$, **, $p<0.01$, ***, $p<0.001$ when compared to their respective untreated control cells.

In transformed, normal, keratinocyte (HaCaT) cells, exposure to SFN (Fig. 3.10a) and IBN (Fig. 3.10b) induced cell cycle arrest at the G1 phase followed by reduced levels of the S

phase at 24hrs of exposure, an effect which was not persistent at 48hrs of similar exposure. In addition, our results showed that BITC growth arrested cells at the G2/M phase which was further accompanied with a reduction of cells in S phase, during 24hrs of exposure (Fig. 3.10d). However, at 48hrs of exposure, the cellular distribution at G2/M and S phases was reduced to control levels together with that of the G1 phase. Moreover, exposure to AITC and PEITC exerted a similar effect (Figs. 3.10c & 3.10e, respectively) indicated as a decrease of cells at the G1 phase along with a slight increase in G2/M and S phases. In addition, a decrease in S phase was observed at 24hrs of exposure (but not at 48hrs) in cells exposed to AITC (Fig. 3.10c). Finally, the number of dead cells (sub-G1 phase) remained quite low even after 48hrs of exposure to all ITCs (Fig. 3.10).

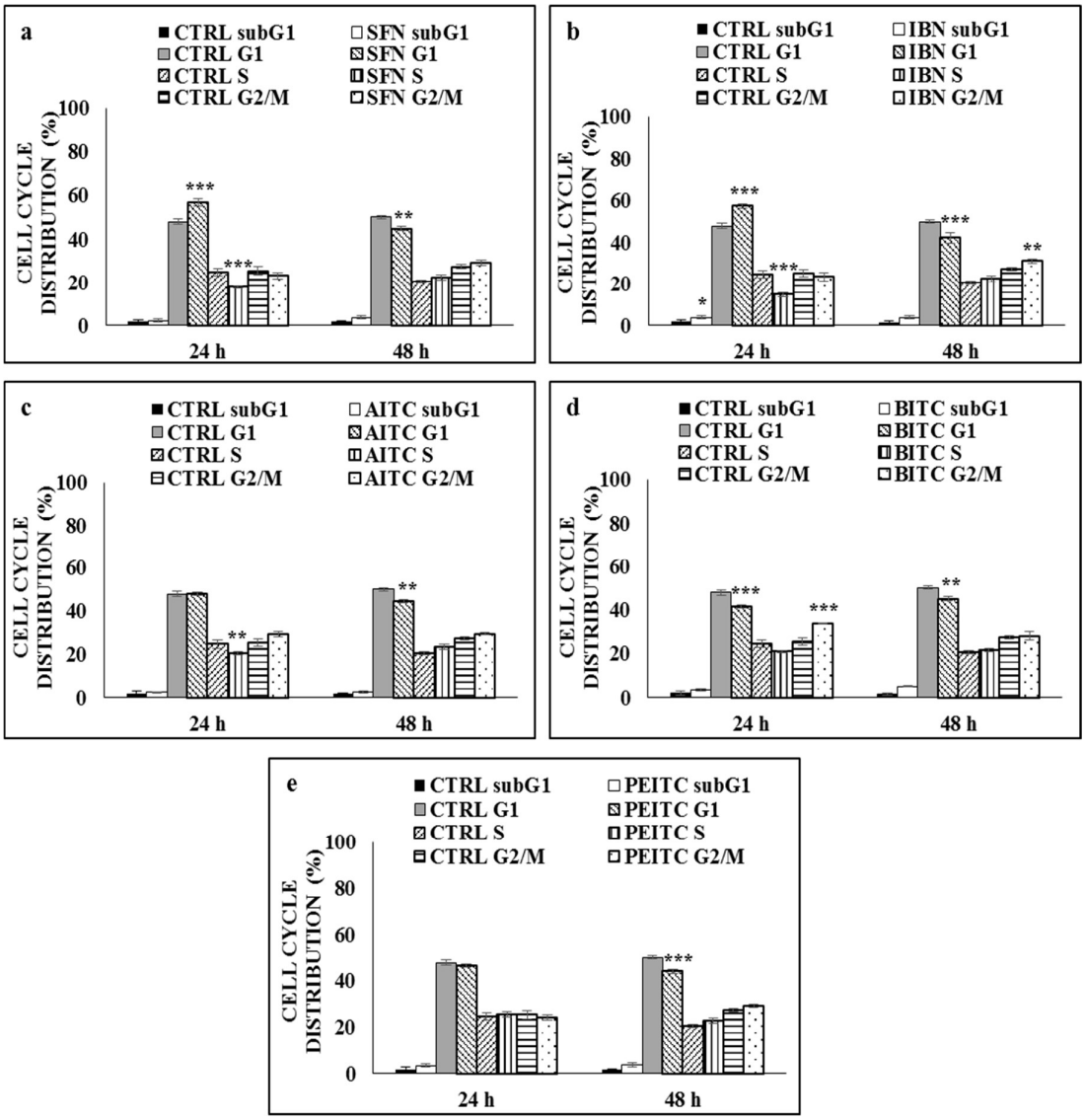

Figure 3.10: The effect of ITCs in cell cycle progression of HaCaT cells. Cells were exposed to10μM of **a**) SFN, **b**) IBN, **c**) AITC, **d**) BITC and **e**) PEITC at 24 and 48hrs of exposure. The distribution of cells in sub-G1, G1, S and G2/M phases of the cell cycle were recorded by flow cytometry and quantified as percentage of cells (based on cellular DNA content) present in each phase of the cell cycle. Results are expressed as mean ± SD of three replicates and are representatives of three independent experiments. Statistical analysis performed by one-way ANOVA with Tukey's test for multiple comparisons. Asterisks indicate statistical significance at *, $p<0.05$, **, $p<0.01$, ***, $p<0.001$ when compared to their respective untreated control cells.

On the other hand, the kinetics of cell cycle growth arrest in B16F10 cells remained relatively unaffected after exposure to any of the ITCs (Fig. 3.11). However, it is noteworthy, that we

observed a slight increase of cells at the G2/M phase, whereas those at the G1 phase were slightly decreased under BITC and PEITC exposure in both time points (Figs 3.11d & 3.11e). Furthermore, PEITC showed an increased accumulation of cells at the S phase and subsequently a diminished G2/M, after 48hrs of exposure (Fig. 3.11e). Overall, our data suggest that exposure to all 5 ITCs exerted a potent effect in growth arresting cells at various phases of the cell cycle when compared to unexposed (control) cells.

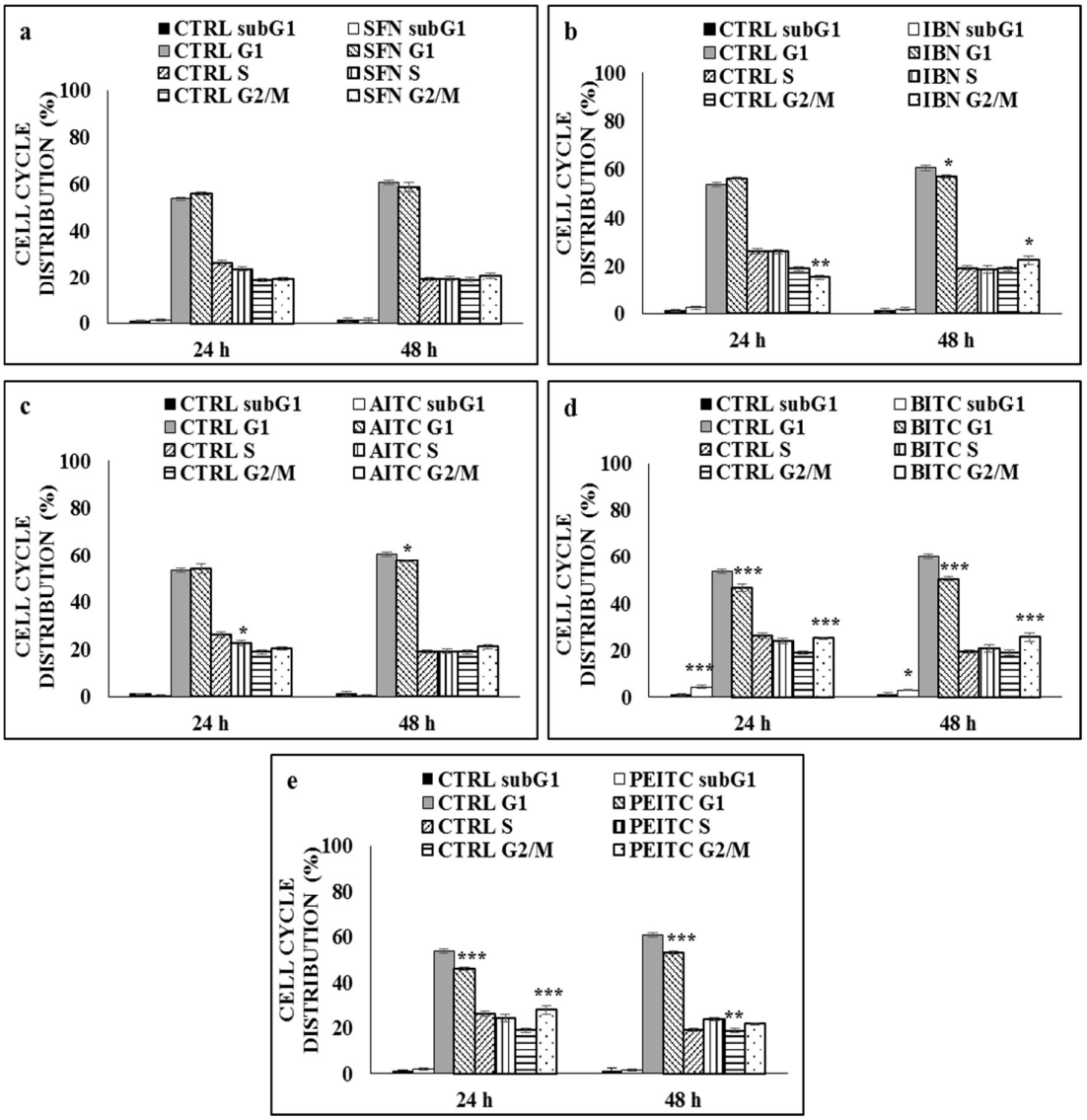

Figure 3.11: The effect of ITCs in cell cycle progression of B16F10 cells. Cells were exposed to10μM of **a**) SFN, **b**) IBN, **c**) AITC, **d**) BITC and **e**) PEITC at 24 and 48hrs of exposure. The distribution of cells in sub-G1, G1, S and G2/M phases of the cell cycle were recorded by flow cytometry and quantified as percentage of cells (based on cellular DNA content) present in each phase of the cell cycle. Results are expressed as mean ± SD of three

replicates and are representatives of three independent experiments. Statistical analysis performed by one-way ANOVA with Tukey's test for multiple comparisons. Asterisks indicate statistical significance at *, $p<0.05$, **, $p<0.01$, ***, $p<0.001$ when compared to their respective untreated control cells.

3.1.3: Cytotoxicity Profile: Determination of Cell Death Induction

In this set of experiments, we used flow cytometry to distinguish between populations of apoptotic and necrotic cells. All cell lines were subjected to 10μM of each one of the 5 ITCs for 24 and 48hrs of exposure. To distinguish between these two modes of cell death, the Cell Event Caspase 3/7 Green detection reagent was utilized as a detector of activated caspase 3 and caspase 7 in apoptotic cells while DAPI was utilized as an indicator of necrosis. Flow cytometry histograms for all experiments are represented in Figure S2 (under supplementary material).

In particular, in A375 cells, our data showed that SFN, IBN, BITC and PEITC were able to induce cell death, during the first 24h, an effect which was intensified over time, in a manner where live cells were reduced, while necro-apoptotic cells increased markedly (Fig. 3.12). Apoptotic induction in these cells was indicated by the increased levels of cells stained positive for activated caspase 3/7 compared to untreated ones. BITC (Fig. 3.12d) was the most potent one in triggering cell death followed by PEITC (Fig. 3.12e). The population of cells that had undergone apoptosis, during 24hrs of exposure to BITC and PEITC, was higher compared to the necrotic one while at 48hrs, a significant elevation of necrosis was noted. Moreover, SFN (Fig. 3.12a) and IBN (Fig. 3.12b) showed similar levels of necrosis and apoptosis, at both time points, while AITC did not significantly affect cell death (Fig. 3.12c).

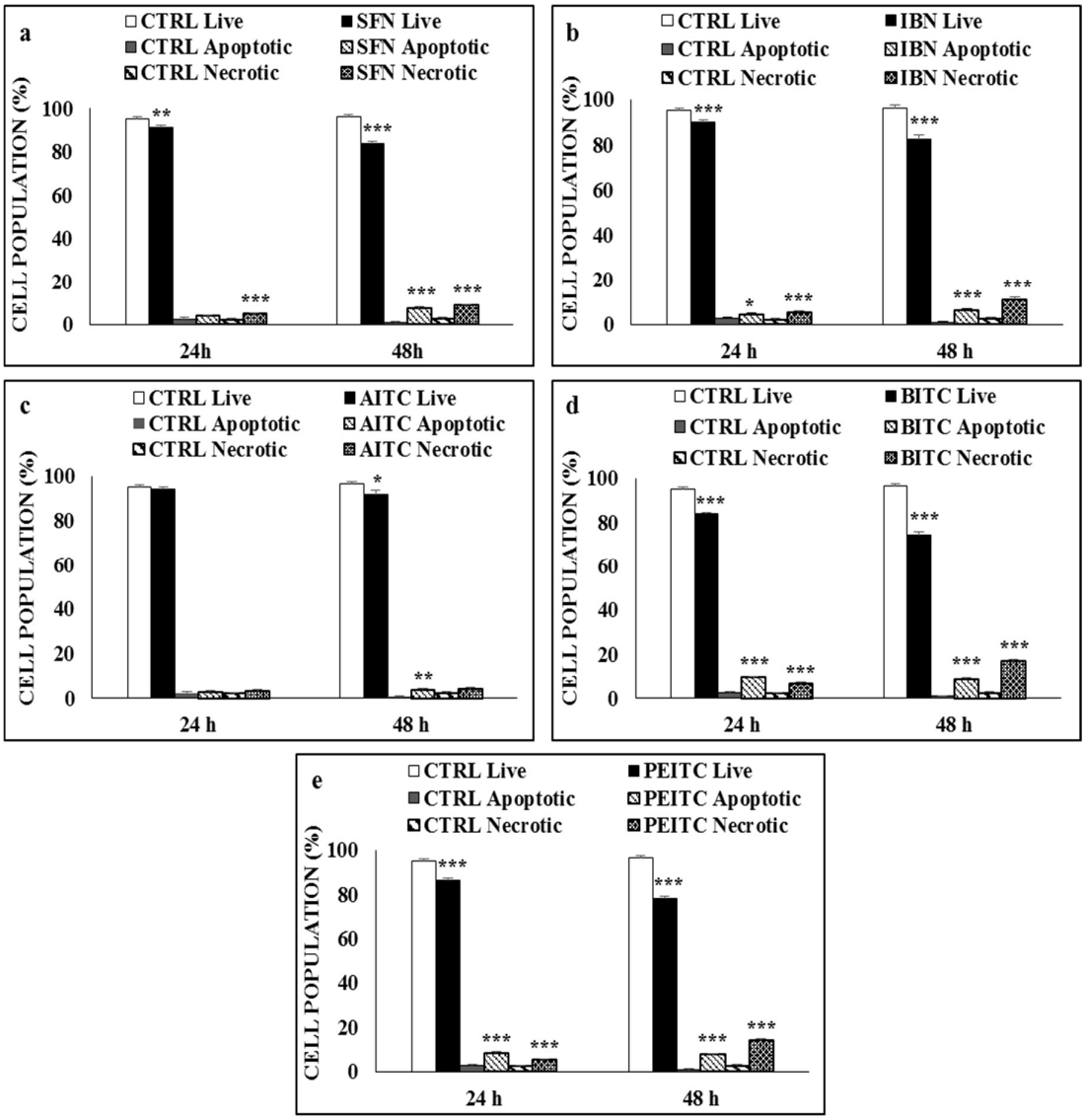

Figure 3.12: ITCs-induced cell death in A375 cells. Cells were exposed to 10μM of **a**) SFN, **b**) IBN, **c**) AITC, **d**) BITC and **e**) PEITC for 24 and 48hrs and the percentage of live, apoptotic and necrotic cells was recorded by flow cytometry. Results are expressed as mean ± SD of three replicates and are representatives of three independent experiments. Statistical analysis performed by one-way ANOVA with Tukey's test for multiple comparisons. Asterisks denote statistical significance at *, $p<0.05$, **, $p<0.01$, ***, $p<0.001$ when compared to their respective untreated control cells.

Next, in Hs294T cells, a slight increase in the percentage of dead cells after 24hrs of exposure to SFN (~18%) and IBN (~16%) was observed as compared to control (~13%) with similar levels being recorded at 48hrs as well (Figs. 3.13a & 3.13b). However, excessive cell death was observed after exposure to BITC and PEITC (Figs. 3.13d & 3.13e, respectively). In

particular, a dramatic reduction in the number of viable cells followed by a marked increase in the number of caspase 3/7 positive-stained (apoptotic) and to a greater extent of DAPI-positive (necrotic) cells was observed at 24hrs post-exposure to BITC and PEITC. Interestingly, at 48hrs of exposure to these two ITCs, the number of apoptotic cells was decreased while the necrotic one increased significantly, reaching approximately 48% and 46% under BITC and PEITC exposure respectively.

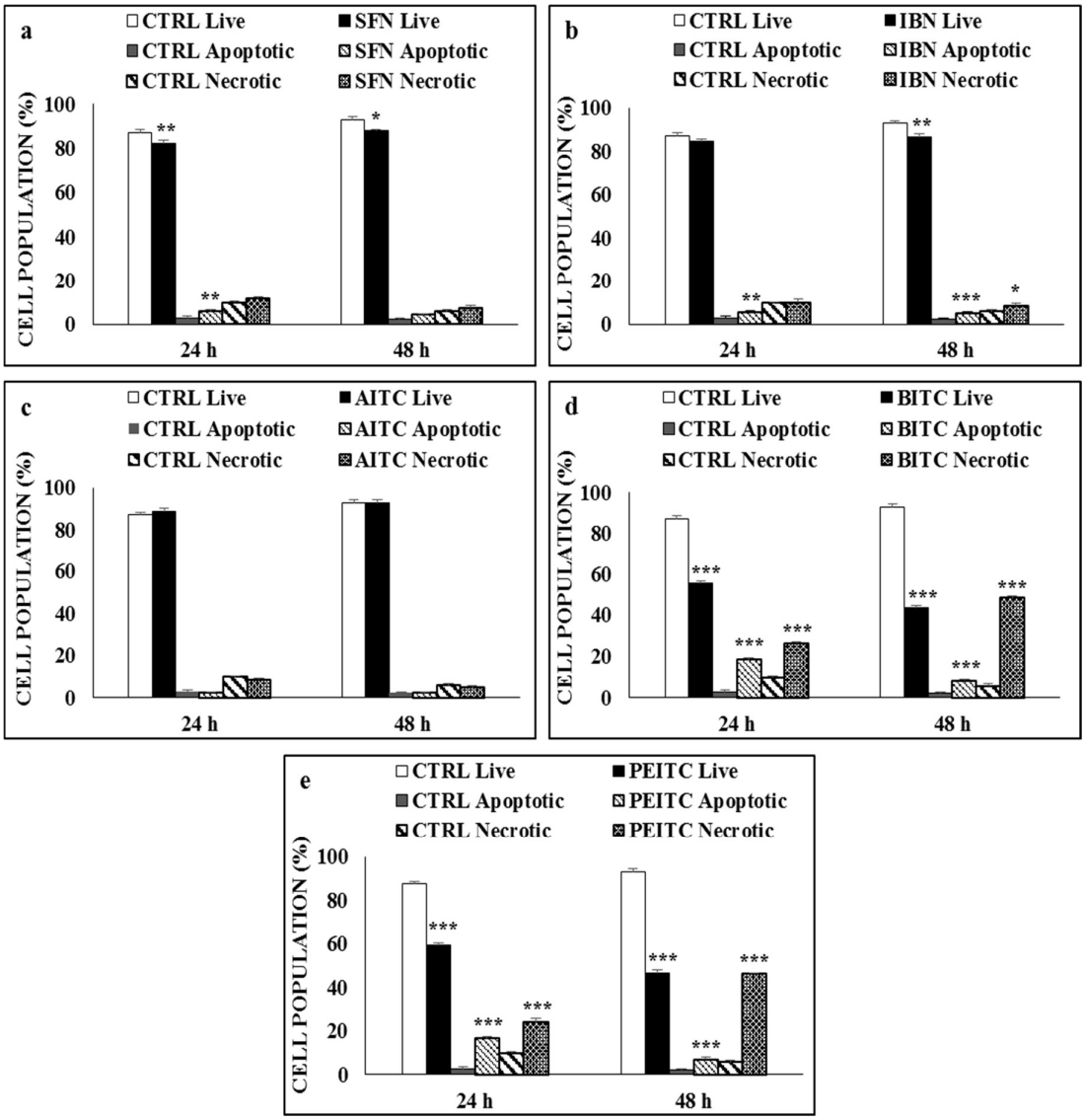

Figure 3.13: ITCs-induced cell death in Hs294T cells. Cells were exposed to 10μM of **a**) SFN, **b**) IBN, **c**) AITC, **d**) BITC and **e**) PEITC for 24 and 48hrs and the percentage of live, apoptotic and necrotic cells was recorded by flow cytometry. Results are expressed as mean ± SD of three replicates and are representatives of three independent experiments. Statistical analysis performd by one-way ANOVA with Tukey's test for multiple comparisons.

Asterisks denote statistical significance at *, $p<0.05$, **, $p<0.01$, ***, $p<0.001$ when compared to their respective untreated control cells.

Furthermore, when VMM1 cells were exposed to all 5 ITCs, an increase in dead cells was observed, especially under exposure to SFN, IBN, BITC and PEITC. However, such effect was not as significant in A375 and Hs294T cells (Fig. 3.14). In contrast, exposure to AITC did not alter the levels of dead cells (Fig. 3.14c). More specifically, at 24hrs of exposure, an elevation in the number of DAPI-positive cells was noted by SFN (Fig. 3.14a), IBN (Fig. 3.14b), BITC (Fig. 3.14d) and PEITC (Fig. 3.14e) while BITC and PEITC also induced apoptosis at this time point. However, at 48hrs, PEITC exposure reduced the number of apoptotic cells whereas BITC and IBN exposure increased the number of apoptotic cells while necrotic ones remained at relatively steady levels.

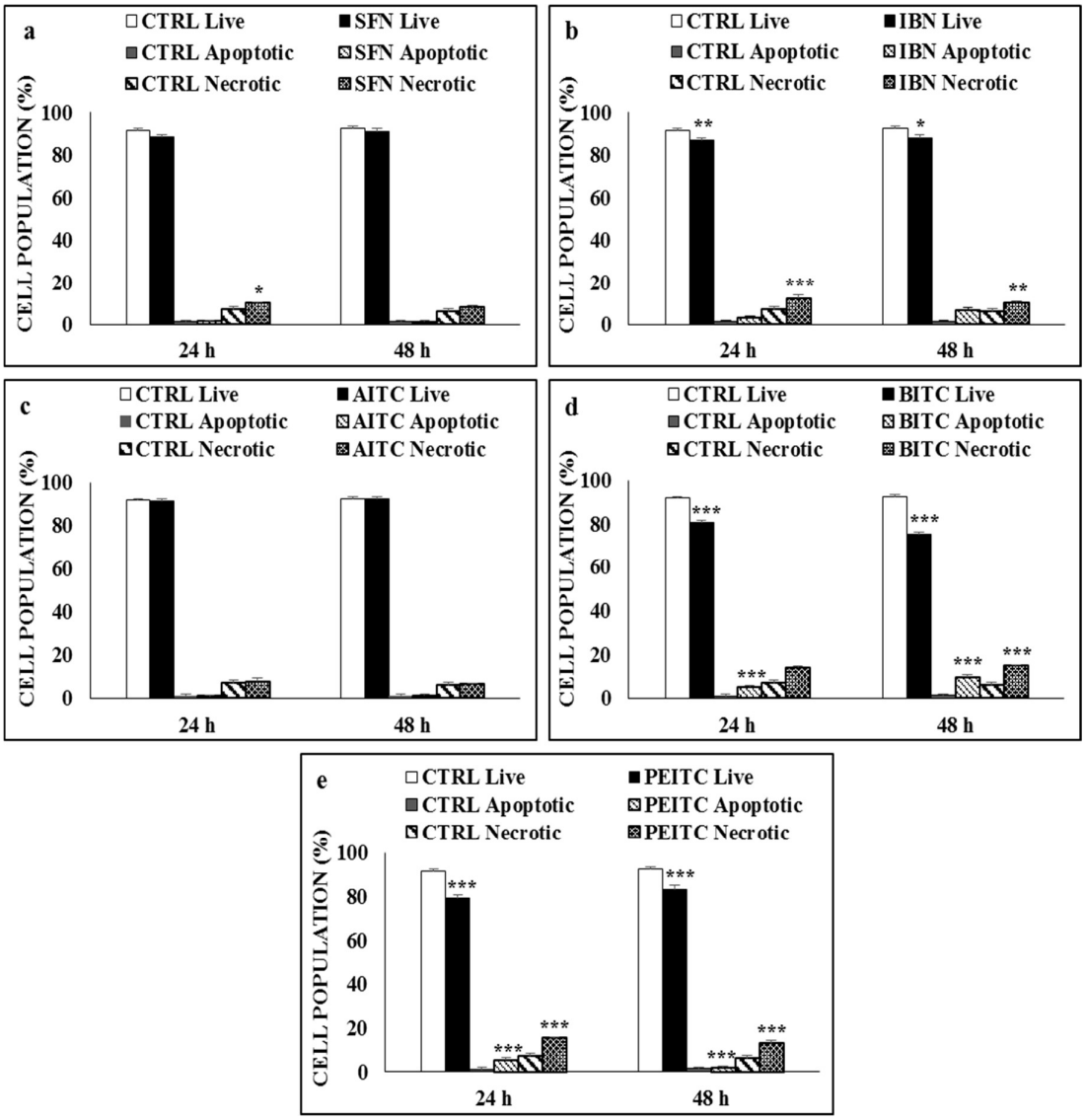

Figure 3.14: ITCs-induced cell death in VMM1 cells. Cells were exposed to 10μM of **a**) SFN, **b**) IBN, **c**) AITC, **d**) BITC and **e**) PEITC for 24 and 48hrs and the percentage of live, apoptotic and necrotic cells was recorded by flow cytometry. Results are expressed as mean ± SD of three replicates and are representatives of three independent experiments. Statistical analysis performd by one-way ANOVA with Tukey's test for multiple comparisons. Asterisks denote statistical significance at *, $p<0.05$, **, $p<0.01$, ***, $p<0.001$ when compared to their respective untreated control cells.

In non-melanoma epidermoid carcinoma (A431) cells, increased levels of cell death were observed after exposure to BITC and PEITC but not with SFN, IBN and AITC (Fig. 3.15). In particular, BITC induced caspase 3/7 activation at 24hrs of exposure (Fig. 3.15d), an effect which was enhanced even after 48hrs of exposure together with necrosis. Finally,

exposure to PEITC resulted in elevated levels of both caspase3/7-positive and DAPI-positive cells but only 48hrs post exposure (Fig. 3.15e).

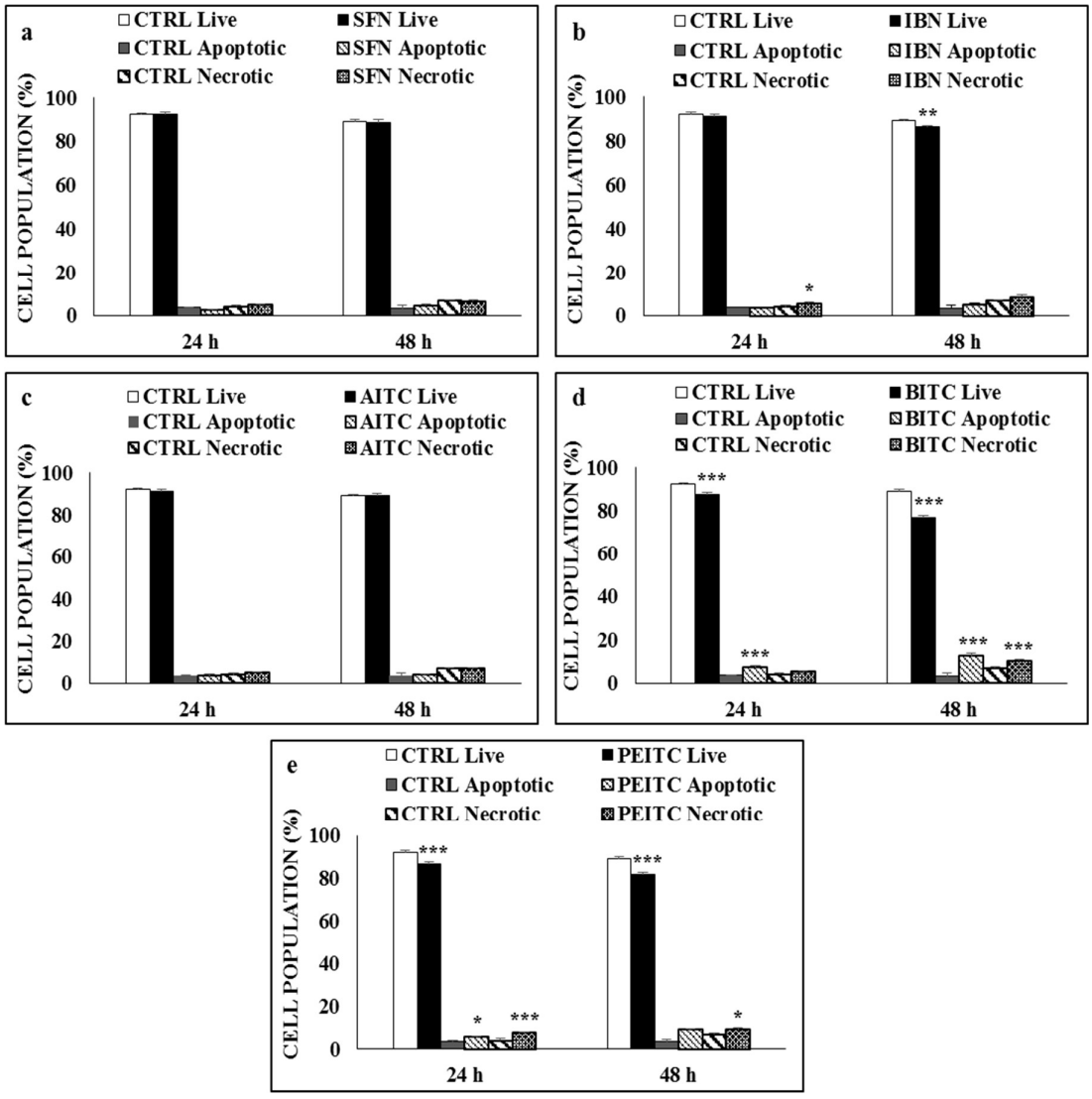

Figure 3.15: ITCs-induced cell death in A431 cells. Cells were exposed to 10μM of **a**) SFN, **b**) IBN, **c**) AITC, **d**) BITC and **e**) PEITC for 24 and 48hrs and the percentage of live, apoptotic and necrotic cells was recorded by flow. Results are expressed as mean ± SD of three replicates and are representatives of three independent experiments. Statistical analysis performd by one-way ANOVA with Tukey's test for multiple comparisons. Asterisks denote statistical significance at *, $p<0.05$, **, $p<0.01$, ***, $p<0.001$ when compared to their respective untreated control cells.

Similarly, in HaCaT cells, no significant induction of cell death was reported under exposure to all 5 ITCs during the initial 24hrs (Fig. 3.16). However, after 48hrs, our data showed an increase in the population of necrotic cells when cells were exposed to IBN (Fig. 3.16b),

PEITC (Fig. 3.16e) and AITC (Fig. 3.16c). In contrast, PEITC showed increased caspase 3/7 activity at this particular time point.

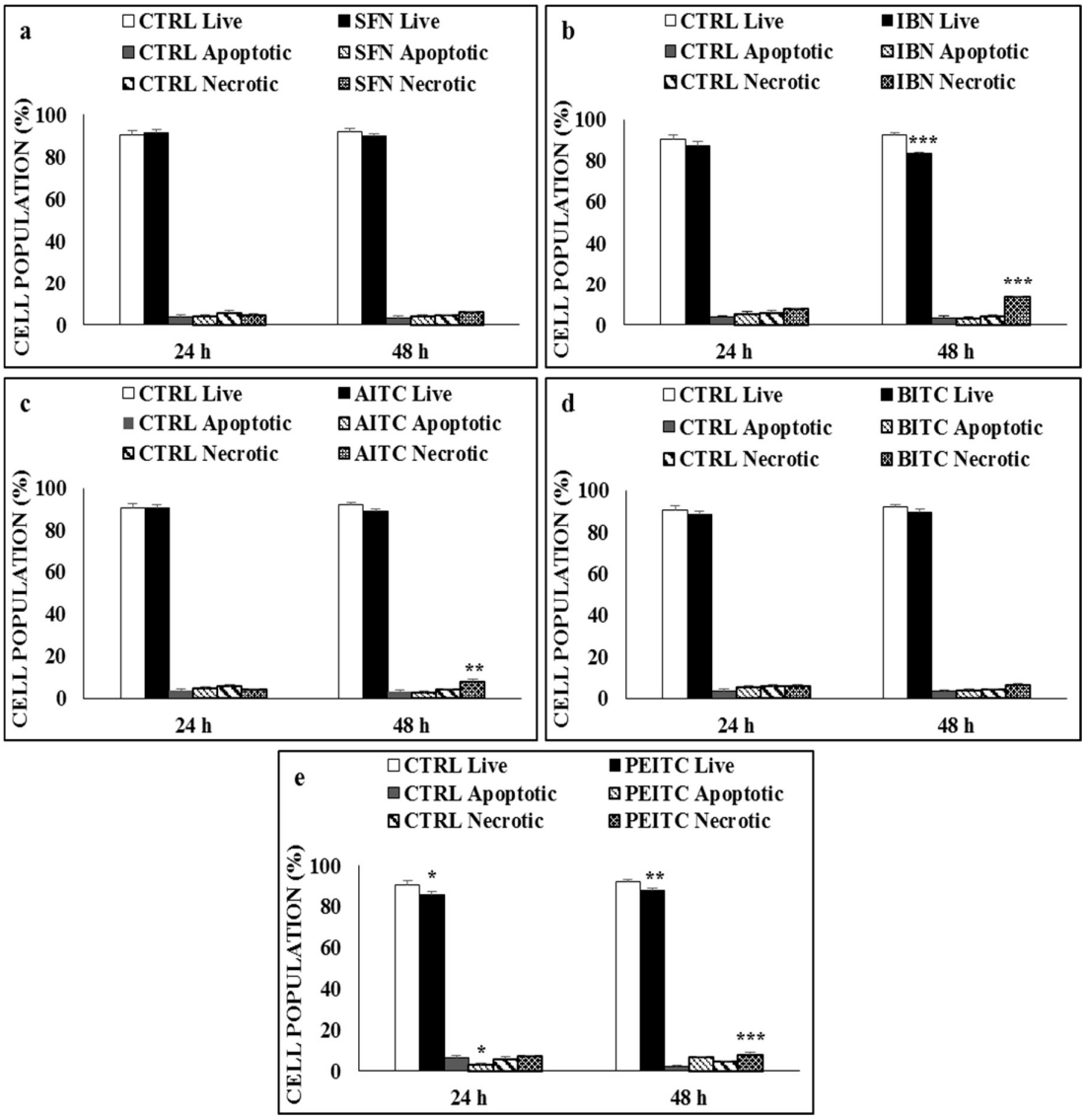

Figure 3.16: ITCs-induced cell death in HaCaT cells. Cells were exposed to 10μM of a) SFN, b) IBN, c) AITC, d) BITC and e) PEITC for 24 and 48hrs and the percentage of live, apoptotic and necrotic cells was recorded by flow. Results are expressed as mean ± SD of three replicates and are representatives of three independent experiments. Statistical analysis performd by one-way ANOVA with Tukey's test for multiple comparisons. Asterisks denote statistical significance at *, $p<0.05$, **, $p<0.01$, ***, $p<0.001$ when compared to their respective untreated control cells

Finally, when B16F10 cells were incubated with each one of the ITCs, the levels of dead cell were shown to be similar to those of the control ones, at both time points of exposure, suggesting that neither apoptosis nor necrosis was induced in this cell line (Fig. 3.17).

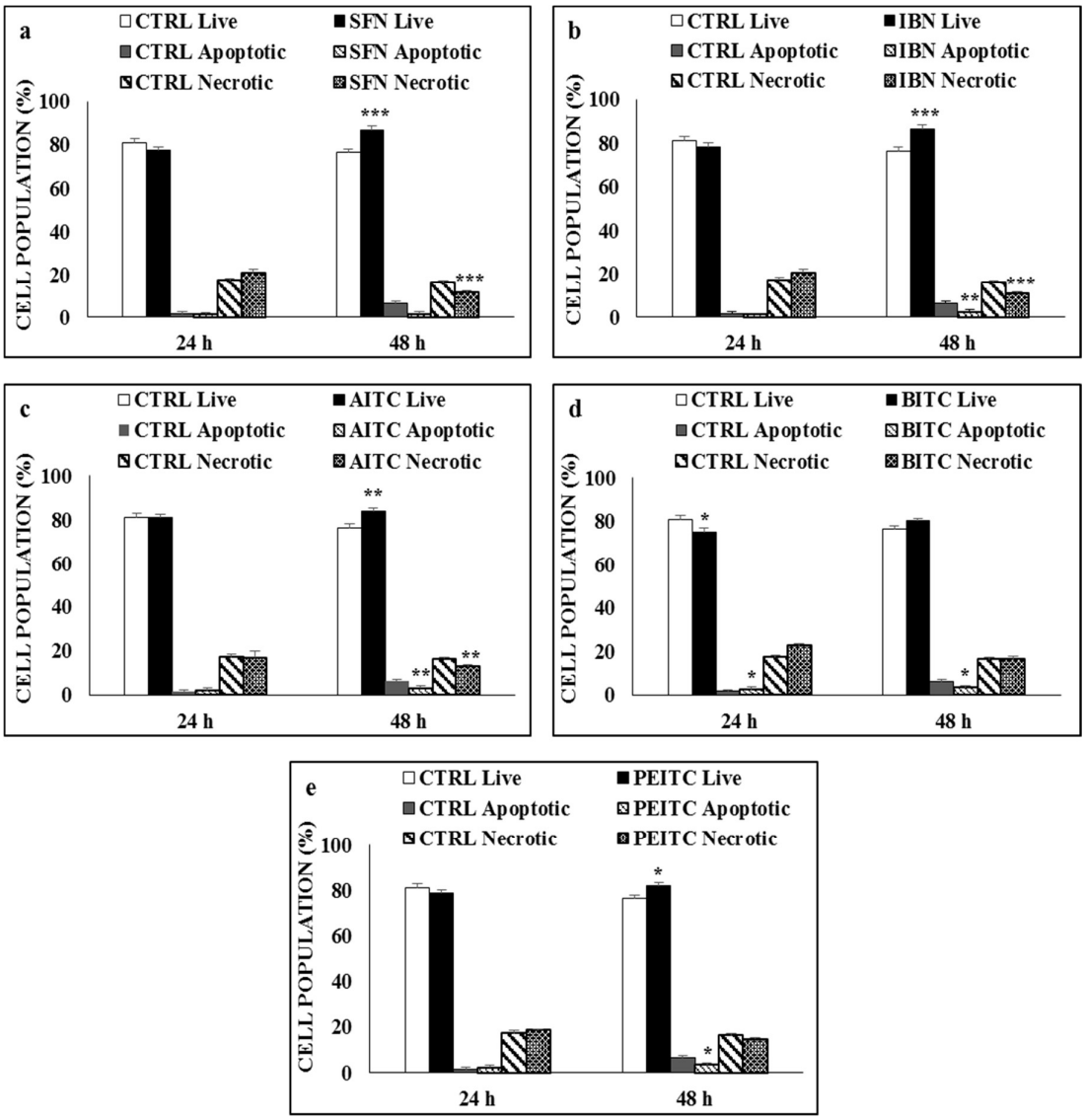

Figure 3.17: ITCs-induced cell death in B16F10 cells. Cells were exposed to 10μM of a) SFN, b) IBN, c) AITC, d) BITC and e) PEITC for 24 and 48hrs and the percentage of live, apoptotic and necrotic cells was recorded by flow. Results are expressed as mean ± SD of three replicates and are representatives of three independent experiments. Statistical analysis performd by one-way ANOVA with Tukey's test for multiple comparisons. Asterisks denote statistical significance at *, $p<0.05$, **, $p<0.01$, ***, $p<0.001$ when compared to their respective untreated control cells

3.1.4 Cytotoxicity Profile: Determination of ROS Induction

Another important aspect in ITC-induced cytotoxicity is the generation of oxidative stress (measured as levels of reactive oxygen species; ROS) and so the capacity of all 5 ITCs to induce ROS production, in our *in vitro* melanoma model, was investigated. For this reason, we evaluated the levels of intracellular ROS generation post-exposure to 10μM of each ITC, using flow cytometry and utilizing a fluorescent DHR 123 probe as a ROS detector. Flow cytometry histograms for all experiments are represented in Figure S3 (under supplementary material).

More specifically, treatment of A375 cells with SFN, IBN, BITC and PEITC induced an increase in intracellular ROS levels, at 24hrs of exposure, which became 2-fold higher after 48hrs when compared to control cells (Fig. 3.18a). ROS generation was also observed in Hs294T cells exposed to the same ITCs at 24hrs, which was sustained even at 48hrs post-exposure (Fig. 3.18c). In contrast, no significant induction of oxidative response was observed in AITC-exposed A375 and Hs294T cells, conditions where ROS levels were close to control ones at both time points (Figs. 3.18a & 3.17c). Regarding B16F10 cells, our data showed that there were no statistically significant differences in ROS levels under SFN, IBN and AITC exposure conditions, at 24 and 48hrs. However, BITC and PEITC showed a capacity to induce ROS production after 48hrs in of exposure (Fig. 3.18f). Interestingly, we observed a decline in intracellular ROS levels at 24hrs of exposure, in VMM1 cells, that reached control levels at 48hrs under all ITCs examined (Fig. 3.18b). In addition, intracellular ROS levels in HaCaT (Fig. 3.18d) and A431 (Fig. 3.18e) were similar to control levels under 24hrs of exposure to all ITCs. At 48hrs of exposure to BITC and PEITC, a 1.5 fold increase in ROS production was observed in HaCaT cells only. Finally, PEITC was shown to exert the capacity to trigger generation of oxidative stress in A431 cells at 48hrs of exposure.

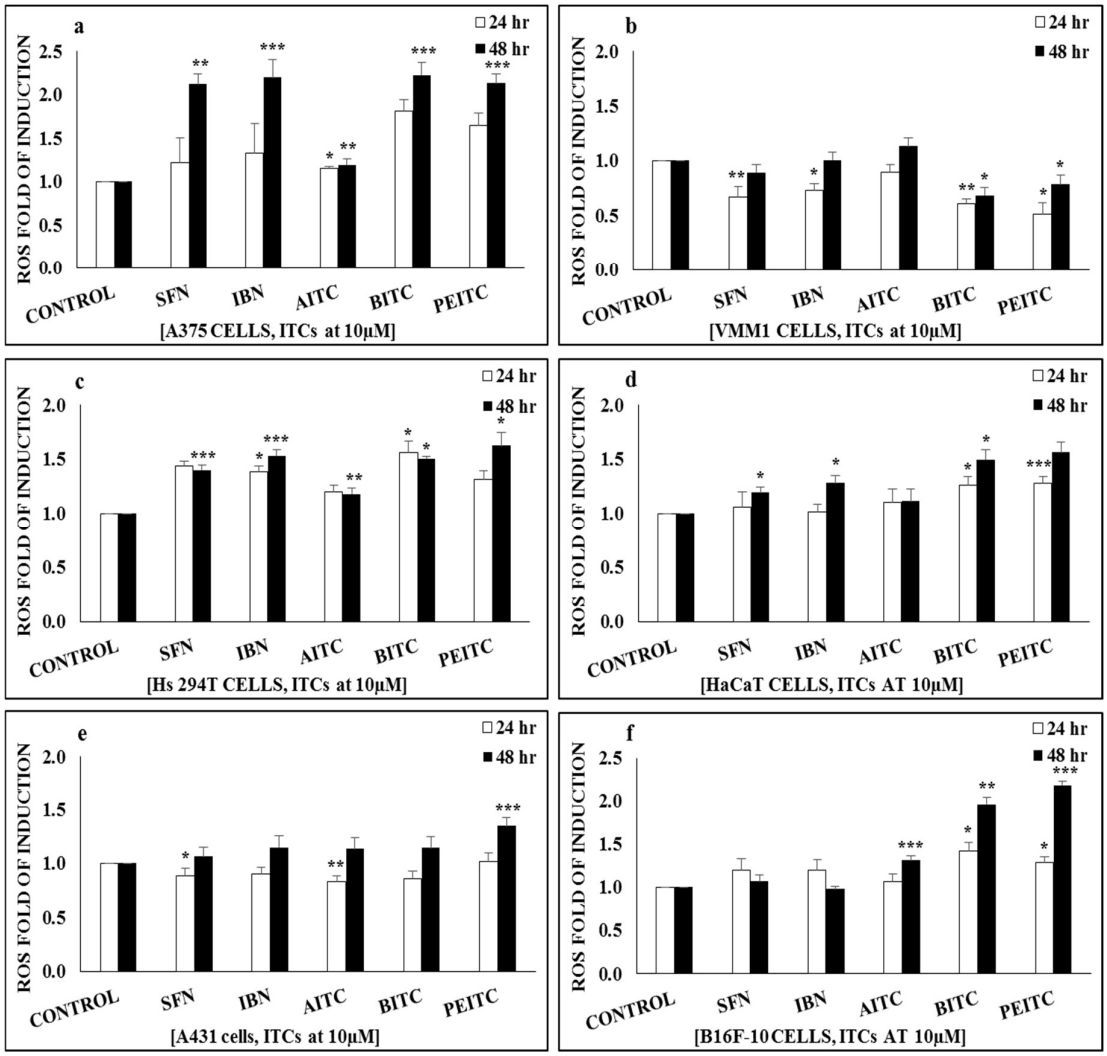

Figure 3.18: ITCs-induce generation of oxidative stress in an *in vitro* model of malignant melanoma. Our *in vitro* model consisted of: **a**) malignant melanoma (A375), **b**) metastatic melanoma derived from brain (VMM1), **c**) metastatic melanoma derived from lymph node (Hs294T), **d**) transformed, normal, keratinocyte (HaCaT), **e**) non-melanoma epidermoid carcinoma (A431) and **f**) murine malignant melanoma (B16F10) cells. All cell lines were treated with 10µM of each of the 5 ITCs for 24 and 48hrs and ROS production was examined by flow cytometry. Data quantitated as fold induction relative to untreated control cells. Results are expressed as mean ± SD of three replicates and are representatives of three independent experiments. Statistical analysis performed by one-way ANOVA with Tukey's test for multiple comparisons. Statistical significance was set at *, $p<0.05$, **, $p<0.01$, ***, $p<0.001$, relative to corresponding untreated controls.

Overall, our data showed that among all cell lines, the FITC spectrum increased dramatically mainly in A375 cells treated with SFN, IBN, BITC and PEITC while AITC had a minor

effect in all cell lines tested. A similar effect was observed in Hs294T cells but not as significant as in A375 cells. Also, our results suggest that most of the cell lines (e.g. B16F10, VMM1, A431 and HaCaT) were resistant to ITC-induced production of oxidative stress suggesting that perhaps such production does not modulate the ITC-induced cytotoxicity observed in these cells. In addition, BITC and PEITC were shown to be the most potent ones in triggering an oxidative stress response in all cells.

3.1.5: Cytotoxicity Profile: Determination of GSH Levels

In this experimental setting, our *in vitro* model was exposed to 10μM of each of the ITCs and the levels of total reduced glutathione (GSH) were evaluated 24 and 48hrs post exposure by using flow cytometry with the utilization of a Thiol Green Dye as reduced GSH detector. Flow cytometry histograms for all experiments are represented in Figure S4 (under supplementary material).

In A375 cells, a marked decrease in GSH levels was observed 24hrs post exposure to all 5 ITCs. However, at 48hrs of exposure, GSH levels were increased significantly when the cells were exposed to SFN, IBN, BITC and PEITC. Under exposure to AITC, these levels were recovered back to control ones (Fig. 3.19a). Similarly, in Hs294T cells, 24hrs after exposure to all 5 ITCs, the total cellular concentration of GSH declined whiles after 48hrs of exposure a significant elevation was observed. However, in SFN-, IBN-, AITC- and PEITC-exposed cells, GSH levels still remained declined and there was no period for recovery of cellular GSH concentration levels. On the contrary, in BITC-exposed Hs294T cells, GSH levels were elevated (Fig. 3.19c). Alternatively, when B16F10 cells were exposed to SFN and IBN, for 24hrs, the GSH levels were increased, an observation that was further enhanced after 48hrs of exposure. In line with these observations, in PEITC-exposed cells, a slight elevation in intracellular GSH levels was observed, at 24hrs, which was persistent all the way through the 48hrs time point of exposure. On the other hand exposure of these cells to BITC resulted in a slight increase of GSH levels only after 48hrs. Interestingly, GSH concentration remained at control levels at both time points of AITC exposure (Fig. 3.19f). In the case of the VMM1 cells, our results showed that BITC induced a significant elevation in GSH, at 24hrs but not at 48hrs of exposure. In contrast, PEITC caused a significant decline in GSH at 24hrs but also not at 48hrs of exposure. On the other hand, exposure to SFN and IBN had no significant effect on cellular GSH levels (Fig. 3.19b). In A431 cells, at 24hrs of exposure, PEITC markedly increased the GSH concentration, an effect that was even further potentiated during 48hrs of exposure. Moreover, BITC significantly increased GSH levels

after 48hrs of exposure whereas AITC diminished those levels at both time points. In addition, in SFN-exposed A431 cells, GSH decreased at 24hrs, followed by a slight increase over 48hrs while during IBN exposure, an increase in GSH levels occurred mainly at 48hrs (Fig. 3.19e). Finally, in HaCaT cells, the GSH concentration declined at 24hrs of exposure to SFN, IBN, AITC and PEITC. However, at 48hrs of exposure, the GSH levels were recovered (to control values) for both IBN and PEITC while increased with Furthermore, exposure to AITC induced a decline in GSH levels at both time points. Finally, BITC exposure did not change significantly the GSH levels, at 24hrs, but increased over 48hrs (Fig. 3.19d).

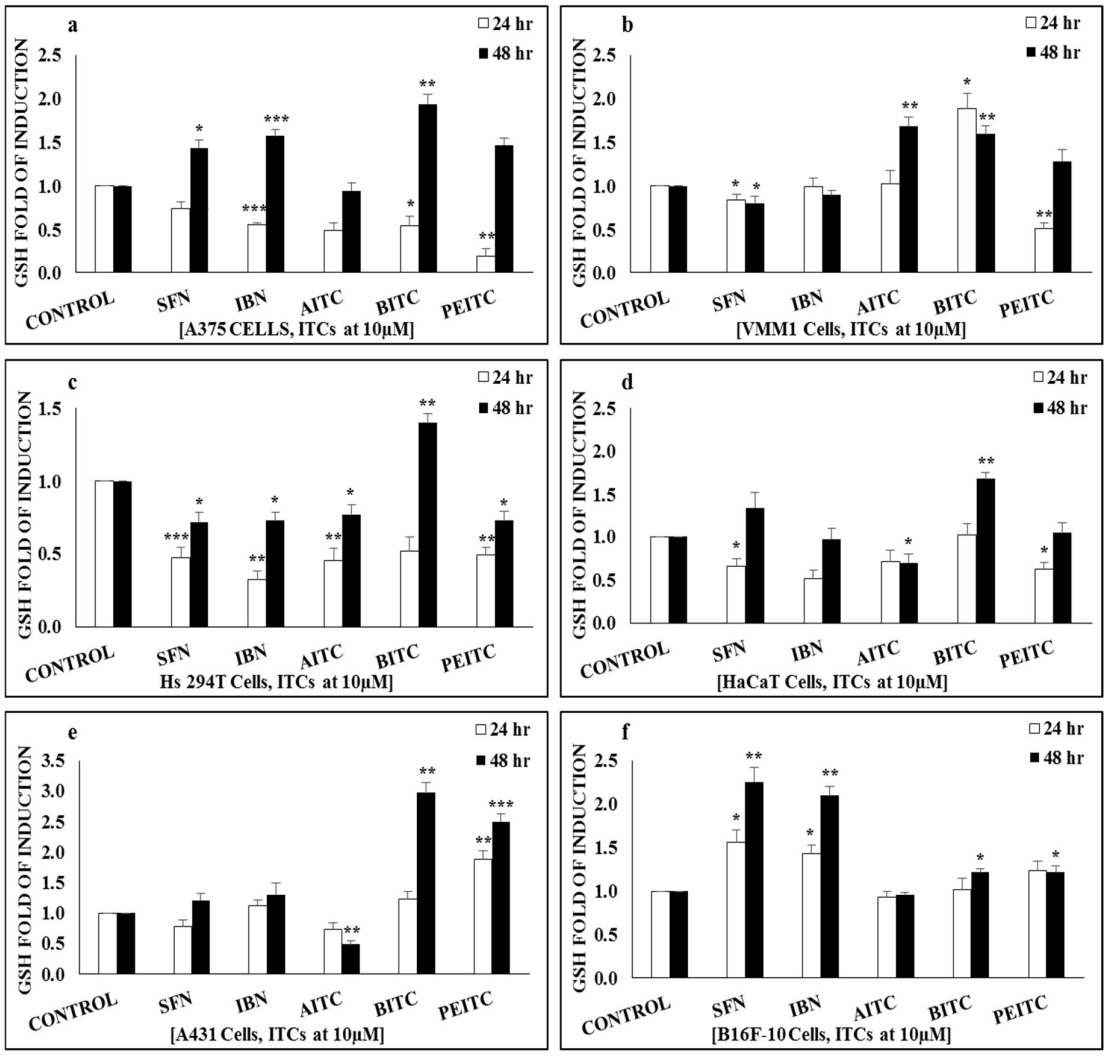

Figure 3.19: The effect of ITCs on total intracellular levels of GSH in an *in vitro* model of malignant melanoma. Our *in vitro* model consisted of: **a**) malignant melanoma (A375), **b**) metastatic melanoma derived from brain (VMM1), **c**) metastatic melanoma derived from lymph node (Hs294T), **d**) transformed, normal, keratinocyte (HaCaT), **e**) non-melanoma

epidermoid carcinoma (A431) and **f**) murine malignant melanoma (B16F10) cells. All cells were exposed to 10μM of each of the 5 ITCs for 24 and 48hrs. Total intracellular GSH levels were recorded by flow cytometry. Data quantitated as fold induction relative to GSH levels of untreated control cells. Results are expressed as mean ± SD of three replicates and are representatives of three independent experiments. Statistical analysis performed by one-way ANOVA with Tukey's test for multiple comparisons. Asterisks denote statistical significance at *, $p<0.05$, **, $p<0.01$, ***, $p<0.001$, relative to corresponding untreated controls.

Based on the detailed characterization of the cytotoxicity profile of each ITC, a concentration of 10μM over 48hrs of exposure were chosen as optimum experimental conditions in order to demonstrate the anti-melanoma effect of all 5ITCs on human malignant melanoma (A375) as well as in melanoma metastatic Hs294T cells. On the other hand, the brain metastatic cell line (VMM1), the non-tumorigenic keratinocyte (HaCaT), non-melanoma epidermoid carcinoma (A431) and murine malignant melanoma (B16F10) cell lines remained relatively unaffected, reflecting a specificity of these ITCs towards human primary and lymph node metastasic melanoma cells.

Chapter 3

Results

Results II – Assessment of apoptotic induction in response to ITC exposure of malignant melanoma cells

3.2 ITCs modulate the Expression Profile of Key Apoptotic Genes in Human Malignant Melanoma (A375) Cells

In order to further investigate the ITC-induced apoptotic response in malignant melanoma cells, a transcriptomic approach for screening multiple critical gene targets involved in various stages of the apoptotic process was used. To do so, we utilized a TaqMan real-time PCR microarray-based gene expression profiling system containing 92 candidate apoptosis-associated genes involved in the initiation of apoptosis, death receptor regulated pathways, the BCL-2 family of pro- and anti-apoptotic molecules, and various caspases in addition to 4 endogenous housekeeping (control) genes. This system allows the profiling of the differential expression pattern of these 92 genes, in response to 10μM of each of the 5 ITCs, 48h post exposure, in A375 cells compared to untreated (control) ones. Apoptotic gene expression was assessed 48h post exposure to the five ITCs, as at this time point a significant increase in cell death induction was observed accompanied with increased levels of cells stained positive for activated caspase 3/7, compared to 24h (as observed from the cell death induction experiments). Our data showed that several genes were differentially expressed (by being either up- or down-regulated) after exposure to each ITC. It should be highlighted that gene expression experiments are still in the early discovery phase and the reported data demonstate prelminary observations requiring futher validation experiments in the future.

In particular, in SFN-exposed A375 cells, we observed 29 genes being differentially expressed in comparison to untreated cells of which 19 were up-regulated (by at least 2-fold). Among them, 5 genes (e.g. *FAS, FASLG, IGF1, IL6* and *MDM2*) were highly expressed (e.g. 4- to 8-fold) while the expression levels of 10 genes were down-regulated (by 2-fold) (Table 3.3):

Table 3.3: List of differentially regulated apoptosis-associated genes as a response to SFN exposure in malignant melanoma (A375) cells

GENE	DESCRIPTION	FOLD INDUCTION SFN
Intrinsic pathway		
AIFM1	Apoptosis Inducing Factor Mitochondria Associated 1 Acts as a pro-apoptotic factor promoting disassembly in apoptotic cells and the release of the apoptogenic proteins cytochrome c and caspase-9	2.0
BBC3	BCL2 Binding Component 3 Member of the BCL-2 family of proteins - Binds to anti-apoptotic Bcl-2 family members to induce mitochondrial dysfunction, caspase activation and apoptosis. Regulates ER stress-induced neuronal apoptosis	2.0

Table 3.3: List of differentially regulated apoptosis-associated genes as a response to SFN exposure in malignant melanoma (A375) cells (continued)		
BCL2L1	Bcl-2-Like Protein 1 Member of the BCL-2 protein family - Acts as anti- or pro-apoptotic regulators and regulate mitochondrial membrane potential, the production of reactive oxygen species and release of cytochrome C	2.0
BID	BH3 Interacting Domain Death Agonist Interacts with either agonist BAX or antagonist BCL2 and regulate apoptosis, mediating mitochondrial damage induced by caspase-8 and triggering cytochrome c release	2.0
CASP9	Caspase 9 Member of the cysteine-aspartic acid protease family - Play a central role in apoptosis and acts as a tumor suppressor, activated by the apoptosome - Induces cleavage and activation of caspase-3 and 7 - Promotes DNA damage-induced apoptosis	2.0
DFFB	DNA Fragmentation Factor Subunit Beta Triggers DNA fragmentation and chromatin condensation during apoptosis	0.5
SLC25A6	Solute Carrier Family 25 Member 6 Member of the mitochondrial carrier subfamily of solute carrier protein genes - Catalyzes the exchange of cytoplasmic ADP with mitochondrial ATP across the mitochondrial inner membrane and is implicated in the function of the permeability transition pore complex (PTPC), which controls the release of mitochondrial products that induce apoptosis	0.5
P53-mediated apoptosis		
BAX	BCL2 Associated X Protein Act as an apoptotic activator triggering loss in mitochondria membrane potential and release of cytochrome c and promotes activation of CASP3	2.0
MDM2	MDM2 proto-oncogene Is an E3 ubiquitin ligase that mediate p53/TP53 inhibition via proteasome degradation and blocks p73/TP73-mediated cell cycle arrest and apoptosis. It is also involved in p53/TP53 stabilization as well as growth and DNA damage response pathways	8.1
ER-stress mediated apoptosis		
BBC3	BCL2 Binding Component 3 Member of the BCL-2 family of proteins - Binds to anti-apoptotic Bcl-2 family members to induce mitochondrial dysfunction, caspase activation and apoptosis. Regulates ER stress-induced neuronal apoptosis	2.0
Extrinsic pathway		
FAS	Fas Cell Surface Death Receptor Member of the TNF-receptor superfamily - Initiates the subsequent cascade of caspases mediating apoptosis promoting the formation of death-inducing signaling complex that includes Fas-associated death domain protein (FADD), caspase 8, and caspase 10	4.0
FASLG	Fas Ligand (TNF Superfamily, Member 6) Member of the tumor necrosis factor superfamily - Transmembrane protein that primarily induce apoptosis triggered by binding to FAS	8.3
TNFSF10	TNF Superfamily Member 10 Member of the tumor necrosis factor (TNF) ligand family – It induces apoptosis preferentially in transformed and tumor cells and has been reported to trigger the activation of MAPK8/JNK, caspase 8 and caspase 3	2.0

Table 3.3: List of differentially regulated apoptosis-associated genes as a response to SFN exposure in malignant melanoma (A375) cells (continued)		
TRADD	TNF Receptor Type 1-Associated DEATH Domain Protein Interacts with TNFRSF1A/TNFR1 and mediates programmed cell death signaling, is involved in the Fas-induced cell death pathway in NFkB activation	2.0
DFFB	DNA Fragmentation Factor Subunit Beta Triggers DNA fragmentation and chromatin condensation during apoptosis	0.5
TRAF2	TNF Receptor Associated Factor 2 Member of the TNF receptor associated factor protein family, required for TNF-alpha-mediated activation of MAPK8/JNK and NF-kappa-B and plays a key role in controlling cell survival and apoptosis	0.5
Other cellular processes: Cell growth, Proliferation, Immune responses and Inflammation		
IGF1	Insulin Like Growth Factor 1 Member of a family of proteins, structurally and functionally related to insulin, involved in mediating growth and development – Regulate activation of the PI3K-AKT/PKB and the Ras-MAPK pathways	7.8
IKBKB	Inhibitor Of Nuclear Factor Kappa B Kinase Subunit Beta Plays an essential role in the NFkB signaling pathway – Activates NFkB and thus induces genes involved in immune response, growth control, or protection against apoptosis	2.0
IKBKG	Inhibitor of Nuclear Factor Kappa B Kinase Subunit Gamma Acts as a regulator of the IKK complex, which once activated, promote activation and release of NFkB	2.0
IL6	Interleukin 6 Is a cytokine involved in inflammation and maturation of B cells as well as in lymphocyte and monocyte differentiation	8.1
KDR	Kinase Insert Domain Receptor or Vascular Endothelial Growth Factor Receptor 2 Plays a key role in the regulation of angiogenesis, vascular development and permeability and promotes proliferation, survival, migration and differentiation. It also induces the reorganization of the actin cytoskeleton	2.0
NFKB2	Nuclear Factor Kappa B Subunit 2 Encodes a subunit of the transcription factor complex NFkB which functions as a central activator of genes involved in biological processes such as inflammation, immunity, differentiation, cell growth, tumorigenesis and apoptosis	2.0
NFKBIA	NF-Kappa-B Inhibitor Alpha Encodes a member of the NFkB inhibitor family and interacts with REL dimers to inhibit NFkB/REL complexes which are involved in inflammatory responses	2.0
TGFB1	Transforming Growth Factor Beta 1 Encodes a secreted ligand of the TGF-beta superfamily of proteins and regulates cell proliferation, differentiation and growth, immune function, and can regulate the activation of other growth factors including interferon gamma and tumor necrosis factor alpha	2.0
CHEK2	Checkpoint Kinase 2 It is a cell cycle checkpoint regulator and tumor suppressor, required for checkpoint-mediated growth arrest, activation of DNA repair and regulates pro-apoptotic genes and apoptosis through p53	0.5

Table 3.3: List of differentially regulated apoptosis-associated genes as a response to SFN exposure in malignant melanoma (A375) cells (continued)		
EGFR	Epidermal Growth Factor Receptor Member of the protein kinase superfamily that interact with members of the epidermal growth factor family and activates complex downstream signaling cascades that regulate cell proliferation.	0.5
PARP1	Poly(ADP-Ribose) Polymerase 1 Encodes the poly(ADP-ribosyl)transferase which is involved in the regulation of various crucial cellular processes such as differentiation, proliferation, tumor transformation and DNA repair	0.5
PIK3CB	Phosphatidylinositol-4,5-Bisphosphate 3-Kinase Catalytic Subunit Beta Is an isoform of the catalytic subunit of phosphoinositide 3-kinase PI3Kbeta (PI3KB) and is implicated in signaling pathways involved in cell growth, survival, proliferation, motility and morphology	0.5
PRKCA	Protein Kinase C Alpha Member of serine- and threonine-specific protein kinase family involved in diverse cellular processes, including cell proliferation, apoptosis, differentiation, migration, adhesion, transformation, angiogenesis, platelet function and inflammation	0.5
RPS6KA2	Ribosomal Protein S6 Kinase A2 Member of the ribosomal S6 kinase family of serine/threonine kinases that functions downstream the MAPK signaling pathway and thus control cell growth, proliferation, survival, differentiation and motility	0.5
RPS6KA5	Ribosomal Protein S6 Kinase A5 Serine/threonine-protein kinase, required for the regulation of inflammatory genes, while mediate activation of several immediate early genes, including proto-oncogenes	0.5

In IBN-exposed A375 cells, a diverse expression pattern regarding 35 genes was noted. Most of these genes showed reduced relative expression levels among which *BCL2* was the one with the lowest fold induction compared to control cells. In contrast, the expression of 12 genes was found to be up-regulated among which *FAS*, *IL6* and *KDR* were shown to be the ones with the highest induction of expression (e.g. 4-fold) (Table 3.4):

Table 3.4: List of differentially regulated apoptosis-associated genes as a response to IBN exposure in malignant melanoma (A375) cells

GENE	DESCRIPTION	FOLD INDUCTION IBN
Intrinsic pathway		
BAD	BCL2 Associated Agonist Of Cell Death Member of the BCL-2 family with pro-apoptotic activity - Promotes cell death by biding to BCL-xL and BCL-2, thus inhibit their death repressor activity	2.0
BID	BH3 Interacting Domain Death Agonist Member of the BCL-2 family - Encodes a death agonist and regulate apoptosis mediating mitochondrial damage induced by caspase-8	2.0

Table 3.4: List of differentially regulated apoptosis-associated genes as a response to IBN exposure in malignant melanoma (A375) cells (continued)		
APAF1	Apoptotic Peptidase Activating Factor 1 Initiator of apoptosis by promoting cytochrome c-induced activation of caspase 9, which then induce the subsequent caspase cascade and commits the cell to apoptosis	0.5
BCL2	BCL2 Apoptosis Regulator Encodes an integral outer mitochondrial membrane protein that reverse the apoptotic death regulating mitochondrial permeability, inhibits caspase activity and may also attenuate inflammation	0.2
BCL2L11	BCL2 Like 11 Member of the BCL-2 protein family - Interacts with other members of the BCL-2 protein family and functions as an apoptotic activator	0.5
CASP3	Caspase 3 Member of the cysteine-aspartic acid protease family – It is an effector caspase having a crucial role in the execution-phase of cell apoptosis. Activates caspases 6, 7, and 9	0.5
CASP7	Caspase 7 Member of the cysteine-aspartic acid protease family – It is an effector caspase having a crucial role in the execution-phase of cell apoptosis	0.5
CYCS	Cytochrome C, Somatic It is a central component of the electron transport chain in mitochondria and plays an important role in apoptosis initiation. Modulate both anti-apoptotic and pro-apoptotic members of the Bcl-2 family, altering mitochondrial membrane permeability, which leads to cytochrome c release	0.5
SLC25A5	Solute Carrier Family 25 Member 5 Member of the mitochondrial carrier subfamily of solute carrier protein genes - Catalyzes the exchange of cytoplasmic ADP with mitochondrial ATP across the mitochondrial inner membrane. Repression of SLC25A5 reported to be associated with apoptosis induction and tumor growth inhibition	0.5
P53-mediated apoptosis		
BAX	BCL2 Associated X Protein Act as an apoptotic activator triggering loss in mitochondria membrane potential and release of cytochrome c and promotes activation of CASP3	2.0
MDM2	MDM2 proto-oncogene Is an E3 ubiquitin ligase that mediate p53/TP53 inhibition via proteasome degradation and blocks p73/TP73-mediated cell cycle arrest and apoptosis. It is also involved in p53/TP53 stabilization as well as growth and DNA damage response pathways	2.0
ATM	ATM Serine/Threonine Kinase Member of the PI3/PI4-kinase family – Acts as a DNA damage sensor and thus induce several genes such as the ones involved in cell cycle checkpoint signaling pathways and the tumor suppressor proteins p53 and BRCA1 maintaining genome stability	0.5
Extrinsic pathway		
FAS	Fas Cell Surface Death Receptor Member of the TNF-receptor superfamily - Initiates the subsequent cascade of caspases mediating apoptosis promoting the formation of death-inducing signaling complex that includes Fas-associated death domain protein (FADD), caspase 8, and caspase 10	4.0

Table 3.4: List of differentially regulated apoptosis-associated genes as a response to IBN exposure in malignant melanoma (A375) cells (continued)		
TRADD	TNF Receptor Type 1-Associated DEATH Domain Protein Interacts with TNFRSF1A/TNFR1 and mediates programmed cell death signaling, is involved in the Fas-induced cell death pathway in NFkB activation	2.0
CASP3	Caspase 3 Member of the cysteine-aspartic acid protease family – It is an effector caspase having a crucial role in the execution-phase of cell apoptosis. Activates caspases 6, 7, and 9	0.5
CASP7	Caspase 7 Member of the cysteine-aspartic acid protease family – It is an effector caspase having a crucial role in the execution-phase of cell apoptosis	0.5
CFLAR	CASP8 and FADD Like Apoptosis Regulator It is an apoptotic regulator, structurally similar to caspase-8 that acts as an important link between cell survival and cell death pathways. It has a dual role acting either as an apoptotic inducer or an anti-apoptotic factor inhibiting TNFRSF-mediated apoptosis	0.5
DAXX	Death Domain Associated Protein It's a multifunctional protein located both in the nucleus and in the cytoplasm. It interacts with various proteins, such as apoptosis antigen Fas. It's also implicated in apoptosis regulation, by inducing JNK pathway activation and thus TNFRSF6-dependent apoptosis. Also mediate p53 stabilization by promoting MDM2 degradation, upon DNA damage	0.5
TRAF2	TNF Receptor Associated Factor 2 Member of the TNF receptor associated factor protein family, required for TNF-alpha-mediated activation of MAPK8/JNK and NF-kappa-B and plays a key role in controlling cell survival and apoptosis	0.5
Other cellular processes: Cell growth, Proliferation, Immune responses and Inflammation		
IKBKB	Inhibitor Of Nuclear Factor Kappa B Kinase Subunit Beta Plays an essential role in the NFkB signaling pathway – Activates NFkB and thus induces genes involved in immune response, growth control, or protection against apoptosis	2.0
IL6	Interleukin 6 Is a cytokine involved in inflammation and maturation of B cells as well as in lymphocyte and monocyte differentiation	3.9
KDR	Kinase Insert Domain Receptor or Vascular Endothelial Growth Factor Receptor 2 Plays a key role in the regulation of angiogenesis, vascular development and permeability and promotes proliferation, survival, migration and differentiation. It also induces the reorganization of the actin cytoskeleton	4.0
NFKBIA	NF-Kappa-B Inhibitor Alpha Encodes a member of the NFkB inhibitor family and interacts with REL dimers to inhibit NFkB/REL complexes which are involved in inflammatory responses	2.0
PIK3R1	Phosphoinositide-3-Kinase Regulatory Subunit 1 Plays a crucial role in insulin-related metabolic actions and regulates various cell functions such as proliferation and survival	2.0
AKT1	AKT Serine/Threonine Kinase 1 Regulate a range of functions including metabolism, proliferation, cell survival, apoptosis, growth and angiogenesis as well as NFkB-dependent gene transcription	0.5

Table 3.4: List of differentially regulated apoptosis-associated genes as a response to IBN exposure in malignant melanoma (A375) cells (continued)		
ATM	ATM Serine/Threonine Kinase Member of the PI3/PI4-kinase family – Acts as a DNA damage sensor and thus induce several genes such as the ones involved in cell cycle checkpoint signaling pathways and the tumor suppressor proteins p53 and BRCA1 maintaining genome stability	0.5
CHEK2	Checkpoint Kinase 2 It is a cell cycle checkpoint regulator and tumor suppressor, required for checkpoint-mediated growth arrest, activation of DNA repair and regulates pro-apoptotic genes and apoptosis through p53	0.5
CHUK	Component Of Inhibitor Of Nuclear Factor Kappa B Kinase Complex Member of the serine/threonine protein kinase family – It is an important regulator of the NF-kappa-B signaling pathway, thus modulating genes involved in immune response, growth control, or protection against apoptosis	0.5
PARP1	Poly(ADP-Ribose) Polymerase 1 Encodes the poly(ADP-ribosyl)transferase which is involved in the regulation of various crucial cellular processes such as differentiation, proliferation, tumor transformation and DNA repair	0.5
PARP2	Poly(ADP-Ribose) Polymerase 2 Encodes the poly(ADP-ribosyl)transferase -like 2 protein plays a key role in DNA repair	0.5
REL	REL Proto-Oncogene, NF-KB Subunit Member of the Rel homology domain/immunoglobulin-like fold, plexin, transcription factor (RHD/IPT) family. Interacts with NFkB and regulate processes such as apoptosis, inflammation, immune response, differentiation, cell growth, tumorigenesis and oncogenic processes	0.5
RPS6KA1	Ribosomal Protein S6 Kinase A1 Member of the ribosomal S6 kinase family of serine/threonine kinases that functions downstream the MAPK signaling pathway and thus control cell growth, proliferation, survival and differentiation. It is also associated with repression of pro-apoptotic function of BAD and DAPK1	0.5
RPS6KA2	Ribosomal Protein S6 Kinase A2 Member of the ribosomal S6 kinase family of serine/threonine kinases that functions downstream the MAPK signaling pathway and thus control cell growth, proliferation, survival, differentiation and motility	0.5
RPS6KA4	Ribosomal Protein S6 Kinase A4 Member of the ribosomal S6 kinase family of serine/threonine kinases - Functions in the regulation of inflammatory genes, in the control of RELA transcriptional activity in response to TNF as well as of cell growth, proliferation, survival, differentiation and motility	0.5
RPS6KA5	Ribosomal Protein S6 Kinase A5 Serine/threonine-protein kinase, required for the regulation of inflammatory genes, while mediate activation of several immediate early genes, including proto-oncogenes	0.5

In AITC-exposed A375 cells, a diverse expression profile of 17 genes was identified. Most of these genes were down-regulated whereas 6 of them were upregulated to a variable degree (e.g. 2- to 8-fold induction). Interestingly, the *F2RL3* gene (known to be involved in

inflammation responses) was shown to be markedly up-regulated (e.g.30-fold induction) suggesting a role of inflammation in AITC-induced cytotoxicity of A375 cells (Table 3.5):

Table 3.5: List of differentially regulated apoptosis-associated genes as a response to AITC exposure in malignant melanoma (A375) cells

GENE	DESCRIPTION	FOLD INDUCTION AITC
Intrinsic pathway		
CASP9	Caspase 9 Member of the cysteine-aspartic acid protease family - Play a central role in apoptosis and acts as a tumor suppressor, activated by the apoptosome - Induces cleavage and activation of caspase-3 and 7 - Promotes DNA damage-induced apoptosis	2.0
APAF1	Apoptotic Peptidase Activating Factor 1 Initiator of apoptosis by promoting cytochrome c-induced activation of caspase 9, which then induce the subsequent caspase cascade and commits the cell to apoptosis	0.5
DFFB	DNA Fragmentation Factor Subunit Beta Triggers DNA fragmentation and chromatin condensation during apoptosis	0.5
P53-mediated apoptosis		
MDM2	MDM2 proto-oncogene Is an E3 ubiquitin ligase that mediate p53/TP53 inhibition via proteasome degradation and blocks p73/TP73-mediated cell cycle arrest and apoptosis. It is also involved in p53/TP53 stabilization as well as growth and DNA damage response pathways	2.0
Extrinsic pathway		
FASLG	Fas Ligand (TNF Superfamily, Member 6) Member of the tumor necrosis factor superfamily - Transmembrane protein that primarily induce apoptosis triggered by binding to FAS	8.0
TNF	Tumor Necrosis Factor Member of the tumor necrosis factor (TNF) superfamily – It binds to TNFRSF1A/TNFR1 and TNFRSF1B/TNFBR receptors and thus regulate various biological processes including cell proliferation, differentiation, apoptosis, lipid metabolism, and coagulation	2.0
DFFB	DNA Fragmentation Factor Subunit Beta Triggers DNA fragmentation and chromatin condensation during apoptosis	0.5
BIRC2	Baculoviral IAP Repeat Containing 2 Member of a family of proteins that inhibits apoptosis – It's a multifactorial protein that binds to tumor necrosis factor receptor-associated factors, TRAF1 and TRAF2 and regulates caspases and apoptosis and modulates inflammatory signaling, immunity, mitogenic kinase signaling, cell proliferation, invasion and metastasis.	0.5
TNFRSF10A	TNF Receptor Superfamily Member 10a Member of the TNF-receptor superfamily – interacts with TNF-related ligand, TNFSF10/TRAIL, and mediates downstream cell death signaling and induces apoptosis and NFkB activation. FADD adaptor protein is required for TNFRSF10A-induced apoptosis, recruiting caspase-8 initiating the subsequent cascade of caspases	0.5

Table 3.5: List of differentially regulated apoptosis-associated genes as a response to AITC exposure in malignant melanoma (A375) cells (continued)		
TNFRSF1A	TNF Receptor Superfamily Member 1A Member of the TNF receptor superfamily – Binding of TNFa in this receptor results in its activation and transduces signals for the regulation of cell functions including cell survival, FADD-mediated apoptosis, and inflammation	0.5
TNFSF12	TNF Superfamily Member 12 Member of the tumor necrosis factor (TNF) ligand family – Interacts with the FN14/TWEAKR receptor and is involved in apoptotic induction in a cell type-specific manner and also mediates NFkB activation, angiogenesis, proliferation and induction of inflammatory cytokines	0.5
TRAF2	TNF Receptor Associated Factor 2 Member of the TNF receptor associated factor protein family, required for TNF-alpha-mediated activation of MAPK8/JNK and NF-kappa-B and plays a key role in controlling cell survival and apoptosis	0.5
Other cellular processes: Cell growth, Proliferation, Immune responses and Inflammation		
RPS6KA3	Ribosomal Protein S6 Kinase A3 Member of the ribosomal S6 kinase family of serine/threonine kinases that functions downstream the MAPK signaling pathway and thus control cell growth, proliferation, survival, differentiation and motility. It is also associated with repression of pro-apoptotic function of BAD and DAPK1	2.0
BIRC2	Baculoviral IAP Repeat Containing 2 Member of a family of proteins that inhibits apoptosis – It's a multifactorial protein that binds to tumor necrosis factor receptor-associated factors, TRAF1 and TRAF2 and regulates caspases and apoptosis and modulates inflammatory signaling, immunity, mitogenic kinase signaling, cell proliferation, invasion and metastasis.	0.5
F2RL3	F2R Like Thrombin Or Trypsin Receptor 3 Member of the protease-activated receptor subfamily - Plays a role in blood coagulation, inflammation and response to pain	29.7
TNF	Tumor Necrosis Factor Member of the tumor necrosis factor (TNF) superfamily – It binds to TNFRSF1A/TNFR1 and TNFRSF1B/TNFBR receptors and thus regulate various biological processes including cell proliferation, differentiation, apoptosis, lipid metabolism, and coagulation	2.0
EGFR	Epidermal Growth Factor Receptor Member of the protein kinase superfamily that interact with members of the epidermal growth factor family and activates complex downstream signaling cascades that regulate cell proliferation	0.5
KIT	KIT Proto-Oncogene, Receptor Tyrosine Kinase Human homolog of the proto-oncogene c-kit – It's a tyrosine-protein kinase involved in the regulation of cell survival and proliferation, hematopoiesis, stem cell maintenance, gametogenesis, mast cell development, migration and function, as well as in melanogenesis.	0.1
PRKCA	Protein Kinase C Alpha Member of serine- and threonine-specific protein kinase family involved in diverse cellular processes, including cell proliferation, apoptosis, differentiation, migration, adhesion, transformation, angiogenesis, platelet function and inflammation	0.5

Table 3.5: List of differentially regulated apoptosis-associated genes as a response to AITC exposure in malignant melanoma (A375) cells (continued)		
PRKCB	Protein Kinase C Beta Member of serine- and threonine-specific protein kinase family involved in diverse cellular processes, including B cell activation, intestinal sugar absorption, cell proliferation, oxidative stress-induced apoptosis and activation of NFkB canonical pathway	0.1
RPS6KA1	Ribosomal Protein S6 Kinase A1 Member of the ribosomal S6 kinase family of serine/threonine kinases that functions downstream the MAPK signaling pathway and thus control cell growth, proliferation, survival and differentiation. It is also associated with repression of pro-apoptotic function of BAD and DAPK1	0.5
RPS6KA4	Ribosomal Protein S6 Kinase A4 Member of the ribosomal S6 kinase family of serine/threonine kinases - Functions in the regulation of inflammatory genes, in the control of RELA transcriptional activity in response to TNF as well as of cell growth, proliferation, survival, differentiation and motility	0.5
TNFRSF1A	TNF Receptor Superfamily Member 1A Member of the TNF receptor superfamily – Binding of TNFa in this receptor results in its activation and transduces signals for the regulation of cell functions including cell survival, FADD-mediated apoptosis, and inflammation	0.5
TNFSF12	TNF Superfamily Member 12 Member of the tumor necrosis factor (TNF) ligand family – Interacts with the FN14/TWEAKR receptor and is involved in apoptotic induction in a cell type-specific manner and also mediates NFkB activation, angiogenesis, proliferation and induction of inflammatory cytokines	0.5

In BITC-exposed A375 cells, we reported an increased number of differentially expressed genes compared to the other ITC exposures. Overall, BITC influenced the expression pattern of 42 genes in a manner where 20 of them were down-regulated with *BCL2* and *EGFR* showing the highest degree of reduction while 22 genes of them were up-regulated and being involved in diverse apoptotic stages [e.g. the BCL2-family (*BBC3*, *BAK1* and *BAX*), death receptors (*FAS* and *FASLG*) and *p53*-related (MDM2), among others] (Table 3.6).

Table 3.6: List of differentially regulated apoptosis-associated genes as a response to BITC exposure in malignant melanoma (A375) cells

GENE	DESCRIPTION	FOLD INDUCTION BITC
Intrinsic pathway		
BAK1	BCL2 Antagonist/Killer 1 Member of the BCL2 protein family – It promotes apoptotic induction via loss of membrane potential resulting in the release of apoptogenic factors such as cytochrome c, promoting the activation of caspase 9. IT also interacts with the p53 tumor suppressor gene under stress stimuli	2.0

Table 3.6: List of differentially regulated apoptosis-associated genes as a response to BITC exposure in malignant melanoma (A375) cells (continued)		
BBC3	BCL2 Binding Component 3 Member of the BCL-2 family of proteins - Binds to anti-apoptotic Bcl-2 family members to induce mitochondrial dysfunction, caspase activation and apoptosis. Regulates ER stress-induced neuronal apoptosis	2.0
PMAIP1	Phorbol-12-Myristate-13-Acetate-Induced Protein 1 Promotes loss of mitochondrial membrane potential and efflux of apoptogenic proteins thus inducing activation of caspases and apoptosis	2.0
APAF1	Apoptotic Peptidase Activating Factor 1 Initiator of apoptosis by promoting cytochrome c-induced activation of caspase 9, which then induce the subsequent caspase cascade and commits the cell to apoptosis	0.5
BCL2	BCL2 Apoptosis Regulator Encodes an integral outer mitochondrial membrane protein that reverse the apoptotic death regulating mitochondrial permeability, inhibits caspase activity and may also attenuate inflammation	0.2
BCL2L1	Bcl-2-Like Protein 1 Member of the BCL-2 protein family - Acts as anti- or pro-apoptotic regulators and regulate mitochondrial membrane potential, the production of reactive oxygen species and release of cytochrome C	0.5
CASP3	Caspase 3 Member of the cysteine-aspartic acid protease family – It is an effector caspase having a crucial role in the execution-phase of cell apoptosis. Activates caspases 6, 7, and 9	0.5
CYCS	Cytochrome C, Somatic It is a central component of the electron transport chain in mitochondria and plays an important role in apoptosis initiation. Modulate both anti-apoptotic and pro-apoptotic members of the Bcl-2 family, altering mitochondrial membrane permeability, which leads to cytochrome c release	0.5
DFFA	DNA Fragmentation Factor Subunit Alpha It's the substrate for caspase-3 and triggers DNA fragmentation during apoptosis and also acts as inhibitor of the caspase-activated DNase (DFF40)	0.5
P53-mediated apoptosis		
BAX	BCL2 Associated X Protein Act as an apoptotic activator triggering loss in mitochondria membrane potential and release of cytochrome c and promotes activation of CASP3	2.0
MDM2	MDM2 proto-oncogene Is an E3 ubiquitin ligase that mediate p53/TP53 inhibition via proteasome degradation and blocks p73/TP73-mediated cell cycle arrest and apoptosis. It is also involved in p53/TP53 stabilization as well as growth and DNA damage response pathways	4.0
ER-stress mediated apoptosis		
BBC3	BCL2 Binding Component 3 Member of the BCL-2 family of proteins - Binds to anti-apoptotic Bcl-2 family members to induce mitochondrial dysfunction, caspase activation and apoptosis. Regulates ER stress-induced neuronal apoptosis	2.0
Extrinsic pathway		

Table 3.6: List of differentially regulated apoptosis-associated genes as a response to BITC exposure in malignant melanoma (A375) cells (continued)		
FAS	Fas Cell Surface Death Receptor Member of the TNF-receptor superfamily - Initiates the subsequent cascade of caspases mediating apoptosis promoting the formation of death-inducing signaling complex that includes Fas-associated death domain protein (FADD), caspase 8, and caspase 10	4.0
FASLG	Fas Ligand (TNF Superfamily, Member 6) Member of the tumor necrosis factor superfamily - Transmembrane protein that primarily induce apoptosis triggered by binding to FAS	2.1
TNF	Tumor Necrosis Factor Member of the tumor necrosis factor (TNF) superfamily – It binds to TNFRSF1A/TNFR1 and TNFRSF1B/TNFBR receptors and thus regulate various biological processes including cell proliferation, differentiation, apoptosis, lipid metabolism, and coagulation	2.0
TNFSF12	TNF Superfamily Member 12 Member of the tumor necrosis factor (TNF) ligand family – Interacts with the FN14/TWEAKR receptor and is involved in apoptotic induction in a cell type-specific manner and also mediates NFkB activation, angiogenesis, proliferation and induction of inflammatory cytokines	2.0
CASP3	Caspase 3 Member of the cysteine-aspartic acid protease family – It is an effector caspase having a crucial role in the execution-phase of cell apoptosis. Activates caspases 6, 7, and 9	0.5
DAXX	Death Domain Associated Protein It's a multifunctional protein located both in the nucleus and in the cytoplasm. It interacts with various proteins, such as apoptosis antigen Fas. It's also implicated in apoptosis regulation, by inducing JNK pathway activation and thus TNFRSF6-dependent apoptosis. Also mediate p53 stabilization by promoting MDM2 degradation, upon DNA damage	0.5
DFFA	DNA Fragmentation Factor Subunit Alpha It's the substrate for caspase-3 and triggers DNA fragmentation during apoptosis and also acts as inhibitor of the caspase-activated DNase (DFF40)	0.5
TRAF2	TNF Receptor Associated Factor 2 Member of the TNF receptor associated factor protein family, required for TNF-alpha-mediated activation of MAPK8/JNK and NF-kappa-B and plays a key role in controlling cell survival and apoptosis	0.5
Other cellular processes: Cell growth, Proliferation, Immune responses and Inflammation		
CDKN2A	Cyclin Dependent Kinase Inhibitor 2A It is a CDK4 kinase inhibitor that regulate cell proliferation by promoting cell cycle arrest in G1 and G2 phases and also acts as a tumor suppressor inducing apoptosis. In addition, acts as a p53 stabilizer via interaction with MDM2.	2.0
IL6	Interleukin 6 Is a cytokine involved in inflammation and maturation of B cells as well as in lymphocyte and monocyte differentiation	2.0

Table 3.6: List of differentially regulated apoptosis-associated genes as a response to BITC exposure in malignant melanoma (A375) cells (continued)		
KDR	Kinase Insert Domain Receptor or Vascular Endothelial Growth Factor Receptor 2 Plays a key role in the regulation of angiogenesis, vascular development and permeability and promotes proliferation, survival, migration and differentiation. It also induces the reorganization of the actin cytoskeleton	2.0
NFKB1	Nuclear Factor Kappa B Subunit 1 This gene produces two transcripts: A 105 kD protein acting as Rel protein-specific transcription inhibitor and a 50 kD protein which is a DNA binding subunit of the NFkB protein complex, thus it is involved in processes including inflammation, immunity, differentiation, cell growth, tumorigenesis and apoptosis	2.0
NFKB2	Nuclear Factor Kappa B Subunit 2 Encodes a subunit of the transcription factor complex NFkB which functions as a central activator of genes involved in biological processes such as inflammation, immunity, differentiation, cell growth, tumorigenesis and apoptosis	4.1
NFKBIA	NF-Kappa-B Inhibitor Alpha Encodes a member of the NFkB inhibitor family and interacts with REL dimers to inhibit NFkB/REL complexes which are involved in inflammatory responses	2.0
NFKBIB	NFKB Inhibitor Beta Member of the NFkB inhibitor family – It inhibits NFkB activation by complexing and trapping it to the cytoplasm	2.0
NFKBIE	NFKB Inhibitor Epsilon Member of the NFkB inhibitor family – It inhibits NFkB activation by complexing and trapping it to the cytoplasm as well as DNA-binding of NFkB subunit complexes	2.0
PRKCB	Protein Kinase C Beta Member of PKC family belonging to serine- and threonine-specific protein kinases - regulate diverse cellular signaling pathways such as the B cell activation, oxidative stress-induced apoptosis, androgen receptor-mediated transcription, insulin signaling and cell proliferation.	8.3
REL	REL Proto-Oncogene, NF-KB Subunit Member of the Rel homology domain/immunoglobulin-like fold, plexin, transcription factor (RHD/IPT) family - Interacts with NFkB and regulate processes such as apoptosis, inflammation, immune response, differentiation, cell growth, tumorigenesis and oncogenic processes	2.0
RELB	RELB Proto-Oncogene, NF-KB Subunit Member of the Rel homology domain/immunoglobulin-like fold, plexin, transcription factor (RHD/IPT) family - Interacts with NFkB2 and NFkB1 and regulates processes including inflammation, immunity, differentiation, cell growth, tumorigenesis and apoptosis.	4.0
TNF	Tumor Necrosis Factor Member of the tumor necrosis factor (TNF) superfamily – It binds to TNFRSF1A/TNFR1 and TNFRSF1B/TNFBR receptors and thus regulate various biological processes including cell proliferation, differentiation, apoptosis, lipid metabolism, and coagulation	2.0

Table 3.6: List of differentially regulated apoptosis-associated genes as a response to BITC exposure in malignant melanoma (A375) cells (continued)		
TNFSF12	TNF Superfamily Member 12 Member of the tumor necrosis factor (TNF) ligand family – Interacts with the FN14/TWEAKR receptor and is involved in apoptotic induction in a cell type-specific manner and also mediates NFkB activation, angiogenesis, proliferation and induction of inflammatory cytokines	2.0
AKT1	AKT Serine/Threonine Kinase 1 Regulate a range of functions including metabolism, proliferation, cell survival, apoptosis, growth and angiogenesis as well as NFkB-dependent gene transcription	0.5
CHEK2	Checkpoint Kinase 2 It is a cell cycle checkpoint regulator and tumor suppressor, required for checkpoint-mediated growth arrest, activation of DNA repair and regulates pro-apoptotic genes and apoptosis through p53	0.5
EGFR	Epidermal Growth Factor Receptor Member of the protein kinase superfamily that interact with members of the epidermal growth factor family and activates complex downstream signaling cascades that regulate cell proliferation	0.2
IGF1R	Insulin Like Growth Factor 1 Receptor Interacts with the insulin-like growth factor and plays a role in cell growth, proliferation and survival, tumor transformation and also functions as an anti-apoptotic agent through inactivation of BAD	0.5
IL2	Interleukin 2 It's a cytokine, important for the proliferation of T and B lymphocytes. Primarily plays a crucial role in the regulation of immune response and also controls cell proliferation, differentiation and survival/apoptosis	0.5
MET	MET Proto-Oncogene, Receptor Tyrosine Kinase Member of the receptor tyrosine kinase family – It's a proto-oncogenic receptor that binds to hepatocyte growth factor/HGF ligand and regulates cellular survival, embryogenesis, and cellular migration and invasion	0.5
PARP1	Poly(ADP-Ribose) Polymerase 1 Encodes the poly(ADP-ribosyl)transferase which is involved in the regulation of various crucial cellular processes such as differentiation, proliferation, tumor transformation and DNA repair	0.5
PIK3CB	Phosphatidylinositol-4,5-Bisphosphate 3-Kinase Catalytic Subunit Beta Is an isoform of the catalytic subunit of phosphoinositide 3-kinase PI3Kbeta (PI3KB) and is implicated in signaling pathways involved in cell growth, survival, proliferation, motility and morphology	0.5
PRKCA	Protein Kinase C Alpha Member of serine- and threonine-specific protein kinase family involved in diverse cellular processes, including cell proliferation, apoptosis, differentiation, migration, adhesion, transformation, angiogenesis, platelet function and inflammation	0.5
RPS6KA1	Ribosomal Protein S6 Kinase A1 Member of the ribosomal S6 kinase family of serine/threonine kinases that functions downstream the MAPK signaling pathway and thus control cell growth, proliferation, survival and differentiation. It is also associated with repression of pro-apoptotic function of BAD and DAPK1	0.5

Table 3.6: List of differentially regulated apoptosis-associated genes as a response to BITC exposure in malignant melanoma (A375) cells (continued)		
RPS6KA5	Ribosomal Protein S6 Kinase A5 Serine/threonine-protein kinase, required for the regulation of inflammatory genes, while mediate activation of several immediate early genes, including proto-oncogenes	0.5
TSPO	Translocator Protein It is located in the mitochondrial compartment of peripheral tissues and promotes the transport of cholesterol across mitochondrial membranes and may also be involved in lipid metabolism. It is involved in cell proliferation, cell cycle progression and mitochondrial-mediated apoptosis	0.5

Finally, the expression profile of 39 genes was found to be differentially regulated after exposure of A375 cells to PEITC. Overall, a number of genes showed an important increase (e.g. 4- to 8-fold induction) in their expression levels, including *FASLG*, *MDM2*, *IGF1*, *CASP9* and *FAS* (Table 3.7):

Table 3.7: List of differentially regulated apoptosis-associated genes as a response to PEITC exposure in malignant melanoma (A375) cells

GENE	DESCRIPTION	FOLD INDUCTION PEITC
Intrinsic pathway		
BAK1	BCL2 Antagonist/Killer 1 Member of the BCL2 protein family – It promotes apoptotic induction via loss of membrane potential resulting in the release of apoptogenic factors such as cytochrome c, promoting the activation of caspase 9. IT also interacts with the p53 tumor suppressor gene under stress stimuli	2.0
BBC3	BCL2 Binding Component 3 Member of the BCL-2 family of proteins - Binds to anti-apoptotic Bcl-2 family members to induce mitochondrial dysfunction, caspase activation and apoptosis. Regulates ER stress-induced neuronal apoptosis	2.0
BCL2L1	Bcl-2-Like Protein 1 Member of the BCL-2 protein family - Acts as anti- or pro-apoptotic regulators and regulate mitochondrial membrane potential, the production of reactive oxygen species and release of cytochrome C	2.0
CASP3	Caspase 3 Member of the cysteine-aspartic acid protease family – It is an effector caspase having a crucial role in the execution-phase of cell apoptosis. Activates caspases 6, 7, and 9	2.0
CASP7	Caspase 7 Member of the cysteine-aspartic acid protease family – It is an effector caspase having a crucial role in the execution-phase of cell apoptosis	2.0
CASP9	Caspase 9 Member of the cysteine-aspartic acid protease family - Play a central role in apoptosis and acts as a tumor suppressor, activated by the apoptosome - Induces cleavage and activation of caspase-3 and 7 - Promotes DNA damage-induced apoptosis	4.0

Table 3.7: List of differentially regulated apoptosis-associated genes as a response to PEITC exposure in malignant melanoma (A375) cells (continued)		
CYCS	Cytochrome C, Somatic It is a central component of the electron transport chain in mitochondria and plays an important role in apoptosis initiation. Modulate both anti-apoptotic and pro-apoptotic members of the Bcl-2 family, altering mitochondrial membrane permeability, which leads to cytochrome c release	2.0
PMAIP1	Phorbol-12-Myristate-13-Acetate-Induced Protein 1 Promotes loss of mitochondrial membrane potential and efflux of apoptogenic proteins thus inducing activation of caspases and apoptosis	2.0
SLC25A6	Solute Carrier Family 25 Member 6 Member of the mitochondrial carrier subfamily of solute carrier protein genes - Catalyzes the exchange of cytoplasmic ADP with mitochondrial ATP across the mitochondrial inner membrane and is implicated in the function of the permeability transition pore complex (PTPC), which controls the release of mitochondrial products that induce apoptosis	0.5
ER-stress mediated apoptosis		
BBC3	BCL2 Binding Component 3 Member of the BCL-2 family of proteins - Binds to anti-apoptotic Bcl-2 family members to induce mitochondrial dysfunction, caspase activation and apoptosis. Regulates ER stress-induced neuronal apoptosis	2.0
P53-mediated apoptosis		
MDM2	MDM2 proto-oncogene Is an E3 ubiquitin ligase that mediate p53/TP53 inhibition via proteasome degradation and blocks p73/TP73-mediated cell cycle arrest and apoptosis. It is also involved in p53/TP53 stabilization as well as growth and DNA damage response pathways	8.2
Extrinsic pathway		
FASLG	Fas Ligand (TNF Superfamily, Member 6) Member of the tumor necrosis factor superfamily - Transmembrane protein that primarily induce apoptosis triggered by binding to FAS	8.3
FAS	Fas Cell Surface Death Receptor Member of the TNF-receptor superfamily - Initiates the subsequent cascade of caspases mediating apoptosis promoting the formation of death-inducing signaling complex that includes Fas-associated death domain protein (FADD), caspase 8, and caspase 10	4.0
DAXX	Death Domain Associated Protein It's a multifunctional protein located both in the nucleus and in the cytoplasm. It interacts with various proteins, such as apoptosis antigen Fas. It's also implicated in apoptosis regulation, by inducing JNK pathway activation and thus TNFRSF6-dependent apoptosis. Also mediate p53 stabilization by promoting MDM2 degradation, upon DNA damage	2.0
CASP3	Caspase 3 Member of the cysteine-aspartic acid protease family – It is an effector caspase having a crucial role in the execution-phase of cell apoptosis. Activates caspases 6, 7, and 9	2.0

Table 3.7: List of differentially regulated apoptosis-associated genes as a response to PEITC exposure in malignant melanoma (A375) cells (continued)		
CASP7	Caspase 7 Member of the cysteine-aspartic acid protease family – It is an effector caspase having a crucial role in the execution-phase of cell apoptosis	2.0
TNF	Tumor Necrosis Factor Member of the tumor necrosis factor (TNF) superfamily – It binds to TNFRSF1A/TNFR1 and TNFRSF1B/TNFBR receptors and thus regulate various biological processes including cell proliferation, differentiation, apoptosis, lipid metabolism, and coagulation	2.0
FADD	Fas Associated Via Death Domain It's an apoptotic adaptor molecule that binds to several cell surface receptors, Fas- or TNFR- receptors, and induces cell apoptotic death via activation of caspase-8 that subsequently induce the downstream caspase cascade. It also implicated in interferon regulation, thus in immune response	0.5
TNFRSF1A	TNF Receptor Superfamily Member 1A Member of the TNF receptor superfamily – Binding of TNFa in this receptor results in its activation and transduces signals for the regulation of cell functions including cell survival, FADD-mediated apoptosis, and inflammation	0.5
TRAF2	TNF Receptor Associated Factor 2 Member of the TNF receptor associated factor protein family, required for TNF-alpha-mediated activation of MAPK8/JNK and NF-kappa-B and plays a key role in controlling cell survival and apoptosis	0.5
Other cellular processes: Cell growth, Proliferation, Immune responses and Inflammation		
CDKN2A	Cyclin Dependent Kinase Inhibitor 2A It is a CDK4 kinase inhibitor that regulate cell proliferation by promoting cell cycle arrest in G1 and G2 phases and also acts as a tumor suppressor inducing apoptosis. In addition, acts as a p53 stabilizer via interaction with MDM2.	2.0
F2RL3	F2R Like Thrombin Or Trypsin Receptor 3 Member of the protease-activated receptor subfamily - Plays a role in blood coagulation, inflammation and response to pain	16.2
IGF1	Insulin Like Growth Factor 1 Member of a family of proteins, structurally and functionally related to insulin, involved in mediating growth and development – Regulate activation of the PI3K-AKT/PKB and the Ras-MAPK pathways	7.2
IKBKG	Inhibitor of Nuclear Factor Kappa B Kinase Subunit Gamma Acts as a regulator of the IKK complex, which once activated, promote activation and release of NFkB	2.0
IL2	Interleukin 2 It's a cytokine, important for the proliferation of T and B lymphocytes. Primarily plays a crucial role in the regulation of immune response and also controls cell proliferation, differentiation and survival/apoptosis	2.0
IL6	Interleukin 6 Is a cytokine involved in inflammation and maturation of B cells as well as in lymphocyte and monocyte differentiation	16.2

Table 3.7: List of differentially regulated apoptosis-associated genes as a response to PEITC exposure in malignant melanoma (A375) cells (continued)		
KDR	Kinase Insert Domain Receptor or Vascular Endothelial Growth Factor Receptor 2 Plays a key role in the regulation of angiogenesis, vascular development and permeability and promotes proliferation, survival, migration and differentiation. It also induces the reorganization of the actin cytoskeleton	2.0
NFKBIA	NF-Kappa-B Inhibitor Alpha Encodes a member of the NFkB inhibitor family and interacts with REL dimers to inhibit NFkB/REL complexes which are involved in inflammatory responses	2.0
PIK3R1	Phosphoinositide-3-Kinase Regulatory Subunit 1 Plays a crucial role in insulin-related metabolic actions and regulates various cell functions such as proliferation and survival	2.0
REL	REL Proto-Oncogene, NF-KB Subunit Member of the Rel homology domain/immunoglobulin-like fold, plexin, transcription factor (RHD/IPT) family. Interacts with NFkB and regulate processes such as apoptosis, inflammation, immune response, differentiation, cell growth, tumorigenesis and oncogenic processes	2.0
TNF	Tumor Necrosis Factor Member of the tumor necrosis factor (TNF) superfamily – It binds to TNFRSF1A/TNFR1 and TNFRSF1B/TNFBR receptors and thus regulate various biological processes including cell proliferation, differentiation, apoptosis, lipid metabolism, and coagulation	2.0
AKT1	AKT Serine/Threonine Kinase 1 Regulate a range of functions including metabolism, proliferation, cell survival, apoptosis, growth and angiogenesis as well as NFkB-dependent gene transcription	0.5
CHEK2	Checkpoint Kinase 2 It is a cell cycle checkpoint regulator and tumor suppressor, required for checkpoint-mediated growth arrest, activation of DNA repair and regulates pro-apoptotic genes and apoptosis through p53	0.5
DAPK3	Death Associated Protein Kinase 3 Member of serine/threonine kinase family – It is involved in the regulation of cell cycle progression and proliferation, autophagy, transcription, translation, actin cytoskeleton reorganization and induces morphological changes in apoptosis	0.5
EGFR	Epidermal Growth Factor Receptor Member of the protein kinase superfamily that interact with members of the epidermal growth factor family and activates complex downstream signaling cascades that regulate cell proliferation	0.5
FADD	Fas Associated Via Death Domain It's an apoptotic adaptor molecule that binds to several cell surface receptors, Fas- or TNFR- receptors, and induces cell apoptotic death via activation of caspase-8 that subsequently induce the downstream caspase cascade. It also implicated in interferon regulation, thus in immune response	0.5
IKBKB	Inhibitor Of Nuclear Factor Kappa B Kinase Subunit Beta Plays an essential role in the NFkB signaling pathway – Activates NFkB and thus induces genes involved in immune response, growth control, or protection against apoptosis	0.5

Table 3.7: List of differentially regulated apoptosis-associated genes as a response to PEITC exposure in malignant melanoma (A375) cells (continued)		
PARP1	Poly(ADP-Ribose) Polymerase 1 Encodes the poly(ADP-ribosyl)transferase which is involved in the regulation of various crucial cellular processes such as differentiation, proliferation, tumor transformation and DNA repair	0.5
PIK3CB	Phosphatidylinositol-4,5-Bisphosphate 3-Kinase Catalytic Subunit Beta Is an isoform of the catalytic subunit of phosphoinositide 3-kinase PI3Kbeta (PI3KB) and is implicated in signaling pathways involved in cell growth, survival, proliferation, motility and morphology	0.5
RPS6KA1	Ribosomal Protein S6 Kinase A1 Member of the ribosomal S6 kinase family of serine/threonine kinases that functions downstream the MAPK signaling pathway and thus control cell growth, proliferation, survival and differentiation. It is also associated with repression of pro-apoptotic function of BAD and DAPK1	0.5
RPS6KA4	Ribosomal Protein S6 Kinase A4 Member of the ribosomal S6 kinase family of serine/threonine kinases - Functions in the regulation of inflammatory genes, in the control of RELA transcriptional activity in response to TNF as well as of cell growth, proliferation, survival, differentiation and motility	0.5
RPS6KA5	Ribosomal Protein S6 Kinase A5 Serine/threonine-protein kinase, required for the regulation of inflammatory genes, while mediate activation of several immediate early genes, including proto-oncogenes	0.5
TNFRSF1A	TNF Receptor Superfamily Member 1A Member of the TNF receptor superfamily – Binding of TNFa in this receptor results in its activation and transduces signals for the regulation of cell functions including cell survival, FADD-mediated apoptosis, and inflammation	0.5
TSPO	Translocator Protein It is located in the mitochondrial compartment of peripheral tissues and promotes the transport of cholesterol across mitochondrial membranes and may also be involved in lipid metabolism. It is involved in cell proliferation, cell cycle progression and mitochondrial-mediated apoptosis	0.5

Taken together, the gene expression data indicated an altered expression pattern of several genes implicated at various stages of the apoptotic process as well as processes important for cell growth and survival based on each ITC exposure. Among them, about 20 genes (summarized in Fig. 3.20 and Table 3.8) were shown to have a common profile among all ITC exposures. More specifically, we reported 19 genes that show a common expression pattern (being either up- or down- regulated) in at least three of the ITCs used, while two genes, MDM2 (*p53*-related pathway) and *TRAF2* (extrinsic pathway) were shown to be highly up- or down-regulated respectively, under exposure to all 5 ITCs. These common gene targets are descriptive of diverse apoptotic pathways, including the i) intrinsic (e.g.

APAF1, BAX, BBC3, CASP9 and *SLC25A6*), ii) extrinsic (e.g. *FAS, FASLG* and *TRAF2*), iii) ER stress-mediated (e.g. *BBC3*) and iv) p53-related (e.g. *BAX, CHEK2* and *MDM2*) ones. In addition, we have reported a differential expression pattern of genes involved in other important cellular processes, that promote apoptosis, including inflammatory and immune responses (e.g. *IL6, NFKBIA, RPS6KA4, RPS6KA5* and *TNF*) as well as cell growth, survival, differentiation, cell adhesion and migration (e.g. *AKT1, EGFR, KDR, PIK3CB, PRKCA*). Overall, our data support the involvement of ITCs in regulating the apoptotic response, as part of their cytotoxic potential, by modulating the expression of various apoptosis-related genes implicated in diverse pathways and cellular functions thereby reflecting their plurality of functions and activities.

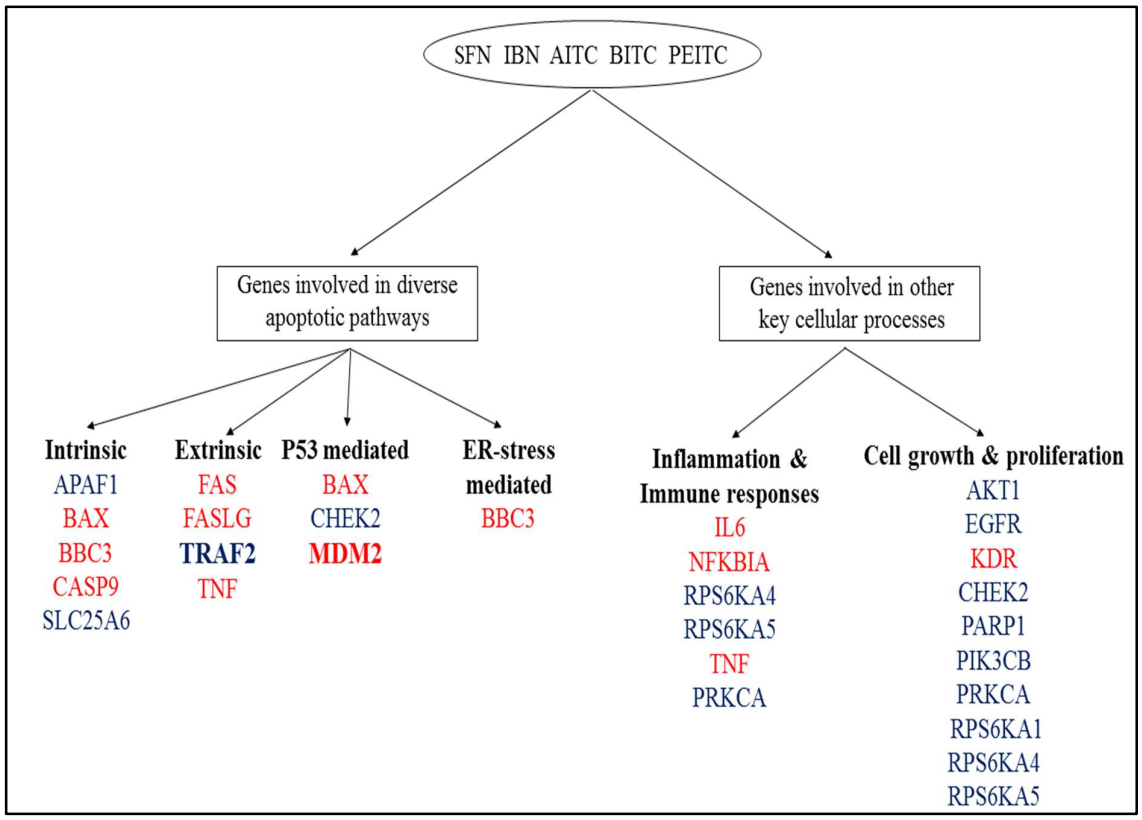

Figure 3.20: Commonly expressed apoptosis-associated genes upon exposure to all 5 ITCs in malignant melanoma (A375) cells. A375 melanoma cells were exposed to 10μM of each of the 5 ITCs for 48hrs and the expression of 92 candidate apoptosis-associated genes was evaluated utilizing a TaqMan real-time PCR array-based gene expression profiling system. **S**everal genes, involved in various stages of the apoptotic process, found to be differentially expressed post exposure to each ITC. Among them, 22 genes found to follow a common expression pattern (being either up- or down- regulated) in at least three of the

ITCs used, which are summarized in this figure. Genes in red refers to upregulated ones, while blue to downregulated, whereas the two genes in bold (***MDM2*** and ***TRAF2)*** found to be regulated, under exposure to all 5 ITCs.

Table 3.8: List of common differentially expressed apoptosis-associated genes upon exposure to all 5 ITCs in malignant melanoma (A375) cells

GENE	DESCRIPTION	SFN	IBN	AITC	BITC	PEITC
Intrinsic pathway						
BBC3	BCL2 Binding Component 3 Member of the BCL-2 family of proteins - Binds to anti-apoptotic Bcl-2 family members to induce mitochondrial dysfunction, caspase activation and apoptosis. Regulates ER stress-induced neuronal apoptosis	2.0	2.0	-	2.0	2.0
CASP9	Caspase 9 Member of the cysteine-aspartic acid protease family - Play a central role in apoptosis and acts as a tumor suppressor, activated by the apoptosome - Induces cleavage and activation of caspase-3 and 7 - Promotes DNA damage-induced apoptosis	2.0	-	2.0	-	4.0
APAF1	Apoptotic Peptidase Activating Factor 1 Initiator of apoptosis by promoting cytochrome c-induced activation of caspase 9, which then induce the subsequent caspase cascade and commits the cell to apoptosis	-	0.5	0.5	0.5	-
SLC25A6	Solute Carrier Family 25 Member 6 Member of the mitochondrial carrier subfamily of solute carrier protein genes - Catalyzes the exchange of cytoplasmic ADP with mitochondrial ATP across the mitochondrial inner membrane and is implicated in the function of the permeability transition pore complex (PTPC), which controls the release of mitochondrial products that induce apoptosis	0.5	0.5	-	-	0.5
ER-stress mediated apoptosis						
BBC3	BCL2 Binding Component 3 Member of the BCL-2 family of proteins - Binds to anti-apoptotic Bcl-2 family members to induce mitochondrial dysfunction, caspase activation and apoptosis. Regulates ER stress-induced neuronal apoptosis	2.0	2.0	-	2.0	2.0
p53-mediated apoptosis						
BAX	BCL2 Associated X Protein Act as an apoptotic activator triggering loss in mitochondria membrane potential and release of cytochrome c and promotes activation of CASP3	2.0	2.0	-	2.0	-

Table 3.8: List of common differentially expressed apoptosis-associated genes upon exposure to all 5 ITCs in malignant melanoma (A375) cells (continued)						
MDM2	MDM2 proto-oncogene Is an E3 ubiquitin ligase that mediate p53/TP53 inhibition via proteasome degradation and blocks p73/TP73-mediated cell cycle arrest and apoptosis. It is also involved in p53/TP53 stabilization as well as growth and DNA damage response pathways	8.1	2.0	2.0	4.0	8.2
Extrinsic pathway						
FAS	Fas Cell Surface Death Receptor Member of the TNF-receptor superfamily - Initiates the subsequent cascade of caspases mediating apoptosis promoting the formation of death-inducing signaling complex that includes Fas-associated death domain protein (FADD), caspase 8, and caspase 10	4.0	4.0	-	4.0	4.0
FASLG	Fas Ligand (TNF Superfamily, Member 6) Member of the tumor necrosis factor superfamily - Transmembrane protein that primarily induce apoptosis triggered by binding to FAS	8.3	-	8.0	2.1	8.3
TNF	Tumor Necrosis Factor Member of the tumor necrosis factor (TNF) superfamily – It binds to TNFRSF1A/TNFR1 and TNFRSF1B/TNFBR receptors and thus regulate various biological processes including cell proliferation, differentiation, apoptosis, lipid metabolism, and coagulation	-	-	2.0	2.0	2.0
TRAF2	TNF Receptor Associated Factor 2 Member of the TNF receptor associated factor protein family, required for TNF-alpha-mediated activation of MAPK8/JNK and NF-kappa-B and plays a key role in controlling cell survival and apoptosis	0.5	0.5	0.5	0.5	0.5
Other cellular processes: Cell growth, Proliferation, Immune responses and Inflammation						
IL6	Interleukin 6 Is a cytokine involved in inflammation and maturation of B cells as well as in lymphocyte and monocyte differentiation	8.1	3.9	-	2.0	16.2
KDR	Kinase Insert Domain Receptor or Vascular Endothelial Growth Factor Receptor 2 Plays a key role in the regulation of angiogenesis, vascular development and permeability and promotes proliferation, survival, migration and differentiation. It also induces the reorganization of the actin cytoskeleton	2.0	4.0	-	2.0	2.0

Table 3.8: List of common differentially expressed apoptosis-associated genes upon exposure to all 5 ITCs in malignant melanoma (A375) cells (continued)						
NFKBIA	NF-Kappa-B Inhibitor Alpha Encodes a member of the NFkB inhibitor family and interacts with REL dimers to inhibit NFkB/REL complexes which are involved in inflammatory responses	2.0	2.0	-	2.0	2.0
TNF	Tumor Necrosis Factor Member of the tumor necrosis factor (TNF) superfamily – It binds to TNFRSF1A/TNFR1 and TNFRSF1B/TNFBR receptors and thus regulate various biological processes including cell proliferation, differentiation, apoptosis, lipid metabolism, and coagulation	-	-	2.0	2.0	2.0
AKT1	AKT Serine/Threonine Kinase 1 Regulate a range of functions including metabolism, proliferation, cell survival, apoptosis, growth and angiogenesis as well as NFkB-dependent gene transcription	-	0.5	-	0.5	0.5
CHEK2	Checkpoint Kinase 2 It is a cell cycle checkpoint regulator and tumor suppressor, required for checkpoint-mediated growth arrest, activation of DNA repair and regulates pro-apoptotic genes and apoptosis through p53	0.5	0.5	-	0.5	0.5
EGFR	Epidermal Growth Factor Receptor Member of the protein kinase superfamily that interact with members of the epidermal growth factor family and activates complex downstream signaling cascades that regulate cell proliferation	0.5	-	0.5	0.2	0.5
PARP1	Poly(ADP-Ribose) Polymerase 1 Encodes the poly(ADP-ribosyl)transferase which is involved in the regulation of various crucial cellular processes such as differentiation, proliferation, tumor transformation and DNA repair	0.5	0.5	-	0.5	0.5
PIK3CB	Phosphatidylinositol-4,5-Bisphosphate 3-Kinase Catalytic Subunit Beta Is an isoform of the catalytic subunit of phosphoinositide 3-kinase PI3Kbeta (PI3KB) and is implicated in signaling pathways involved in cell growth, survival, proliferation, motility and morphology	0.5	-	-	0.5	0.5
PRKCA	Protein Kinase C Alpha Member of serine- and threonine-specific protein kinase family involved in diverse cellular processes, including cell proliferation, apoptosis, differentiation, migration, adhesion, transformation, angiogenesis, platelet function and inflammation	0.5	-	0.5	0.5	-

Table 3.8: List of common differentially expressed apoptosis-associated genes upon exposure to all 5 ITCs in malignant melanoma (A375) cells (continued)						
RPS6KA1	Ribosomal Protein S6 Kinase A1 Member of the ribosomal S6 kinase family of serine/threonine kinases that functions downstream the MAPK signaling pathway and thus control cell growth, proliferation, survival and differentiation. It is also associated with repression of pro-apoptotic function of BAD and DAPK1	-	0.5	0.5	0.5	0.5
RPS6KA4	Ribosomal Protein S6 Kinase A4 Member of the ribosomal S6 kinase family of serine/threonine kinases - Functions in the regulation of inflammatory genes, in the control of RELA transcriptional activity in response to TNF as well as of cell growth, proliferation, survival, differentiation and motility	-	0.5	0.5	-	0.5
RPS6KA5	Ribosomal Protein S6 Kinase A5 Serine/threonine-protein kinase, required for the regulation of inflammatory genes, while mediate activation of several immediate early genes, including proto-oncogenes	0.5	0.5	-	0.5	0.5

Chapter 3

Results

Results III – Characterization of the epigenetic response in respect to ITC exposure of malignant melanoma cells

3.3 Characteristic Epigenetic Histone Modifications of A375 Cells in Response to ITCs Exposure

In this part of the study, I aimed to characterize the epigenetic response, focusing on histone posttranslational modifications, in A375 cells, post exposure to 10 μM of each of the 5 ITCs for a period of 48hrs. To this end, we focused on determining protein expression levels of several enzymes involved in the epigenetic machinery as well as on their corresponding epigenetic marks on specific residues on two core histone proteins, H3 and H4 respectively. It should be noted, that western immunoblot data did not show any significant changes in differential expression patterns when compared to untreated (control) cells (presented in the supplementary section).

3.3.1 ITCs Modulate Specific HDAC and HAT Protein Expression and Activity Levels in A375 Cells

The effect of each ITC on protein expression levels of various HDACs (e.g. 1, 2, 4 and 6) and HATs (e.g. CBP, Acetyl CBP/p300, PCAF, and GCN5L2) was characterized in nuclear cell lysates of A375 cells exposed to 10 μM of each ITC over a period of 48hrs. Our data showed a significant decrease in protein expression levels of HDAC1, HDAC2, HDAC4 and HDAC6 after exposure to SFN, IBN, BITC and PEITC (Figs. 3.21a and c) while exposure to AITC diminished markedly the expression of HDAC4 and HDAC6 only when compared to untreated (control) cells (Figs. 3.21b and S5). Overall, our results showed a more profound reduction of HDAC 6 protein expression levels post exposure to all 5 ITCs. Among them, BITC exhibited a more potent effect followed by SFN and PEITC.

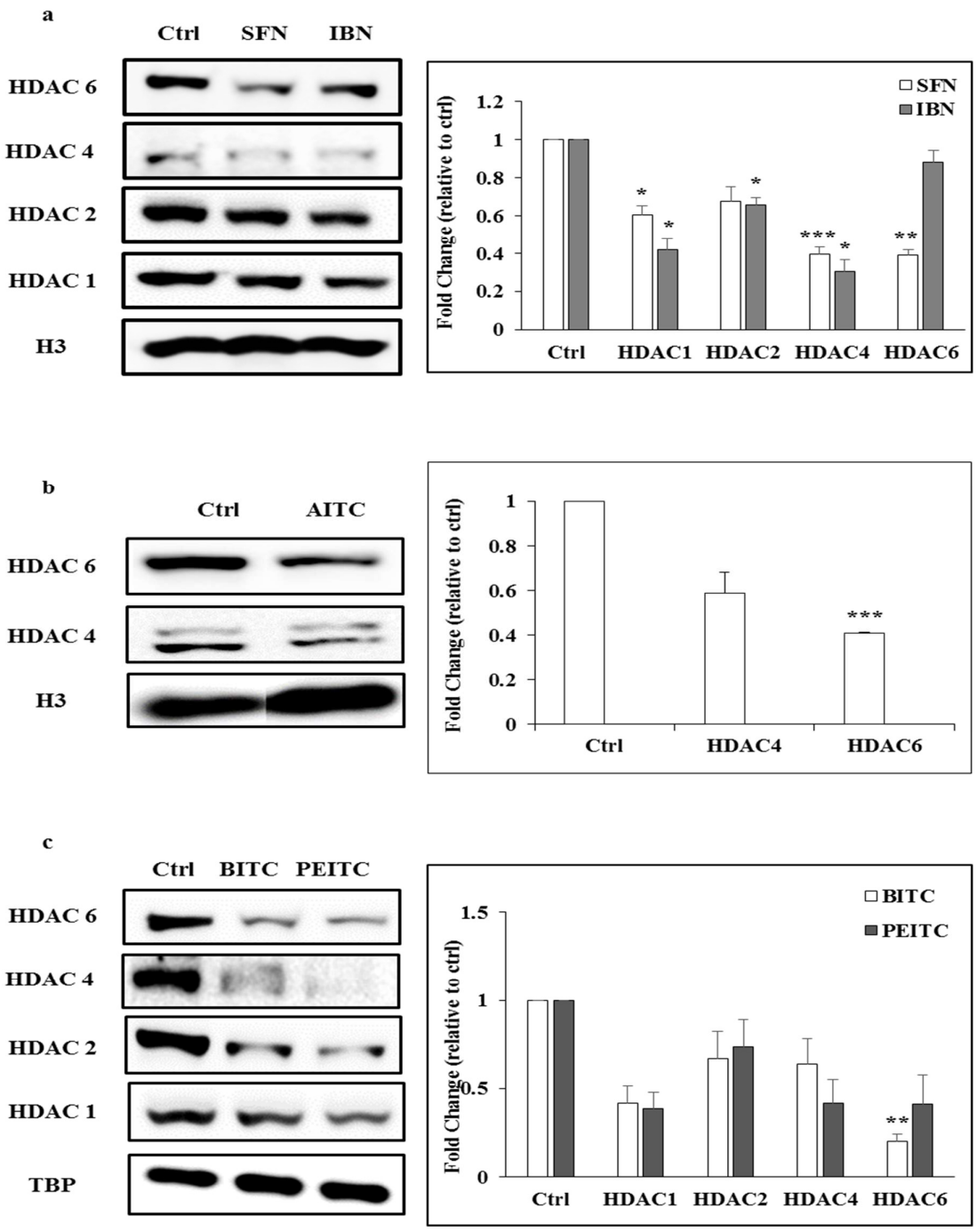

Figure 3.21: ITCs effect on HDAC protein expression levels in A375 cells. Cells were exposed to 10 μM of **a**) SFN or IBN, **b**) AITC and **c**) BITC or PEITC for 48 hrs. Western immunoblotting was used, in nuclear extracts, to determine the expression levels of HDACs 1, 2, 4 and 6. Protein expression levels were quantified by densitometry relative to H3 or TBP and the data were normalized to the untreated control (Ctrl). Western blots are

representative of three independent experiments. Statistical analysis performed by Student's *t*-test and significance was set at $*p < 0.05$, $**p < 0.01$, $***p < 0.001$ relative to corresponding controls.

Furthermore, treatment of A375 cells with each ITC also reduced protein expression levels of specific HAT enzymes, notably CBP and acetyl CBP/p300. Interestingly, AITC was more potent against CBP (Fig. 3.22c) followed by BITC and PEITC (Fig. 3.22d) while all 5 ITCs exerted a similar inhibitory effect on acetyl CBP/p300 expression levels (Fig. 3.22). In addition, PCAF expression was diminished only by SFN (Fig. 3.22a) whereas a slight increase was reported after treatment with PEITC (Fig. 3.22d). In contrast, PCAF expression levels were similar to control under exposure to IBN, AITC and BITC (Figs. S6b, c and d). Finally, GCN5L2 expression levels were similar to control after exposure to all ITCs under investigation (Fig. S6)

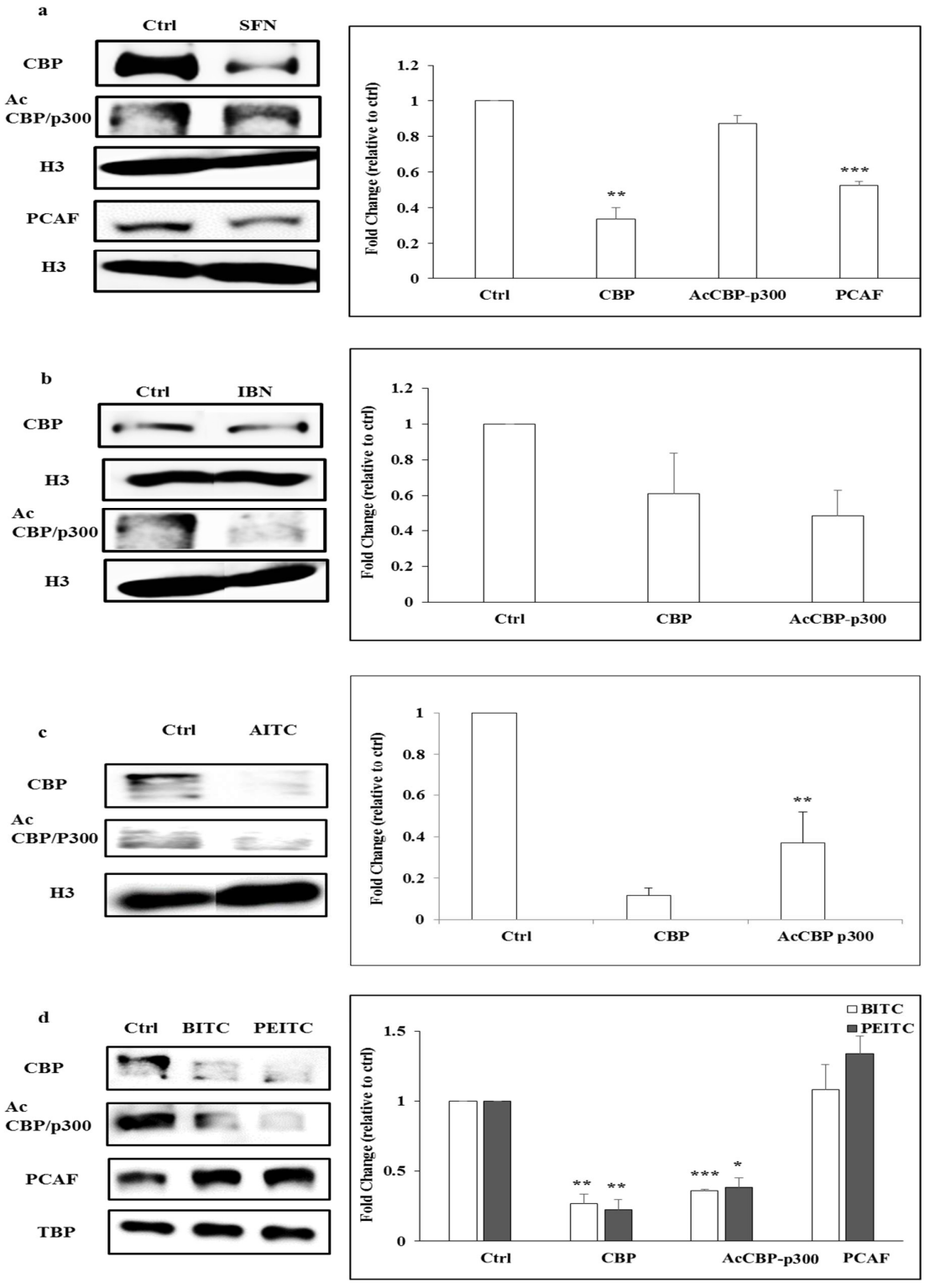

Figure 3.22: ITCs effect on HAT protein expression levels in A375 cells. Western immunoblotting was used, in A375 nuclear extracts, to determine the expression levels of CBP, Acetyl-CBP/p300, PCAF and GCN5L2 after exposure to 10 μM of **a**) SFN, **b**) IBN,

c) AITC and **d**) BITC or PEITC for 48 hrs. Densitometry was used to quantify the protein expression levels relative to H3 or TBP, Data were normalized to the untreated control (Ctrl) levels. Western blots are representative of three independent experiments. Statistical analysis performed by Student's *t*-test and significance was set at $*p < 0.05$, $**p < 0.01$, $***p < 0.001$ relative to corresponding controls.

Next, we determined the effect of ITCs on total nuclear HDAC and HAT activity levels under the same experimental conditions mentioned above. In general, exposure of A375 cells to each of the ITCs resulted in a slight, but statistically significant, reduction in total HDACs activities (Fig. 3.23a). When nuclear HATs activities were evaluated, our results showed that their levels were reduced in AITC-, BITC-and PEITC-exposed cells. Furthermore, BITC and PEITC were shown to exert a more potent inhibitory effect on total HAT activity. On the other hand, an increase in total HATs activity levels was observed under exposure to SFN and IBN when compared to control levels (Fig. 3.23b).

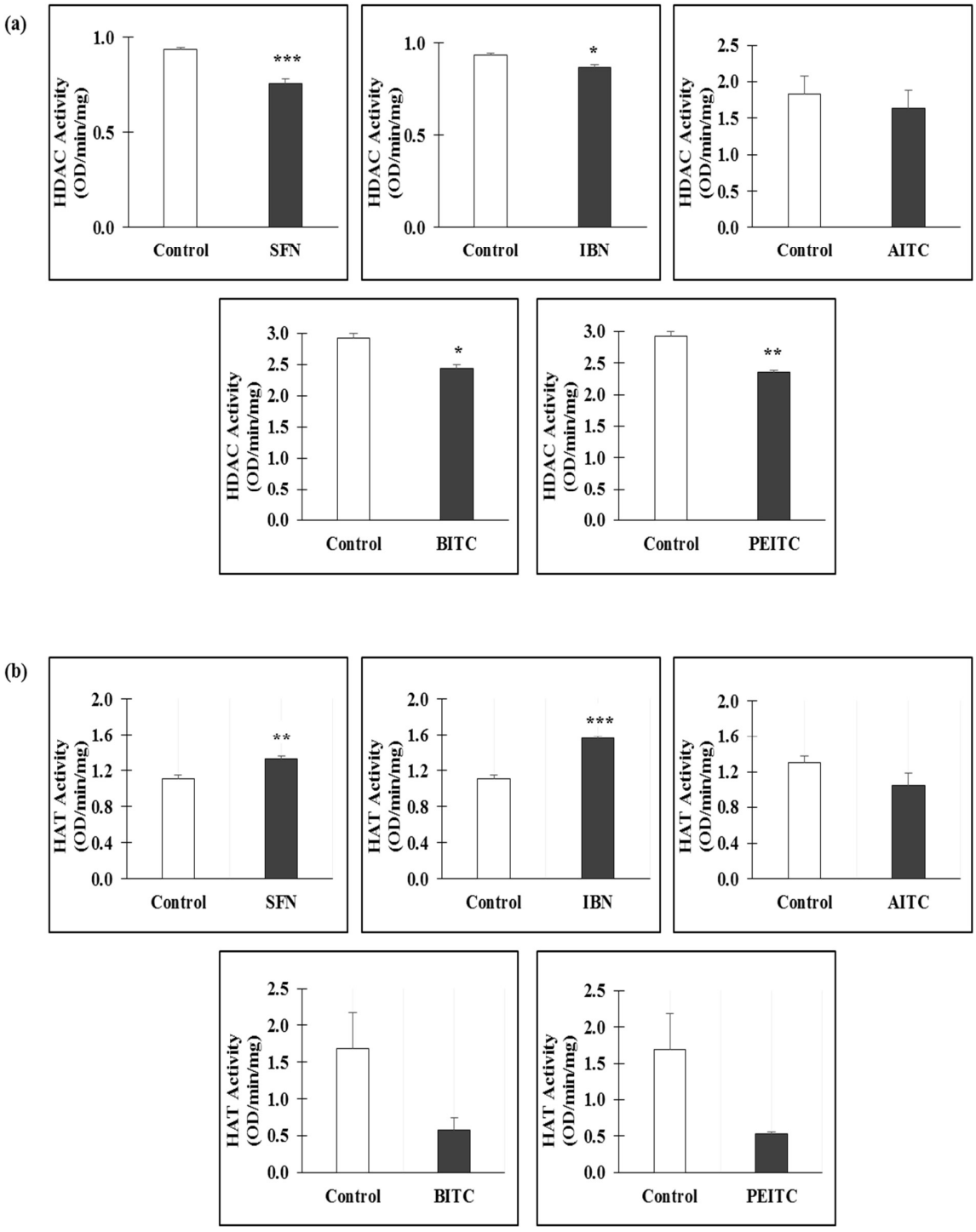

Figure 3.23: The effect of ITCs on total HDAC and HAT activity levels in A375 cells. Cells were exposed to 10 μM of each ITC for 48 hrs and then **a**) total HDAC and **b**) total HAT activity levels were assessed using the Epigenase HDAC Activity/Inhibition Direct and the Epigenase HDAC Activity/Inhibition Direct assay kits, respectively. Data were normalized to the corresponding untreated control (Ctrl) and are best representative of three

independent experiments. Statistical analysis performed by Student's *t*-test and significance was set at *$p < 0.05$, **$p < 0.01$, ***$p < 0.001$ relative to corresponding controls.

3.3.2 Exposure to ITCs Affect the Expression of Specific Histone H4 and H3 Lysine Acetylation Marks in A375 Cells

To further elucidate the effect of the observed changes of HDACs and HATs expression and activity levels, upon exposure to each ITC, we next focused on characterizing the acetylation profile of specific lysine residues on the tails of both H3 and H4 core histone proteins. To this end, total histone extracts of A375 cells exposed to 10μM of each ITC, were utilized for the determination of the acetylation patterns of H4 on lysines (K) 5, 8 and 12 and of H3 on lysines 9, 14, 18, 27 and 56. Diminished expression levels of AcH4K5, AcH4K8 and AcH4K12 were observed with SFN, AITC and BITC while IBN and PEITC reduced the expression of AcH4K8 and AcH4K12 only, relative to control (Fig. 3.24). In general, our results showed that AITC was more potent in inhibiting AcH4K8 and AcH4K12 protein expression levels,followed by BITC and PEITC, respectively. Finally, BITC exhibited a more potent effect against AcH4K5 protein expression levels.

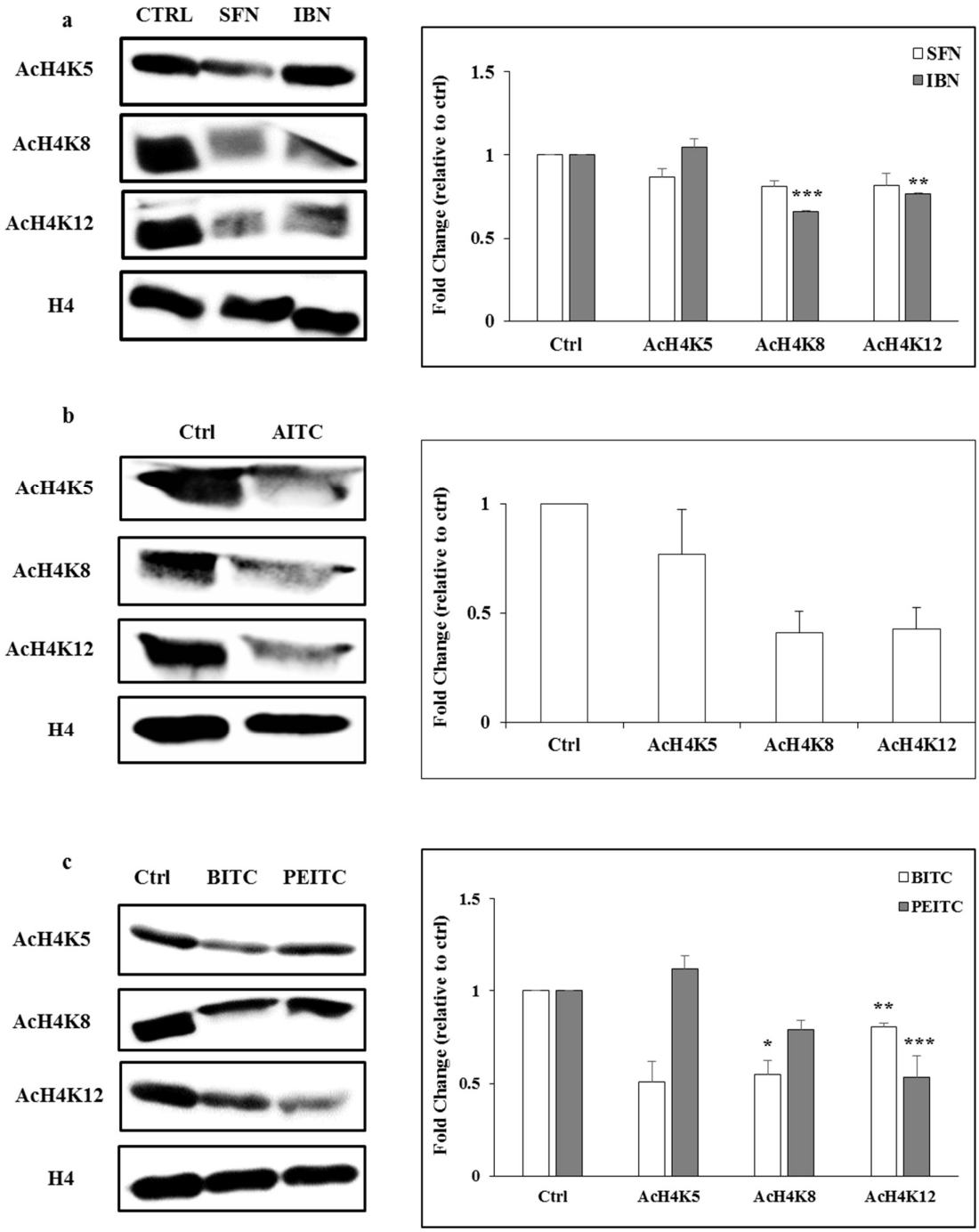

Figure 3.24: The effect of ITCs on specific lysine acetylation marks on H4 in A375 cells. Cells were exposed to 10 μM of **a**) SFN or IBN, **b**) AITC and **c**) BITC or PEITC for 48 hrs. Western immunoblotting was used, in total histone extracts, in order to assess the expression levels of the acetylation status of H4K5, H4K8 and H4K12. Protein expression levels were quantified by densitometry, relative to H4, and data were normalized to the untreated control

(Ctrl). In all experiments, blots are representative of three independent experiments. Statistical analysis performed by Student's *t*-test and significance was set at *$p < 0.05$, **$p < 0.01$, ***$p < 0.001$ relative to corresponding controls.

Regarding the acetylation pattern of H3, both SFN (Fig. 3.25a) and BITC (Fig. 3.25b) exerted a similar effect, resulting in the reduced expression of AcH3K9, AcH3K14 and AcH3K27. Moreover, BITC influenced to a greater extent the reduction in the expression of these marks and especially that of AcH3K56. On another note, PEITC slightly increased the levels of AcH3K14 and AcH3K56, without affecting the pattern of AcH3K9, AcH3K18 and AcH3K27 (Fig. 3.25b). In addition, IBN was shown to slightly decrease the acetylated levels of AcH3K27 while did not induce any significant changes in those of AcH3K9, AcH3K14 and AcH3K18 (Fig. 3.25a). Interestingly, AITC had no effect on the acetylation profile of none of the H3 lysine residues under investigation (Fig. S7).

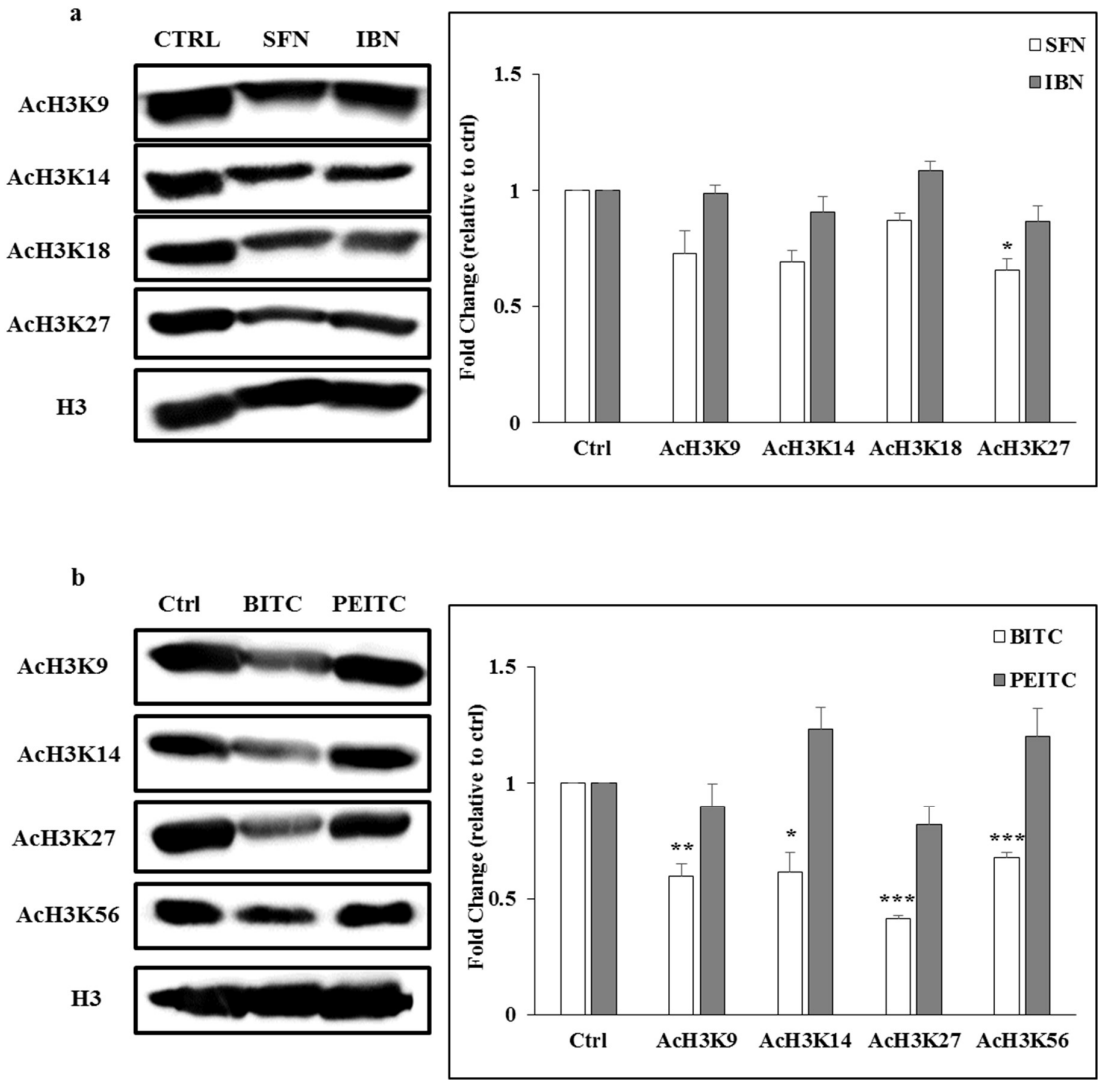

Figure 3.25: The effect of ITCs on specific lysine acetylation marks on H3 in A375 cells. Cells were exposed to 10 μM of **a**) SFN or IBN and **b**) BITC or PEITC for 48 hrs. Western immunoblotting was used, in total histone extracts, in order to evaluate the expression levels of the acetylation status of H3K9, H3K14, H3K18, H3K27 and H3K36. Protein expression levels were quantified by densitometry relative to H3 and the data were normalized to the untreated control (Ctrl). In all experiments, blots are representative of three independent experiments. Statistical analysis performed by Student's *t*-test and significance was set at $*p < 0.05$, $**p < 0.01$, $***p < 0.001$ relative to corresponding controls.

3.3.3 ITCs Modulate the Protein Expression Levels of Specific HMTs

To assess the effect of each ITC on the protein expression levels of specific HMTs, western immunoblotting was utilized, on nuclear cell lysates of A375 cells exposed to each ITC for 48hrs against various HMTs (e.g. G9a/EHMT2, ESET, RBBP, ASH2L, SET8 and SET7-9). Of those, only the expression levels of SET8, SET7-9 and ESET were affected after exposure to each ITC while the expression of G9a/EHMT2, RBBP and ASH2L were similar to those of the untreated control levels (Fig. S8) More specifically, our results showed that the expression levels of SET8 were significantly diminished in A375 cells exposed to IBN (Fig. 3.26a) while unaffected under AITC (Fig. S8c) exposure. In contrast, its expression increased markedly under treatment with BITC and PEITC when compared to untreated cells (Fig. 3.26c). Furthermore, protein expression levels of SET7-9, showed a significant over-expression post exposure to SFN and IBN (Fig. 3.26a) whereas in AITC, BITC and PEITC exposure those levels were significantly reduced (Figs. 3.26b and c). Finally, a significant elevation of ESET protein expression levels was observed after exposure to BITC and PEITC (Fig. 3.26c).

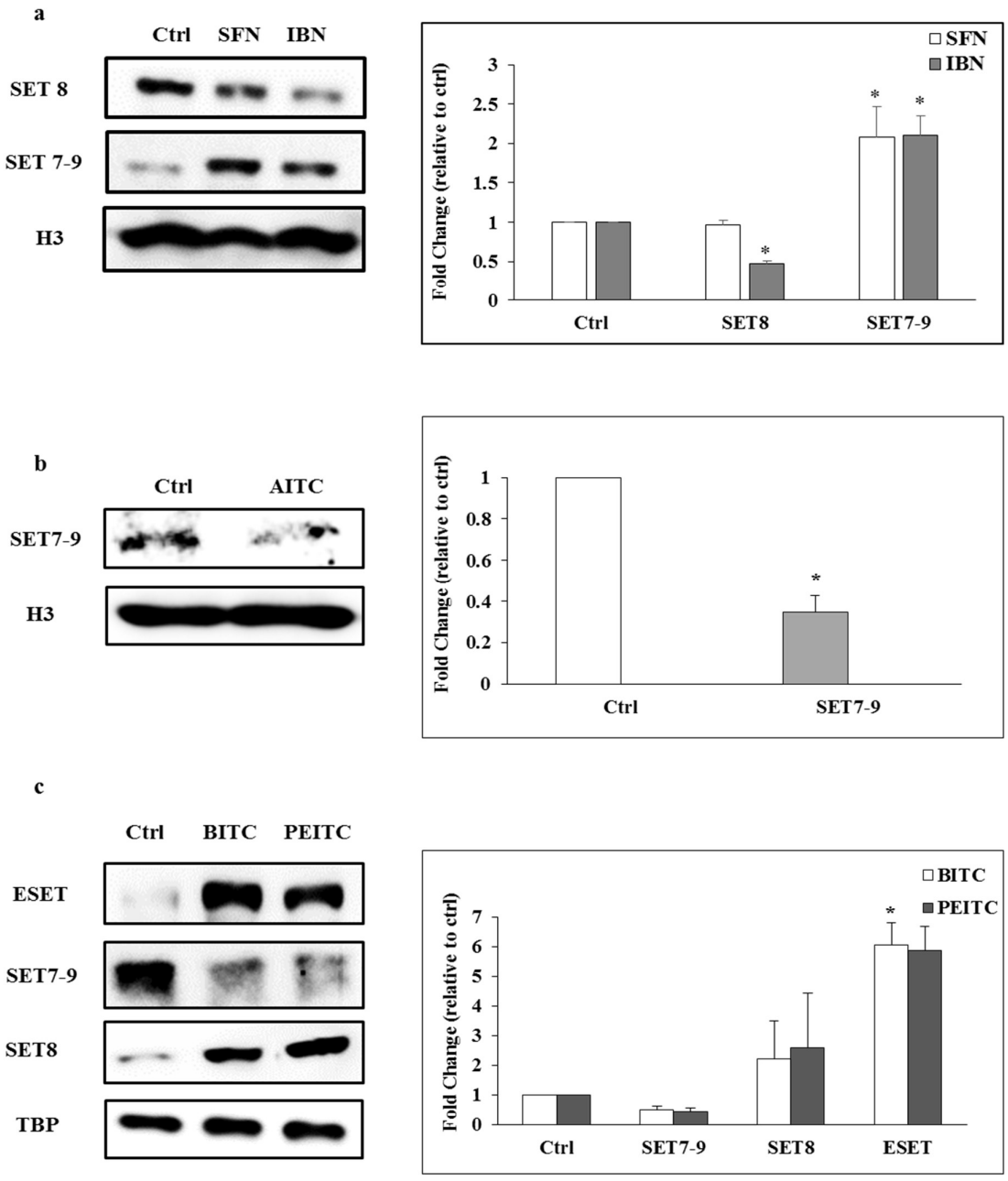

Figure 3.26: The effect of ITCs on specific HMTs protein expression levels in A375 cells. Cells were exposed to 10 μM of **a**) SFN or IBN, **b**) AITC and **c**) BITC or PEITC, for 48 hrs. Western immunoblotting was used in nuclear extracts to determine the expression levels of SET8, SET7-9 and ESET. Protein expression levels were quantified by densitometry relative to H3 or TBP and data were normalized to the untreated control (Ctrl). All blots are representative of three independent experiments. Statistical analysis performed

by Student's *t*-test and significance was set at *p < 0.05, **p < 0.01, ***p < 0.001 relative to corresponding controls.

3.3.4 Di- and tri-methylation Marks of Specific Lysine Residues on Histone H3 Found Differentially Affected in A375 Cells Treated with ITCs

Next, we determined the effect of all 5 ITCs on the di- and tri-methylation levels of lysines (K) 4, 9, 27, 36 and 79 on histone H3. It was shown that exposure to SFN, IBN, BITC and PEITC over-expressed both di- and tri-methylation levels of K9 with BITC and PEITC having a more potent effect on H3K9me2, while IBN and PEITC against H3K9me3 (Figs. 3.27 and 3.28). Furthermore, our results showed an increase in the protein levels of both di- and tri-methylation of K36 and 79, on H3, under exposure to SFN and IBN (Fig. 3.27a and Figs. 3.28a and b). On the other hand, BITC and PEITC did not significantly affect the expression of H3K36me3 and H3K79me3 (Fig. S9d) while they enhanced H3K79me2 levels (Fig. 3.28c). Also, BITC caused a reduction in H3K36me2 which, in turn, was not affected by PEITC (Fig. 3.28c). In addition, exposure to BITC and PEITC downregulated the expression levels of H3K27me2 (Fig. 3.28c), an effect which was not observed with SFN, IBN and AITC (Fig. S9). Also, AITC and BITC, significantly reduced the tri-methylation levels of H3K4 (Figs. 3.27b and c). Finally, AITC was shown to be more effective in downregulating H3K4me3 whereas did not affect the tri-methylation status of the other lysines (Figs. S9c and g).

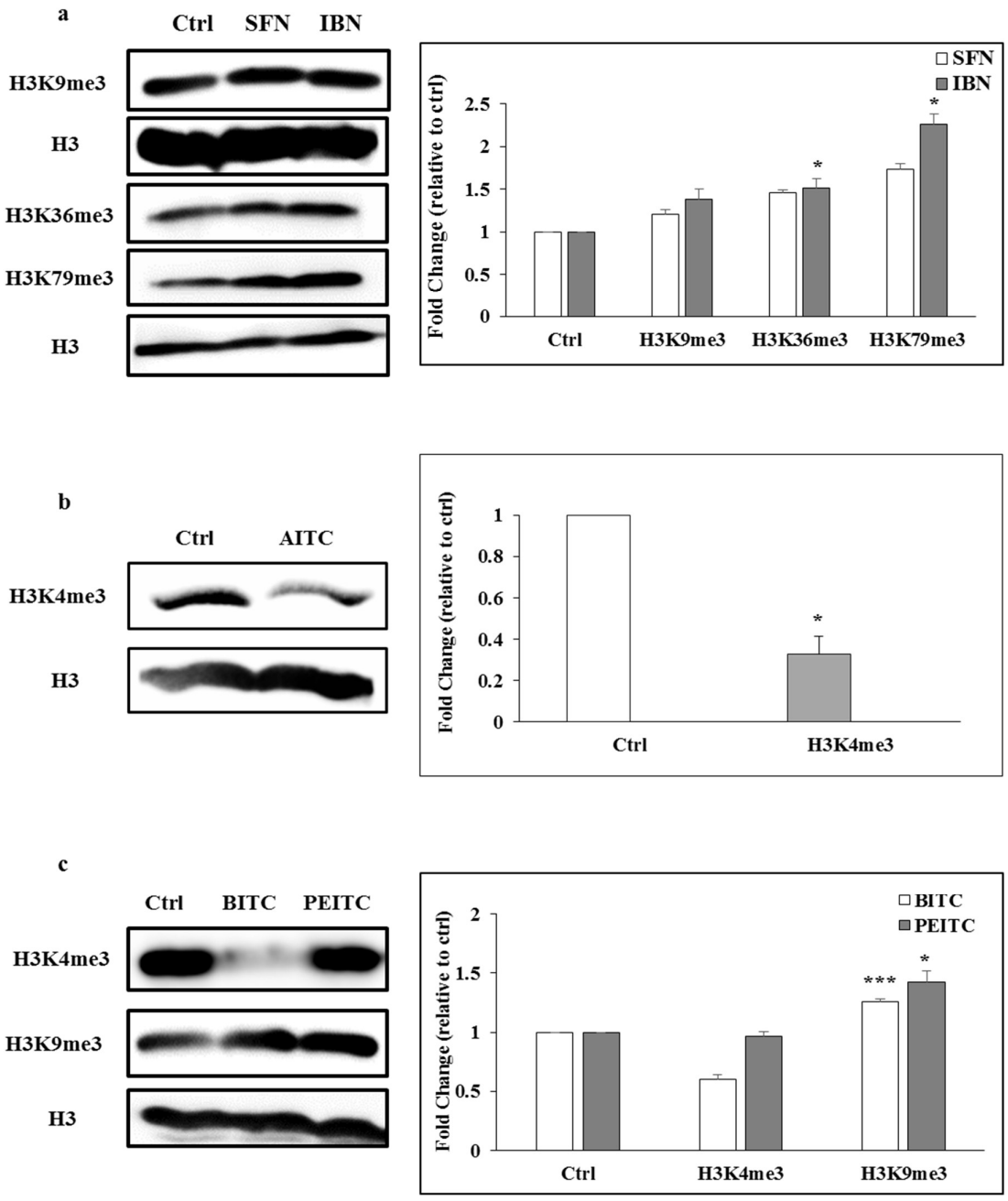

Figure 3.27: ITCs effect on the tri-methylation status of H3 specific lysine residues in A375 cells. Western immunoblotting was used in total histone extracts of A375 cells exposed to 10 μM of **a**) SFN or IBN, **b**) AITC and **c**) BITC or PEITC, for 48hrs, in order to assess the tri-methylation status of lysines (K) 4, 9, 36 and 79 on histone H3. Protein expression levels were quantified by densitometry relative to H3 and the data were normalized to the untreated control (Ctrl). All blots are representative of three independent experiments. Statistical analysis performed by Student's *t*-test and significance was set at $*p < 0.05$, $**p < 0.01$, $***p < 0.001$ relative to corresponding controls.

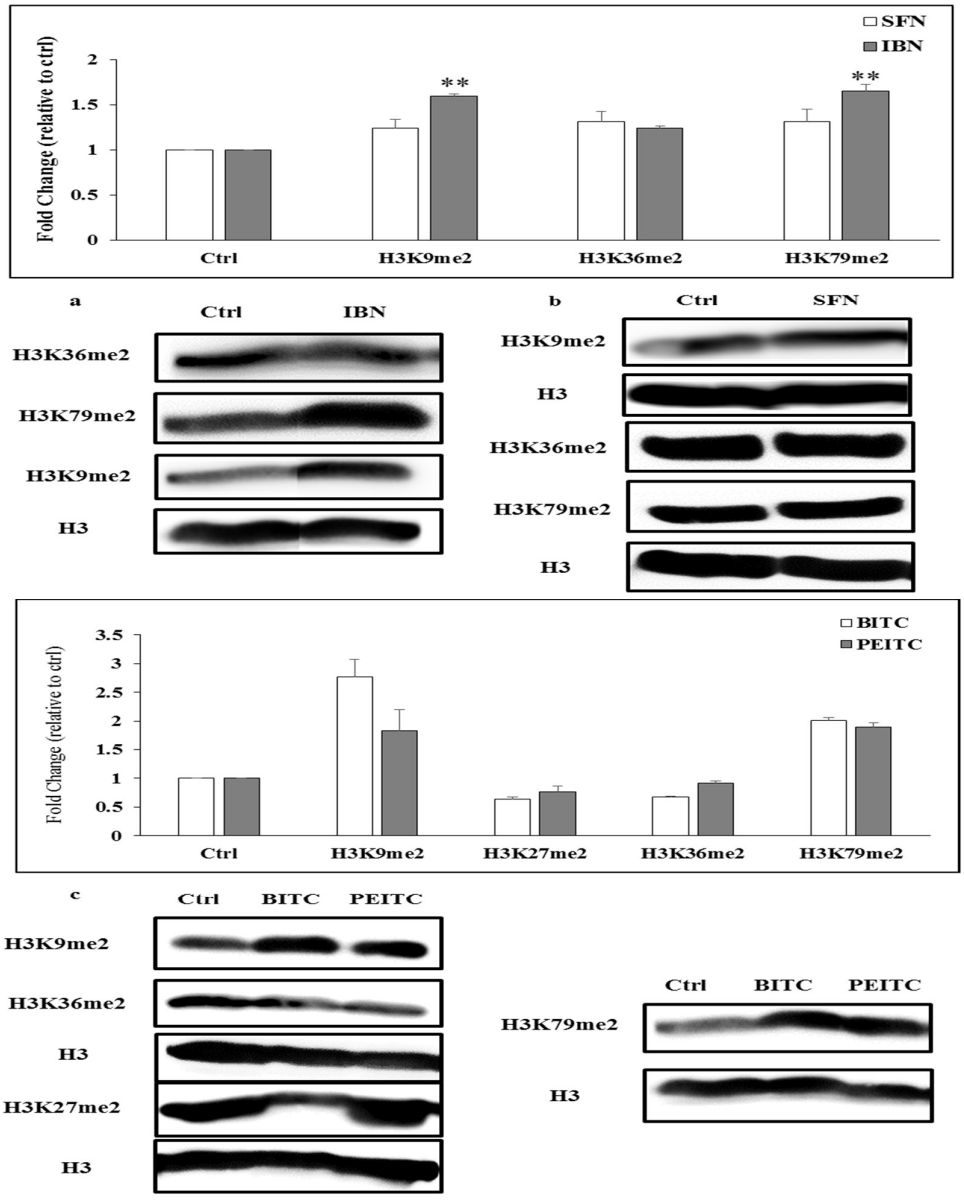

Figure 3.28: ITCs effect on the di-methylation status of H3 specific lysine residues in A375 cells. Cells were exposed to 10 μM of **a**) IBN, **b**) SFN and **c**) BITC or PEITC for 48 hrs and western immunoblotting was used, in total histone extracts, in order to determine the expression levels of di-methylated lysines (K) 9, 27, 36 and 79 on histone H3. Protein expression levels were quantified by densitometry relative to H3 and the data were normalized to the untreated control (Ctrl). All blots are representative of three independent experiments. Statistical analysis performed by Student's *t*-test and significance was set at $*p < 0.05$, $**p < 0.01$, $***p < 0.001$ relative to corresponding controls.

Chapter 4

Discussion

The use of naturally occurring compounds, such as isothiocyanates (ITCs), to prevent melanoma initiation and progression has gained an increasing interest over the last years. Various studies, have focused on the potential of ITCs to inhibit melanogenesis, both *in vitro* (Arcidiacono et al., 2017; Hamsa et al., 2011; Huang et al., 2014; Huang et al., 2012; Lai et al., 2017; Y. S. Ma et al., 2017; Mantso et al., 2019; Mantso et al., 2016; Mitsiogianni, Mantso, et al., 2019; Mitsiogianni et al., 2020; Rudolf et al., 2014; Yuanfeng et al., 2015) and *in vivo* (Bansal et al., 2015; Do et al., 2010; Fisher et al., 2016; Ni et al., 2013; Ni et al., 2014; Pradhan et al., 2010; P. Thejass & G. Kuttan, 2007b). All of these studies have demonstrated the multifactorial effect of ITCs in promoting melanoma cell death, via triggering multiple pathways, including apoptotic induction, cell cycle progression disruption, ROS production and mitochondrial depolarization, as well as blocking invasion and metastasis. In line with these observations, in this study, we have demonstrated that 5 ITCs, namely SFN, IBN, AITC, BITC and PEITC were able to induce cytotoxicity, promote ROS formation, G2/M and G1 cell cycle growth arrest and cell death, *in vitro* in a range of human and rodent malignant melanoma cell lines. Our results showed that exposure to these ITCs, inhibited melanoma cancer cell growth in a concentration- and time-dependent manner in human A375 and murine B16F-10 melanoma as well as in human lymph node-derived metastatic melanoma Hs 294T cells. While human brain-derived metastaticVMM1 melanoma on-melanoma epidermoid carcinoma (A431) and normal transformed (HaCaT) keratinocyte cells were found to be more resistant as indicated from their respective EC_{50} values (Table 3.1). These findings are in agreement with the literature, as a number of studies have also documented that ITCs exert a diversecytotoxic effect among cancer cells and have a different sensitivity between cancer and normal cells (Hać et al., 2019; Konic-Ristic et al., 2016; Nomura et al., 2005; Powolny & Singh, 2010; Trachootham et al., 2006; Tripathi et al., 2015). Differences in cell susceptibility in response to ITC exposure have been reported to be complex due to being attributed to multiple signalling pathways. According to such observations, possible explanations acountable for such versatile responses may involve the following: i) magnitude of ROS formation (an excessive increase in ROS level production above and beyond a particular threshold enhances cellular vulnerability to excess oxidative damage) (Loo, 2003; Powolny & Singh, 2010; Syed Alwi et al., 2012; Trachootham et al., 2006); ii) glutathione (GSH) metabolism alongside with the glutathione S-transferase (GSTs) isoforms that are present in cells (intracellular GSH levels play a crucial role in ITC cellular accumulation and subsequently cytotoxicity) (Konic-Ristic et al., 2016; Syed Alwi et al., 2012; Xu & Thornalley, 2001); iii) basal transcriptional activity of

genes important in cell survival such as *NRF2, NFκB, Apaf-1* and *Bax*) (Batra et al., 2010; Choi et al., 2007; Syed Alwi et al., 2012).

To this end, in order to better characterize the anti-proliferative effect of ITCs, in our *in vitro* model, we assessed the ability of all 5 ITCs to induce oxidative stress as a means of promoting cell death. According to our observations, ITCs stimulated an oxidative stress response in all 6 cell lines but the magnitude of ROS production was variable among different cell types as well as among different ITCs (Fig. 3.17 and Fig. S3). Particularly, our results demonstrated that ROS induction in primary melanoma cell line was considerably higher compared to metastatic one (mainly Hs294T) and non-malignant epidermoid carcinoma (A431), with the effect being intensified over longer periods of exposure. Interestingly, we observed a selective specificity of SFN, IBN, BITC and PEITC towards human malignant melanoma (A375) cells as far as ROS induction. A375 cells have been previously reported to be more vulnerable in oxidative stress induced by these ITCs. Furthermore, both BITC and PEITC have triggered ROS production at a highest magnitude in B16F-10, A431 and HaCaT cells. In line with these observations, other studies have also reported that ROS induction is a main mechanism capable of mediating cell death in various cancer cell models including prostate (J. F. Lin et al., 2017), thyroid (Wang et al., 2015), breast cancer (Xiao et al., 2008), hepatocellular (P. Pocasap et al., 2018), osteosarcoma (de Oliveira et al., 2014; Wu et al., 2011) and melanoma (Huang et al., 2014; Huang et al., 2012). Persistent ROS production seems to sensitize cancer cells to apoptosis-induced cell death as a mechanism by which anti-cancer agents (including ITCs) exert their cytotoxicity. A possible explanation for this effect is that although malignant cells are characterized by high levels of oxidative stress, being able to increase these levels even further (such as by ITCs) can trigger cell death and thus be toxic to these cells. On the contrary, normal cells usually have lower intracellular ROS levels and are therefore more resistant to ROS-inducing compounds thereby allowing the targeting of cancer cells (Gupta et al., 2014; Konic-Ristic et al., 2016; Trachootham et al., 2006). Apart from constitutive intracellular ROS levels, other important factor for the cancer cell fate are the GSH levels as well as the ITCs accumulation rate. In the literature, it is well documented that the mode of action and the intracellular accumulation of ITCs is based primarily on their ability to conjugate with intracellular GSH. ITCs accumulation depends on the cellular GSH levels and leads to GSH depletion. Exposure of cells to ITCs results in the rapid and high intracellular accumulation mainly through simple diffusion. ITCs-GSH conjugation by GSH transferases (GSTs), is also the major driving force for ITC accumulation by means of the enhanced intracellular

trapping that prevents from diffusive efflux (Nakamura et al., 2018, Zhang, 2012). Zhang et al., investigated the molecular mechanism responsible for ITCs accumulation in human breast cancer cells and murine hepatoma cells (Zhang, 2000; Zhang, 2001). The initial ITC cellular uptake rates found to be closely correlated with ITC-GSH conjugation reaction, with increased cellular GSH levels resulting in enhanced cellular ITC uptake. Similarly, it was reported that ITC uptake rate was increased proportionaly with an increase in cellular GST activity levels. These set of experiments strongly suggests that ITCs are predominantly taken up by cells through GSH conjugation reactions and cellular GST promotes ITC uptake by enhancing the conjugation reaction (Zhang, 2000; Zhang, 2001).

Therefore, GSH levels are of particular importance (for ITCs accumulation) in the context that a high intracellular GSH concentration results in greater ITCs influx. Rapid ITC accumulation in cells and the subsequent depletion of GSH due to ITC conjugation, increases cellular vulnerability to ROS-induced damage. This may explain ITCs selectivity towards cancer cells, as these cells reported to have higher intracellular GSH levels compared to normal cells and thus tend to be more sensitive to ITCs' anticancer function (Gupta et al., 2014; Konic-Ristic et al., 2016). In order to further delineate the ITCs' mode of action, with respect to ROS generation, we assessed the intracellular GSH levels post exposure to each of the 5 ITCs. We observed a profound decrease of cellular GSH, mainly in A375 and Hs294T cells during the first 24hrs of exposure in comparison to GSH elevated levels upon prolonged exposure periods, suggesting the reduced capacity of GSH biosynthesis (Fig. 3.18 and Fig. S4). In agreement, Zhang et al., showed that the rapid accumulation of BITC and SFN into murine hepatoma cells, led to a significant drop in GSH, while its levels reported to be rapidly replenished through synthesis. Interestingly it was mentioned that chronic exposure of cells to low concentration of ITCs (>24h) was associated with a mark increase in GSH levels, suggesting that a cycling mechanism is formed, where ITCs deplete GSH, subsequently stimulating its biosynthesis, which in turn may lead to more ITC accumulation in cells (Zhang, 2000). In addition, another proposed mechanism for the observed GSH recovery is based on the *de novo* synthesis of GSH. Specifically. it was reported that ITC-GSH conjugates, once exported from cells, are not stable and they are hydrolyzed extracellularly into GSH and ITC. GSH found to be further degraded to cysteine and cysteine both of which are reabsorbed into cells, triggering GSH synthesis thus, resulting into a burst elevation of GSH (Xu & Thornalley, 2001). Overall, many studies agree in that the net balance of ITC effects (e.g. on detoxification and pro-oxidant pathways) could influence the magnitude of ITC-mediated cellular toxicity (Chen et al., 2011; Overby et al., 2015; Pham

et al., 2004; Singh et al., 2005). In this study, we observed a differential response regarding ROS and GSH levels among all cell lines of our model, which could contribute to the observed selective toxicity of all 5 ITCs, a speculation that requires further investigation.

To further characterize the cytotoxicity profile of all ITCs, we investigated their ability to inhibit cell cycle progression and promote cell death. The potential of ITCs to stimulate cell cycle arrest has been well-documented in the literature. Numerous studies have indicated ITCs association with G2/M cell cycle growth arrest and apoptotic induction in various cancer cell lines (Huang et al., 2014; Huang et al., 2012; Lau et al., 2010; K. C. Liu et al., 2016; Mantso et al., 2019; Visanji et al., 2004; Wu et al., 2011). However, ITCs have been also found to effectively induce cell cycle arrest at different phases depending on the specific cell line used (Arumugam et al., 2020; P. Y. Chen et al., 2012; Cheng et al., 2019; Jadhav et al., 2007). For instance, exposure of human osteosarcoma cells to PEITC growth arrested cells in the G2/M phase while in the case of human oral squamous carcinoma cells, PEITC exposure resulted in G0/G1 growth arrest (P. Y. Chen et al., 2012; Huang et al., 2014). In line with these observations, exposure of two neuroblastoma cell lines (HT92 and SK-N/-SH) with IBN inhibited cell cycle growth at G2/M and G0/G1 phases, respectively (Jadhav et al., 2007). Similarly, assessing the cell cycle distribution in our *in vitro* model, a quite similar pattern was illustrated as all ITCs had the capacity to induce cell cycle growth arrest at the G2/M phase in most cell lines that were utilized. The only exception was in the case of keratinocytes where exposure to SFN and IBN growth arrested cells at the G0/G1 phase of the cell cycle while in the case of VMM1 cells exposed to AITC, there was an accumulation of these cells in the S phase. These observations strongly support the notion that the effect of ITCs on cell cycle distribution depends significantly on the particular type of cancer cell utilized. In addition, we further characterized the effect of these 5 ITCs on their ability to promote cell death and apoptosis. To this end, we investigated the mode of cell death activation, by means of microarray-based RT-PCR expression profiling of various apoptosis-related genes as well as of flow cytometry analysis of relative levels of cellular apoptosis and/or necrosis. According to our results, it was apparent that all ITCs were capable of modulating the apoptotic response by mediating the differential expression of a number of genes representative of various stages in the apoptotic cascade (e.g., intrinsic, extrinsic, p53-dependent apoptosis, etc.) as well as of processes implicated in cell growth and survival in A375 cells (see Tables 3.2, 3.3, 3.4, 3.5, 3.6 and 3.7 – preliminary experiments). Interestingly, our results did not show the potent apoptotic induction (by means of caspase 3/7 activation) we expected, while in A375 and Hs294T cells , higher

levels of necrosis were observed and especially upon exposure to BITC and PEITC. The only exception was the case of Hs294T where significant apoptotic induction was reported. On the contrary, in A431 and HaCaT cells neither apoptosis nor necrosis were stimulated, demonstrating their resistance to the effect of ITCs. In the literature, there are reports demonstrating the unresponsiveness of melanoma cells to diverse apoptosis-mediated chemotherapeutics and that some of these agents could deviate from the typical, caspase-dependent apoptotic processes, with a shift towards necrotic activation (Mijatovic et al., 2011; Soengas & Lowe, 2003). This death mode switch is considered to be partially due to alterations in mitochondrial permeability and bioenergetics. Excessive ROS formation can lead to mitochondrial membrane permeabilization and disturb mitochondrial respiratory capacity and ATP production, resulting in programmed necrosis activation (Armstrong et al., 2018; Ouyang et al., 2012; Troyano et al., 2003). In another study, BITC was found to alter the mode of cell death in human cervical cancer HeLa cells from apoptosis to necrosis, by modulating the intracellular ATP levels. This study demonstrated the importance of ATP levels as well as ITCs concentration in the switching between apoptosis and necrosis (Miyoshi et al., 2008). In addition, other studies have shown the ability of ITCs to promote both apoptotic and necrotic cancer cell death (Piman Pocasap et al., 2018; Trachootham et al., 2006) however, they do suggest that such exposure can favor the activation of necrosis but further studies are needed in order to enhance our current understanding.

Another important observation in this study, is the differential cytotoxic activity of each of the 5 ITCs. According to their cytotoxicity profile, the following trend of potency was noticed: BEITC~PEITC > SFN~IBN>AITC. A similar toxicity pattern was also observed in leukemia cells exposed to SFN, ERN (erucin), IBN, AITC, BITC and PEITC (BITC~PEITC > ERN~IBN > AITC > SFN) (Jakubikova et al., 2005). These observations are in agreement with the current literature data, suggesting that the anti-cancer potential of ITCs is strongly associated with their structure and more specifically with specific differences such as those of the existence of functional groups like double bonds, benzene rings, sulfur or hydroxyl moiety etc. on their side chains. To this end, it is generally considered that the aromatic ITCs (e.g. BITC and PEITC) are more potent than the aliphatic (e.g. SFN and AITC) ones. In addition, the impact of a particular ITC activity may depend on the mechanism of biological function, cell type, etc. (Crichlow et al., 2012; Piman Pocasap et al., 2018; Rajendran et al., 2013; X. Wang et al., 2011). To this end, a study has demonstrated that exposure of human colon cancer cells to AITC, SFN and other SFN-related ITCs (e.g. 6-SFN and 9-SFN) resulted in the inhibition of HDAC activity and consequently increased apoptosis as well as

cell cycle growth arrest. Moreover, in the same study, it was shown that the potency of the ITC cytotoxicity increased proportionally based on the length of the alkyl chain in a manner where AITC<SFN < 6-SFN < 9-SFN (Rajendran et al., 2013). In another study, it was reported that the oxidation state of the sulfur atom as well as the presence of an aromatic ring on the ITC's side chain are both important factors in modifying the anti-cancer potency of ITCs in hepatocellular cancer cells (Piman Pocasap et al., 2018). Overall, the results from both studies are in agreement with our data thereby strongly supporting the fact that structural variations largely affect the potency of anti-cancer capacity of any ITC.

Then, we focused on investigating the interaction of ITCs with the epigenetic machinery in an attempt to enhance our current understanding as to how structurally distinct ITCs can influence gene expression and thus the potency of their function. For this reason, we concentrated on investigating the acetylation and methylation of specific lysine (K) residues on two major core histone proteins (H3 and H4) in human malignant melanoma (A375) cells. In general, it is well known that such histone posttranslational modifications are associated with the transcriptional regulation of various genes involved in very diverse functions like cell growth, proliferation as well as migration and so aberrant alterations in the expression levels of these proteins are considered to be implicated in the development and progression of melanoma (Boyle et al., 2005; Penta et al., 2018; K. Saha et al., 2013; Sarkar et al., 2015). Particularly, overexpression of class I and II HDACs has been associated with cancer progression and cell survival (Bai et al., 2015; J. Liu et al., 2016; Pan et al., 2010; Tsunoda et al., 2011; Z. Wang et al., 2014) as well as drug resistance (Krumm et al., 2016). Therefore, the pharmacological use of a range of HDAC inhibitors (HDACi) can potentially i) promote apoptosis and cell cycle growth arrest (Flørenes et al., 2004; Peltonen et al., 2005; Yokoyama et al., 2008), ii) overcome resistance against various drugs currently used in clinical settings (Booth et al., 2017; Gallagher et al., 2018; Heijkants et al., 2017; Lai et al., 2012; Maertens et al., 2019) and iii) enhance immunogenicity (Cheng et al., 2016; Laino et al., 2019; Lienlaf et al., 2016; Woan et al., 2015; Woods et al., 2015). To these ends, ITCs have been shown to exhibit an epigenetic modulatory capability thereby acting as potent HDAC inhibitors by disrupting the HAT/HDAC ratio and so inhibit cancer cell growth through regulation of the expression of critical tumor suppressor genes (Abbaoui et al., 2017; Boyanapalli et al., 2016; Okonkwo et al., 2018; Paul et al., 2018; Pledgie-Tracy et al., 2007; Rajendran et al., 2013; Yuanfeng et al., 2015). In agreement to these observations, we have also reported herein that SFN, IBN, BITC and PEITC significantly reduced the protein expression levels of several HDAC enzymes (e.g. HDAC1, HDAC2, HDAC4 and HDAC6)

whereas AITC decreased only the expression of type II HDACs in human malignant melanoma (A375) cells. Finally, the reduction on the expression of class I (e.g. HDAC1, HDAC2) and class II (e.g. HDAC4, HDAC6) HDACs was shown to be accompanied by a decline of total HDAC activity levels, under exposure to all 5 ITCs.

On another note, we also reported diminished expression levels of specific HATs, namely CBP and AcetylCBP/p300, in A375 cells, under exposure to all 5 ITCs. In addition PCAF protein levels were also found to be affected, but only under SFN and PEITC exposures by being either reduced or slightly increased respectively. These observations were followed by a reduction in total HAT activity levels, with a marked decrease noticed by BITC and PEITC exposures. In agreement with our data, PEITC and BITC have been also shown to inhibit both HDAC and HAT enzymes and consequently repress cancer cell growth (Batra et al., 2010; C. Yu, A. Y. Gong, D. Chen, D. S. Leon, et al., 2013). On another note, HATs have long been known to act as important mediators in processes essential for cell survival including cell proliferation and cell cycle progression. It has been documented that down-regulation of HATs, results in suppression of cell proliferation and apoptotic induction in various cancer cell lines (Gajer et al., 2015; Lu et al., 2018; Suryanarayanan et al., 2018; Suryanarayanan & Singh, 2015). Regarding melanoma, inhibition of these enzymes has been reported to stimulate a senescence-like phenotype and suppress cell growth (Bandyopadhyay et al., 2002; R. Wang et al., 2018; Yan et al., 2013). Although, a large body of evidence supports the significance of repressing these enzymes thereby inhibit cancer development, yet, there are reports that describe a tumour suppressor function for HATs, through p53 acetylation (Jia et al., 2016; Kramer et al., 2015; Q. Li et al., 2016; Liu et al., 1999; Sakaguchi et al., 1998). This controversy lays on the diverse role of HATs that has been described in participating to both tumor-suppressive and pro-oncogenic processes. Consequently, targeting HATs in order to manage malignant development has gained great interest, over the last years, and so far a number of small molecule inhibitors have been developed and tested in preclinical trials as “next generation” cancer therapeutics (Attar & Kurdistani, 2017; Di Martile et al., 2016; Goodman & Smolik, 2000). Furthermore, we have assessed the impact of ITC on the acetylation status of specific lysine residues on the N-terminus tails of H3 and H4. Overall, we have observed reduced levels of specific histone acetylation marks on both H3 and H4, observations that are in agreement with the observed down-regulation of CBP/p300 and PCAF enzymes. It is generally known, that important target sites for the action of CBP/p300 are H4K8 and H4K5 as well as H3K14, H3K18, H3K27 and H3K56 whereas PCAF preferentially acetylates H3K14. PCAF has also been shown to regulate

H4K8 and H3K9 acetylation (Attar & Kurdistani, 2017; Das et al., 2009; Dekker & Haisma, 2009; Jin et al., 2011). Particularly, in this study, we observed diminished acetylation levels of H4K8 and H4K12, under exposure to all 5 ITCs. In addition, the acetylation levels of H4K5 were also found to be decreased, but only by SFN, AITC and BITC. Regarding the acetylation pattern of H3, reduced levels of AcH3K9, AcH3K14 and notably AcH3K27 were reported mainly by SFN and BITC exposure, while BITC also impaired the acetylation of K56. Loss of acetylation of these marks in various tumours, alongside with HAT inhibition, has been reported by others as well (Gajer et al., 2015; Lasko et al., 2018; Lu et al., 2018; Shidal et al., 2017), and have been associated with decreased cancer cell growth and metastatic potential. Alterations in the acetylation of histone marks have been linked with disease progression and so could act as potential diagnostic and/or prognostic biomarkers.

Another important aspect in gene transcriptional regulation is methylation of histone proteins which is also associated with the extent of histone protein acetylation. To this end, we next investigated the expression levels of specific HMTs and subsequently of their corresponding methylation target marks. Among the methyltransferases we have investigated, only 3 (e.g. SET8, SET7/9 and ESET) were found to be differentially regulated, by ITCs, in human malignant melanoma (A375) cells. Particularly, our results showed that all 5 ITCs differentially affected the expression of SET7/9. In particular, we observed a dramatic reduction on the protein expression levels of this histone methyltransferase after exposure of cells to AITC, BITC and PEITC whereas SFN and IBN significantly increased its expression. Similarly, SET8 was also found to be differentially affected by means of IBN exposure resulting in its diminished expression levels while BITC and PEITC increased its expression. In addition, BITC and PEITC exposure resulted in an overexpression of ESET. All these methyltransferases are important mediators of the methylation of H4K20 (SET8 and SET7/9), H3K4 (SET7/9) and H3K9 (ESET) and play an important role in DNA damage responses, cell cycle progression and carcinogenesis. Apart from the effect on histones, these HMTs also regulate the methylation status of non-histone proteins, such as p53 (Dhayalan et al., 2011; Fei et al., 2015; Kouzarides, 2007; Montenegro et al., 2015; Wagner & Jung, 2012). The role of SET7/9 in carcinogenesis seems to be controversial, exerting both tumour suppressor (Kurash et al., 2008; Liu et al., 2011) as well as oncogenic functions (Gu et al., 2018; Takemoto et al., 2016) depending on different cancer types and cell context. For instance, in acute myeloid leukaemia, breast and gastric cancer, SET7/9 has been reported to induce apoptosis and prevent cell proliferation and migration (Akiyama et al., 2016; Gu et al., 2017; Song et al., 2016). While on the other hand, in non-small cell lung cancer it had

the opposite effect, by inhibiting the apoptotic process (Gu et al., 2017). SET8 is another HMT with a controversial function. A large body of evidence supports the oncogenic role of this methyltransferase. In particular, increased levels of SET8 have been reported to be associated with decreased survival of gastric cancer and hepatocellular carcinoma cells (Guo et al., 2012; Shi et al., 2015). Furthermore, SET8 has been shown to increment prostate cancer proliferation through interaction with the androgen receptor (AR) (Yao et al., 2014) and enhance metastatic potential and invasiveness of breast cancer cells (Yang et al., 2012). In addition, SET8 downregulation resulted in reduced cell proliferation, prevented cell migration and sensitized breast cancer cells to DNA damage (B. Liu et al., 2016; N. Yu et al., 2013). On the other hand, down-regulation of SET8 decreased cell invasiveness and triggered metastasis in prostate cancer cells (Hou et al., 2016). Moreover, stabilization and activation of SET8 reported to be essential for induction of senescence in melanoma cells treated with pevonedistat (Benamar et al., 2016). Also, reduced levels of H4K20 mono-methylation (i.e. the main target of SET8) have been observed in melanoma tissues and are associated with increased proliferation rate of melanoma cells (Davis et al., 2017; Wang et al., 2012). Regarding ESET methyltransferase, its over-expression has been documented in various cancers by being associated with cancer progression and aggressiveness. In addition, increased levels of ESET are a common finding in human hepatocellular carcinomas where it promotes its progression and metastasis and is also a poor prognostic factor for these patients (Wong et al., 2016). Similar observations have been described in glioma (Spyropoulou et al., 2014) and prostate (Sun et al., 2014) cancer cell lines while ESET inhibition, in these cells, resulted in apoptosis and cell cycle growth arrest induction and decreased invasiveness and migratory ability. In melanoma, increased levels of ESET methyltransferase were shown to enhance melanoma onset and progression (Ceol et al., 2011; Orouji et al., 2019). Moreover, the oncogenic role of this methyltransferase has been also described in other cancer models through its capacity to modulate cell proliferation, migration and drug sensitivity thereby suggesting its possible role as a potential target for new therapeutic strategies (Lu et al., 2019; Rodriguez-Paredes et al., 2014; Wu et al., 2018). In contrast, increased expression of ESET was shown to suppress leukemic transformation, by negatively regulating the expression of acute myeloid pro-leukemic genes (Ropa et al., 2019). In agreement, ESET was also found to prevent tumor development by repressing target genes of the WNT signaling cascade (Kim et al., 2012) and to indirectly regulate hypoxia-induced p53-dependent apoptosis (Olcina et al., 2016). In addition, it also suppressed epithelial–mesenchymal transition (EMT), in breast cancer cells, while

decreased expression of ESET has been reported to facilitate cancer progression and promote drug resistance (Du et al., 2018). To conclude, it is obvious that the available information regarding the role of HATs and HMTs in cancer aetiology are contradictory, with a number of studies indicating a tumour suppressor function while others show their involvement in tumour progression. Obviously, further studies are needed in order to improve our understanding on the wide range of functions of these enzymes as well as their interactions with other components of the epigenetic machinery during carcinogenesis.

Given that these enzymes catalyze histone methylation, we next focused on the methylation landscape on the N-terminal tail of the H3 protein. In general, histone methylation, alongside with histone acetylation, are characteristic of the transcriptional state of their target genes. It is generally considered that actively transcribed genes are characterized by methylation on H3K4, H3K36 and H3K79 while methylation of H3K9, H3K27 and H4K20 are usually associated with gene silencing. However, the link between methylation and transcriptional activity is more complex, as the degree and the position of the methylation also determine gene transcriptional state. For example, tri-methylation of H3K9 and H3K27 is associated with gene transcriptional repression, while mono- and di-methylation of H3K9 usually results in activation of transcription. Increasing evidence supports the contribution of these epigenetic alterations to carcinogenesis and that dietary agents, including ITCs, are able to alter a number of these epigenetic events thereby regulating the transcriptional state of gene-targets in cancer (Fuentes et al., 2015; Kouzarides, 2007; Penta et al., 2018; Varier & Timmers, 2011). To this end, we have assessed the methylation status of specific K residues on H3 post-exposure to all 5 ITCs. According to our results, both di- and tri- methylation status of specific K (H3K4, H3K9, H3K27, H3K36 and H3K79) residues were shown to be differentially affected by all ITCs. Common targets of most exposures were shown to be H3K9, H3K36 and H3K79. In particular, exposure to SFN, IBN, BITC and PEITC resulted in elevated levels of di- and tri-methylation of H3K9 as well as of di-methylation of H3K79. In addition, we observed an increase in H3K36me2 by SFN and IBN but diminished levels when exposed to BITC. Other studies have also demonstrated the potential of ITCs to target these marks and thus to modify the expression of multiple genes involved in processes important for cancer cell survival. PEITC exposure of human prostate cancer cells reported to increase the methylation content (mono-, di- and tri-methylation) of H3K4, alongside with an increase in H3 acetylation), while reduced the level of tri-methylated lysine 9 of H3 thereby promoting cell cycle growth arrest and inhibition of cancer growth (Wang et al., 2007; Wang et al., 2008). A similar pattern was observed under treatment with phenylhexyl

isothiocyanate (PHI) in human leukemia cells. PHI enhanced significantly the content of acetylated histones H3 and H4 and further mediated methylation of H3K4 accompanied with a reduction on tri-methylated H3K9 levels as well as inducing cell cycle growth arrest and apoptotic cell death (Ma et al., 2006). In agreement to these observations, in skin cancer cells, SFN exposure decreased the expression of polycomb group (PcG) proteins and consequently reduced H3K27me3 resulting in the accumulation of cells in the G2/M phase (Balasubramanian et al., 2011). SFN was also shown to induce apoptosis and cell cycle growth arrest in human breast cancer cells via increased H3 and H4 acetylation and decreased content of H3K9me3 and H3K27me3 (Meeran et al., 2010; Sinha et al., 2015).

The diverse patterns of these epigenetic marks can also give useful prognostic, diagnostic and therapeutic information in cancer (Park et al., 2008; Seligson et al., 2005). For instance, low levels of H3K4me2 is considered as a poor prognostic factor in breast cancer (Elsheikh et al., 2009). In accordance, decreased levels of H3K4me2, alongside with low levels of H3K9me2 and AcH3K18, were found to be associated with an overall decreased survival of pancreatic adenocarcinoma cells (Manuyakorn et al., 2010). Low cellular levels of H3K4me2 and H3K18ac are also correlated with poorer clinical outcome in lung and kidney cancer patients (Seligson et al., 2009). Another significant prognostic marker in breast, ovarian and pancreatic cancers is H3K27me3, with lower levels indicating poorer patient's survival probabilities (Wei et al., 2008). Therefore, the characterization of the distribution of these epigenetic marks in cancer, could lead to the identification and development of potential predictive or therapeutic biomarkers.

Chapter 5

Conclusions

The beneficial effects of phytochemicals in preventing chronic diseases, including cancer has been the subject of extensive studies during the last few decades. Among such phytochemicals, ITCs have raised the scientific interest due to their unique cancer chemo-preventive properties. So far, a number of studies have provided evidence about the capacity of ITCs to exert multiple cytotoxic effects, including modulation of phase I and II enzymes, oxidative stress generation, inhibition of cell cycle progression, induction of apoptosis, prevention of metastasis and regulation of the epigenetic machinery. Overall, the ability of these agents to preferentially target cancer rather than normal cells, makes them excellent candidates for the development of new strategies against tumorigenesis. Among the various tumor-inhibitory effects of ITCs, their interactions with the epigenetic machinery have raised the scientific interest. Increasing evidence strongly supports their implication in a wide range of epigenetic components in various cancer models. However, in some cases the literature data seem to be controversial suggesting that further studies are needed in order to better understand the effect of these compounds on the complex epigenetic landscape.

In this study we have focused our analysis on the potential of 5 ITCs, abundant in the most commonly consumed cruciferous vegetables, (e.g. SFN, IBN, AITC, BITC and PEITC) to act as epigenetic regulators in malignant melanoma. To do so, we firstly assessed the anti-melanoma effect of these ITCs in an *in vitro* model of malignant melanoma consisting of human [A375 (primary melanoma), VMM1 (brain metastasis), Hs294T (lymph node metastasis)] and murine (B16F-10) melanoma as well as human non-melanoma epidermoid carcinoma (A431) and non-tumorigenic immortalized keratinocyte (HaCaT) cell lines. Overall, our study provides evidence that ITCs are capable of exerting an anti-melanoma potential by inducing cell cycle growth arrest and apoptotic cell death in the above-mentioned, well-defined *in vitro* experimental model.

We observed, herein, a significant decrease in the viability of A375, Hs294T and B16F10 while VMM1, A431 and HaCaT cells were less sensitive to ITCs exposure. More specifically, it was shown that the cytotoxicity potency was of the following order: BEITC~PEITC>SFN~IBN>AITC. Moreover, the observation that our experimental conditions of exposure to each of the ITCs do not induce damage to normal keratinocytes, (the cell type that surrounds melanocytes) raises hopes for the potential development of a "safer" treatment option (i.e. potentially less side effects of toxicity to the surrounding normal, healthy keratinocytes) against melanoma. At the same time, the observed reduction in cell viability was accompanied with increased levels of ROS, an oxidative stress response shown to be of a variable degree of induction among all cell lines. Alongside with the

enhancement of oxidative stress, a transient reduction of cellular GSH levels was observed but which were rapidly replenished upon longer exposure to each ITC. Such differential response to both ROS and GSH levels may contribute to the observed preferential targeting among the different cell types utilized in our *in vitro* melanoma model. However, this is more of a speculation than data-derived conclusion and so further studies are needed in order to investigate how alterations in oxidative stress and GSH homeostasis can affect intracellular accumulation of ITCs and consequently impact the potency of their cytotoxicity.

ROS induction has also been implicated in ITCs-induced modulation of cell cycle growth arrest as well as apoptotic cell death. Our data demonstrated the capacity of ITCs to accumulate cells at the G2/M phase (for most cell lines), G0/G1 phase (for HaCaT keratinocytes) and S phase (for VMM1 cells), suggesting that ITCs differentially affect cell cycle progression depending on the particular type of cancer cell. Furthermore, we observed an increase in necro-apoptotic cell populations, although in low levels in most cell lines, suggesting that the observed significant reduction in cell viability levels was probably attributed to cell cycle growth arrest instead of cell death. To this end, further work needed, focused on the investigation of the role of ROS in the stimulation of cell cycle growth arrest as well as cell death and how this is required for ITC-induced toxicity.

The effect of ITCs in modulating the apoptotic process was also further assessed by utilizing an RT-PCR-based microarray approach. Specifically, various apoptosis-related genes were found to be diversely regulated in response to ITCs exposure. About 20 genes implicated in various apoptotic stages (e.g. intrinsic, extrinsic, p53-related, ER-mediated) and other functions important for cell survival and growth were shown to share a common profile among most of these exposures. In particular, two genes namely MDM2 (shown to be up-regulated) and TRAF2 (shown to be down-regulated) appeared to be targeted by all 5 ITCs. Overall, these data support ITCs involvement in apoptotic processes, however, further work in needed in order to better understand the involvement of these critical genes in regulating the ITCs-induced apoptotic cell death processes.

Finally, we have characterized the epigenetic profile of each ITC exposure in human malignant melanoma (A375) cells by means of assessing specific histone post-translational modifications. In general, all 5 ITCs exhibited the capacity to modulate the epigenetic machinery by acting as potent inhibitors of specific HDACs and HATs. These observations were accompanied by a significant reduction on the acetylation levels of H4K8 and H4K12 as well as H3K9, H3K14 and H3K27. At the same time, the expression levels of specific

HMTs (e.g. SET8, SET7/9 and ESET) were shown to be affected in a way where i) SET 7/9 was a target for all 5 ITCS, ii) SET8 was targeted by IBN, BITC and PEITC while iii) ESET by BITC and PEITC only. Alongside with these observations, ITCs affected the di- and tri-methylation status of specific lysine (K) residues (e.g. H3K4, H3K9, H3K27, H3K36 and H3K79) of which H3K9, H3K36 and H3K79 appeared to be common targets under exposure to all ITCs. The influence of the five ITCs in A375 cells is summarized in figure 5.1, showing the comon epigenetic targets, identified in this study, for at least three of the ITCs of interest. Although these data strongly support the ability of ITCs to interact with the epigenome, further work is needed in order to elucidate how these epigenetic effects regulate gene transcriptional activity and subsequently cell survival and death. To my mind, these findings highlight novel insights as to how these 5 major ITCs differentially regulate the epigenome in ways compatible with their anti-cancer action in malignant melanoma. Overall, we have reported that ITCs could act as potent epigenetic regulators by inhibiting melanoma growth through modulation of methylation and acetylation marks thereby altering the transcriptional activity of various genes critical in processes that regulate cell growth, proliferation and mobility. Thus, the significance of our project lays on the detailed characterization of ITCs-induced anti-melanoma function and their involvement in modulating the epigenome in ways compatible with such function. In this way, it is safe to assume their potential utilization as promising "next generation" epigenetic therapeutic agents for the better clinical management of malignant melanoma.

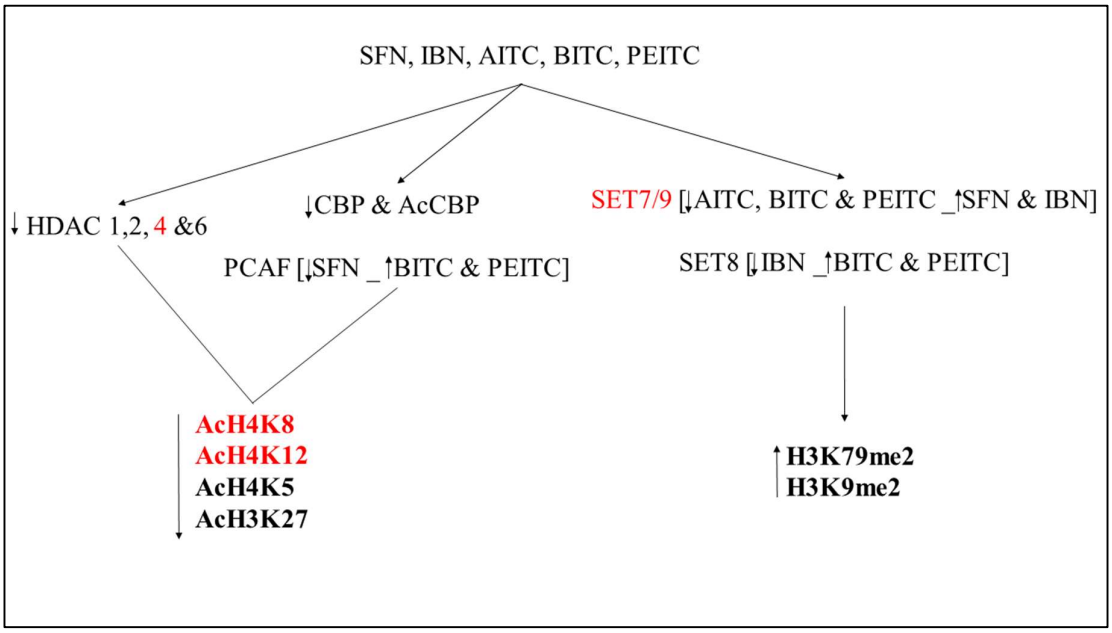

Figure 5.1: Common Epigenetic targets of SFN, IBN, AITC, BITC and PEITC in malignant melanoma (A375) cells. A375 melanoma cells were exposed to 10μM of each

of the 5 ITCs for 48hrs and the expression of the protein level of specific histone acetyltransferases (HAT), deacetylases (HDAC) and methyltransferases (HMT) together with acetylation and methylation marks on histones were evaluated by Western Immunoblotting. ITCs found to influence the expression and activity of various components of the epigenome. Epigenetic components, identified to be common targets of at least three of the ITCs used, are summarized in this figure. Targets in red found to be influenced by all 5 ITCs.

Bibliography

Abbaoui, B., Telu, K. H., Lucas, C. R., Thomas-Ahner, J. M., Schwartz, S. J., Clinton, S. K., Freitas, M. A., & Mortazavi, A. (2017). The impact of cruciferous vegetable isothiocyanates on histone acetylation and histone phosphorylation in bladder cancer. *Journal of Proteomics, 156*, 94-103.

Abel, E. L., Boulware, S., Fields, T., McIvor, E., Powell, K. L., DiGiovanni, J., Vasquez, K. M., & MacLeod, M. C. (2013). Sulforaphane induces phase II detoxication enzymes in mouse skin and prevents mutagenesis induced by a mustard gas analog. *Toxicology and Applied Pharmacology, 266*(3), 439-442.

Agerbirk, N., & Olsen, C. E. (2012). Glucosinolate structures in evolution. *Phytochemistry, 77*, 16-45.

Akiyama, Y., Koda, Y., Byeon, S.-j., Shimada, S., Nishikawaji, T., Sakamoto, A., Chen, Y., Kojima, K., Kawano, T., & Eishi, Y. (2016). Reduced expression of SET7/9, a histone mono-methyltransferase, is associated with gastric cancer progression. *Oncotarget, 7*(4), 3966.

Albert, M., & Helin, K. (2010). Histone methyltransferases in cancer. *Seminars in Cell & Developmental Biology, 21*(2), 209-220.

Amaravadi, R., Kimmelman, A. C., & White, E. (2016). Recent insights into the function of autophagy in cancer. *Genes & Development, 30*(17), 1913-1930.

Ambrosone, C. B., McCann, S. E., Freudenheim, J. L., Marshall, J. R., Zhang, Y., & Shields, P. G. (2004). Breast cancer risk in premenopausal women is inversely associated with consumption of broccoli, a source of isothiocyanates, but is not modified by GST genotype. *The Journal of nutrition, 134*(5), 1134-1138.

Andréasson, E., & Jørgensen, L. B. (2003). Chapter four Localization of plant myrosinases and glucosinolates. *Recent advances in phytochemistry, 37*, 79-99.

Andréasson, E., Jørgensen, L. B., Höglund, A.-S., Rask, L., & Meijer, J. (2001). Different myrosinase and idioblast distribution in Arabidopsis and Brassica napus. *Plant Physiology, 127*(4), 1750-1763.

Angelino, D., Dosz, E. B., Sun, J., Hoeflinger, J. L., Van Tassell, M. L., Chen, P., Harnly, J. M., Miller, M. J., & Jeffery, E. H. (2015). Myrosinase-dependent and–independent formation and control of isothiocyanate products of glucosinolate hydrolysis. *Frontiers in plant science, 6*.

Angelino, D., & Jeffery, E. (2014). Glucosinolate hydrolysis and bioavailability of resulting isothiocyanates: focus on glucoraphanin. *Journal of Functional Foods, 7*, 67-76.

Arcidiacono, P., Ragonese, F., Stabile, A., Pistilli, A., Kuligina, E., Rende, M., Bottoni, U., Calvieri, S., Crisanti, A., & Spaccapelo, R. (2017). Antitumor activity and expression profiles of genes induced by sulforaphane in human melanoma cells. *European Journal of Nutrition*, 1-23.

Armstrong, J. A., Cash, N. J., Ouyang, Y., Morton, J. C., Chvanov, M., Latawiec, D., Awais, M., Tepikin, A. V., Sutton, R., & Criddle, D. N. (2018). Oxidative stress alters mitochondrial bioenergetics and modifies pancreatic cell death independently of cyclophilin D, resulting in an apoptosis-to-necrosis shift. *Journal of Biological Chemistry, 293*(21), 8032-8047.

Arumugam, A., Ibrahim, M. D., Kntayya, S. B., Mohd Ain, N., Iori, R., Galletti, S., Ioannides, C., & Abdull Razis, A. F. (2020). Induction of Apoptosis by Gluconasturtiin-Isothiocyanate (GNST-ITC) in Human Hepatocarcinoma HepG2 Cells and Human Breast Adenocarcinoma MCF-7 Cells. *Molecules, 25*(5).

Athar, M., Li, C., Kim, A. L., Spiegelman, V. S., & Bickers, D. R. (2014). Sonic hedgehog signaling in basal cell nevus syndrome. *Cancer research, 74*(18), 4967-4975.

Attar, N., & Kurdistani, S. K. (2017). Exploitation of EP300 and CREBBP Lysine Acetyltransferases by Cancer. *Cold Spring Harbor Perspectives in Medicine, 7*(3).

Avner, P., & Heard, E. (2001). X-chromosome inactivation: counting, choice and initiation. *Nature Reviews Genetics, 2*(1), 59-67.

Baer, C., Claus, R., & Plass, C. (2013). Genome-Wide Epigenetic Regulation of miRNAs in Cancer. *Cancer research, 73*(2), 473-477.

Bai, J., Lei, Y., An, G.-l., & He, L. (2015). Down-Regulation of Deacetylase HDAC6 Inhibits the Melanoma Cell Line A375.S2 Growth through ROS-Dependent Mitochondrial Pathway. *PloS One, 10*(3), e0121247.

Balasubramanian, S., Chew, Y. C., & Eckert, R. L. (2011). Sulforaphane suppresses polycomb group protein level via a proteasome-dependent mechanism in skin cancer cells. *Molecular pharmacology, 80*(5), 870-878.

Bandyopadhyay, D., Okan, N. A., Bales, E., Nascimento, L., Cole, P. A., & Medrano, E. E. (2002). Down-regulation of p300/CBP histone acetyltransferase activates a senescence checkpoint in human melanocytes. *Cancer Research, 62*(21), 6231-6239.

Bansal, P., Medhe, S., Ganesh, N., & Srivastava, M. M. (2015). Antimelanoma Potential of Eruca sativa Seed Oil and its Bioactive Principles. *Indian Journal of Pharmaceutical Sciences, 77*(2), 208-217.

Barba, F. J., Nikmaram, N., Roohinejad, S., Khelfa, A., Zhu, Z., & Koubaa, M. (2016). Bioavailability of glucosinolates and their breakdown products: Impact of processing. *Frontiers in nutrition, 3*.

Basten, G. P., Bao, Y., & Williamson, G. (2002). Sulforaphane and its glutathione conjugate but not sulforaphane nitrile induce UDP-glucuronosyl transferase (UGT1A1) and glutathione transferase (GSTA1) in cultured cells. *Carcinogenesis, 23*(8), 1399-1404.

Batra, S., Sahu, R. P., Kandala, P. K., & Srivastava, S. K. (2010). Benzyl isothiocyanate–mediated inhibition of histone deacetylase leads to NF-κB turnoff in human pancreatic carcinoma cells. *Molecular Cancer Therapeutics, 9*(6), 1596-1608.

Baxter, J. M., Patel, A. N., & Varma, S. (2012). Facial basal cell carcinoma. *Bmj, 345*, e5342.

Becker, P. B., & Horz, W. (2002). ATP-dependent nucleosome remodeling. *Annual Review of Biochemistry , 71*, 247-273.

Becker, T. M., Haferkamp, S., Dijkstra, M. K., Scurr, L. L., Frausto, M., Diefenbach, E., Scolyer, R. A., Reisman, D. N., Mann, G. J., Kefford, R. F., & Rizos, H. (2009). The chromatin remodelling factor BRG1 is a novel binding partner of the tumor suppressor p16INK4a [journal article]. *Molecular cancer, 8*(1), 4.

Bemis, L. T., Chen, R., Amato, C. M., Classen, E. H., Robinson, S. E., Coffey, D. G., Erickson, P. F., Shellman, Y. G., & Robinson, W. A. (2008). MicroRNA-137 Targets Microphthalmia-Associated Transcription Factor in Melanoma Cell Lines. *Cancer research, 68*(5), 1362-1368.

Benamar, M., Guessous, F., Du, K., Corbett, P., Obeid, J., Gioeli, D., Slingluff, C. L., & Abbas, T. (2016). Inactivation of the CRL4-CDT2-SET8/p21 ubiquitylation and degradation axis underlies the therapeutic efficacy of pevonedistat in melanoma. *EBioMedicine, 10*, 85-100.

Berdasco, M., & Esteller, M. (2010). Aberrant Epigenetic Landscape in Cancer: How Cellular Identity Goes Awry. *Developmental Cell, 19*(5), 698-711.

Berger, S. L. (2007). The complex language of chromatin regulation during transcription. *Nature, 447*(7143), 407-412.

Bhattacharya, A., Li, Y., Wade, K. L., Paonessa, J. D., Fahey, J. W., & Zhang, Y. (2010). Allyl isothiocyanate-rich mustard seed powder inhibits bladder cancer growth and muscle invasion. *Carcinogenesis, 31*(12), 2105-2110.

Bishop, K. S., & Ferguson, L. R. (2015). The interaction between epigenetics, nutrition and the development of cancer. *Nutrients, 7*(2), 922-947.

Biswas, S., & Rao, C. M. (2017). Epigenetics in cancer: Fundamentals and Beyond. *Pharmacology & Therapeutics, 173*, 118-134.

Boddupalli, S., Mein, J. R., Lakkanna, S., & James, D. R. (2012). Induction of phase 2 antioxidant enzymes by broccoli sulforaphane: perspectives in maintaining the antioxidant activity of vitamins a, C, and e. *Frontiers in Genetics, 3*, 7.

Bommareddy, A., Hahm, E.-R., Xiao, D., Powolny, A. A., Fisher, A. L., Jiang, Y., & Singh, S. V. (2009). Atg5 Regulates Phenethyl Isothiocyanate–Induced Autophagic and Apoptotic Cell Death in Human Prostate Cancer Cells. *Cancer Research, 69*(8), 3704-3712.

Bonasio, R., Tu, S., & Reinberg, D. (2010). Molecular signals of epigenetic states. *Science, 330*(6004), 612-616.

Bones, A. M., & Rossiter, J. T. (2006). The enzymic and chemically induced decomposition of glucosinolates. *Phytochemistry, 67*(11), 1053-1067.

Booth, L., Roberts, J. L., Sander, C., Lee, J., Kirkwood, J. M., Poklepovic, A., & Dent, P. (2017). The HDAC inhibitor AR42 interacts with pazopanib to kill trametinib/dabrafenib-resistant melanoma cells in vitro and in vivo. *Oncotarget, 8*(10), 16367-16386.

Boreddy, S. R., Pramanik, K. C., & Srivastava, S. K. (2011). Pancreatic tumor suppression by benzyl isothiocyanate is associated with inhibition of PI3K/AKT/FOXO pathway. *Clinical Cancer Research, 17*(7), 1784-1795.

Boreddy, S. R., Sahu, R. P., & Srivastava, S. K. (2011). Benzyl isothiocyanate suppresses pancreatic tumor angiogenesis and invasion by inhibiting HIF-α/VEGF/Rho-GTPases: pivotal role of STAT-3. *PloS one, 6*(10), e25799.

Borges, A., Simões, L. C., Saavedra, M. J., & Simões, M. (2014). The action of selected isothiocyanates on bacterial biofilm prevention and control. *International Biodeterioration & Biodegradation, 86*, 25-33.

Bosserhoff, A. K. (2006). Novel biomarkers in malignant melanoma. *Clinica Chimica Acta, 367*(1), 28-35.

Boumber, Y., & Issa, J. P. (2011). Epigenetics in cancer: what's the future? *Oncology, 25*(3), 220-226, 228.

Boyanapalli, S. S., Li, W., Fuentes, F., Guo, Y., Ramirez, C. N., Gonzalez, X.-P., Pung, D., & Kong, A.-N. T. (2016). Epigenetic reactivation of RASSF1A by phenethyl isothiocyanate (PEITC) and promotion of apoptosis in LNCaP cells. *Pharmacological Research, 114*, 175-184.

Boyle, G. M., Martyn, A. C., & Parsons, P. G. (2005). Histone deacetylase inhibitors and malignant melanoma. *Pigment Cell Research, 18*(3), 160-166.

Brash, D. E. (2015). UV Signature Mutations. *Photochemistry and Photobiology, 91*(1), 15-26.

Brennan, P., Hsu, C. C., Moullan, N., Szeszenia-Dabrowska, N., Lissowska, J., Zaridze, D., Rudnai, P., Fabianova, E., Mates, D., & Bencko, V. (2005). Effect of cruciferous vegetables on lung cancer in patients stratified by genetic status: a mendelian randomisation approach. *The Lancet, 366*(9496), 1558-1560.

Brown, V. L., Harwood, C. A., Crook, T., Cronin, J. G., Kelsell, D. P., & Proby, C. M. (2004). p16INK4a and p14ARF Tumor Suppressor Genes Are Commonly Inactivated in Cutaneous Squamous Cell Carcinoma. *Journal of Investigative Dermatology, 122*(5), 1284-1292.

Bustos, M. A., Ono, S., Marzese, D. M., Oyama, T., Iida, Y., Cheung, G., Nelson, N., Hsu, S. C., Yu, Q., & Hoon, D. S. B. (2017). MiR-200a Regulates CDK4/6 Inhibitor Effect by Targeting CDK6 in Metastatic Melanoma. *Journal of Investigative Dermatology, 137*(9), 1955-1964.

Cai, X., Yang, L., Chen, H., & Wang, C. (2014). An updated meta-analysis of the association between GSTM1 polymorphism and colorectal cancer in Asians. *Tumor Biology, 35*(2), 949-953.

Calin, G. A., Dumitru, C. D., Shimizu, M., Bichi, R., Zupo, S., Noch, E., Aldler, H., Rattan, S., Keating, M., Rai, K., Rassenti, L., Kipps, T., Negrini, M., Bullrich, F., & Croce, C. M. (2002). Frequent deletions and down-regulation of micro- RNA genes miR15 and miR16 at 13q14 in chronic lymphocytic leukemia. *Proceedings of the National Academy of Sciences, 99*(24), 15524-15529.

Cancer, I. A. f. R. o. (2004). *Cruciferous vegetables, isothiocyanates and indoles*. IARC.

Carpenter, E. L., Le, M. N., Miranda, C. L., Reed, R. L., Stevens, J. F., Indra, A. K., & Ganguli-Indra, G. (2018). Photoprotective Properties of Isothiocyanate and Nitrile

Glucosinolate Derivatives From Meadowfoam (Limnanthes alba) Against UVB Irradiation in Human Skin Equivalent. *Frontiers in Pharmacology, 9*, 477.

Catanzaro, E., Calcabrini, C., Turrini, E., Sestili, P., & Fimognari, C. (2017). Nrf2: a potential therapeutic target for naturally occurring anticancer drugs? *Expert Opinion on Therapeutic Targets, 21*(8), 781-793.

Ceol, C. J., Houvras, Y., Jane-Valbuena, J., Bilodeau, S., Orlando, D. A., Battisti, V., Fritsch, L., Lin, W. M., Hollmann, T. J., Ferre, F., Bourque, C., Burke, C. J., Turner, L., Uong, A., Johnson, L. A., Beroukhim, R., Mermel, C. H., Loda, M., Ait-Si-Ali, S., Garraway, L. A., Young, R. A., & Zon, L. I. (2011). The histone methyltransferase SETDB1 is recurrently amplified in melanoma and accelerates its onset. *Nature, 471*(7339), 513-517.

Chaiprasongsuk, A., Lohakul, J., Soontrapa, K., Sampattavanich, S., Akarasereenont, P., & Panich, U. (2017). Activation of Nrf2 Reduces UVA-Mediated MMP-1 Upregulation via MAPK/AP-1 Signaling Cascades: The Photoprotective Effects of Sulforaphane and Hispidulin. *The Journal of pharmacology and experimental therapeutics, 360*(3), 388-398.

Chakravarthi, B. V. S. K., Nepal, S., & Varambally, S. (2016). Genomic and Epigenomic Alterations in Cancer. *The American Journal of Pathology, 186*(7), 1724-1735.

Chang, N.-B., Feng, R., Gao, Z., & Gao, W. (2010). Skin cancer incidence is highly associated with ultraviolet-B radiation history. *International Journal of Hygiene and Environmental Health, 213*(5), 359-368.

Charron, C. S., Saxton, A. M., & Sams, C. E. (2005). Relationship of climate and genotype to seasonal variation in the glucosinolate–myrosinase system. I. Glucosinolate content in ten cultivars of Brassica oleracea grown in fall and spring seasons. *Journal of the Science of Food and Agriculture, 85*(4), 671-681.

Chen, G., Chen, Z., Hu, Y., & Huang, P. (2011). Inhibition of mitochondrial respiration and rapid depletion of mitochondrial glutathione by beta-phenethyl isothiocyanate: mechanisms for anti-leukemia activity. *Antioxidants & Redox Signaling, 15*(12), 2911-2921.

Chen, H.-E., Lin, J.-F., Tsai, T.-F., Lin, Y.-C., Chou, K.-Y., & Hwang, T. I.-S. (2018). Allyl Isothiocyanate Induces Autophagy through the Up-Regulation of Beclin-1 in Human Prostate Cancer Cells. *The American journal of Chinese medicine, 46*(07), 1625-1643.

Chen, P.-Y., Lin, K.-C., Lin, J.-P., Tang, N.-Y., Yang, J.-S., Lu, K.-W., & Chung, J.-G. (2012). Phenethyl Isothiocyanate (PEITC) inhibits the growth of human oral squamous carcinoma HSC-3 cells through G0/G1 phase arrest and mitochondria-mediated apoptotic cell death. *Evidence-based Complementary and Alternative Medicine, 2012*.

Chen, P. Y., Lin, K. C., Lin, J. P., Tang, N. Y., Yang, J. S., Lu, K. W., & Chung, J. G. (2012). Phenethyl Isothiocyanate (PEITC) Inhibits the Growth of Human Oral Squamous Carcinoma HSC-3 Cells through G(0)/G(1) Phase Arrest and Mitochondria-Mediated Apoptotic Cell Death. *Evidence-based Complementary and Alternative Medicine, 2012*.

Chen, Y., Song, Y-X., & Wang Z-N. (2013). The MicroRNA-148/152 Family: Multi-faceted Players. *Molecular Cancer,*12:43.

Cheng, A. C., Shen, C. J., Hung, C. M., & Hsu, Y. C. (2019). Sulforaphane Decrease of SERTAD1 Expression Triggers G1/S Arrest in Breast Cancer Cells. *Journal of Medicinal Food, 22*(5), 444-450.

Cheng, F., Laino, A. S., Wang, H., Chen, J., Villagra, A., Woods, D. M., Weber, J. S., Quayle, S., Jones, S. S., & Sotomayor, E. M. (2016). In vitro and in vivo anti-melanoma activity of ricolinostat, a selective HDAC6 inhibitor with immunomodulatory properties. *Journal of Clinical Oncology, 34*(15_suppl), e21075-e21075.

Cheng, Y.-M., Tsai, C.-C., & Hsu, Y.-C. (2016). Sulforaphane, a dietary isothiocyanate, induces G2/M arrest in Cervical cancer cells through CyclinB1 downregulation and GADD45β/CDC2 association. *International journal of molecular sciences, 17*(9), 1530.

Cheung, K. L., Khor, T. O., Yu, S., & Kong, A.-N. T. (2008). PEITC induces G1 cell cycle arrest on HT-29 cells through the activation of p38 MAPK signaling pathway. *The AAPS journal, 10*(2), 277.

Cheung, K. L., & Kong, A.-N. (2010). Molecular targets of dietary phenethyl isothiocyanate and sulforaphane for cancer chemoprevention. *The AAPS journal, 12*(1), 87-97.

Chew, Y. C., Adhikary, G., Wilson, G. M., Xu, W., & Eckert, R. L. (2012). Sulforaphane induction of p21Cip1 cyclin-dependent kinase inhibitor expression requires p53 and Sp1 transcription factors and is p53-dependent. *Journal of Biological Chemistry, 287*(20), 16168-16178.

Cho, H. J., Lim, D. Y., Kwon, G. T., Kim, J. H., Huang, Z., Song, H., Oh, Y. S., Kang, Y. H., Lee, K. W., Dong, Z., & Park, J. H. (2016). Benzyl Isothiocyanate Inhibits Prostate Cancer Development in the Transgenic Adenocarcinoma Mouse Prostate (TRAMP) Model, Which Is Associated with the Induction of Cell Cycle G1 Arrest. *International Journal of Molecular Sciences, 17*(2), 264.

Choi, S., Lew, K. L., Xiao, H., Herman-Antosiewicz, A., Xiao, D., Brown, C. K., & Singh, S. V. (2007). D,L-Sulforaphane-induced cell death in human prostate cancer cells is regulated by inhibitor of apoptosis family proteins and Apaf-1. *Carcinogenesis, 28*(1), 151-162.

Chou, Y. C., Chang, M. Y., Wang, M. J., Yu, F. S., Liu, H. C., Harnod, T., Hung, C. H., Lee, H. T., & Chung, J. G. (2015). PEITC inhibits human brain glioblastoma GBM 8401 cell migration and invasion through the inhibition of uPA, Rho A, and Ras with inhibition of MMP-2, -7 and -9 gene expression. *Oncology Reports, 34*(5), 2489-2496.

Chuang, J. C., & Jones, P. A. (2007). Epigenetics and MicroRNAs. *Pediatric Research, 61*(7), 24-29.

Ciska, E., Martyniak-Przybyszewska, B., & Kozlowska, H. (2000). Content of glucosinolates in cruciferous vegetables grown at the same site for two years under different climatic conditions. *Journal of agricultural and food chemistry, 48*(7), 2862-2867.

Clarke, D. B. (2010). Glucosinolates, structures and analysis in food. *Analytical Methods, 2*(4), 310-325.

Cohen, J. H., Kristal, A. R., & Stanford, J. L. (2000). Fruit and vegetable intakes and prostate cancer risk. *Journal of the National Cancer Institute, 92*(1), 61-68.

Costello, J. F., & Plass, C. (2001). Methylation matters. *Journal of Medical Genetics, 38*(5), 285-303.

Crea, F., Fornaro, L., Bocci, G., Sun, L., Farrar, W. L., Falcone A., & Danesi, R. (2012). EZH2 inhibition: targeting the crossroad of tumor invasion and angiogenesis. *Cancer and Metastasis Reviews, 31*(3-4), 753–761.

Crichlow, G. V., Fan, C., Keeler, C., Hodsdon, M., & Lolis, E. J. (2012). Structural interactions dictate the kinetics of macrophage migration inhibitory factor inhibition by different cancer-preventive isothiocyanates. *Biochemistry, 51*(38), 7506-7514.

Cuadrado, A., Martin-Moldes, Z., Ye, J., & Lastres-Becker, I. (2014). Transcription factors NRF2 and NF-kappaB are coordinated effectors of the Rho family, GTP-binding

protein RAC1 during inflammation. J*ournal of Biological Chemistry, 289*(22), 15244-15258.

D'Arcangelo, D., Tinaburri, L., & Dellambra, E. (2017). The Role of p16(INK4a) Pathway in Human Epidermal Stem Cell Self-Renewal, Aging and Cancer. *International Journal of Molecular Sciences, 18*(7).

Dahl, C., & Guldberg, P. (2007). The genome and epigenome of malignant melanoma. *Apmis, 115*(10), 1161-1176.

Darido, C., Georgy, Smitha R., Wilanowski, T., Dworkin, S., Auden, A., Zhao, Q., Rank, G., Srivastava, S., Finlay, Moira J., Papenfuss, Anthony T., Pandolfi, Pier P., Pearson, Richard B., & Jane, Stephen M. (2011). Targeting of the Tumor Suppressor GRHL3 by a miR-21-Dependent Proto-Oncogenic Network Results in PTEN Loss and Tumorigenesis. *Cancer Cell, 20*(5), 635-648.

Das, C., Lucia, M. S., Hansen, K. C., & Tyler, J. K. (2009). CBP/p300-mediated acetylation of histone H3 on lysine 56. *Nature, 459*(7243), 113-117.

Davis, L. E., Byrum, S. D., Mackintosh, S. G., Shalin, S., & Tackett, A. J. (2017). Identification of Misregulated Histone Post Translational Modifications in Melanoma. *The FASEB Journal, 31*(1_supplement), lb62-lb62.

Dawson, M. A., & Kouzarides, T. (2012). Cancer epigenetics: from mechanism to therapy. *Cell, 150*(1), 12-27.

de Oliveira, J. M. P. F., Costa, M., Pedrosa, T., Pinto, P., Remédios, C., Oliveira, H., Pimentel, F., Almeida, L., & Santos, C. (2014). Sulforaphane induces oxidative stress and death by p53-independent mechanism: implication of impaired glutathione recycling. *PloS one, 9*(3), e92980.

Deb, G., Thakur, V.S., & Gupta, S. (2013). Multifaceted role of EZH2 in breast and prostate tumorigenesis: Epigenetics and beyond. *Epigenetics, 8*(5), 464-476.

Dekker, F. J., & Haisma, H. J. (2009). Histone acetyl transferases as emerging drug targets. *Drug Discovery Today, 14*(19), 942-948.

del Carmen Martinez-Ballesta, M., & Carvajal, M. (2015). Myrosinase in Brassicaceae: the most important issue for glucosinolate turnover and food quality. *Phytochemistry Reviews, 14*(6), 1045-1051.

Del Prete, A., Allavena, P., Santoro, G., Fumarulo, R., Corsi, M. M., & Mantovani, A. (2011). Molecular pathways in cancer-related inflammation. *Biochemia Medica, 21*(3), 264-275.

Deng, Q., Zinoviadou, K. G., Galanakis, C. M., Orlien, V., Grimi, N., Vorobiev, E., Lebovka, N., & Barba, F. J. (2015). The effects of conventional and non-conventional processing on glucosinolates and its derived forms, isothiocyanates: extraction, degradation, and applications. *Food Engineering Reviews, 7*(3), 357-381.

Devine, C., Srinivasan, B., Sayan, A., & Ilankovan, V. (2017). Epidemiology of basal cell carcinoma: a 10-year comparative study. *British Journal of Oral and Maxillofacial Surgery*.

Dhayalan, A., Kudithipudi, S., Rathert, P., & Jeltsch, A. (2011). Specificity Analysis-Based Identification of New Methylation Targets of the SET7/9 Protein Lysine Methyltransferase. *Chemistry & Biology, 18*(1), 111-120.

Di Domenico, F., Foppoli, C., Coccia, R., & Perluigi, M. (2012). Antioxidants in cervical cancer: chemopreventive and chemotherapeutic effects of polyphenols. *Biochimica et Biophysica Acta (BBA)-Molecular Basis of Disease, 1822*(5), 737-747.

Di Martile, M., Del Bufalo, D., & Trisciuoglio, D. (2016). The multifaceted role of lysine acetylation in cancer: prognostic biomarker and therapeutic target. *Oncotarget, 7*(34), 55789-55810.

Dias, C., Aires, A., & Saavedra, M. J. (2014). Antimicrobial activity of isothiocyanates from cruciferous plants against methicillin-resistant Staphylococcus aureus (MRSA). *International journal of molecular sciences, 15*(11), 19552-19561.

Diaz-Moralli, S., Tarrado-Castellarnau, M., Miranda, A., & Cascante, M. (2013). Targeting cell cycle regulation in cancer therapy. *Pharmacology & Therapeutics, 138*(2), 255-271.

Dickinson, S. E., Melton, T. F., Olson, E. R., Zhang, J., Saboda, K., & Bowden, G. T. (2009). Inhibition of activator protein-1 by sulforaphane involves interaction with cysteine in the cFos DNA-binding domain: implications for chemoprevention of UVB-induced skin cancer. *Cancer research, 69*(17), 7103-7110.

Dickinson, S. E., Rusche, J. J., Bec, S. L., Horn, D. J., Janda, J., Rim, S. H., Smith, C. L., & Bowden, G. T. (2015). The effect of sulforaphane on histone deacetylase activity in keratinocytes: Differences between in vitro and in vivo analyses. *Molecular Carcinogenesis, 54*(11), 1513-1520.

Diepgen, T., & Mahler, V. (2002). The epidemiology of skin cancer. *British Journal of Dermatology, 146*(s61), 1-6.

Dinkova-Kostova, A. T., Fahey, J. W., Benedict, A. L., Jenkins, S. N., Ye, L., Wehage, S. L., & Talalay, P. (2010). Dietary glucoraphanin-rich broccoli sprout extracts protect

against UV radiation-induced skin carcinogenesis in SKH-1 hairless mice. *Photochemical & photobiological sciences, 9*(4), 597-600.

Dinkova-Kostova, A. T., Fahey, J. W., Wade, K. L., Jenkins, S. N., Shapiro, T. A., Fuchs, E. J., Kerns, M. L., & Talalay, P. (2007). Induction of the Phase 2 Response in Mouse and Human Skin by Sulforaphane-containing Broccoli Sprout Extracts. *Cancer Epidemiology Biomarkers & Prevention, 16*(4), 847-851.

Dinkova-Kostova, A. T., Jenkins, S. N., Fahey, J. W., Ye, L., Wehage, S. L., Liby, K. T., Stephenson, K. K., Wade, K. L., & Talalay, P. (2006). Protection against UV-light-induced skin carcinogenesis in SKH-1 high-risk mice by sulforaphane-containing broccoli sprout extracts. *Cancer Letters, 240*(2), 243-252.

Dinkova-Kostova, A. T., & Kostov, R. V. (2012). Glucosinolates and isothiocyanates in health and disease. *Trends in molecular medicine, 18*(6), 337-347.

Do, D., Pai, S., Rizvi, S. A., & D'Souza, M. J. (2010). Development of sulforaphane-encapsulated microspheres for cancer epigenetic therapy. *International Journal of Pharmaceutics, 386*(1), 114-121.

Donaldson, M. S. (2004). Nutrition and cancer: a review of the evidence for an anti-cancer diet. *Nutrition Journal, 3*, 19.

Drobnica, Ľ., Zemanova, M., Nemec, P., Antoš, K., Kristian, P., Štullerová, A., & Knoppova, V. (1967). Antifungal activity of isothiocyanates and related compounds I. Naturally occurring isothiocyanates and their analogues. *Applied Microbiology, 15*(4), 701-709.

Du, D., Katsuno, Y., Meyer, D., Budi, E. H., Chen, S. H., Koeppen, H., Wang, H., Akhurst, R. J., & Derynck, R. (2018). Smad3-mediated recruitment of the methyltransferase SETDB1/ESET controls Snail1 expression and epithelial-mesenchymal transition. *EMBO Reports, 19*(1), 135-155.

Dufour, V., Stahl, M., & Baysse, C. (2015). The antibacterial properties of isothiocyanates. *Microbiology, 161*(2), 229-243.

Eckschlager, T., Plch, J., Stiborova, M., & Hrabeta, J. (2017). Histone Deacetylase Inhibitors as Anticancer Drugs. *International Journal of Molecular Sciences, 18*(7), 1414.

Eden, A., Gaudet, F., Waghmare, A., & Jaenisch, R. (2003). Chromosomal Instability and Tumors Promoted by DNA Hypomethylation. *Science, 300*(5618), 455-455.

Egger, G., Liang, G., Aparicio, A., & Jones, P. A. (2004). Epigenetics in human disease and prospects for epigenetic therapy. *Nature, 429*(6990), 457-463.

Egner, P. A., Kensler, T. W., Chen, J.-G., Gange, S. J., Groopman, J. D., & Friesen, M. D. (2008). Quantification of sulforaphane mercapturic acid pathway conjugates in human urine by high-performance liquid chromatography and isotope-dilution tandem mass spectrometry. *Chemical research in toxicology, 21*(10), 1991-1996.

Elsheikh, S. E., Green, A. R., Rakha, E. A., Powe, D. G., Ahmed, R. A., Collins, H. M., Soria, D., Garibaldi, J. M., Paish, C. E., Ammar, A. A., Grainge, M. J., Ball, G. R., Abdelghany, M. K., Martinez-Pomares, L., Heery, D. M., & Ellis, I. O. (2009). Global Histone Modifications in Breast Cancer Correlate with Tumor Phenotypes, Prognostic Factors, and Patient Outcome. *Cancer Research, 69*(9), 3802-3809.

Emmert, S., Schön, M. P., & Haenssle, H. A. (2014). Molecular biology of basal and squamous cell carcinomas. *Advances in Experimental Medicine and Biology, 810*, 234-252).

Erb, P., Ji, J., Kump, E., Mielgo, A., & Wernli, M. (2008). Apoptosis and pathogenesis of melanoma and nonmelanoma skin cancer. *Advances in Experimental Medicine and Biology, 624*, 283-295.

Ernst, I. M., Wagner, A. E., Schuemann, C., Storm, N., Höppner, W., Döring, F., Stocker, A., & Rimbach, G. (2011). Allyl-, butyl-and phenylethyl-isothiocyanate activate Nrf2 in cultured fibroblasts. *Pharmacological Research, 63*(3), 233-240.

Fahey, J. W., Zalcmann, A. T., & Talalay, P. (2001). The chemical diversity and distribution of glucosinolates and isothiocyanates among plants. *Phytochemistry, 56*(1), 5-51.

Farazi, T. A., Spitzer, J. I., Morozov, P., & Tuschl, T. (2011). miRNAs in human cancer. *The Journal of pathology, 223*(2), 102-115.

Fei, Q., Shang, K., Zhang, J., Chuai, S., Kong, D., Zhou, T., Fu, S., Liang, Y., Li, C., Chen, Z., Zhao, Y., Yu, Z., Huang, Z., Hu, M., Ying, H., Chen, Z., Zhang, Y., Xing, F., Zhu, J., Xu, H., Zhao, K., Lu, C., Atadja, P., Xiao, Z.-X., Li, E., & Shou, J. (2015). Histone methyltransferase SETDB1 regulates liver cancer cell growth through methylation of p53. *Nature communications, 6*, 8651-8651.

Feinberg, A. P., & Vogelstein, B. (1983). Hypomethylation distinguishes genes of some human cancers from their normal counterparts. *Nature, 301*(5895), 89-92.

Ferguson-Smith, A. C., & Surani, M. A. (2001). Imprinting and the epigenetic asymmetry between parental genomes. *Science, 293*(5532), 1086-1089.

Fernald, K., & Kurokawa, M. (2013). Evading apoptosis in cancer. *Trends in Cell Biology, 23*(12), 620-633.

Fimognari, C., Nüsse, M., Berti, F., Iori, R., Cantelli-Forti, G., & Hrelia, P. (2004). A mixture of isothiocyanates induces cyclin B1-and p53-mediated cell-cycle arrest and apoptosis of human T lymphoblastoid cells. *Mutation Research/Fundamental and Molecular Mechanisms of Mutagenesis, 554*(1), 205-214.

Fimognari, C., Nüsse, M., Cesari, R., Iori, R., Cantelli-Forti, G., & Hrelia, P. (2002). Growth inhibition, cell-cycle arrest and apoptosis in human T-cell leukemia by the isothiocyanate sulforaphane. *Carcinogenesis, 23*(4), 581-586.

Fisher, M. L., Adhikary, G., Grun, D., Kaetzel, D. M., & Eckert, R. L. (2016). The Ezh2 polycomb group protein drives an aggressive phenotype in melanoma cancer stem cells and is a target of diet derived sulforaphane. *Molecular Carcinogenesis, 55*(12), 2024-2036.

Fitsiou, E., Anestopoulos, I., Chlichlia, K., Galanis, A., Kourkoutas, I., Panayiotidis, M. I., & Pappa, A. (2016). Antioxidant and Antiproliferative Properties of the Essential Oils of Satureja thymbra and Satureja parnassica and their Major Constituents. *Anticancer Research, 36*(11), 5757-5763.

Flørenes, V. A., Skrede, M., Jørgensen, K., & Nesland, J. M. (2004). Deacetylase inhibition in malignant melanomas: impact on cell cycle regulation and survival. *Melanoma Research, 14*(3), 173-181.

Fowke, J. H., Gao, Y.-T., Chow, W.-H., Cai, Q., Shu, X.-O., Li, H.-l., Ji, B.-T., Rothman, N., Yang, G., Chung, F.-L., & Zheng, W. (2011). Urinary isothiocyanate levels and lung cancer risk among non-smoking women: A prospective investigation. *Lung Cancer, 73*(1), 18-24.

Fraga, M. F., Herranz, M., Espada, J., Ballestar, E., Paz, M. F., Ropero, S., Erkek, E., Bozdogan, O., Peinado, H., & Niveleau, A. (2004). A mouse skin multistage carcinogenesis model reflects the aberrant DNA methylation patterns of human tumors. *Cancer research, 64*(16), 5527-5534.

Freije, A., Molinuevo, R., Ceballos, L., Cagigas, M., Alonso-Lecue, P., Rodriguez, R., Menendez, P., Aberdam, D., De Diego, E., & Gandarillas, A. (2014). Inactivation of p53 in Human Keratinocytes Leads to Squamous Differentiation and Shedding via Replication Stress and Mitotic Slippage. *Cell Reports, 9*(4), 1349-1360.

Freitas, E., Aires, A., Rosa, E., & Saavedra, M. J. (2013). Antibacterial activity and synergistic effect between watercress extracts, 2-phenylethyl isothiocyanate and antibiotics against 11 isolates of Escherichia coli from clinical and animal source. *Letters in applied microbiology, 57*(4), 266-273.

Friedrich, M., Pracht, K., Mashreghi, M-F., Jäck, H-M., Radbruch, A., & Seliger, B. (2017). The role of the miR-148/-152 family in physiology and disease. *European Journal of Immunology, 47*(12), 2026-2038.

Fuentes, F., Paredes-Gonzalez, X., & Kong, A.-N. T. (2015). Dietary glucosinolates sulforaphane, phenethyl isothiocyanate, indole-3-carbinol/3, 3′-diindolylmethane: Antioxidative stress/inflammation, Nrf2, epigenetics/epigenomics and in vivo cancer chemopreventive efficacy. *Current pharmacology reports, 1*(3), 179-196.

Fuks, F., Hurd, P. J., Deplus, R., & Kouzarides, T. (2003). The DNA methyltransferases associate with HP1 and the SUV39H1 histone methyltransferase. *Nucleic acids research, 31*(9), 2305-2312.

Furfaro, A., Traverso, N., Domenicotti, C., Piras, S., Moretta, L., Marinari, U., Pronzato, M., & Nitti, M. (2016). The Nrf2/HO-1 axis in cancer cell growth and chemoresistance. *Oxidative Medicine and Cellular Longevity, 2016*.

Füllgrabe, J., Kavanagh, E., & Joseph, B. (2011). Histone onco-modifications. *Oncogene, 30*(31), 3391.

Gajer, J. M., Furdas, S. D., Gründer, A., Gothwal, M., Heinicke, U., Keller, K., Colland, F., Fulda, S., Pahl, H. L., Fichtner, I., Sippl, W., & Jung, M. (2015). Histone acetyltransferase inhibitors block neuroblastoma cell growth in vivo [Original Article]. *Oncogenesis, 4*, e137.

Gallagher, S. J., Gunatilake, D., Beaumont, K. A., Sharp, D. M., Tiffen, J. C., Heinemann, A., Weninger, W., Haass, N. K., Wilmott, J. S., Madore, J., Ferguson, P. M., Rizos, H., & Hersey, P. (2018). HDAC inhibitors restore BRAF-inhibitor sensitivity by altering PI3K and survival signalling in a subset of melanoma. *International Journal of Cancer, 142*(9), 1926-1937.

Gao, S. S., Chen, X. Y., Zhu, R. Z., Choi, B. M., & Kim, B. R. (2010). Sulforaphane induces glutathione S-transferase isozymes which detoxify aflatoxin B1-8, 9-epoxide in AML 12 cells. *BioFactors, 36*(4), 289-296.

Geu-Flores, F., Møldrup, M. E., Böttcher, C., Olsen, C. E., Scheel, D., & Halkier, B. A. (2011). Cytosolic γ-glutamyl peptidases process glutathione conjugates in the biosynthesis of glucosinolates and camalexin in Arabidopsis. *The Plant Cell, 23*(6), 2456-2469.

Ghosh, S., & Karin, M. (2002). Missing Pieces in the NF-κB Puzzle. *Cell, 109*(2), S81-S96.

Gills, J. J., Jeffery, E. H., Matusheski, N. V., Moon, R. C., Lantvit, D. D., & Pezzuto, J. M. (2006). Sulforaphane prevents mouse skin tumorigenesis during the stage of promotion. *Cancer Letters, 236*(1), 72-79.

Gokul, G., & Khosla, S. (2013). DNA Methylation and Cancer. *Subcellular Biochemistry*,*61,* 597-625.

Golbabapour, S., Abdulla, M. A., & Hajrezaei, M. (2011). A concise review on epigenetic regulation: insight into molecular mechanisms. *International journal of molecular sciences, 12*(12), 8661-8694.

Gonzalez, C. A. (2006). Nutrition and cancer: the current epidemiological evidence. *British Journal of Nutriioon, 96*(1), 42-45.

Goodman, R. H., & Smolik, S. (2000). CBP/p300 in cell growth, transformation, and development. *Genes & Development, 14*(13), 1553-1577.

Gordon, R. (2013). Skin Cancer: An Overview of Epidemiology and Risk Factors. *Seminars in Oncology Nursing, 29*(3), 160-169.

Goto, N., Bazar, G., Kovacs, Z., Kunisada, M., Morita, H., Kizaki, S., Sugiyama, H., Tsenkova, R., & Nishigori, C. (2015). Detection of UV-induced cyclobutane pyrimidine dimers by near-infrared spectroscopy and aquaphotomics. *Scientific Reports, 5*, 11808.

Graser, G., Schneider, B., Oldham, N. J., & Gershenzon, J. (2000). The methionine chain elongation pathway in the biosynthesis of glucosinolates in Eruca sativa (Brassicaceae). *Archives of Biochemistry and Biophysics, 378*(2), 411-419.

Greaney, A. J., Maier, N. K., Leppla, S. H., & Moayeri, M. (2016). Sulforaphane inhibits multiple inflammasomes through an Nrf2-independent mechanism. *Journal of Leukocyte Biology, 99*(1), 189-199.

Greenberg, E. S., Chong, K. K., Huynh, K. T., Tanaka, R., & Hoon, D. S. (2014). Epigenetic biomarkers in skin cancer. *Cancer Letters, 342*(2), 170-177.

Greer, E. L., & Shi, Y. (2012). Histone methylation: a dynamic mark in health, disease and inheritance. *Nature reviews Genetics, 13*(5), 343-357.

Greger, V., Passarge, E., Hopping, W., Messmer, E., & Horsthemke, B. (1989). Epigenetic changes may contribute to the formation and spontaneous regression of retinoblastoma. *Human Genetics, 83*(2), 155-158.

Greinert, R. (2009). Skin cancer: new markers for better prevention. *Pathobiology, 76*(2), 64-81.

Grubb, C. D., & Abel, S. (2006). Glucosinolate metabolism and its control. *Trends in plant science, 11*(2), 89-100.

Grzywa, R., Winiarski, L., Psurski, M., Rudnicka, A., Wietrzyk, J., Gajda, T., & Oleksyszyn, J. (2016). Synthesis and biological activity of diisothiocyanate-derived mercapturic acids. *Bioorganic & Medicinal Chemistry Letters, 26*(2), 667-671.

Gu, Y., Wang, X., Liu, H., Li, G., Yu, W., & Ma, Q. (2018). SET7/9 promotes hepatocellular carcinoma progression through regulation of E2F1. *Oncology Reports, 40*(4), 1863-1874.

Gu, Y., Wang, Y., Wang, X., Gao, L., Yu, W., & Dong, W.-F. (2017). Opposite Effects of SET7/9 on Apoptosis of Human Acute Myeloid Leukemia Cells and Lung Cancer Cells. *Journal of Cancer, 8*(11), 2069-2078.

Guo, Z., Wu, C., Wang, X., Wang, C., Zhang, R., & Shan, B. (2012). A polymorphism at the miR-502 binding site in the 3′-untranslated region of the histone methyltransferase SET8 is associated with hepatocellular carcinoma outcome. *International Journal of Cancer, 131*(6), 1318-1322.

Gupta, B., Chiang, L., Chae, K., & Lee, D.-H. (2013). Phenethyl isothiocyanate inhibits hypoxia-induced accumulation of HIF-1α and VEGF expression in human glioma cells. *Food Chemistry, 141*(3), 1841-1846.

Gupta, P., Adkins, C., Lockman, P., & Srivastava, S. K. (2013). Metastasis of breast tumor cells to brain is suppressed by phenethyl isothiocyanate in a novel in vivo metastasis model. *PloS one, 8*(6), e67278.

Gupta, P., Wright, S. E., Kim, S.-H., & Srivastava, S. K. (2014). Phenethyl isothiocyanate: A comprehensive review of anti-cancer mechanisms. *Biochimica et Biophysica Acta (BBA)-Reviews on Cancer, 1846*(2), 405-424.

Guttilla, I. K., & White, B. A. (2009). Coordinate regulation of FOXO1 by miR-27a, miR-96, and miR-182 in breast cancer cells. *J Biol Chem, 284*(35), 23204-23216.

Haflidadottir, B. S., Bergsteinsdottir, K., Praetorius, C., & Steingrimsson, E. (2010). miR-148 regulates Mitf in melanoma cells. *PloS one, 5*(7), e11574.

Halkier, B. A., & Du, L. (1997). The biosynthesis of glucosinolates. *Trends in plant science, 2*(11), 425-431.

Halliday, G. M. (2005). Inflammation, gene mutation and photoimmunosuppression in response to UVR-induced oxidative damage contributes to photocarcinogenesis. *Mutation Research/Fundamental and Molecular Mechanisms of Mutagenesis, 571*(1), 107-120.

Hamsa, T. P., Thejass, P., & Kuttan, G. (2011). Induction of apoptosis by sulforaphane in highly metastatic B16F-10 melanoma cells. *Drug and Chemical Toxicology, 34*(3), 332-340.

Hanschen, F. S., Platz, S., Mewis, I., Schreiner, M., Rohn, S., & Kroh, L. W. (2012). Thermally induced degradation of sulfur-containing aliphatic glucosinolates in broccoli sprouts (Brassica oleracea var. italica) and model systems. *Journal of agricultural and food chemistry, 60*(9), 2231-2241.

Hassler, M. R., & Egger, G. (2012). Epigenomics of cancer – emerging new concepts. *Biochimie, 94*(11), 2219-2230.

Hayashita, Y., Osada, H., Tatematsu, Y., Yamada, H., Yanagisawa, K., Tomida, S., Yatabe, Y., Kawahara, K., Sekido, Y., & Takahashi, T. (2005). A polycistronic microRNA cluster, miR-17-92, is overexpressed in human lung cancers and enhances cell proliferation. *Cancer Research, 65*(21), 9628-9632.

Hać, A., Brokowska, J., Rintz, E., Bartkowski, M., Węgrzyn, G., & Herman-Antosiewicz, A. (2019). Mechanism of selective anticancer activity of isothiocyanates relies on differences in DNA damage repair between cancer and healthy cells. *European Journal of Nutrition*.

Hee Kim, Y., Kim, K. Y., Jun do, Y., Kim, J. S., & Kim, Y. H. (2016). Inhibition of autophagy enhances dynamin inhibitor-induced apoptosis via promoting Bak activation and mitochondrial damage in human Jurkat T cells. *Biochemical and Biophysical Research Communications, 478*(4), 1609-1616.

Heffelfinger, C., Ouyang, Z., Engberg, A., Leffell, D. J., Hanlon, A. M., Gordon, P. B., Zheng, W., Zhao, H., Snyder, M. P., & Bale, A. E. (2012). Correlation of global microRNA expression with basal cell carcinoma subtype. *G3: Genes, Genomes, Genetics, 2*(2), 279-286.

Heijkants, R., Willekens, K., Schoonderwoerd, M., Teunisse, A., Nieveen, M., Radaelli, E., Hawinkels, L., Marine, J.-C., & Jochemsen, A. (2017). Combined inhibition of CDK and HDAC as a promising therapeutic strategy for both cutaneous and uveal metastatic melanoma. *Oncotarget, 9*(5), 6174-6187.

Hemberger, M. (2007). Epigenetic landscape required for placental development. *Cellular and Molecular Life Sciences, 64*(18), 2422-2436.

Herman-Antosiewicz, A., Johnson, D. E., & Singh, S. V. (2006). Sulforaphane causes autophagy to inhibit release of cytochrome C and apoptosis in human prostate cancer cells. *Cancer Research, 66*(11), 5828-5835.

Herman-Antosiewicz, A., Xiao, H., Lew, K. L., & Singh, S. V. (2007). Induction of p21 protein protects against sulforaphane-induced mitotic arrest in LNCaP human prostate cancer cell line. *Molecular Cancer Therapeutics, 6*(5), 1673-1681.

Higdon, J. V., Delage, B., Williams, D. E., & Dashwood, R. H. (2007). Cruciferous vegetables and human cancer risk: epidemiologic evidence and mechanistic basis. *Pharmacological Research, 55*(3), 224-236.

Ho, E., Clarke, J. D., & Dashwood, R. H. (2009). Dietary sulforaphane, a histone deacetylase inhibitor for cancer prevention. *The Journal of nutrition, 139*(12), 2393-2396.

Hocker, T. L., Singh, M. K., & Tsao, H. (2008). Melanoma Genetics and Therapeutic Approaches in the 21st Century: Moving from the Benchside to the Bedside. *Journal of Investigative Dermatology, 128*(11), 2575-2595.

Horwacik, I., Gaik, M., Durbas, M., Boratyn, E., Zajac, G., Szychowska, K., Szczodrak, M., Koloczek, H., & Rokita, H. (2015). Inhibition of autophagy by 3-methyladenine potentiates sulforaphane-induced cell death of BE(2)-C human neuroblastoma cells. *Molecular Medicine Reports, 12*(1), 535-542.

Hou, L., Li, Q., Yu, Y., Li, M., & Zhang, D. (2016). SET8 induces epithelial-mesenchymal transition and enhances prostate cancer cell metastasis by cooperating with ZEB1. *Molecular Medicine Reports, 13*(2), 1681-1688.

Hsu, A., Wong, C. P., Yu, Z., Williams, D. E., Dashwood, R. H., & Ho, E. (2011). Promoter de-methylation of cyclin D2 by sulforaphane in prostate cancer cells. *Clinical Epigenetics, 3*, 3.

Hu, R., Xu, C., Shen, G., Jain, M. R., Khor, T. O., Gopalkrishnan, A., Lin, W., Reddy, B., Chan, J. Y., & Kong, A.-N. T. (2006). Gene expression profiles induced by cancer chemopreventive isothiocyanate sulforaphane in the liver of C57BL/6J mice and C57BL/6J/Nrf2 (−/−) mice. *Cancer letters, 243*(2), 170-192.

Huang, C., Ma, W.-y., Li, J., Hecht, S. S., & Dong, Z. (1998). Essential role of p53 in phenethyl isothiocyanate-induced apoptosis. *Cancer Research, 58*(18), 4102-4106.

Huang, S., Hsu, M., Hsu, S., Yang, J., Huang, W., Huang, A., Hsiao, Y., Yu, C., & Chung, J. (2014). Phenethyl isothiocyanate triggers apoptosis in human malignant melanoma A375. S2 cells through reactive oxygen species and the mitochondria-dependent pathways. *Human & Experimental Toxicology, 33*(3), 270-283.

Huang, S.-H., Wu, L.-W., Huang, A.-C., Yu, C.-C., Lien, J.-C., Huang, Y.-P., Yang, J.-S., Yang, J.-H., Hsiao, Y.-P., & Wood, W. G. (2012). Benzyl isothiocyanate (BITC) induces G2/M phase arrest and apoptosis in human melanoma A375. S2 cells through

reactive oxygen species (ROS) and both mitochondria-dependent and death receptor-mediated multiple signaling pathways. *Journal of agricultural and food chemistry, 60*(2), 665-675.

Issa, A. Y., Volate, S. R., & Wargovich, M. J. (2006). The role of phytochemicals in inhibition of cancer and inflammation: New directions and perspectives. *Journal of Food Composition and Analysis, 19*(5), 405-419.

Jackson, S. J. T., Singletary, K. W., & Venema, R. C. (2007). Sulforaphane suppresses angiogenesis and disrupts endothelial mitotic progression and microtubule polymerization. *Vascular Pharmacology, 46*(2), 77-84.

Jadhav, U., Ezhilarasan, R., Vaughn, S. F., Berhow, M. A., & Mohanam, S. (2007). Iberin induces cell cycle arrest and apoptosis in human neuroblastoma cells. *International journal of molecular medicine, 19*(3), 353-361.

Jain, M. G., Hislop, G. T., Howe, G. R., & Ghadirian, P. (1999). Plant foods, antioxidants, and prostate cancer risk: findings from case-control studies in Canada. *Nutrition and Cancer, 34*(2), 173-184.

Jakubikova, J., Bao, Y., & Sedlak, J. (2005). Isothiocyanates induce cell cycle arrest, apoptosis and mitochondrial potential depolarization in HL-60 and multidrug-resistant cell lines. *Anticancer Research, 25*(5), 3375-3386.

Jakubíková, J., Sedlák, J., Mithen, R., & Bao, Y. (2005). Role of PI3K/Akt and MEK/ERK signaling pathways in sulforaphane-and erucin-induced phase II enzymes and MRP2 transcription, G 2/M arrest and cell death in Caco-2 cells. *Biochemical pharmacology, 69*(11), 1543-1552.

Jansson, M. D., & Lund, A. H. (2012). MicroRNA and cancer. *Molecular Oncology, 6*(6), 590-610.

Jaramillo, M. C., & Zhang, D. D. (2013). The emerging role of the Nrf2–Keap1 signaling pathway in cancer. *Genes & Development, 27*(20), 2179-2191.

Javaid, N., & Choi, S. (2017). Acetylation- and Methylation-Related Epigenetic Proteins in the Context of Their Targets. *Genes, 8*(8), 196.

Jensen, K., Slattery, E., Housley, L., & Hansen, E. (2019). Sulforaphane Impacts Invasion Capacity and Proliferation of Triple Negative Breast Cancer Cells Grown in the Presence of Tumor-associated Macrophages (P05-003-19). *Current Developments in Nutrition, 3(1)*, nzz030.P005-003-019.

Jia, Y.-L., Xu, M., Dou, C.-W., Liu, Z.-K., Xue, Y.-M., Yao, B.-W., Ding, L.-L., Tu, K.-S., Zheng, X., & Liu, Q.-G. (2016). P300/CBP-associated factor (PCAF) inhibits the

growth of hepatocellular carcinoma by promoting cell autophagy. *Cell Death and Disease, 7*, e2400.

Jiang, L.-L., Zhou, S.-J., Zhang, X.-M., Chen, H.-Q., & Liu, W. (2016). Sulforaphane suppresses in vitro and in vivo lung tumorigenesis through downregulation of HDAC activity. *Biomedicine and Pharmacotherapy, 78*, 74-80.

Jiang, S., Ma, X., Huang, Y., Xu, Y., Zheng, R., & Chiao, J.-W. (2010). Reactivating aberrantly hypermethylated p15 gene in leukemic T cells by a phenylhexyl isothiocyanate mediated inter-active mechanism on DNA and chromatin. *Journal of Hematology & Oncology, 3*(1), 48.

Jiang, Z., Liu, X., Chang, K., Liu, X., & Xiong, J. (2016). Allyl Isothiocyanate Inhibits the Proliferation of Renal Carcinoma Cell Line GRC-1 by Inducing an Imbalance Between Bcl2 and Bax. *Medical science monitor: international medical journal of experimental and clinical research, 22*, 4283.

Jin, Q., Yu, L. R., Wang, L., Zhang, Z., Kasper, L. H., Lee, J. E., Wang, C., Brindle, P. K., Dent, S. Y., & Ge, K. (2011). Distinct roles of GCN5/PCAF-mediated H3K9ac and CBP/p300-mediated H3K18/27ac in nuclear receptor transactivation. The *Embo journal, 30*(2), 249-262.

Johnson, I. T. (2007). Phytochemicals and cancer. *Proceedings of the Nutrition Society, 66*(02), 207-215.

Jun-Hee, K., Ki, H. K., Jung, J.-Y., Han, H.-S., Shim, J. H., Oh, S., Choi, K.-H., Choi, E.-S., Shin, J.-A., & Leem, D.-H. (2009). Sulforaphane increases cyclin-dependent kinase inhibitor, p21 protein in human oral carcinoma cells and nude mouse animal model to induce G2/M cell cycle arrest. *Journal of Clinical Biochemistry and Nutrition, 46*(1), 60-67.

Kaiser, S. J., Mutters, N. T., Blessing, B., & Günther, F. (2017). Natural isothiocyanates express antimicrobial activity against developing and mature biofilms of Pseudomonas aeruginosa. *Fitoterapia, 119*, 57-63.

Kanavy, H. E., & Gerstenblith, M. R. (2011). Ultraviolet radiation and melanoma. Seminars in cutaneous medicine and surgery, *30*(4), 222-228

Kanemaru, H., Fukushima, S., Yamashita, J., Honda, N., Oyama, R., Kakimoto, A., Masuguchi, S., Ishihara, T., Inoue, Y., & Jinnin, M. (2011). The circulating microRNA-221 level in patients with malignant melanoma as a new tumor marker. *Journal of Dermatological Science, 61*(3), 187-193.

Kang, N. J., Shin, S. H., Lee, H. J., & Lee, K. W. (2011). Polyphenols as small molecular inhibitors of signaling cascades in carcinogenesis. *Pharmacology & Therapeutics, 130*(3), 310-324.

Kanwal, R., & Gupta, S. (2012). Epigenetic modifications in cancer. *Clinical genetics, 81*(4), 303-311.

Kaufman-Szymczyk, A., Majewski, G., Lubecka-Pietruszewska, K., & Fabianowska-Majewska, K. (2015). The Role of Sulforaphane in Epigenetic Mechanisms, Including Interdependence between Histone Modification and DNA Methylation. *International Journal of Molecular Sciences, 16*(12), 29732-29743.

Kerr, C., Adhikary, G., Grun, D., George, N., & Eckert, R. L. (2018). Combination cisplatin and sulforaphane treatment reduces proliferation, invasion, and tumor formation in epidermal squamous cell carcinoma. *Molecular Carcinogenesis, 57*(1), 3-11.

Keum, Y.-S., Jeong, W.-S., & Kong, A. T. (2004). Chemoprevention by isothiocyanates and their underlying molecular signaling mechanisms. *Mutation Research/Fundamental and Molecular Mechanisms of Mutagenesis, 555*(1), 191-202.

Khurana, N., Kim, H., Chandra, P. K., Talwar, S., Sharma, P., Abdel-Mageed, A. B., Sikka, S. C., & Mondal, D. (2017). Multimodal actions of the phytochemical sulforaphane suppress both AR and AR-V7 in 22Rv1 cells: Advocating a potent pharmaceutical combination against castration-resistant prostate cancer. *Oncology Reports, 38*(5), 2774-2786.

Kim, B. K., Kim, I., & Yoon, S. K. (2015). Identification of miR-199a-5p target genes in the skin keratinocyte and their expression in cutaneous squamous cell carcinoma. *Journal of Dermatological Science, 79*(2), 137-147.

Kim, D. H., Sung, B., Kang, Y. J., Hwang, S. Y., Kim, M. J., Yoon, J.-H., Im, E., & Kim, N. D. (2015). Sulforaphane inhibits hypoxia-induced HIF-1α and VEGF expression and migration of human colon cancer cells. *International journal of oncology, 47*(6), 2226-2232.

Kim, H. A., Koo, B. K., Cho, J. H., Kim, Y. Y., Seong, J., Chang, H. J., Oh, Y. M., Stange, D. E., Park, J. G., Hwang, D., & Kong, Y. Y. (2012). Notch1 counteracts WNT/beta-catenin signaling through chromatin modification in colorectal cancer. *Journal of Clinical Investigation, 122*(9), 3248-3259.

Kim, J., Samaranayake, M., & Pradhan, S. (2009). Epigenetic mechanisms in mammals. *Cellular and molecular life sciences, 66*(4), 596-612.

Kim, S.-i., Jin, S.-G., & Pfeifer, G. P. (2013). Formation of cyclobutane pyrimidine dimers at dipyrimidines containing 5-hydroxymethylcytosine. *Photochemical & photobiological sciences, 12*(8), 1409-1415.

Kissen, R., Rossiter, J. T., & Bones, A. M. (2009). The 'mustard oil bomb': not so easy to assemble?! Localization, expression and distribution of the components of the myrosinase enzyme system. *Phytochemistry Reviews, 8*(1), 69-86.

Kleszczynski, K., Ernst, I. M., Wagner, A. E., Kruse, N., Zillikens, D., Rimbach, G., & Fischer, T. W. (2013). Sulforaphane and phenylethyl isothiocyanate protect human skin against UVR-induced oxidative stress and apoptosis: role of Nrf2-dependent gene expression and antioxidant enzymes. *Pharmacological Research, 78*, 28-40.

Kliebenstein, D. J., Kroymann, J., Brown, P., Figuth, A., Pedersen, D., Gershenzon, J., & Mitchell-Olds, T. (2001). Genetic control of natural variation in Arabidopsis glucosinolate accumulation. *Plant Physiology, 126*(2), 811-825.

Kliebenstein, D. J., Kroymann, J., & Mitchell-Olds, T. (2005). The glucosinolate–myrosinase system in an ecological and evolutionary context. *Current Opinion in Plant Biology, 8*(3), 264-271.

Klose, R. J., & Bird, A. P. (2006). Genomic DNA methylation: the mark and its mediators. *Trends in biochemical sciences, 31*(2), 89-97.

Ko, J. M., & Fisher, D. E. (2011). A new era: melanoma genetics and therapeutics. *The Journal of pathology, 223*(2), 242-251.

Ko, M.-o., Kim, M.-B., & Lim, S.-b. (2016). Relationship between Chemical Structure and Antimicrobial Activities of Isothiocyanates from Cruciferous Vegetables against Oral Pathogens. *Journal of microbiology and biotechnology, 26*(12), 2036-2042.

Kohonen-Corish, M. R., Cooper, W. A., Saab, J., Thompson, J. F., Trent, R. J., & Millward, M. J. (2006). Promoter hypermethylation of the O(6)-methylguanine DNA methyltransferase gene and microsatellite instability in metastatic melanoma. *Journal of Investigative Dermatology, 126*(1), 167-171.

Kondo, Y. (2009). Epigenetic Cross-Talk between DNA Methylation and Histone Modifications in Human Cancers. *Yonsei Medical Journal, 50*(4), 455-463.

Konic-Ristic, A., Stanojkovic, T., Srdic-Rajic, T., Dilber, S., Dordevic, B., Stankovic, I., & Juranic, Z. (2016). In vitro assessment of antiproliferative action selectivity of dietary sothiocyanates for tumor versus normal human cells. *Vojnosanitetski Pregled , 73*(7), 636-642.

Konicke, K., López-Luna, A., Muñoz-Carrillo, J. L., Servín-González, L. S., Flores-de la Torre, A., Olasz, E., & Lazarova, Z. (2018). The microRNA landscape of cutaneous squamous cell carcinoma. *Drug Discovery Today*.

Koprivova, A., & Kopriva, S. (2016). Sulfation pathways in plants. *Chemico-biological interactions, 259*, 23-30.

Koroleva, O. A., Davies, A., Deeken, R., Thorpe, M. R., Tomos, A. D., & Hedrich, R. (2000). Identification of a new glucosinolate-rich cell type in Arabidopsis flower stalk. *Plant Physiology, 124*(2), 599-608.

Kouzarides, T. (2007). Chromatin modifications and their function. *Cell, 128*(4), 693-705.

Kramer, D., Schön, M., Bayerlová, M., Bleckmann, A., Schön, M. P., Zörnig, M., & Dobbelstein, M. (2015). A pro-apoptotic function of iASPP by stabilizing p300 and CBP through inhibition of BRMS1 E3 ubiquitin ligase activity. *Cell Death Disease, 6*, e1634.

Krumm, A., Barckhausen, C., Kücük, P., Tomaszowski, K.-H., Loquai, C., Fahrer, J., Krämer, O. H., Kaina, B., & Roos, W. P. (2016). Enhanced histone deacetylase activity in malignant melanoma provokes RAD51 and FANCD2 triggered drug resistance. *Cancer Research*, 2680.2015.

Kulis, M., & Esteller, M. (2010). DNA methylation and cancer. *Adv Genet, 70*(10), 27-56.

Kurash, J. K., Lei, H., Shen, Q., Marston, W. L., Granda, B. W., Fan, H., Wall, D., Li, E., & Gaudet, F. (2008). Methylation of p53 by Set7/9 Mediates p53 Acetylation and Activity In Vivo. *Molecular Cell, 29*(3), 392-400.

Kurepina, N., Kreiswirth, B. N., & Mustaev, A. (2013). Growth-inhibitory activity of natural and synthetic isothiocyanates against representative human microbial pathogens. *Journal of applied microbiology, 115*(4), 943-954.

Lai, F., Jin, L., Gallagher, S., Mijatov, B., Zhang, X. D., & Hersey, P. (2012). Histone deacetylases (HDACs) as mediators of resistance to apoptosis in melanoma and as targets for combination therapy with selective BRAF inhibitors. In *Advances in Pharmacology*, *65*, 27-43.

Lai, K.-C., Huang, A.-C., Hsu, S.-C., Kuo, C.-L., Yang, J.-S., Wu, S.-H., & Chung, J.-G. (2010). Benzyl isothiocyanate (BITC) inhibits migration and invasion of human colon cancer HT29 cells by inhibiting matrix metalloproteinase-2/-9 and urokinase plasminogen (uPA) through PKC and MAPK signaling pathway. *Journal of agricultural and food chemistry, 58*(5), 2935-2942.

Lai, K.-C., Lu, C.-C., Tang, Y.-J., Chiang, J.-H., Kuo, D.-H., Chen, F.-A., Chen, I.-L., & Yang, J.-S. (2014). Allyl isothiocyanate inhibits cell metastasis through suppression of the MAPK pathways in epidermal growth factor-stimulated HT29 human colorectal adenocarcinoma cells. *Oncology Reports, 31*(1), 189-196.

Lai, K. C., Hsiao, Y. T., Yang, J. L., Ma, Y. S., Huang, Y. P., Chiang, T. A., & Chung, J. G. (2017). Benzyl isothiocyanate and phenethyl isothiocyanate inhibit murine melanoma B16F10 cell migration and invasion in vitro. *International Journal of Oncology, 51*(3), 832-840.

Laino, A. S., Betts, B. C., Veerapathran, A., Dolgalev, I., Sarnaik, A., Quayle, S. N., Jones, S. S., Weber, J. S., & Woods, D. M. (2019). HDAC6 selective inhibition of melanoma patient T-cells augments anti-tumor characteristics [journal article]. *Journal for ImmunoTherapy of Cancer, 7*(1), 33.

Lan, F., Pan, Q., Yu, H., & Yue, X. (2015). Sulforaphane enhances temozolomide-induced apoptosis because of down-regulation of miR-21 via Wnt/beta-catenin signaling in glioblastoma. J*ournal of Neurochemistry, 134*(5), 811-818.

Lasko, L. M., Jakob, C. G., Edalji, R. P., Qiu, W., Montgomery, D., Digiammarino, E. L., Hansen, T. M., Risi, R. M., Frey, R., Manaves, V., Shaw, B., Algire, M., Hessler, P., Lam, L. T., Uziel, T., Faivre, E., Ferguson, D., Buchanan, F. G., Martin, R. L., Torrent, M., Chiang, G. G., Karukurichi, K., Langston, J. W., Weinert, B. T., Choudhary, C., de Vries, P., Kluge, A. F., Patane, M. A., Van Drie, J. H., Wang, C., McElligott, D., Kesicki, E. A., Marmorstein, R., Sun, C., Cole, P. A., Rosenberg, S. H., Michaelides, M. R., Lai, A., & Bromberg, K. D. (2018). Author Correction: Discovery of a selective catalytic p300/CBP inhibitor that targets lineage-specific tumours. *Nature, 558*(7710).

Lau, W. S., Chen, T., & Wong, Y. S. (2010). Allyl isothiocyanate induces G2/M arrest in human colorectal adenocarcinoma SW620 cells through down-regulation of Cdc25B and Cdc25C. *Molecular Medicine Reports, 3*(6), 1023-1030.

Lawrence, M., Daujat, S., & Schneider, R. (2016). Lateral Thinking: How Histone Modifications Regulate Gene Expression. *Trends in Genetics, 32*(1), 42-56.

Lee, Y.-J., & Lee, S.-H. (2011). Sulforaphane induces antioxidative and antiproliferative responses by generating reactive oxygen species in human bronchial epithelial BEAS-2B cells. *Journal of Korean medical science, 26*(11), 1474-1482.

Lee, Y. J., & Lee, S. H. (2017). Pro-oxidant activity of sulforaphane and cisplatin potentiates apoptosis and simultaneously promotes autophagy in malignant mesothelioma cells. *Molecular Medicine Reports, 16*(2), 2133-2141.

Levine, B. (2007). Autophagy and cancer. *Nature, 446*, 745.

Li, A.-N., Li, S., Zhang, Y.-J., Xu, X.-R., Chen, Y.-M., & Li, H.-B. (2014). Resources and biological activities of natural polyphenols. *Nutrients, 6*(12), 6020-6047.

Li, B., Carey, M., & Workman, J. L. (2007). The role of chromatin during transcription. *Cell, 128*(4), 707-719.

Li, E., Beard, C., & Jaenisch, R. (1993). Role for DNA methylation in genomic imprinting. *Nature, 366*(6453), 362-365.

Li, M., Li, J., Ding, X., He, M., & Cheng, S.-Y. (2010). microRNA and cancer. *The AAPS journal, 12*(3), 309-317.

Li, Q., Liu, Z., Xu, M., Xue, Y., Yao, B., Dou, C., Jia, Y., Wang, Y., Tu, K., Zheng, X., & Yao, Y. (2016). PCAF inhibits hepatocellular carcinoma metastasis by inhibition of epithelial-mesenchymal transition by targeting Gli-1. *Cancer Letters, 375*(1), 190-198.

Li, W., Guo, Y., Zhang, C., Wu, R., Yang, A. Y., Gaspar, J., & Kong, A.-N. T. (2016). Dietary phytochemicals and cancer chemoprevention: a perspective on oxidative stress, inflammation, and epigenetics. *Chemical research in toxicology, 29*(12), 2071-2095.

Li, W., Khor, T. O., Xu, C., Shen, G., Jeong, W. S., Yu, S., & Kong, A. N. (2008). Activation of Nrf2-antioxidant signaling attenuates NFkappaB-inflammatory response and elicits apoptosis. *Biochemical Pharmacology, 76*(11), 1485-1489.

Lienlaf, M., Perez-Villarroel, P., Knox, T., Pabon, M., Sahakian, E., Powers, J., Woan, K., Lee, C., Cheng, F., & Deng, S. (2016). Essential role of HDAC6 in the regulation of PD-L1 in melanoma. *Molecular Oncology, 10*(5), 735-750.

Lin, C.-M., Kim, J., Du, W.-X., & Wei, C.-I. (2000). Bactericidal activity of isothiocyanate against pathogens on fresh produce. *Journal of food protection, 63*(1), 25-30.

Lin, J.-F., Liao, P.-C., Lin, Y.-H., Chen, H.-E., Lin, Y.-C., Chou, K.-Y., Tsai, T.-F., & Hwang, T. I.-S. (2012). Benzyl isothiocyanate induces protective autophagy in human prostate cancer cells via inhibition of mTOR signaling. *Carcinogenesis, 34*(2), 406-414.

Lin, J.-F., Tsai, T.-F., Yang, S.-C., Lin, Y.-C., Chen, H.-E., Chou, K.-Y., & Hwang, T. I. S. (2017). Benzyl isothiocyanate induces reactive oxygen species-initiated autophagy and apoptosis in human prostate cancer cells. *Oncotarget, 8*(12), 20220-20234.

Lin, J. F., Tsai, T. F., Yang, S. C., Lin, Y. C., Chen, H. E., Chou, K. Y., & Hwang, T. I. (2017). Benzyl isothiocyanate induces reactive oxygen species-initiated autophagy and apoptosis in human prostate cancer cells. *Oncotarget, 8*(12), 20220-20234.

Lin-Feng, C., & Greene, W. C. (2004). Shaping the nuclear action of NF-[kappa] B. *Nature reviews. Molecular cell biology, 5*(5), 392.

Liu, B., Zhang, X., Song, F., Zheng, H., Zhao, Y., Li, H., Zhang, L., Yang, M., Zhang, W., & Chen, K. (2016). MiR-502/SET8 regulatory circuit in pathobiology of breast cancer. *Cancer Letters, 376*(2), 259-267.

Liu, H. J., Wang, L., Kang, L., Du, J., Li, S., & Cui, H. X. (2018). Sulforaphane-N-Acetyl-Cysteine Induces Autophagy Through Activation of ERK1/2 in U87MG and U373MG Cells. *Cellular Physiology and Biochemistry, 51*(2), 528-542.

Liu, J., Gu, J., Feng, Z., Yang, Y., Zhu, N., Lu, W., & Qi, F. (2016). Both HDAC5 and HDAC6 are required for the proliferation and metastasis of melanoma cells. *Journal of Translational Medicine, 14*(1), 7.

Liu, K. C., Shih, T. Y., Kuo, C. L., Ma, Y. S., Yang, J. L., Wu, P. P., Huang, Y. P., Lai, K. C., & Chung, J. G. (2016). Sulforaphane Induces Cell Death Through G2/M Phase Arrest and Triggers Apoptosis in HCT 116 Human Colon Cancer Cells. *American Journal of Chinese Medicine, 44*(6), 1289-1310.

Liu, L., Scolnick, D. M., Trievel, R. C., Zhang, H. B., Marmorstein, R., Halazonetis, T. D., & Berger, S. L. (1999). p53 Sites Acetylated In Vitro by PCAF and p300 Are Acetylated In Vivo in Response to DNA Damage. *Molecular and Cellular Biology, 19*(2), 1202-1209.

Liu, R. H. (2004). Potential synergy of phytochemicals in cancer prevention: mechanism of action. *The Journal of nutrition, 134*(12), 3479S-3485S.

Liu, X., Chen, X., Yu, X., Tao, Y., Bode, A. M., Dong, Z., & Cao, Y. (2013). Regulation of microRNAs by epigenetics and their interplay involved in cancer. *Journal of Experimental and Clinical Cancer Research, 32*, 96.

Liu, X., Takano, C., Shimizu, T., Yokobe, S., Abe-Kanoh, N., Zhu, B., Nakamura, T., Munemasa, S., Murata, Y., & Nakamura, Y. (2017). Inhibition of phosphatidylinositide 3-kinase ameliorates antiproliferation by benzyl

isothiocyanate in human colon cancer cells. *Biochemical and Biophysical Research Communications, 491*(1), 209-216.

Liu, X., Wang, D., Zhao, Y., Tu, B., Zheng, Z., Wang, L., Wang, H., Gu, W., Roeder, R. G., & Zhu, W.-G. (2011). Methyltransferase Set7/9 regulates p53 activity by interacting with Sirtuin 1 (SIRT1). *Proceedings of the National Academy of Sciences, 108*(5), 1925-1930.

Loo, G. (2003). Redox-sensitive mechanisms of phytochemical-mediated inhibition of cancer cell proliferation (review). *Journal of Nutritional Biochemistry, 14*(2), 64-73.

Loriot, A., De Plaen, E., Boon, T., & De Smet, C. (2006). Transient down-regulation of DNMT1 methyltransferase leads to activation and stable hypomethylation of MAGE-A1 in melanoma cells. *Journal of Biological Chemistry, 281*(15), 10118-10126.

Lu, J., Getz, G., Miska, E. A., Alvarez-Saavedra, E., Lamb, J., Peck, D., Sweet-Cordero, A., Ebert, B. L., Mak, R. H., Ferrando, A. A., Downing, J. R., Jacks, T., Horvitz, H. R., & Golub, T. R. (2005). MicroRNA expression profiles classify human cancers. *Nature, 435*, 834.

Lu, W., Xiong, H., Chen, Y., Wang, C., Zhang, H., Xu, P., Han, J., Xiao, S., Ding, H., Chen, Z., Lu, T., Wang, J., Zhang, Y., Yue, L., Liu, Y.-C., Zhang, C., Yang, Y., Jiang, H., Chen, K., Zhou, B., & Luo, C. (2018). Discovery and biological evaluation of thiobarbituric derivatives as potent p300/CBP inhibitors. *Bioorganic & Medicinal Chemistry, 26*(20), 5397-5407.

Lu, Y., Feng, Y., Yi-Yi, L., Yi-Zhi, Z., Yang, L., Hong-Mei, Y., Yuan, F., Yu-Wen, X., Feng-Jiao, Z., Long-Hua, C., Yi, D., & Ke-Li, C. (2019). Histone Methyltransferase SETDB1 Promotes Colorectal Cancer Proliferation through the STAT1-CCND1/CDK6 Axis. *Carcinogenesis*.

Luo, J. L., Tong, W. M., Yoon, J. H., Hergenhahn, M., Koomagi, R., Yang, Q., Galendo, D., Pfeifer, G. P., Wang, Z. Q., & Hollstein, M. (2001). UV-induced DNA damage and mutations in Hupki (human p53 knock-in) mice recapitulate p53 hotspot alterations in sun-exposed human skin. *Cancer Research, 61*(22), 8158-8163.

M de Figueiredo, S., S Binda, N., A Nogueira-Machado, J., A Vieira-Filho, S., & B Caligiorne, R. (2015). The antioxidant properties of organosulfur compounds (sulforaphane). *Recent patents on endocrine, metabolic & immune drug discovery, 9*(1), 24-39.

Ma, X., Fang, Y., Beklemisheva, A., Dai, W., Feng, J., Ahmed, T., Liu, D., & Chiao, J. (2006). Phenylhexyl isothiocyanate inhibits histone deacetylases and remodels chromatins to induce growth arrest in human leukemia cells. *International Journal of Oncology, 28*(5), 1287-1293.

Ma, X., Fang, Y., Beklemisheva, A., Dai, W., Feng, J., Ahmed, T., Liu, D., & Chiao, J. W. (2006). Phenylhexyl isothiocyanate inhibits histone deacetylases and remodels chromatins to induce growth arrest in human leukemia cells. *International Journal of Oncology, 28*(5), 1287-1293.

Ma, Y.-S., Hsiao, Y.-T., Lin, J.-J., Liao, C.-L., Lin, C.-C., & Chung, J.-G. (2017). Phenethyl isothiocyanate (PEITC) and benzyl isothiocyanate (BITC) inhibit human melanoma A375. S2 cell migration and invasion by affecting MAPK signaling pathway in vitro. *Anticancer research, 37*(11), 6223-6234.

Ma, Y. S., Hsiao, Y. T., Lin, J. J., Liao, C. L., Lin, C. C., & Chung, J. G. (2017). Phenethyl Isothiocyanate (PEITC) and Benzyl Isothiocyanate (BITC) Inhibit Human Melanoma A375.S2 Cell Migration and Invasion by Affecting MAPK Signaling Pathway In Vitro. *Anticancer Research, 37*(11), 6223-6234.

Madan, V., Lear, J. T., & Szeimies, R.-M. (2010). Non-melanoma skin cancer. *The Lancet, 375*(9715), 673-685.

Maertens, O., Kuzmickas, R., Manchester, H. E., Emerson, C. E., Gavin, A. G., Guild, C. J., Wong, T. C., De Raedt, T., Bowman-Colin, C., Hatchi, E., Garraway, L. A., Flaherty, K. T., Pathania, S., Elledge, S. J., & Cichowski, K. (2019). MAPK Pathway Suppression Unmasks Latent DNA Repair Defects and Confers a Chemical Synthetic Vulnerability in BRAF-, NRAS-, and NF1-Mutant Melanomas. *Cancer Discovery, 9*(4), 526-545.

Maltepe, E., Bakardjiev, A. I., & Fisher, S. J. (2010). The placenta: transcriptional, epigenetic, and physiological integration during development. *The Journal of clinical investigation, 120*(4), 1016-1025.

Malumbres, M. (2013). miRNAs and cancer: An epigenetics view. *Molecular Aspects of Medicine, 34*(4), 863-874.

Manesh, C., & Kuttan, G. (2003). Effect of naturally occurring allyl and phenyl isothiocyanates in the inhibition of experimental pulmonary metastasis induced by B16F-10 melanoma cells. *Fitoterapia, 74*(4), 355-363.

Mantso, T., Anestopoulos, I., Lamprianidou, E., Kotsianidis, I., Pappa, A., & Panayiotidis, M. I. (2019). Isothiocyanate-induced Cell Cycle Arrest in a Novel In Vitro Exposure

Protocol of Human Malignant Melanoma (A375) Cells. *Anticancer Research, 39*(2), 591-596.

Mantso, T., Sfakianos, A. P., Atkinson, A., Anestopoulos, I., Mitsiogianni, M., Botaitis, S., Perente, S., Simopoulos, C., Vasileiadis, S., Franco, R., Pappa, A., & Panayiotidis, M. I. (2016). Development of a Novel Experimental In Vitro Model of Isothiocyanate-induced Apoptosis in Human Malignant Melanoma Cells. *Anticancer Research, 36*(12), 6303-6309.

Manuyakorn, A., Paulus, R., Farrell, J., Dawson, N. A., Tze, S., Cheung-Lau, G., Hines, O. J., Reber, H., Seligson, D. B., Horvath, S., Kurdistani, S. K., Guha, C., & Dawson, D. W. (2010). Cellular histone modification patterns predict prognosis and treatment response in resectable pancreatic adenocarcinoma: results from RTOG 9704. *Journal of clinical oncology : official journal of the American Society of Clinical Oncology, 28*(8), 1358-1365.

Manyes, L., Luciano, F. B., Mañes, J., & Meca, G. (2015). In vitro antifungal activity of allyl isothiocyanate (AITC) against Aspergillus parasiticus and Penicillium expansum and evaluation of the AITC estimated daily intake. *Food and Chemical Toxicology, 83*, 293-299.

Mar-Aguilar, F., Mendoza-Ramirez, J. A., Malagon-Santiago, I., Espino-Silva, P. K., Santuario-Facio, S. K., Ruiz-Flores, P., Rodriguez-Padilla, C., & Resendez-Perez, D. (2013). Serum circulating microRNA profiling for identification of potential breast cancer biomarkers. *Disease Markers, 34*(3), 163-169.

Margueron, R., & Reinberg, D. (2010). Chromatin structure and the inheritance of epigenetic information. *Nature Reviews Genetics, 11*(4), 285-296.

Martin, C., & Zhang, Y. (2005). The diverse functions of histone lysine methylation. *Nature reviews Molecular cell biology, 6*(11), 838-849.

Martin-Gorgojo, A., Llinares, M., Viros, A., Requena, C., Garcia-Casado, Z., Traves, V., Kumar, R., & Nagore, E. (2017). Cutaneous melanoma primary site is linked to nevus density. *Oncotarget, 8*(58), 98876-98886.

Matsui, T.-a., Murata, H., Sakabe, T., Sowa, Y., Horie, N., Nakanishi, R., Sakai, T., & Kubo, T. (2007). Sulforaphane induces cell cycle arrest and apoptosis in murine osteosarcoma cells in vitro and inhibits tumor growth in vivo. *Oncology Reports, 18*(5), 1263-1268.

Mayne, S. T., Playdon, M. C., & Rock, C. L. (2016). Diet, nutrition, and cancer: past, present and future. *Nature Reviews Clinical Oncology, 13*(8), 504-515.

Mazar, J., DeBlasio, D., Govindarajan, S. S., Zhang, S., & Perera, R. J. (2011). Epigenetic regulation of microRNA-375 and its role in melanoma development in humans. *FEBS Letters, 585*(15), 2467-2476.

McCabe, M. T., Graves, A. P., Ganji, G., Diaz, E., Halsey, W. S., Jiang, Y., Smitheman, K. N., Ott, H. M., Pappalardi, M. B., Allen, K. E., Chen, S. B., Della Pietra, A., Dul, E., Hughes, A. M., Gilbert, S. A., Thrall, S. H., Tummino, P. J., Kruger, R. G., Brandt, M., Schwartz, B., & Creasy, C. L. (2012). Mutation of A677 in histone methyltransferase EZH2 in human B-cell lymphoma promotes hypertrimethylation of histone H3 on lysine 27 (H3K27). *Proceedings of the national academy of sciences, 109*(8), 2989-2994.

McWalter, G. K., Higgins, L. G., McLellan, L. I., Henderson, C. J., Song, L., Thornalley, P. J., Itoh, K., Yamamoto, M., & Hayes, J. D. (2004). Transcription factor Nrf2 is essential for induction of NAD (P) H: quinone oxidoreductase 1, glutathione S-transferases, and glutamate cysteine ligase by broccoli seeds and isothiocyanates. *The Journal of nutrition, 134*(12), 3499S-3506S.

Meeran, S. M., Patel, S. N., Li, Y., Shukla, S., & Tollefsbol, T. O. (2012). Bioactive dietary supplements reactivate ER expression in ER-negative breast cancer cells by active chromatin modifications. *PloS One, 7*(5), e37748.

Meeran, S. M., Patel, S. N., & Tollefsbol, T. O. (2010). Sulforaphane causes epigenetic repression of hTERT expression in human breast cancer cell lines. *PloS one, 5*(7), e11457.

Meeran, S. M., Punathil, T., & Katiyar, S. K. (2008). IL-12 Deficiency Exacerbates Inflammatory Responses in UV-Irradiated Skin and Skin Tumors. *Journal of Investigative Dermatology, 128*(11), 2716-2727.

Mi, L., Di Pasqua, A. J., & Chung, F. L. (2011). Proteins as binding targets of isothiocyanates in cancer prevention. *Carcinogenesis, 32*(10), 1405-1413.

Mijatovic, S. A., Timotijevic, G. S., Miljkovic, D. M., Radovic, J. M., Maksimovic-Ivanic, D. D., Dekanski, D. P., & Stosic-Grujicic, S. D. (2011). Multiple antimelanoma potential of dry olive leaf extract. *International Journal of Cancer, 128*(8), 1955-1965.

Milczarek, M., Wiktorska, K., Mielczarek, L., Koronkiewicz, M., Dąbrowska, A., Lubelska, K., Matosiuk, D., & Chilmonczyk, Z. (2018). Autophagic cell death and premature senescence: New mechanism of 5-fluorouracil and sulforaphane synergistic

anticancer effect in MDA-MB-231 triple negative breast cancer cell line. *Food and Chemical Toxicology, 111*, 1-8.

Milkiewicz, M., Roudier, E., Doyle, J. L., Trifonova, A., Birot, O., & Haas, T. L. (2011). Identification of a Mechanism Underlying Regulation of the Anti-Angiogenic Forkhead Transcription Factor FoxO1 in Cultured Endothelial Cells and Ischemic Muscle. *The American Journal of Pathology, 178*(2), 935-944.

Mithen, R. F., Dekker, M., Verkerk, R., Rabot, S., & Johnson, I. T. (2000). The nutritional significance, biosynthesis and bioavailability of glucosinolates in human foods. *Journal of the Science of Food and Agriculture, 80*(7), 967-984.

Mitsiogianni, M., Amery, T., Franco, R., Zoumpourlis, V., Pappa, A., & Panayiotidis, M. I. (2018). From chemo-prevention to epigenetic regulation: The role of isothiocyanates in skin cancer prevention. *Pharmacology & Therapeutics, 190*, 187-201.

Mitsiogianni, M., Koutsidis, G., Mavroudis, N., Trafalis, D. T., Botaitis, S., Franco, R., Zoumpourlis, V., Amery, T., Galanis, A., Pappa, A., & Panayiotidis, M. I. (2019). The Role of Isothiocyanates as Cancer Chemo-Preventive, Chemo-Therapeutic and Anti-Melanoma Agents. *Antioxidants (Basel), 8*(4).

Mitsiogianni, M., Mantso, T., Trafalis, D. T., Vasantha Rupasinghe, H. P., Zoumpourlis, V., Franco, R., Botaitis, S., Pappa, A., & Panayiotidis, M. I. (2019). Allyl isothiocyanate regulates lysine acetylation and methylation marks in an experimental model of malignant melanoma. *European Journal of Nutrition*.

Mitsiogianni, M., Trafalis, D. T., Franco, R., Zoumpourlis, V., Pappa, A., & Panayiotidis, M. I. (2020). Sulforaphane and iberin are potent epigenetic modulators of histone acetylation and methylation in malignant melanoma. *European Journal of Nutrition*.

Miyoshi, N., Uchida, K., Osawa, T., & Nakamura, Y. (2004). Benzyl isothiocyanate modifies expression of the G2/M arrest-related genes. *BioFactors, 21*(1-4), 23-26.

Miyoshi, N., Watanabe, E., Osawa, T., Okuhira, M., Murata, Y., Ohshima, H., & Nakamura, Y. (2008). ATP depletion alters the mode of cell death induced by benzyl isothiocyanate. *Biochimica et Biophysica Acta (BBA) - Molecular Basis of Disease, 1782*(10), 566-573.

Moan, J., Grigalavicius, M., Baturaite, Z., Dahlback, A., & Juzeniene, A. (2015). The relationship between UV exposure and incidence of skin cancer. *Photodermatology, photoimmunology & photomedicine, 31*(1), 26-35.

Moison, C., Guieysse-Peugeot, A.-L., & Arimondo, P. B. (2014). DNA methylation in cancer. *Atlas of Genetics and Cytogenetics in Oncology and Haematology,*

Mondal, A., Biswas, R., Rhee, Y.-H., Kim, J., & Ahn, J.-C. (2016). Sulforaphene promotes Bax/Bcl2, MAPK-dependent human gastric cancer AGS cells apoptosis and inhibits migration via EGFR, p-ERK1/2 down-regulation. *General physiology and biophysics, 35*(1), 25-34.

Montenegro, M., Sanchez-del-Campo, L., Fernandez-Perez, M., Saez-Ayala, M., Cabezas-Herrera, J., & Rodriguez-Lopez, J. (2015). Targeting the epigenetic machinery of cancer cells. *Oncogene, 34*(2), 135.

Moore, L. D., Le, T., & Fan, G. (2013). DNA methylation and its basic function. *Neuropsychopharmacology : official publication of the American College of Neuropsychopharmacology, 38*(1), 23-38.

Mori, T., Martinez, S. R., O'Day, S. J., Morton, D. L., Umetani, N., Kitago, M., Tanemura, A., Nguyen, S. L., Tran, A. N., & Wang, H.-J. (2006). Estrogen receptor-α methylation predicts melanoma progression. *Cancer research, 66*(13), 6692-6698.

Moserle, L., & Casanovas, O. (2013). Anti-angiogenesis and metastasis: a tumour and stromal cell alliance. *Journal of Internal Medicine, 273*(2), 128-137.

Moutinho, C., & Esteller, M. (2017). MicroRNAs and Epigenetics. *Advances in Cancer Research, 135*, 189-220.

Mugford, S. G., Yoshimoto, N., Reichelt, M., Wirtz, M., Hill, L., Mugford, S. T., Nakazato, Y., Noji, M., Takahashi, H., & Kramell, R. (2009). Disruption of adenosine-5′-phosphosulfate kinase in Arabidopsis reduces levels of sulfated secondary metabolites. *The Plant Cell, 21*(3), 910-927.

Munday, C. M. (2002). Selective induction of phase II enzymes in the urinary bladder of rats by allyl isothiocyanate, a compound derived from Brassica vegetables. *Nutrition and Cancer, 44*(1), 52-59.

Murao, K., Kubo, Y., Ohtani, N., Hara, E., & Arase, S. (2006). Epigenetic abnormalities in cutaneous squamous cell carcinomas: frequent inactivation of the RB1/p16 and p53 pathways. *British Journal of Dermatology, 155*(5), 999-1005.

Murr, R. (2010). Interplay between different epigenetic modifications and mechanisms. *Advances in Genetics, 70*, 101-141.

Myzak, M. C., Hardin, K., Wang, R., Dashwood, R. H., & Ho, E. (2005). Sulforaphane inhibits histone deacetylase activity in BPH-1, LnCaP and PC-3 prostate epithelial cells. *Carcinogenesis, 27*(4), 811-819.

Myzak, M. C., Karplus, P. A., Chung, F.-L., & Dashwood, R. H. (2004). A novel mechanism of chemoprotection by sulforaphane. *Cancer Research, 64*(16), 5767-5774.

Myzak, M. C., Tong, P., Dashwood, W.-M., Dashwood, R. H., & Ho, E. (2007). Sulforaphane retards the growth of human PC-3 xenografts and inhibits HDAC activity in human subjects. *Experimental Biology and Medicine, 232*(2), 227-234.

Nakamura, T., Abe-Kanoh, N., & Nakamura, Y. (2018). Physiological relevance of covalent protein modification by dietary isothiocyanates. *Journal of Clinical Biochemistry and Nutrition, 62*(1), 11-19.

Nandakumar, V., Vaid, M., Tollefsbol, T. O., & Katiyar, S. K. (2011). Aberrant DNA hypermethylation patterns lead to transcriptional silencing of tumor suppressor genes in UVB-exposed skin and UVB-induced skin tumors of mice. *Carcinogenesis, 32*(4), 597-604.

Narayanan, D. L., Saladi, R. N., & Fox, J. L. (2010). Ultraviolet radiation and skin cancer. *International journal of dermatology, 49*(9), 978-986.

Navarro, S. L., Li, F., & Lampe, J. W. (2011). Mechanisms of action of isothiocyanates in cancer chemoprevention: an update. *Food & Function, 2*(10), 579-587.

Nebbioso, A., Tambaro, F. P., Dell'Aversana, C., & Altucci, L. (2018). Cancer epigenetics: Moving forward. *PLoS genetics, 14*(6), e1007362-e1007362.

Nguyen, N., Sharma, A., Nguyen, N., Sharma, A. K., Desai, D., Huh, S. J., Amin, S., Meyers, C., & Robertson, G. P. (2011). Melanoma chemoprevention in skin reconstructs and mouse xenografts using isoselenocyanate-4. *Cancer Prevention Research, 4*(2), 248-258.

Nguyen, T., Kuo, C., Nicholl, M. B., Sim, M. S., Turner, R. R., Morton, D. L., & Hoon, D. S. (2011). Downregulation of microRNA-29c is associated with hypermethylation of tumor-related genes and disease outcome in cutaneous melanoma. *Epigenetics, 6*(3), 388-394.

Nguyen, T. H., & Ho, D. Q.-D. (2002). Nonmelanoma skin cancer. *Current treatment options in oncology, 3*(3), 193-203.

Ni, W.-Y., Hsiao, Y.-P., Hsu, S.-C., Hsueh, S.-C., Chang, C.-H., Ji, B.-C., Yang, J.-S., Lu, H.-F., & Chung, J.-G. (2013). Oral administration of benzyl-isothiocyanate inhibits in vivo growth of subcutaneous xenograft tumors of human malignant melanoma A375. S2 cells. *In Vivo, 27*(5), 623-626.

Ni, W. Y., Lu, H. F., Hsu, S. C., Hsiao, Y. P., Liu, K. C., Liu, J. Y., Ji, B. C., Hsueh, S. C., Hung, F. M., Shang, H. S., & Chung, J. G. (2014). Phenethyl isothiocyanate inhibits in vivo growth of subcutaneous xenograft tumors of human malignant melanoma A375.S2 cells. *In Vivo, 28*(5), 891-894.

No, J. H., Kim, Y.-B., & Song, Y. S. (2014). Targeting Nrf2 Signaling to Combat Chemoresistance. *Journal of Cancer Prevention, 19*(2), 111-117.

Nohynek, L. J., Alakomi, H.-L., Kähkönen, M. P., Heinonen, M., Helander, I. M., Oksman-Caldentey, K.-M., & Puupponen-Pimiä, R. H. (2006). Berry phenolics: antimicrobial properties and mechanisms of action against severe human pathogens. *Nutrition and Cancer, 54*(1), 18-32.

Nomura, T., Shinoda, S., Yamori, T., Sawaki, S., Nagata, I., Ryoyama, K., & Fuke, Y. (2005). Selective sensitivity to wasabi-derived 6-(methylsulfinyl) hexyl isothiocyanate of human breast cancer and melanoma cell lines studied in vitro. *Cancer detection and prevention, 29*(2), 155-160.

Norval, M., & Halliday, G. M. (2011). The Consequences of UV-Induced Immunosuppression for Human Health. *Photochemistry and Photobiology, 87*(5), 965-977.

O'Brien, J., Hayder, H., Zayed, Y., & Peng, C. (2018). Overview of MicroRNA Biogenesis, Mechanisms of Actions, and Circulation. *Frontiers in endocrinology, 9*, 402-402.

Ohtsuka, M., Ling, H., Doki, Y., Mori, M., & Calin, G. A. (2015). MicroRNA processing and human cancer. *Journal of clinical medicine, 4*(8), 1651-1667.

Okonkwo, A., Mitra, J., Johnson, G. S., Li, L., Dashwood, W. M., Hegde, M., Yue, C., Dashwood, R. H., & Rajendran, P. (2018). Heterocyclic Analogs of Sulforaphane Trigger DNA Damage and Impede DNA Repair in Colon Cancer Cells: Interplay of HATs and HDACs. *Molecular Nutrition & Food Research*, 1800228.

Olcina, M. M., Leszczynska, K. B., Senra, J. M., Isa, N. F., Harada, H., & Hammond, E. M. (2016). H3K9me3 facilitates hypoxia-induced p53-dependent apoptosis through repression of APAK. *Oncogene, 35*(6), 793-799.

Orouji, E., Federico, A., Larribere, L., Novak, D., Lipka, D. B., Assenov, Y., Sachindra, S., Huser, L., Granados, K., Gebhardt, C., Plass, C., Umansky, V., & Utikal, J. (2019). Histone methyltransferase SETDB1 contributes to melanoma tumorigenesis and serves as a new potential therapeutic target. **I***nternational Journal of Cancer, 145*(12), 3462-3477.

Otto, T., & Sicinski, P. (2017). Cell cycle proteins as promising targets in cancer therapy. *Nature Reviews Cancer, 17*(2), 93-115.

Ouyang, L., Shi, Z., Zhao, S., Wang, F. T., Zhou, T. T., Liu, B., & Bao, J. K. (2012). Programmed cell death pathways in cancer: a review of apoptosis, autophagy and programmed necrosis. *Cell Proliferation, 45*(6), 487-498.

Overby, A., Stokland, R. A., Asberg, S. E., Sporsheim, B., & Bones, A. M. (2015). Allyl isothiocyanate depletes glutathione and upregulates expression of glutathione S-transferases in Arabidopsis thaliana. *Frontiers in Plant Science, 6*, 277.

Palliyaguru, D. L., Yuan, J. M., Kensler, T. W., & Fahey, J. W. (2018). Isothiocyanates: Translating the Power of Plants to People. *Molecular Nutrition & Food Research, 62*(18), e1700965.

Pan, L., Pan, H., Jiang, H., Du, J., Wang, X., Huang, B., & Lu, J. (2010). HDAC4 inhibits the transcriptional activation of mda-7/IL-24 induced by Sp1. *Cellular & Molecular Immunology, 7*(3), 221.

Panning, B., & Jaenisch, R. (1998). RNA and the epigenetic regulation of X chromosome inactivation. *Cell, 93*(3), 305-308.

Pappa, G., Lichtenberg, M., Iori, R., Barillari, J., Bartsch, H., & Gerhäuser, C. (2006). Comparison of growth inhibition profiles and mechanisms of apoptosis induction in human colon cancer cell lines by isothiocyanates and indoles from Brassicaceae. *Mutation Research/Fundamental and Molecular Mechanisms of Mutagenesis, 599*(1), 76-87.

Park, Y. S., Jin, M. Y., Kim, Y. J., Yook, J. H., Kim, B. S., & Jang, S. J. (2008). The global histone modification pattern correlates with cancer recurrence and overall survival in gastric adenocarcinoma. *Annals of Surgical Oncology, 15*(7), 1968-1976.

Parnaud, G., Li, P., Cassar, G., Rouimi, P., Tulliez, J., Combaret, L., & Gamet-Payrastre, L. (2004). Mechanism of sulforaphane-induced cell cycle arrest and apoptosis in human colon cancer cells. *Nutrition and cancer, 48*(2), 198-206.

Parzych, K. R., & Klionsky, D. J. (2014). An overview of autophagy: morphology, mechanism, and regulation. *Antioxidants and Redox Signaling, 20*(3), 460-473.

Paul, B., Li, Y., & Tollefsbol, T. (2018). The effects of combinatorial genistein and sulforaphane in breast tumor inhibition: role in epigenetic regulation. *International Journal of Molecular Sciences, 19*(6), 1754.

Pawlik, A., Wała, M., Hać, A., Felczykowska, A., & Herman-Antosiewicz, A. (2017). Sulforaphene, an isothiocyanate present in radish plants, inhibits proliferation of human breast cancer cells. *Phytomedicine, 29*, 1-10.

Peltonen, K., Kiviharju, T. M., Järvinen, P. M., Ra, R., & Laiho, M. (2005). Melanoma cell lines are susceptible to histone deacetylase inhibitor TSA provoked cell cycle arrest and apoptosis. *Pigment Cell Research, 18*(3), 196-202.

Penta, D., Somashekar, B. S., & Meeran, S. M. (2018). Epigenetics of skin cancer: Interventions by selected bioactive phytochemicals. *Photodermatology, Photoimmunology and Photomedicine, 34*(1), 42-49.

Peschansky, V. J., & Wahlestedt, C. (2014). Non-coding RNAs as direct and indirect modulators of epigenetic regulation. *Epigenetics, 9*(1), 3-12.

Pfeifer, G. P., & Besaratinia, A. (2012). UV wavelength-dependent DNA damage and human non-melanoma and melanoma skin cancer. *Photochemical & photobiological sciences, 11*(1), 90-97.

Pham, N. A., Jacobberger, J. W., Schimmer, A. D., Cao, P., Gronda, M., & Hedley, D. W. (2004). The dietary isothiocyanate sulforaphane targets pathways of apoptosis, cell cycle arrest, and oxidative stress in human pancreatic cancer cells and inhibits tumor growth in severe combined immunodeficient mice. *Molecular Cancer Therapeutics, 3*(10), 1239-1248.

Pietrocola, F., Pol, J., Vacchelli, E., Baracco, E. E., Levesque, S., Castoldi, F., Maiuri, M. C., Madeo, F., & Kroemer, G. (2016). Autophagy induction for the treatment of cancer. *Autophagy, 12*(10), 1962-1964.

Pledgie-Tracy, A., Sobolewski, M. D., & Davidson, N. E. (2007). Sulforaphane induces cell type–specific apoptosis in human breast cancer cell lines. *Molecular Cancer Therapeutics, 6*(3), 1013-1021.

Pocasap, P., Weerapreeyakul, N., & Thumanu, K. (2018). Structures of isothiocyanates attributed to reactive oxygen species generation and microtubule depolymerization in HepG2 cells. *Biomed Pharmacother, 101*, 698-709.

Pocasap, P., Weerapreeyakul, N., & Thumanu, K. (2018). Structures of isothiocyanates attributed to reactive oxygen species generation and microtubule depolymerization in HepG2 cells. *Biomedicine and Pharmacotherapy, 101*, 698-709.

Powolny, A. A., & Singh, S. V. (2010). Differential response of normal (PrEC) and cancerous human prostate cells (PC-3) to phenethyl isothiocyanate-mediated changes in expression of antioxidant defense genes. *Pharm Res, 27*(12), 2766-2775.

Pradhan, S. J., Mishra, R., Sharma, P., & Kundu, G. C. (2010). Quercetin and sulforaphane in combination suppress the progression of melanoma through the down-regulation of matrix metalloproteinase-9. *Experimental and Therapeutic Medicine, 1*(6), 915-920.

Probst, A. V., Dunleavy, E., & Almouzni, G. (2009). Epigenetic inheritance during the cell cycle. *Nature reviews Molecular cell biology, 10*(3), 192-206.

Qi, Y., Wang, D., Jin, T., Yang, L., Wu, H., Li, Y., Zhao, J., Du, F., Song, M., & Wang, R. (2016). HEDD: the human epigenetic drug database. *Database, 2016*.

Qu, X., Pröll, M., Neuhoff, C., Zhang, R., Cinar, M. U., Hossain, M. M., Tesfaye, D., Große-Brinkhaus, C., Salilew-Wondim, D., & Tholen, E. (2015). Sulforaphane epigenetically regulates innate immune responses of porcine monocyte-derived dendritic cells induced with lipopolysaccharide. *PloS one, 10*(3), e0121574.

Rajendran, P., Delage, B., Dashwood, W. M., Yu, T.-W., Wuth, B., Williams, D. E., Ho, E., & Dashwood, R. H. (2011). Histone deacetylase turnover and recovery in sulforaphane-treated colon cancer cells: competing actions of 14-3-3 and Pin1 in HDAC3/SMRT corepressor complex dissociation/reassembly. *Molecular Cancer, 10*(1), 68.

Rajendran, P., Kidane, A. I., Yu, T.-W., Dashwood, W.-M., Bisson, W. H., Löhr, C. V., Ho, E., Williams, D. E., & Dashwood, R. H. (2013). HDAC turnover, CtIP acetylation and dysregulated DNA damage signaling in colon cancer cells treated with sulforaphane and related dietary isothiocyanates. *Epigenetics, 8*(6), 612-623.

Ratert, N., Meyer, H. A., Jung, M., Lioudmer, P., Mollenkopf, H. J., Wagner, I., Miller, K., Kilic, E., Erbersdobler, A., Weikert, S., & Jung, K. (2013). miRNA profiling identifies candidate mirnas for bladder cancer diagnosis and clinical outcome. *Journal of Molecular Diagnostics, 15*(5), 695-705.

Rice, J. C., & Allis, C. D. (2001). Histone methylation versus histone acetylation: new insights into epigenetic regulation. *Current opinion in cell biology, 13*(3), 263-273.

Rodriguez-Paredes, M., Martinez de Paz, A., Simo-Riudalbas, L., Sayols, S., Moutinho, C., Moran, S., Villanueva, A., Vazquez-Cedeira, M., Lazo, P. A., Carneiro, F., Moura, C. S., Vieira, J., Teixeira, M. R., & Esteller, M. (2014). Gene amplification of the histone methyltransferase SETDB1 contributes to human lung tumorigenesis. *Oncogene, 33*(21), 2807-2813.

Romagnolo, D. F., & Selmin, O. I. (2012). Flavonoids and cancer prevention: a review of the evidence. *Journal of Nutrition in Gerontology and Geriatrics, 31*(3), 206-238.

Ropa, J., Saha, N., Hu, H., Peterson, L. F., Talpaz, M., & Muntean, A. G. (2019). SETDB1 mediated histone H3 lysine 9 methylation suppresses MLL-fusion target expression and leukemic transformation. *Haematologica*.

Rudek, M. A., Venitz, J., & Figg, W. D. (2002). Matrix metalloproteinase inhibitors: do they have a place in anticancer therapy? *Pharmacotherapy: The Journal of Human Pharmacology and Drug Therapy, 22*(6), 705-720.

Rudolf, E., Andělová, H., & Červinka, M. (2009). Activation of several concurrent proapoptic pathways by sulforaphane in human colon cancer cells SW620. *Food and Chemical Toxicology, 47*(9), 2366-2373.

Rudolf, K., Cervinka, M., & Rudolf, E. (2014). Sulforaphane-induced apoptosis involves p53 and p38 in melanoma cells. *Apoptosis, 19*(4), 734-747.

Rupasinghe, H. P., Sekhon-Loodu, S., Mantso, T., & Panayiotidis, M. I. (2016). Phytochemicals in regulating fatty acid beta-oxidation: Potential underlying mechanisms and their involvement in obesity and weight loss. *Pharmacology & Therapeutics, 165*, 153-163.

Russo, G. L. (2007). Ins and outs of dietary phytochemicals in cancer chemoprevention. *Biochemical pharmacology, 74*(4), 533-544.

Rünger, T. M. (2008). C→T Transition Mutations Are Not Solely UVB-Signature Mutations, Because They Are Also Generated by UVA. *Journal of Investigative Dermatology, 128*(9), 2138-2140.

Sage, E., Girard, P.-M., & Francesconi, S. (2012). Unravelling UVA-induced mutagenesis. *Photochemical & photobiological sciences, 11*(1), 74-80.

Saha, K., Fisher, M. L., Adhikary, G., Grun, D., & Eckert, R. L. (2017). Sulforaphane suppresses PRMT5/MEP50 function in epidermal squamous cell carcinoma leading to reduced tumor formation. *Carcinogenesis, 38*(8), 827-836.

Saha, K., Hornyak, T. J., & Eckert, R. L. (2013). Epigenetic cancer prevention mechanisms in skin cancer. *The AAPS Journal, 15*(4), 1064-1071.

Saha, K., Hornyak, T. J., & Eckert, R. L. (2013). Epigenetic Cancer Prevention Mechanisms in Skin Cancer. *The AAPS Journal, 15*(4), 1064-1071.

Sahu, R. P. (2015). Expression of the platelet-activating factor receptor enhances benzyl isothiocyanate-induced apoptosis in murine and human melanoma cells. *Molecular Medicine Reports, 12*(1), 394-400.

Sakaguchi, K., Herrera, J. E., Saito, S. i., Miki, T., Bustin, M., Vassilev, A., Anderson, C. W., & Appella, E. (1998). DNA damage activates p53 through a phosphorylation–acetylation cascade. *Genes & Development, 12*(18), 2831-2841.

Sand, M., Gambichler, T., Skrygan, M., Sand, D., Scola, N., Altmeyer, P., & Bechara, F. G. (2010). Expression levels of the microRNA processing enzymes Drosha and dicer in epithelial skin cancer. *Cancer investigation, 28*(6), 649-653.

Sand, M., Sand, D., Altmeyer, P., & Bechara, F. G. (2012). MicroRNA in non-melanoma skin cancer. *Cancer Biomarkers, 11*(6), 253-257.

Sandoval, J., & Esteller, M. (2012). Cancer epigenomics: beyond genomics. *Current opinion in genetics & development, 22*(1), 50-55.

Sapienza, C., & Issa, J. P. (2016). Diet, Nutrition, and Cancer Epigenetics. *Annual Review of Nutrition, 36*, 665-681.

Sarkar, D., Leung, E. Y., Baguley, B. C., Finlay, G. J., & Askarian-Amiri, M. E. (2015). Epigenetic regulation in human melanoma: past and future. *Epigenetics, 10*(2), 103-121.

Sarkar, R., Mukherjee, S., Biswas, J., & Roy, M. (2012). Sulphoraphane, a naturally occurring isothiocyanate induces apoptosis in breast cancer cells by targeting heat shock proteins. *Biochemical and Biophysical Research Communications, 427*(1), 80-85.

Sato, F., Tsuchiya, S., Meltzer, S. J., & Shimizu, K. (2011). MicroRNAs and epigenetics. *The FEBS Journal, 278*(10), 1598-1609.

Saw, C. L., Huang, M. T., Liu, Y., Khor, T. O., Conney, A. H., & Kong, A. N. (2011). Impact of Nrf2 on UVB-induced skin inflammation/photoprotection and photoprotective effect of sulforaphane. *Moleculr Carcinogenesis, 50*(6), 479-486.

Sawan, C., & Herceg, Z. (2010). 3 - Histone Modifications and Cancer. In Z. Herceg & T. Ushijima (Eds.), *Advances in Genetics*, *70*, 57-85.

Schinke, C., Mo, Y., Yu, Y., Amiri, K., Sosman, J., Greally, J., & Verma, A. (2010). Aberrant DNA methylation in malignant melanoma. *Melanoma research, 20*(4), 253.

Schwarz, A., Noordegraaf, M., Maeda, A., Torii, K., Clausen, B. E., & Schwarz, T. (2010). Langerhans Cells Are Required for UVR-Induced Immunosuppression. *Journal of Investigative Dermatology, 130*(5), 1419-1427.

Seebode, C., Lehmann, J., & Emmert, S. (2016). Photocarcinogenesis and skin cancer prevention strategies. *Anticancer Research, 36*(3), 1371-1378.

Segura, M. F., Hanniford, D., Menendez, S., Reavie, L., Zou, X., Alvarez-Diaz, S., Zakrzewski, J., Blochin, E., Rose, A., Bogunovic, D., Polsky, D., Wei, J., Lee, P., Belitskaya-Levy, I., Bhardwaj, N., Osman, I., & Hernando, E. (2009). Aberrant miR-182 expression promotes melanoma metastasis by repressing FOXO3 and microphthalmia-associated transcription factor. *Proceedings of the National Academy of Sciences of the United States of America, 106*(6), 1814-1819.

Sehrawat, A., Croix, C. S., Baty, C. J., Watkins, S., Tailor, D., Singh, R. P., & Singh, S. V. (2016). Inhibition of mitochondrial fusion is an early and critical event in breast

cancer cell apoptosis by dietary chemopreventative benzyl isothiocyanate. *Mitochondrion, 30*, 67-77.

Seligson, D. B., Horvath, S., McBrian, M. A., Mah, V., Yu, H., Tze, S., Wang, Q., Chia, D., Goodglick, L., & Kurdistani, S. K. (2009). Global levels of histone modifications predict prognosis in different cancers. *The American Journal of Pathology, 174*(5), 1619-1628.

Seligson, D. B., Horvath, S., Shi, T., Yu, H., Tze, S., Grunstein, M., & Kurdistani, S. K. (2005). Global histone modification patterns predict risk of prostate cancer recurrence. *Nature, 435*(7046), 1262-1266.

Seow, A., Vainio, H., & Mimi, C. Y. (2005). Effect of glutathione-S-transferase polymorphisms on the cancer preventive potential of isothiocyanates: an epidemiological perspective. *Mutation Research/Fundamental and Molecular Mechanisms of Mutagenesis, 592*(1), 58-67.

Seow, A., Yuan, J.-M., Sun, C.-L., Van Den Berg, D., Lee, H.-P., & Yu, M. C. (2002). Dietary isothiocyanates, glutathione S-transferase polymorphisms and colorectal cancer risk in the Singapore Chinese Health Study. *Carcinogenesis, 23*(12), 2055-2061.

Serrano, L., Martínez-Redondo, P., Marazuela-Duque, A., Vazquez, B. N., Dooley, S. J., Voigt, P., Beck, D. B., Kane-Goldsmith, N., Tong, Q., & Rabanal, R. M. (2013). The tumor suppressor SirT2 regulates cell cycle progression and genome stability by modulating the mitotic deposition of H4K20 methylation. *Genes & development, 27*(6), 639-653.

Shan, Y., Lin, N., Yang, X., Tan, J., Zhao, R., Dong, S., & Wang, S. (2012). Sulphoraphane inhibited the expressions of intercellular adhesion molecule-1 and vascular cell adhesion molecule-1 through MyD88-dependent toll-like receptor-4 pathway in cultured endothelial cells. *Nutrition, Metabolism and Cardiovascular Diseases, 22*(3), 215-222.

Shan, Y., Sun, C., Zhao, X., Wu, K., Cassidy, A., & Bao, Y. (2006). Effect of sulforaphane on cell growth, G0/G1 phase cell progression and apoptosis in human bladder cancer T24 cells. *International Journal of Oncology, 29*(4), 883-888.

Shan, Y., Zhang, L., Bao, Y., Li, B., He, C., Gao, M., Feng, X., Xu, W., Zhang, X., & Wang, S. (2013). Epithelial-mesenchymal transition, a novel target of sulforaphane via COX-2/MMP2, 9/Snail, ZEB1 and miR-200c/ZEB1 pathways in human bladder cancer cells. *The Journal of Nutritional Biochemistry, 24*(6), 1062-1069.

Sharma, A., Sharma, A. K., Madhunapantula, S. V., Desai, D., Huh, S. J., Mosca, P., Amin, S., & Robertson, G. P. (2009). Targeting Akt3 signaling in malignant melanoma using isoselenocyanates. *Clinical Cancer Research, 15*(5), 1674-1685.

Sharma, A. K., Sharma, A., Desai, D., Madhunapantula, S. V., Huh, S. J., Robertson, G. P., & Amin, S. (2008). Synthesis and anticancer activity comparison of phenylalkyl isoselenocyanates with corresponding naturally occurring and synthetic isothiocyanates. *Journal of Medicinal Chemistry, 51*(24), 7820-7826.

Sharma, S., Kelly, T. K., & Jones, P. A. (2010). Epigenetics in cancer. *Carcinogenesis, 31*(1), 27-36.

Shi, X., Guo, Z., Wang, X., Liu, X., & Shi, G. (2015). SET8 expression is associated with overall survival in gastric cancer. *Genetics and Molecular Research, 14*, 15609-15615.

Shidal, C., Inaba, J.-I., Yaddanapudi, K., & Davis, K. R. (2017). The soy-derived peptide Lunasin inhibits invasive potential of melanoma initiating cells. *Oncotarget, 8*(15), 25525-25541.

Shtivelman, E., Davies, M. Q., Hwu, P., Yang, J., Lotem, M., Oren, M., Flaherty, K. T., & Fisher, D. E. (2014). Pathways and therapeutic targets in melanoma. *Oncotarget, 5*(7), 1701-1752.

Shukla, G. C., Singh, J., & Barik, S. (2011). MicroRNAs: Processing, Maturation, Target Recognition and Regulatory Functions. *Molecular and cellular pharmacology, 3*(3), 83-92.

Siegfried, Z., & Simon, I. (2010). DNA methylation and gene expression. *Wiley Interdisciplinary Reviews: Systems Biology and Medicine, 2*(3), 362-371.

Sigalotti, L., Covre, A., Fratta, E., Parisi, G., Colizzi, F., Rizzo, A., Danielli, R., Nicolay, H. J., Coral, S., & Maio, M. (2010). Epigenetics of human cutaneous melanoma: setting the stage for new therapeutic strategies. *Journal of translational medicine, 8*(1), 56.

Singh, S. V., Srivastava, S. K., Choi, S., Lew, K. L., Antosiewicz, J., Xiao, D., Zeng, Y., Watkins, S. C., Johnson, C. S., & Trump, D. L. (2005). Sulforaphane-induced cell death in human prostate cancer cells is initiated by reactive oxygen species. *Journal of Biological Chemistry, 280*(20), 19911-19924.

Sinha, S., Shukla, S., Khan, S., Tollefsbol, T. O., & Meeran, S. M. (2015). Epigenetic reactivation of p21CIP1/WAF1 and KLOTHO by a combination of bioactive dietary supplements is partially ERalpha-dependent in ERalpha-negative human breast cancer cells. *Molecular and Cellular Endocrinology, 406*, 102-114.

Sk, U. H., Gowda, A. P., Crampsie, M. A., Yun, J. K., Spratt, T. E., Amin, S., & Sharma, A. K. (2011). Development of novel naphthalimide derivatives and their evaluation as potential melanoma therapeutics. *European Journal of Medicinal Chemistry, 46*(8), 3331-3338.

Slaby, O., Sachlova, M., Brezkova, V., Hezova, R., Kovarikova, A., Bischofová, S., Sevcikova, S., Bienertova-Vasku, J., Vasku, A., & Svoboda, M. (2013). Identification of microRNAs regulated by isothiocyanates and association of polymorphisms inside their target sites with risk of sporadic colorectal cancer. *Nutrition and cancer, 65*(2), 247-254.

Slawson, D. L., Fitzgerald, N., & Morgan, K. T. (2013). Position of the Academy of Nutrition and Dietetics: the role of nutrition in health promotion and chronic disease prevention. *Journal of the Academy of Nutrition and Dietetics, 113*(7), 972-979.

Soengas, M. S., & Lowe, S. W. (2003). Apoptosis and melanoma chemoresistance. *Oncogene, 22*(20), 3138-3151.

Song, L., & Thornalley, P. J. (2007). Effect of storage, processing and cooking on glucosinolate content of Brassica vegetables. *Food and Chemical Toxicology, 45*(2), 216-224.

Song, Y., Zhang, J., Tian, T., Fu, X., Wang, W., Li, S., Shi, T., Suo, A., Ruan, Z., Guo, H., & Yao, Y. (2016). SET7/9 inhibits oncogenic activities through regulation of Gli-1 expression in breast cancer [journal article]. *Tumor Biology, 37*(7), 9311-9322.

Spencer, E. S., Dale, E. J., Gommans, A. L., Rutledge, M. T., Vo, C. T., Nakatani, Y., Gamble, A. B., Smith, R. A. J., Wilbanks, S. M., Hampton, M. B., & Tyndall, J. D. A. (2015). Multiple binding modes of isothiocyanates that inhibit macrophage migration inhibitory factor. *European Journal of Medicinal Chemistry, 93*, 501-510.

Spyropoulou, A., Gargalionis, A., Dalagiorgou, G., Adamopoulos, C., Papavassiliou, K. A., Lea, R. W., Piperi, C., & Papavassiliou, A. G. (2014). Role of histone lysine methyltransferases SUV39H1 and SETDB1 in gliomagenesis: modulation of cell proliferation, migration, and colony formation. *Neuromolecular Med, 16*(1), 70-82.

Srijyothi, L., Saravanaraman, P., Prathama, T., Cheemala, A., & Baluchamy, S. (2018). Roles of Non-Coding RNAs in Transcriptional Regulation. In.

Srivastava, S. K., Xiao, D., Lew, K. L., Hershberger, P., Kokkinakis, D. M., Johnson, C. S., Trump, D. L., & Singh, S. V. (2003). Allyl isothiocyanate, a constituent of cruciferous vegetables, inhibits growth of PC-3 human prostate cancer xenografts in vivo. *Carcinogenesis, 24*(10), 1665-1670.

Stan, S. D., Singh, S. V., Whitcomb, D. C., & Brand, R. E. (2014). Phenethyl isothiocyanate inhibits proliferation and induces apoptosis in pancreatic cancer cells in vitro and in a MIAPaca2 xenograft animal model. *Nutrition and cancer, 66*(4), 747-755.

Straume, O., Smeds, J., Kumar, R., Hemminki, K., & Akslen, L. A. (2002). Significant Impact of Promoter Hypermethylation and the 540 C>T Polymorphism of CDKN2A in Cutaneous Melanoma of the Vertical Growth Phase. *The American Journal of Pathology, 161*(1), 229-237.

Su, Z.-Y., Zhang, C., Lee, J. H., Shu, L., Wu, T.-Y., Khor, T. O., Conney, A. H., Lu, Y.-P., & Kong, A.-N. T. (2014). Requirement and epigenetics reprogramming of Nrf2 in suppression of tumor promoter TPA-induced mouse skin cell transformation by sulforaphane. *Cancer prevention research, 7*(3), 319-329.

Sun, Y., Wei, M., Ren, S.-C., Chen, R., Xu, W.-D., Wang, F.-B., Lu, J., Shen, J., Yu, Y.-W., Hou, J.-G., Xu, C.-L., Huang, J.-T., & Sun, Y.-H. (2014). Histone methyltransferase SETDB1 is required for prostate cancer cell proliferation, migration and invasion. *Asian journal of andrology, 16*(2), 319-324.

Supic, G., Jagodic, M., & Magic, Z. (2013). Epigenetics: a new link between nutrition and cancer. *Nutrition and cancer, 65*(6), 781-792.

Surh, Y.-J., & Na, H.-K. (2008). NF-κB and Nrf2 as prime molecular targets for chemoprevention and cytoprotection with anti-inflammatory and antioxidant phytochemicals. *Genes & nutrition, 2*(4), 313-317.

Suryanarayanan, V., Rajavel, T., Devi, K. P., & Singh, S. K. (2018). Structure based identification and biological evaluation of novel and potent inhibitors of PCAF catalytic domain. *International Journal of Biological Macromolecules, 120*, 823-834.

Suryanarayanan, V., & Singh, S. K. (2015). Assessment of dual inhibition property of newly discovered inhibitors against PCAF and GCN5 through in silico screening, molecular dynamics simulation and DFT approach. *Journal of Receptors and Signal Transduction, 35*(5), 370-380.

Syed Alwi, S. S., Cavell, B. E., Donlevy, A., & Packham, G. (2012). Differential induction of apoptosis in human breast cancer cell lines by phenethyl isothiocyanate, a glutathione depleting agent. *Cell Stress Chaperones, 17*(5), 529-538.

Sønderby, I. E., Geu-Flores, F., & Halkier, B. A. (2010). Biosynthesis of glucosinolates–gene discovery and beyond. *Trends in plant science, 15*(5), 283-290.

Taby, R., & Issa, J. P. (2010). Cancer epigenetics. *CA: A Cancer Journal for Clinicians, 60*(6), 376-392.

Takemoto, Y., Ito, A., Niwa, H., Okamura, M., Fujiwara, T., Hirano, T., Handa, N., Umehara, T., Sonoda, T., & Ogawa, K. (2016). Identification of cyproheptadine as an inhibitor of SET domain containing lysine methyltransferase 7/9 (Set7/9) that regulates estrogen-dependent transcription. *Journal of Medicinal Chemistry, 59*(8), 3650-3660.

Talalay, P., & Fahey, J. W. (2001). Phytochemicals from cruciferous plants protect against cancer by modulating carcinogen metabolism. *The Journal of Nutrition, 131*(11), 3027S-3033S.

Talalay, P., Fahey, J. W., Healy, Z. R., Wehage, S. L., Benedict, A. L., Min, C., & Dinkova-Kostova, A. T. (2007). Sulforaphane mobilizes cellular defenses that protect skin against damage by UV radiation. *Proceedings of the national academy of sciences, 104*(44), 17500-17505.

Tan, X.-L., Shi, M., Tang, H., Han, W., & Spivack, S. D. (2010). Candidate dietary phytochemicals modulate expression of phase II enzymes GSTP1 and NQO1 in human lung cells. *The Journal of nutrition, 140*(8), 1404-1410.

Tan, Z., Feng, M., Luo, Y., Sun, C., Fan, Z., Tan, Y., Fu, B., & Lang, J. (2013). GSTP1 Ile105Val polymorphism and colorectal cancer risk: An updated analysis. *Gene, 527*(1), 275-282.

Tanemura, A., Terando, A. M., Sim, M. S., van Hoesel, A. Q., de Maat, M. F., Morton, D. L., & Hoon, D. S. (2009). CpG island methylator phenotype predicts progression of malignant melanoma. *Clinical Cancer Research, 15*(5), 1801-1807.

Tang, L., Zirpoli, G. R., Jayaprakash, V., Reid, M. E., McCann, S. E., Nwogu, C. E., Zhang, Y., Ambrosone, C. B., & Moysich, K. B. (2010). Cruciferous vegetable intake is inversely associated with lung cancer risk among smokers: a case-control study. *BMC cancer, 10*(1), 1-9.

Telang, U., & Morris, M. E. (2010). Effect of orally administered phenethyl isothiocyanate on hepatic gene expression in rats. *Molecular Nutrition & Food Research, 54*(12), 1802-1806.

Tellez, C. S., Shen, L., Estécio, M. R., Jelinek, J., Gershenwald, J. E., & Issa, J.-P. J. (2009). CpG island methylation profiling in human melanoma cell lines. *Melanoma research, 19*(3), 146-155.

Thangstad, O. P., Gilde, B., Chadchawan, S., Seem, M., Husebye, H., Bradley, D., & Bones, A. M. (2004). Cell specific, cross-species expression of myrosinases in Brassica napus, Arabidopsis thaliana and Nicotiana tabacum. *Plant molecular biology, 54*(4), 597-611.

Thejass, P., & Kuttan, G. (2007). Allyl isothiocyanate (AITC) and phenyl isothiocyanate (PITC) inhibit tumour-specific angiogenesis by downregulating nitric oxide (NO) and tumour necrosis factor-α (TNF-α) production. *Nitric Oxide, 16*(2), 247-257.

Thejass, P., & Kuttan, G. (2007a). Inhibition of endothelial cell differentiation and proinflammatory cytokine production during angiogenesis by allyl isothiocyanate and phenyl isothiocyanate. *Integrative Cancer Therapies, 6*(4), 389-399.

Thejass, P., & Kuttan, G. (2007b). Modulation of cell-mediated immune response in B16F-10 melanoma-induced metastatic tumor-bearing C57BL/6 mice by sulforaphane. *Immunopharmacology and Immunotoxicology, 29*(2), 173-186.

Thornalley, P. (2004). Cruciferous Vegetables, Isothiocyanates and Indoles (IARC Handbooks of Cancer Prevention). In, 1-261).

Tian, J., Shen, R., Yan, Y., & Deng, L. (2018). miR-186 promotes tumor growth in cutaneous squamous cell carcinoma by inhibiting apoptotic protease activating factor-1. *Experimental and Therapeutic Medicine, 16*(5), 4010-4018.

Ting, W., Schultz, K., Cac, N. N., Peterson, M., & Walling, H. W. (2007). Tanning bed exposure increases the risk of malignant melanoma. *The International Journal of Dermatology, 46*(12), 1253-1257.

Trachootham, D., Zhou, Y., Zhang, H., Demizu, Y., Chen, Z., Pelicano, H., Chiao, P. J., Achanta, G., Arlinghaus, R. B., Liu, J., & Huang, P. (2006). Selective killing of oncogenically transformed cells through a ROS-mediated mechanism by beta-phenylethyl isothiocyanate. *Cancer Cell, 10*(3), 241-252.

Trio, P. Z., Kawahara, A., Tanigawa, S., Sakao, K., & Hou, D.-X. (2017). DNA Microarray Profiling Highlights Nrf2-Mediated Chemoprevention Targeted by Wasabi-Derived Isothiocyanates in HepG2 Cells. *Nutrition and Cancer, 69*(1), 105-116.

Tripathi, K., Hussein, U. K., Anupalli, R., Barnett, R., Bachaboina, L., Scalici, J., Rocconi, R. P., Owen, L. B., Piazza, G. A., & Palle, K. (2015). Allyl isothiocyanate induces replication-associated DNA damage response in NSCLC cells and sensitizes to ionizing radiation. *Oncotarget, 6*(7), 5237-5252.

Troyano, A., Sancho, P., Fernández, C., de Blas, E., Bernardi, P., & Aller, P. (2003). The selection between apoptosis and necrosis is differentially regulated in hydrogen

peroxide-treated and glutathione-depleted human promonocytic cells. *Cell Death & Differentiation, 10*(8), 889-898.

Tsai, H.-C., & Baylin, S. B. (2011). Cancer epigenetics: linking basic biology to clinical medicine. *Cell research, 21*(3), 502-517.

Tsai, S.-C., Huang, W.-W., Huang, W.-C., Lu, C.-C., Chiang, J.-H., Peng, S.-F., Chung, J.-G., Lin, Y.-H., Hsu, Y.-M., & Amagaya, S. (2012). ERK-modulated intrinsic signaling and G2/M phase arrest contribute to the induction of apoptotic death by allyl isothiocyanate in MDA-MB-468 human breast adenocarcinoma cells. *International journal of oncology, 41*(6), 2065-2072.

Tsunoda, K., Oikawa, H., Tada, H., Tatemichi, Y., Muraoka, S., Miura, S., Shibazaki, M., Maeda, F., Takahashi, K., Akasaka, T., Masuda, T., & Maesawa, C. (2011). Nucleus Accumbens-Associated 1 Contributes to Cortactin Deacetylation and Augments the Migration of Melanoma Cells. *Journal of Investigative Dermatology, 131*(8), 1710-1719.

Tyndall, J. D., Lue, H., Rutledge, M. T., Bernhagen, J., Hampton, M. B., & Wilbanks, S. M. (2012). Macrophage migration inhibitory factor covalently complexed with phenethyl isothiocyanate. *Acta Crystallographica Section F: Structural Biology and Crystallization Communications, 68*(9), 999-1002.

Ullah, M., Bhat, S., Husain, E., Abu-Duhier, F., Hadi, S. M., Sarkar, F., & Ahmad, A. (2014). Cancer chemopreventive pharmacology of phytochemicals derived from plants of dietary and non-dietary origin: Implication for alternative and complementary approaches. *Phytochemistry Reviews, 13*, 811-833.

Valencia-Sanchez, M. A., Liu, J., Hannon, G. J., & Parker, R. (2006). Control of translation and mRNA degradation by miRNAs and siRNAs. *Genes & Development, 20*(5), 515-524.

van den Hurk, K., Niessen, H. E. C., Veeck, J., van den Oord, J. J., van Steensel, M. A. M., zur Hausen, A., van Engeland, M., & Winnepenninckx, V. J. L. (2012). Genetics and epigenetics of cutaneous malignant melanoma: A concert out of tune. *Biochimica et Biophysica Acta (BBA) - Reviews on Cancer, 1826*(1), 89-102.

Varier, R. A., & Timmers, H. T. M. (2011). Histone lysine methylation and demethylation pathways in cancer. *Biochimica et Biophysica Acta (BBA) - Reviews on Cancer, 1815*(1), 75-89.

Velasco, P., Cartea, M. E., González, C., Vilar, M., & Ordás, A. (2007). Factors affecting the glucosinolate content of kale (Brassica oleracea acephala group). *Journal of agricultural and food chemistry, 55*(3), 955-962.

Verkerk, R., Schreiner, M., Krumbein, A., Ciska, E., Holst, B., Rowland, I., De Schrijver, R., Hansen, M., Gerhäuser, C., & Mithen, R. (2009). Glucosinolates in Brassica vegetables: the influence of the food supply chain on intake, bioavailability and human health. *Molecular nutrition & food research, 53*(S2), S219-S219.

Visanji, J. M., Duthie, S. J., Pirie, L., Thompson, D. G., & Padfield, P. J. (2004). Dietary isothiocyanates inhibit Caco-2 cell proliferation and induce G2/M phase cell cycle arrest, DNA damage, and G2/M checkpoint activation. *Journal of Nutrition, 134*(11), 3121-3126.

Vogtmann, E., Xiang, Y.-B., Li, H.-L., Cai, Q., Wu, Q.-J., Xie, L., Li, G.-L., Yang, G., Waterbor, J. W., Levitan, E. B., Zhang, B., Zheng, W., & Shu, X.-O. (2014). Cruciferous vegetables, glutathione S-transferase polymorphisms, and the risk of colorectal cancer among Chinese men. *Annals of Epidemiology, 24*(1), 44-49.

Volinia, S., Calin, G. A., Liu, C.-G., Ambs, S., Cimmino, A., Petrocca, F., Visone, R., Iorio, M., Roldo, C., & Ferracin, M. (2006). A microRNA expression signature of human solid tumors defines cancer gene targets. *Proceedings of the National Academy of Sciences of the United States of America, 103*(7), 2257-2261.

von Weymarn, L. B., Chun, J. A., & Hollenberg, P. F. (2006). Effects of benzyl and phenethyl isothiocyanate on P450s 2A6 and 2A13: potential for chemoprevention in smokers. *Carcinogenesis, 27*(4), 782-790.

Wagner, A. E., Ernst, I., Iori, R., Desel, C., & Rimbach, G. (2010). Sulforaphane but not ascorbigen, indole-3-carbinole and ascorbic acid activates the transcription factor Nrf2 and induces phase-2 and antioxidant enzymes in human keratinocytes in culture. *Experimental Dermatology, 19*(2), 137-144.

Wagner, A. E., Terschluesen, A. M., & Rimbach, G. (2013). Health promoting effects of brassica-derived phytochemicals: from chemopreventive and anti-inflammatory activities to epigenetic regulation. *Oxidative medicine and cellular longevity, 2013*.

Wagner, T., & Jung, M. (2012). New lysine methyltransferase drug targets in cancer. *Nature Biotechnology, 30*, 622.

Wahid, F., Shehzad, A., Khan, T., & Kim, Y. Y. (2010). MicroRNAs: Synthesis, mechanism, function, and recent clinical trials. *Biochimica et Biophysica Acta (BBA) - Molecular Cell Research, 1803*(11), 1231-1243.

Wang, C., Guo, Z., Wu, C., Li, Y., & Kang, S. (2012). A polymorphism at the miR-502 binding site in the 3′ untranslated region of the SET8 gene is associated with the risk of epithelial ovarian cancer. *Cancer Genetics, 205*(7), 373-376.

Wang, D. X., Zou, Y. J., Zhuang, X. B., Chen, S. X., Lin, Y., Li, W. L., Lin, J. J., & Lin, Z. Q. (2017). Sulforaphane suppresses EMT and metastasis in human lung cancer through miR-616-5p-mediated GSK3beta/beta-catenin signaling pathways. *Acta Pharmacologica Sinica, 38*(2), 241-251.

Wang, H., Wang, L., Cao, L., Zhang, Q., Song, Q., Meng, Z., Wu, X., & Xu, K. (2018). Inhibition of autophagy potentiates the anti-metastasis effect of phenethyl isothiocyanate through JAK2/STAT3 pathway in lung cancer cells. *Molecular Carcinogenesis, 57*(4), 522-535.

Wang, H., Wu, J., Sun, S., Liu, B., Cheng, F., Sun, R., & Wang, X. (2011). Glucosinolate biosynthetic genes in Brassica rapa. *Gene, 487*(2), 135-142.

Wang, J., Han, L., Zhang, W., Wang, J., Ni, Q., Shen, M., & Gao, Y. (2014). [A case-control study on the association between urinary levels of isothiocyanates and the risk of pancreatic cancer]. *Zhonghua Yu Fang Yi Xue Za Zhi. Chinese Journal of Preventive Medicine, 48*(3), 172-176.

Wang, L., Tian, Z., Yang, Q., Li, H., Guan, H., Shi, B., Hou, P., & Ji, M. (2015). Sulforaphane inhibits thyroid cancer cell growth and invasiveness through the reactive oxygen species-dependent pathway. *Oncotarget, 6*(28), 25917-25931.

Wang, L. G., Beklemisheva, A., Liu, X. M., Ferrari, A. C., Feng, J., & Chiao, J. W. (2007). Dual action on promoter demethylation and chromatin by an isothiocyanate restored GSTP1 silenced in prostate cancer. *Molecular Carcinogenesis, 46*(1), 24-31.

Wang, L. G., Liu, X. M., Fang, Y., Dai, W., Chiao, F. B., Puccio, G. M., Feng, J., Liu, D., & Chiao, J. W. (2008). De-repression of the p21 promoter in prostate cancer cells by an isothiocyanate via inhibition of HDACs and c-Myc. *International Journal of Oncology, 33*(2), 375-380.

Wang, R., He, Y., Robinson, V., Yang, Z., Hessler, P., Lasko, L. M., Lu, X., Bhathena, A., Lai, A., Uziel, T., & Lam, L. T. (2018). Targeting Lineage-specific MITF Pathway in Human Melanoma Cell Lines by A-485, the Selective Small-molecule Inhibitor of p300/CBP. *Molecular Cancer Therapeutics, 17*(12), 2543-2550.

Wang, S., Cao, K. E., He, Q., Yin, Z., & Zhou, J. (2016). miR-199a-5p induces cell invasion by suppressing E-cadherin expression in cutaneous squamous cell carcinoma. *Oncology Letters, 12*(1), 97-101.

Wang, W., Wang, S., Howie, A. F., Beckett, G. J., Mithen, R., & Bao, Y. (2005). Sulforaphane, erucin, and iberin up-regulate thioredoxin reductase 1 expression in human MCF-7 cells. *Journal of agricultural and food chemistry, 53*(5), 1417-1421.

Wang, X., Di Pasqua, A. J., Govind, S., McCracken, E., Hong, C., Mi, L., Mao, Y., Wu, J. Y., Tomita, Y., Woodrick, J. C., Fine, R. L., & Chung, F. L. (2011). Selective depletion of mutant p53 by cancer chemopreventive isothiocyanates and their structure-activity relationships. *Journal of Medicinal Chemistry, 54*(3), 809-816.

Wang, Z., Qin, G., & Zhao, T. C. (2014). HDAC4: mechanism of regulation and biological functions. *Epigenomics, 6*(1), 139-150.

Wang, Z., Zang, C., Cui, K., Schones, D. E., Barski, A., Peng, W., & Zhao, K. (2009). Genome-wide mapping of HATs and HDACs reveals distinct functions in active and inactive genes. *Cell, 138*(5), 1019-1031.

Wei, Y., Xia, W., Zhang, Z., Liu, J., Wang, H., Adsay, N. V., Albarracin, C., Yu, D., Abbruzzese, J. L., Mills, G. B., Bast, R. C., Jr., Hortobagyi, G. N., & Hung, M. C. (2008). Loss of trimethylation at lysine 27 of histone H3 is a predictor of poor outcome in breast, ovarian, and pancreatic cancers. *Molecular Carcinogenesis, 47*(9), 701-706.

Welsh, M. M., Karagas, M. R., Kuriger, J. K., Houseman, A., Spencer, S. K., Perry, A. E., & Nelson, H. H. (2011). Genetic determinants of UV-susceptibility in non-melanoma skin cancer. *PloS one, 6*(7), e20019.

Weng, C.-J., & Yen, G.-C. (2012). Chemopreventive effects of dietary phytochemicals against cancer invasion and metastasis: phenolic acids, monophenol, polyphenol, and their derivatives. *Cancer Treatment Reviews, 38*(1), 76-87.

White, E. (2012). Deconvoluting the context-dependent role for autophagy in cancer. *Nature Reviews Cancer, 12*(6), 401.

Wikonkal, N. M., & Brash, D. E. (1999). Ultraviolet radiation induced signature mutations in photocarcinogenesis. *Journal of Investigative Dermatology Symposium Proceedings, 4*(1), 6-10.

Willett, W. C. (2010). Fruits, vegetables, and cancer prevention: turmoil in the produce section. *Journal of the National Cancer Institute*, *102*, 510-511).

Wilson, A. E., Bergaentzlé, M., Bindler, F., Marchioni, E., Lintz, A., & Ennahar, S. (2013). In vitro efficacies of various isothiocyanates from cruciferous vegetables as antimicrobial agents against foodborne pathogens and spoilage bacteria. *Food Control, 30*(1), 318-324.

Wiseman, M. J. (2019). Nutrition and cancer: prevention and survival. *British Journal of Nutrition, 122*(5), 481-487.

Wittstock, U., & Halkier, B. A. (2002). Glucosinolate research in the Arabidopsis era. *Trends in Plant Science, 7*(6), 263-270.

Woan, K., Lienlaf, M., Perez-Villaroel, P., Lee, C., Cheng, F., Knox, T., Woods, D., Barrios, K., Powers, J., & Sahakian, E. (2015). Targeting histone deacetylase 6 mediates a dual anti-melanoma effect: Enhanced antitumor immunity and impaired cell proliferation. *Molecular Oncology, 9*(7), 1447-1457.

Wong, C. M., Wei, L., Law, C. T., Ho, D. W., Tsang, F. H., Au, S. L., Sze, K. M., Lee, J. M., Wong, C. C., & Ng, I. O. (2016). Up-regulation of histone methyltransferase SETDB1 by multiple mechanisms in hepatocellular carcinoma promotes cancer metastasis. *Hepatology, 63*(2), 474-487.

Wong, C. P., Hsu, A., Buchanan, A., Palomera-Sanchez, Z., Beaver, L. M., Houseman, E. A., Williams, D. E., Dashwood, R. H., & Ho, E. (2014). Effects of sulforaphane and 3,3'-diindolylmethane on genome-wide promoter methylation in normal prostate epithelial cells and prostate cancer cells. *PloS one, 9*(1), e86787.

Woodcock, C. L., & Ghosh, R. P. (2010). Chromatin higher-order structure and dynamics. *Cold Spring Harbor Perspectives in Biology, 2*(5), a000596.

Woods, D. M., Sodré, A. L., Villagra, A., Sarnaik, A., Sotomayor, E. M., & Weber, J. (2015). HDAC Inhibition Upregulates PD-1 Ligands in Melanoma and Augments Immunotherapy with PD-1 Blockade. *Cancer Immunology Research, 3*(12), 1375-1385.

Wu, C. L., Huang, A. C., Yang, J. S., Liao, C. L., Lu, H. F., Chou, S. T., Ma, C. Y., Hsia, T. C., Ko, Y. C., & Chung, J. G. (2011). Benzyl isothiocyanate (BITC) and phenethyl isothiocyanate (PEITC)-mediated generation of reactive oxygen species causes cell cycle arrest and induces apoptosis via activation of caspase-3, mitochondria dysfunction and nitric oxide (NO) in human osteogenic sarcoma U-2 OS cells. *Journal of Orthopaedic Research, 29*(8), 1199-1209.

Wu, J., Zhang, J.-R., & Qin, J. (2014). Clinical significance of methylation of E-cadherin and p14ARF gene promoters in skin squamous cell carcinoma tissues. *International journal of clinical and experimental medicine, 7*(7), 1808.

Wu, M., Fan, B., Guo, Q., Li, Y., Chen, R., Lv, N., Diao, Y., & Luo, Y. (2018). Knockdown of SETDB1 inhibits breast cancer progression by miR-381-3p-related regulation. *Journal of Biological Research, 51*(1), 39.

Wu, Q. J., Wang, J., Gao, J., Zhang, W., Han, L. H., Gao, S., Gao, Y. T., Ji, B. T., Zheng, W., Shu, X. O., & Xiang, Y. B. (2014). Urinary isothiocyanates level and liver cancer risk: a nested case-control study in Shanghai, China. *Nutrition and Cancer, 66*(6), 1023-1029.

Wu, X., Zhou, Q.-h., & Xu, K. (2009). Are isothiocyanates potential anti-cancer drugs? *Acta Pharmacologica Sinica, 30*(5), 501-512.

Xiao, D., Bommareddy, A., Kim, S. H., Sehrawat, A., Hahm, E. R., & Singh, S. V. (2012). Benzyl isothiocyanate causes FoxO1-mediated autophagic death in human breast cancer cells. *PloS One, 7*(3), e32597.

Xiao, D., Powolny, A. A., & Singh, S. V. (2008). Benzyl isothiocyanate targets mitochondrial respiratory chain to trigger reactive oxygen species-dependent apoptosis in human breast cancer cells. *Journal of Biological Chemistry, 283*(44), 30151-30163.

Xiao, D., & Singh, S. V. (2007). Phenethyl isothiocyanate inhibits angiogenesis in vitro and ex vivo. *Cancer Research, 67*(5), 2239-2246.

Xiao, D., Srivastava, S. K., Lew, K. L., Zeng, Y., Hershberger, P., Johnson, C. S., Trump, D. L., & Singh, S. V. (2003). Allyl isothiocyanate, a constituent of cruciferous vegetables, inhibits proliferation of human prostate cancer cells by causing G2/M arrest and inducing apoptosis. *Carcinogenesis, 24*(5), 891-897.

Xiao, D., Vogel, V., & Singh, S. V. (2006). Benzyl isothiocyanate–induced apoptosis in human breast cancer cells is initiated by reactive oxygen species and regulated by Bax and Bak. *Molecular Cancer Therapeutics, 5*(11), 2931-2945.

Xiao, J., Gong, A. Y., Eischeid, A. N., Chen, D., Deng, C., Young, C. Y., & Chen, X. M. (2012). miR-141 modulates androgen receptor transcriptional activity in human prostate cancer cells through targeting the small heterodimer partner protein. *Prostate, 72*(14), 1514-1522.

Xie, B., Nagalingam, A., Kuppusamy, P., Muniraj, N., Langford, P., Gyorffy, B., Saxena, N. K., & Sharma, D. (2017). Benzyl Isothiocyanate potentiates p53 signaling and antitumor effects against breast cancer through activation of p53-LKB1 and p73-LKB1 axes. *Sciemtific Reports, 7*, 40070.

Xie, J. (2008). Molecular biology of basal and squamous cell carcinomas. *Advances in Experimental Medicine and Biology, 624*, 241-251.

Xu, C., Huang, M. T., Shen, G., Yuan, X., Lin, W., Khor, T. O., Conney, A. H., & Kong, A. N. (2006). Inhibition of 7,12-dimethylbenz(a)anthracene-induced skin tumorigenesis

in C57BL/6 mice by sulforaphane is mediated by nuclear factor E2-related factor 2. *Cancer Research, 66*(16), 8293-8296.

Xu, C., Shen, G., Chen, C., Gélinas, C., & Ah-Ng, T. K. (2005). Suppression of NF-[kappa] B and NF-[kappa] B-regulated gene expression by sulforaphane and PEITC through I [kappa] B [alpha], IKK pathway in human prostate cancer PC-3 cells. *Oncogene, 24*(28), 4486.

Xu, C., Shen, G., Yuan, X., Kim, J.-h., Gopalkrishnan, A., Keum, Y.-S., Nair, S., & Kong, A.-N. T. (2006). ERK and JNK signaling pathways are involved in the regulation of activator protein 1 and cell death elicited by three isothiocyanates in human prostate cancer PC-3 cells. *Carcinogenesis, 27*(3), 437-445.

Xu, C., Yuan, X., Pan, Z., Shen, G., Kim, J.-H., Yu, S., Khor, T. O., Li, W., Ma, J., & Kong, A.-N. T. (2006). Mechanism of action of isothiocyanates: the induction of ARE-regulated genes is associated with activation of ERK and JNK and the phosphorylation and nuclear translocation of Nrf2. *Molecular Cancer Therapeutics, 5*(8), 1918-1926.

Xu, K., & Thornalley, P. J. (2001). Involvement of glutathione metabolism in the cytotoxicity of the phenethyl isothiocyanate and its cysteine conjugate to human leukaemia cells in vitro. *Biochemical Pharmacology, 61*(2), 165-177.

Yamane, K., Jinnin, M., Etoh, T., Kobayashi, Y., Shimozono, N., Fukushima, S., Masuguchi, S., Maruo, K., Inoue, Y., & Ishihara, T. (2013). Down-regulation of miR-124/-214 in cutaneous squamous cell carcinoma mediates abnormal cell proliferation via the induction of ERK. *Journal of Molecular Medicine, 91*(1), 69-81.

Yan, C., & Boyd, D. D. (2006). Histone H3 acetylation and H3 K4 methylation define distinct chromatin regions permissive for transgene expression. *Molecular and cellular biology, 26*(17), 6357-6371.

Yan, G., Eller, M. S., Elm, C., Larocca, C. A., Ryu, B., Panova, I. P., Dancy, B. M., Bowers, E. M., Meyers, D., & Lareau, L. (2013). Selective inhibition of p300 HAT blocks cell cycle progression, induces cellular senescence, and inhibits the DNA damage response in melanoma cells. *Journal of Investigative Dermatology, 133*(10), 2444-2452.

Yang, F., Sun, L., Li, Q., Han, X., Lei, L., Zhang, H., & Shang, Y. (2012). SET8 promotes epithelial–mesenchymal transition and confers TWIST dual transcriptional activities. *The EMBO Journal, 31*(1), 110-123.

Yang, F., Wang, F., Liu, Y., Wang, S., Li, X., Huang, Y., Xia, Y., & Cao, C. (2018). Sulforaphane induces autophagy by inhibition of HDAC6-mediated PTEN activation in triple negative breast cancer cells. *Life Sciences, 213*, 149-157.

Yang, G., Gao, Y. T., Shu, X. O., Cai, Q., Li, G. L., Li, H. L., Ji, B. T., Rothman, N., Dyba, M., Xiang, Y. B., Chung, F. L., Chow, W. H., & Zheng, W. (2010). Isothiocyanate exposure, glutathione S-transferase polymorphisms, and colorectal cancer risk. *American Journal of Clinical Nutrition, 91*(3), 704-711.

Yang, H., Yang, S., Liu, J., Shao, F., Wang, H., & Wang, Y. (2015). The association of GSTM1 deletion polymorphism with lung cancer risk in Chinese population: evidence from an updated meta-analysis. *Scientific Reports, 5*.

Yang, Q., Proll, M. J., Salilew-Wondim, D., Zhang, R., Tesfaye, D., Fan, H., Cinar, M. U., Grosse-Brinkhaus, C., Tholen, E., Islam, M. A., Holker, M., Schellander, K., Uddin, M. J., & Neuhoff, C. (2016). LPS-induced expression of CD14 in the TRIF pathway is epigenetically regulated by sulforaphane in porcine pulmonary alveolar macrophages. Journal of *Innate Immunity, 22*(8), 682-695.

Yang, Z. J., Chee, C. E., Huang, S., & Sinicrope, F. A. (2011). The role of autophagy in cancer: therapeutic implications. *Molecular Cancer Therapeutics, 10*(9), 1533-1541.

Yao, L., Li, Y., Du, F., Han, X., Li, X., Niu, Y., Ren, S., & Sun, Y. (2014). Histone H4 Lys 20 methyltransferase SET8 promotes androgen receptor-mediated transcription activation in prostate cancer. *Biochemical and Biophysical Research Communications, 450*(1), 692-696.

Yao, Q., Chen, Y., & Zhou, X. (2019). The roles of microRNAs in epigenetic regulation. *Current Opinion in Chemical Biology, 51*, 11-17.

Yokoyama, S., Feige, E., Poling, L. L., Levy, C., Widlund, H. R., Khaled, M., Kung, A. L., & Fisher, D. E. (2008). Pharmacologic suppression of MITF expression via HDAC inhibitors in the melanocyte lineage. *Pigment Cell & Melanoma Research, 21*(4), 457-463.

Yoxall, V., Kentish, P., Coldham, N., Kuhnert, N., Sauer, M. J., & Ioannides, C. (2005). Modulation of hepatic cytochromes P450 and phase II enzymes by dietary doses of sulforaphane in rats: Implications for its chemopreventive activity. *International Journal of Cancer, 117*(3), 356-362.

Yu, C., Gong, A. Y., Chen, D., Leon, D. S., Young, C. Y., & Chen, X. M. (2013). Phenethyl isothiocyanate inhibits androgen receptor-regulated transcriptional activity in

prostate cancer cells through suppressing PCAF. *Molecular Nutrition & Food Research, 57*(10), 1825-1833.

Yu, C., Gong, A. Y., Chen, D., Solelo Leon, D., Young, C. Y., & Chen, X. M. (2013). Phenethyl isothiocyanate inhibits androgen receptor-regulated transcriptional activity in prostate cancer cells through suppressing PCAF. *Molecular Nutrition & Food Research, 57*(10), 1825-1833.

Yu, N., Huangyang, P., Yang, X., Han, X., Yan, R., Jia, H., Shang, Y., & Sun, L. (2013). microRNA-7 suppresses the invasive potential of breast cancer cells and sensitizes cells to DNA damages by targeting histone methyltransferase SET8. *Journal of Biological Chemistry, 288*(27), 19633-19642.

Yu, R., Mandlekar, S., Harvey, K. J., Ucker, D. S., & Kong, A. N. (1998). Chemopreventive isothiocyanates induce apoptosis and caspase-3-like protease activity. *Cancer Research, 58*(3), 402-408.

Yu, S. H., Bordeaux, J. S., & Baron, E. D. (2014). The immune system and skin cancer. *Advances in Experimental Medicine and Biology, 810*, 182-191.

Yuanfeng, W., Gongnian, X., Jianwei, M., Shiwang, L., Jun, H., & Lehe, M. (2015). Dietary sulforaphane inhibits histone deacetylase activity in B16 melanoma cells. *Journal of Functional Foods, 18*, 182-189.

Zhang, C., Shu, L., Kim, H., Khor, T. O., Wu, R., Li, W., & Kong, A. N. (2016). Phenethyl isothiocyanate (PEITC) suppresses prostate cancer cell invasion epigenetically through regulating microRNA-194. *Molecular Nutrition & Food Research, 60*(6), 1427-1436.

Zhang, C., Shu, L., Kim, H., Khor, T. O., Wu, R., Li, W., & Kong, A. N. T. (2016). Phenethyl isothiocyanate (PEITC) suppresses prostate cancer cell invasion epigenetically through regulating microRNA-194. *Molecular Nutrition & Food Research, 60*(6), 1427-1436.

Zhang, C., Su, Z. Y., Khor, T. O., Shu, L., & Kong, A. N. (2013). Sulforaphane enhances Nrf2 expression in prostate cancer TRAMP C1 cells through epigenetic regulation. *Biochemical Pharmacology, 85*(9), 1398-1404.

Zhang, P., Wu, W., Chen, Q., & Chen, M. (2019). Non-Coding RNAs and their Integrated Networks. *Journal of integrative bioinformatics, 16*(3), 20190027.

Zhang, Q.-c., Pan, Z.-h., Liu, B.-n., Meng, Z.-w., Wu, X., Zhou, Q.-h., & Xu, K. (2017). Benzyl isothiocyanate induces protective autophagy in human lung cancer cells

through an endoplasmic reticulum stress-mediated mechanism. *Acta Pharmacologica Sinica, 38*(4), 539.

Zhang, R., Loganathan, S., Humphreys, I., & Srivastava, S. K. (2006). Benzyl isothiocyanate-induced DNA damage causes G2/M cell cycle arrest and apoptosis in human pancreatic cancer cells. *Journal of Nutrition, 136*(11), 2728-2734.

Zhang, Y. (2001). Molecular mechanism of rapid cellular accumulation of anticarcinogenic isothiocyanates. *Carcinogenesis, 22*(3), 425-431.

Zhang, Y. (2000). Role of glutathione in the accumulation of anticarcinogenic isothiocyanates and their glutathione conjugates by murine hepatoma cells. *Carcinogenesis, 21*(6), 1175-1182.

Zhang, Y. (2012a). The 1,2-benzenedithiole-based cyclocondensation assay: a valuable tool for the measurement of chemopreventive isothiocyanates. *Critical Reviews in Food Science and Nutrition, 52*(6), 525-532.

Zhang, Y. (2012b). The molecular basis that unifies the metabolism, cellular uptake and chemopreventive activities of dietary isothiocyanates. *Carcinogenesis, 33*(1), 2-9.

Zhao, B., Seow, A., Lee, E. J., Poh, W.-T., Teh, M., Eng, P., Wang, Y.-T., Tan, W.-C., Mimi, C. Y., & Lee, H.-P. (2001). Dietary isothiocyanates, glutathione S-transferase-M1,-T1 polymorphisms and lung cancer risk among Chinese women in Singapore. *Cancer Epidemiology Biomarkers & Prevention, 10*(10), 1063-1067.

Zhao, H., Lin, J., Grossman, H. B., Hernandez, L. M., Dinney, C. P., & Wu, X. (2007). Dietary isothiocyanates, GSTM1, GSTT1, NAT2 polymorphisms and bladder cancer risk. *International Journal of Cancer, 120*(10), 2208-2213.

Zhao, Y., Wang, B., Hu, K., Wang, J., Lu, S., Zhang, Y., Lu, W., Zhao, E., & Yuan, L. (2015). Glutathione S-transferase θ1 polymorphism contributes to lung cancer susceptibility: A meta-analysis of 26 case-control studies. *Oncology Letters, 9*(4), 1947-1953.

Zhou, W., Fong, M. Y., Min, Y., Somlo, G., Liu, L., Palomares, M. R., Yu, Y., Chow, A., O'Connor, S. T., Chin, A. R., Yen, Y., Wang, Y., Marcusson, E. G., Chu, P., Wu, J., Wu, X., Li, A. X., Li, Z., Gao, H., Ren, X., Boldin, M. P., Lin, P. C., & Wang, S. E. (2014). Cancer-secreted miR-105 destroys vascular endothelial barriers to promote metastasis. *Cancer Cell, 25*(4), 501-515.

Zhu, Y., Zhang, L., Zhang, G.-D., Wang, H.-O., Liu, M.-Y., Jiang, Y., Qi, L.-S., Li, Q., & Yang, P. (2014). Potential mechanisms of benzyl isothiocyanate suppression of

invasion and angiogenesis by the U87MG human glioma cell line. *Asian Pacific Journal of Cancer Prevention, 15*(19), 8225-8228.

Ziech, D., Anestopoulos, I., Hanafi, R., Voulgaridou, G. P., Franco, R., Georgakilas, A. G., Pappa, A., & Panayiotidis, M. I. (2012). Pleiotrophic effects of natural products in ROS-induced carcinogenesis: the role of plant-derived natural products in oral cancer chemoprevention. *Cancer Letters, 327*(1-2), 16-25.

Ziech, D., Franco, R., Pappa, A., Malamou-Mitsi, V., Georgakila, S., Georgakilas, A. G., & Panayiotidis, M. I. (2010). The role of epigenetics in environmental and occupational carcinogenesis. *Chemico-biological interactions, 188*(2), 340-349.

Zingg, D., Debbache, J., Schaefer, S. M., Tuncer, E., Frommel, S. C., Cheng, P., Arenas-Ramirez, N., Haeusel, J., Zhang, Y., Bonalli, M., McCabe, M. T., Creasy, C. L., Levesque, M. P., Boyman, O., Santoro, R., Shakhova, O., Dummer, R., & Sommer, L. (2015). The epigenetic modifier EZH2 controls melanoma growth and metastasis through silencing of distinct tumour suppressors. *Nature Communications, 6*, 6051.

Zörnig, M., Hueber, A.-O., Baum, W., & Evan, G. (2001). Apoptosis regulators and their role in tumorigenesis. *Biochimica et Biophysica Acta (BBA) - Reviews on Cancer, 1551*(2), 1-37.

Śmiechowska, A., Bartoszek, A., & Namieśnik, J. (2010). Determination of Glucosinolates and Their Decomposition Products—Indoles and Isothiocyanates in Cruciferous Vegetables. *Critical Reviews in Analytical Chemistry, 40*(3), 202-216.

Supplementary Material

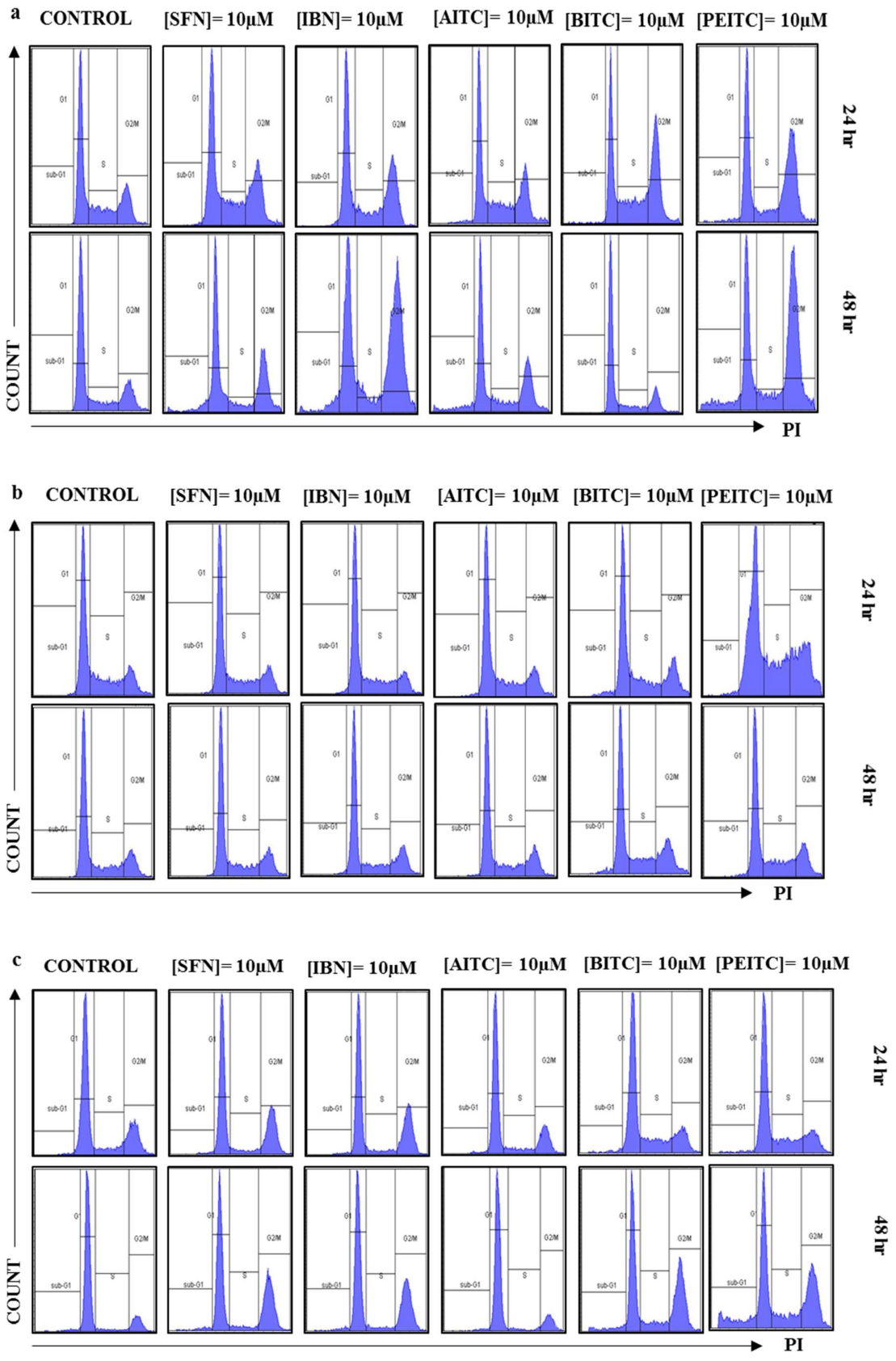

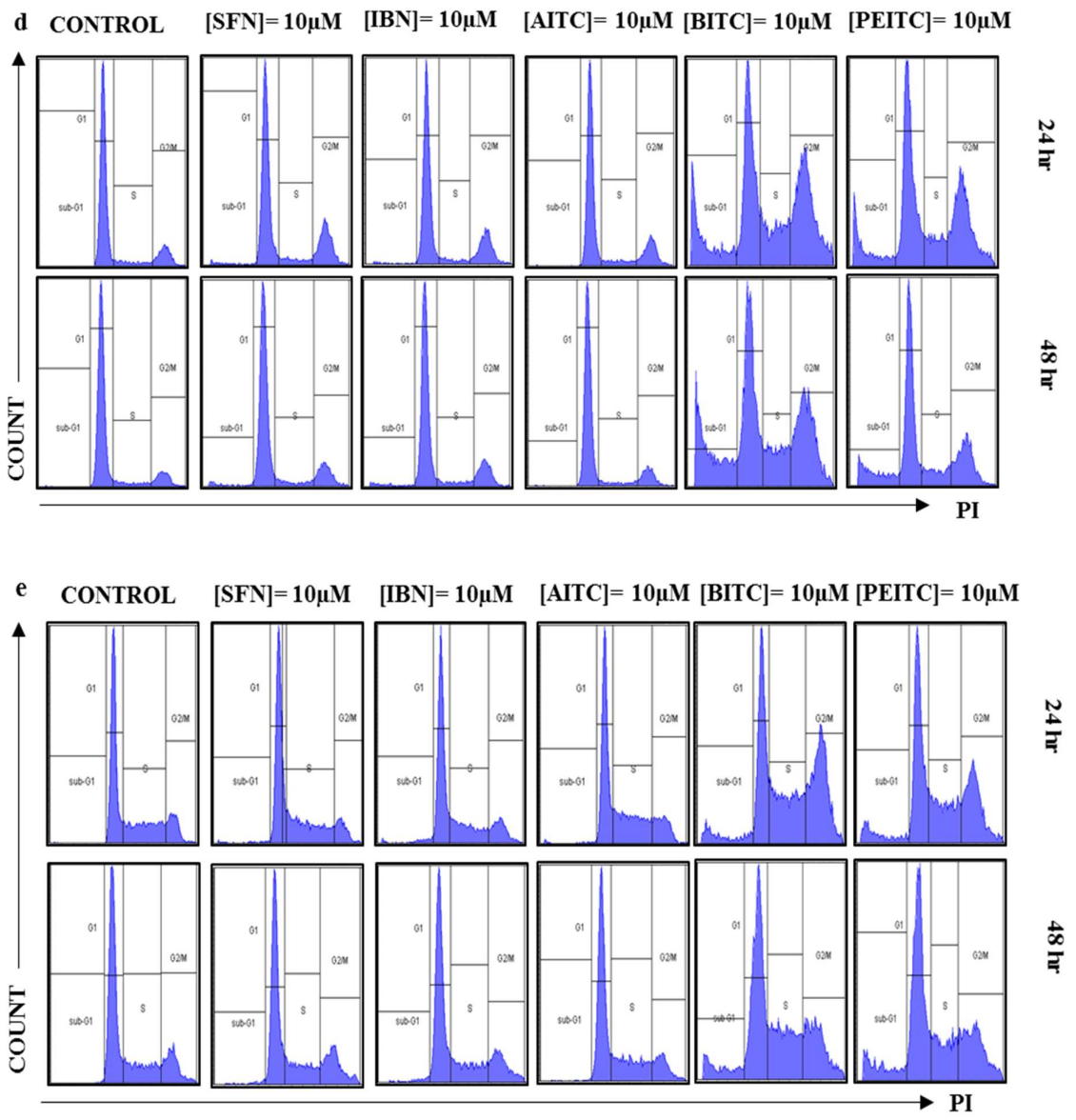
d
CONTROL
[SFN]= 10µM
[IBN]= 10µM
[AITC]= 10µM
[BITC]= 10µM
[PEITC]= 10µM
24 hr
48 hr
COUNT
PI
G1
S
G2/M
sub-G1
e
CONTROL
[SFN]= 10µM
[IBN]= 10µM
[AITC]= 10µM
[BITC]= 10µM
[PEITC]= 10µM
24 hr
48 hr
COUNT
PI
G1
S
G2/M
sub-G1

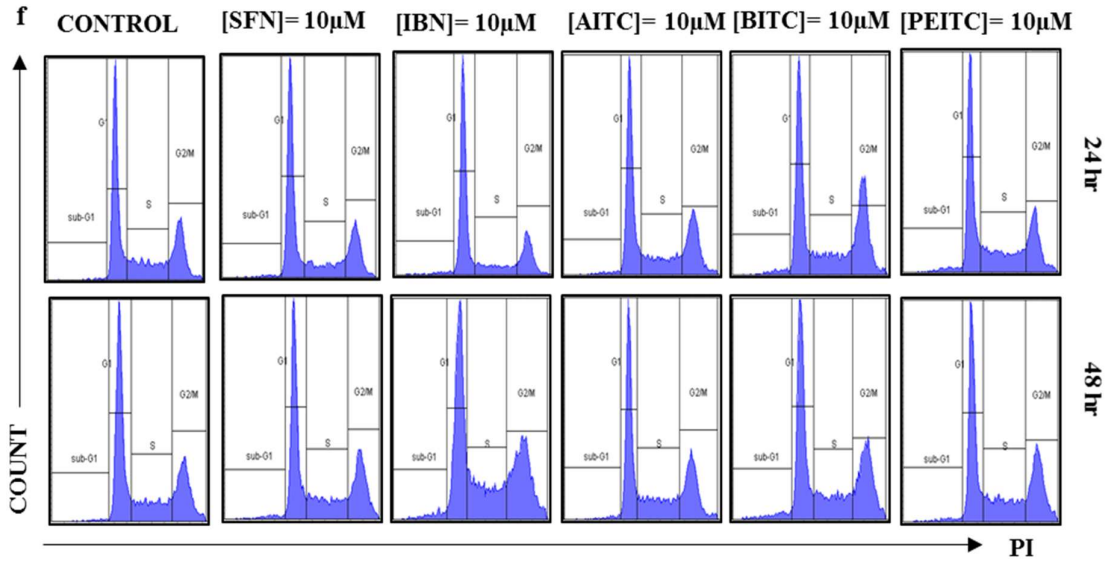

Figure S1: The ability of SFN, IBN, AITC, BITC and PEITC to induce cell cycle growth arrest in an *in vitro* model of malignant melanoma consisting of **a**) human malignant melanoma (A375), **b**) murine malignant melanoma (B16F10), **c**) brain-derived human metastatic melanoma (VMM1), **d**) lymph node-derived human metastatic melanoma (Hs294T), **e**) human non-melanoma epidermoid carcinoma (A431) and (**f**) human immortalized keratinocytes (HaCaT) cell lines. All cells were seeded in 100 mm dishes and next day were exposed to 10 µM of each ITC (separately) for 24 and 48 hrs. DNA accumulation in each phase of the cell cycle was determined by staining the pre-fixed cells with FxCycle PI/RNase fluorescent probe and measured the relative intensity of each phase in the PI region.

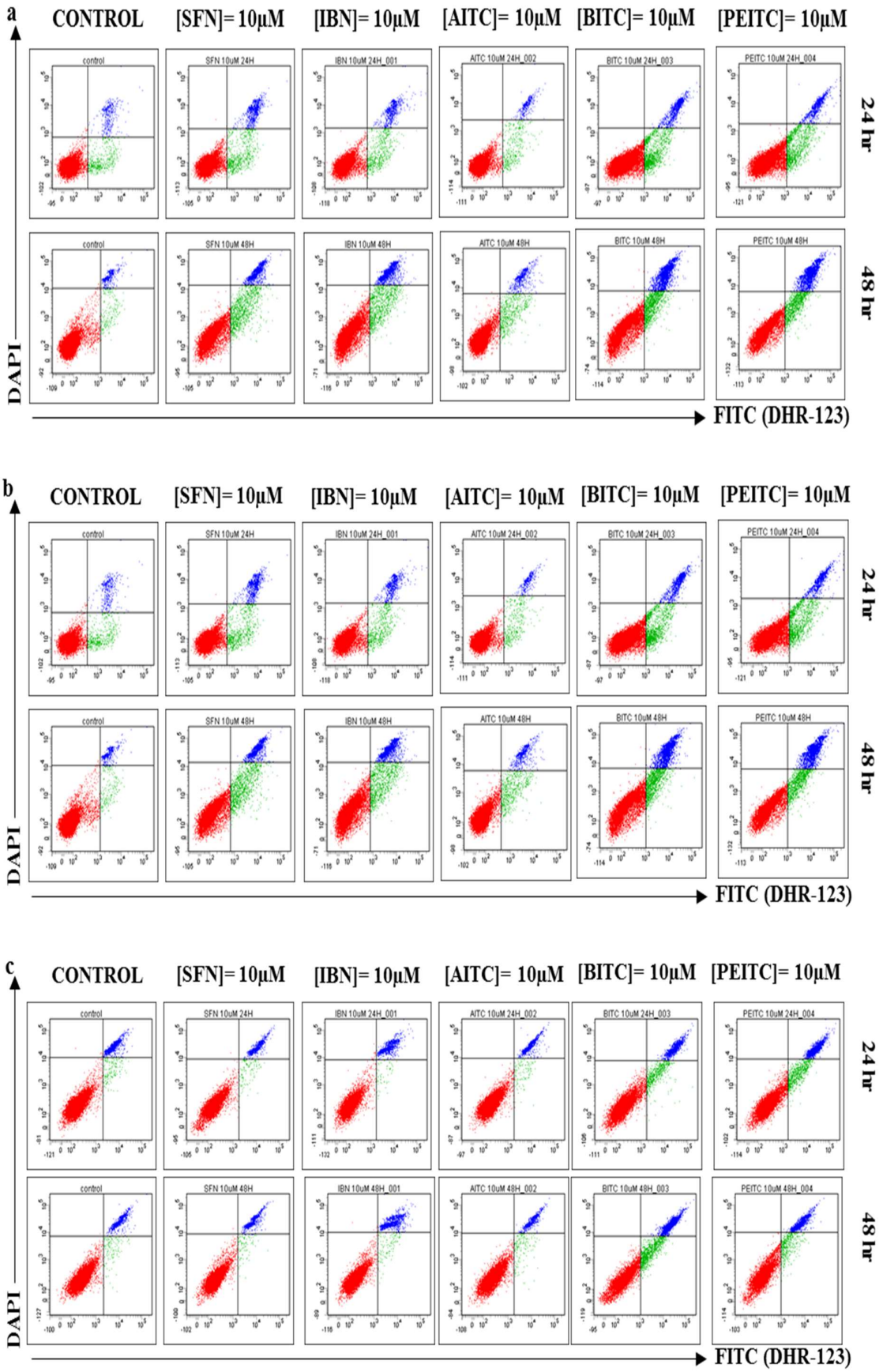
a
CONTROL
[SFN]= 10µM
[IBN]= 10µM
[AITC]= 10µM
[BITC]= 10µM
[PEITC]= 10µM
24 hr
48 hr
DAPI
FITC (DHR-123)
b
CONTROL
[SFN]= 10µM
[IBN]= 10µM
[AITC]= 10µM
[BITC]= 10µM
[PEITC]= 10µM
24 hr
48 hr
DAPI
FITC (DHR-123)
c
CONTROL
[SFN]= 10µM
[IBN]= 10µM
[AITC]= 10µM
[BITC]= 10µM
[PEITC]= 10µM
24 hr
48 hr
DAPI
FITC (DHR-123)

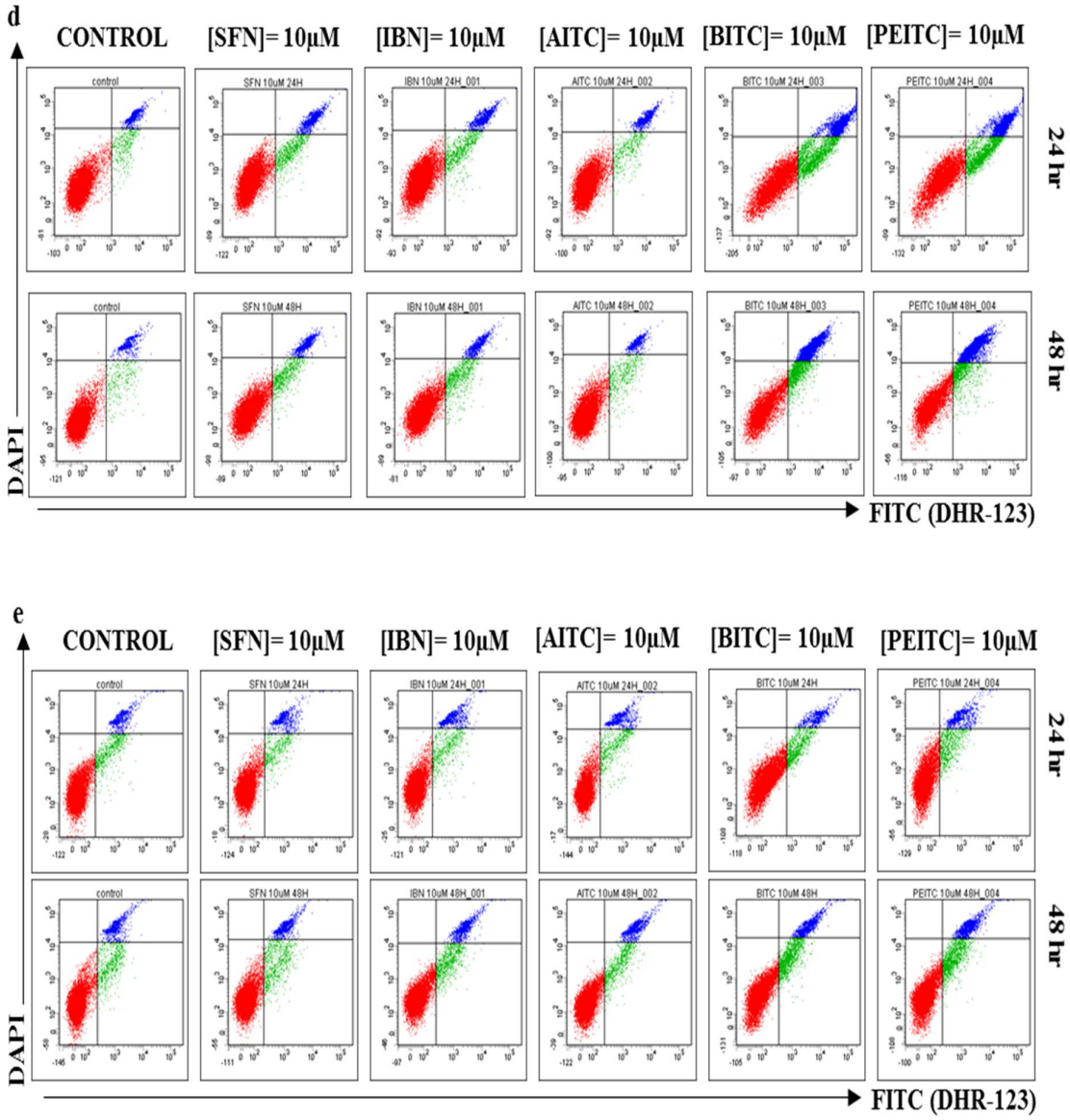
d
CONTROL
[SFN]= 10µM
[IBN]= 10µM
[AITC]= 10µM
[BITC]= 10µM
[PEITC]= 10µM
24 hr
48 hr
DAPI
FITC (DHR-123)
e
CONTROL
[SFN]= 10µM
[IBN]= 10µM
[AITC]= 10µM
[BITC]= 10µM
[PEITC]= 10µM
24 hr
48 hr
DAPI
FITC (DHR-123)

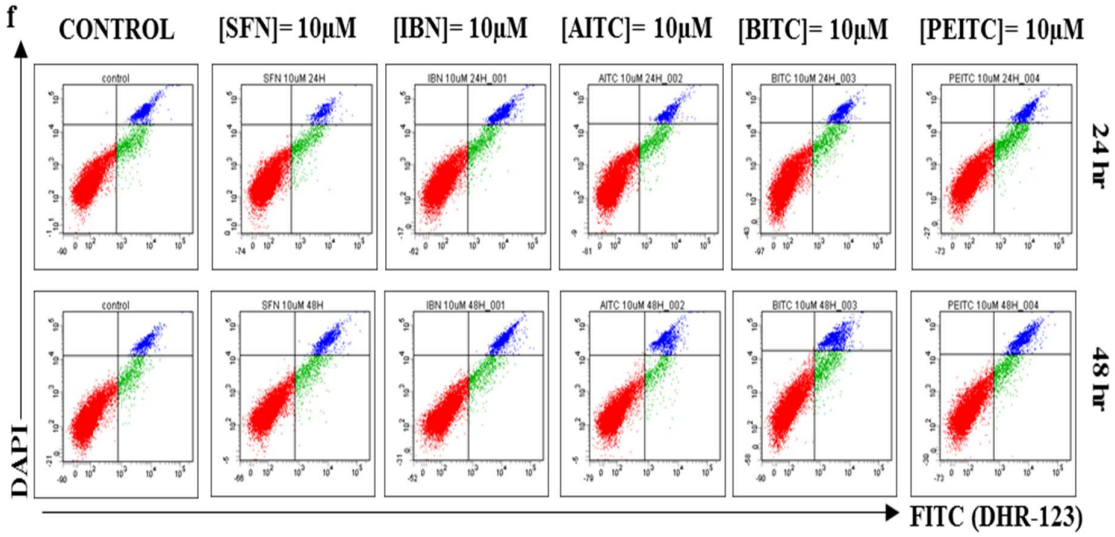

Figure S2: The ability of SFN, IBN, AITC, BITC and PEITC to induce cell death (e.g. apoptosis and necrosis) in an *in vitro* model of malignant melanoma consisting of **a**) human malignant melanoma (A375), **b**) murine malignant melanoma (B16F10), **c**) brain-derived human metastatic melanoma (VMM1), **d**) lymph node-derived human metastatic melanoma (Hs294T), **e**) non-melanoma human epidermoid carcinoma (A431) and **f**) human immortalized keratinocytes (HaCaT) cell lines. All cells were seeded in 100 mm dishes and next day were exposed to 10 µM of each ITC (separately) for 24 and 48 hrs. The mode of cell death was distinguished by the use of a caspase 3/7 fluorescent probe (for apoptosis) and DAPI (for necrosis).

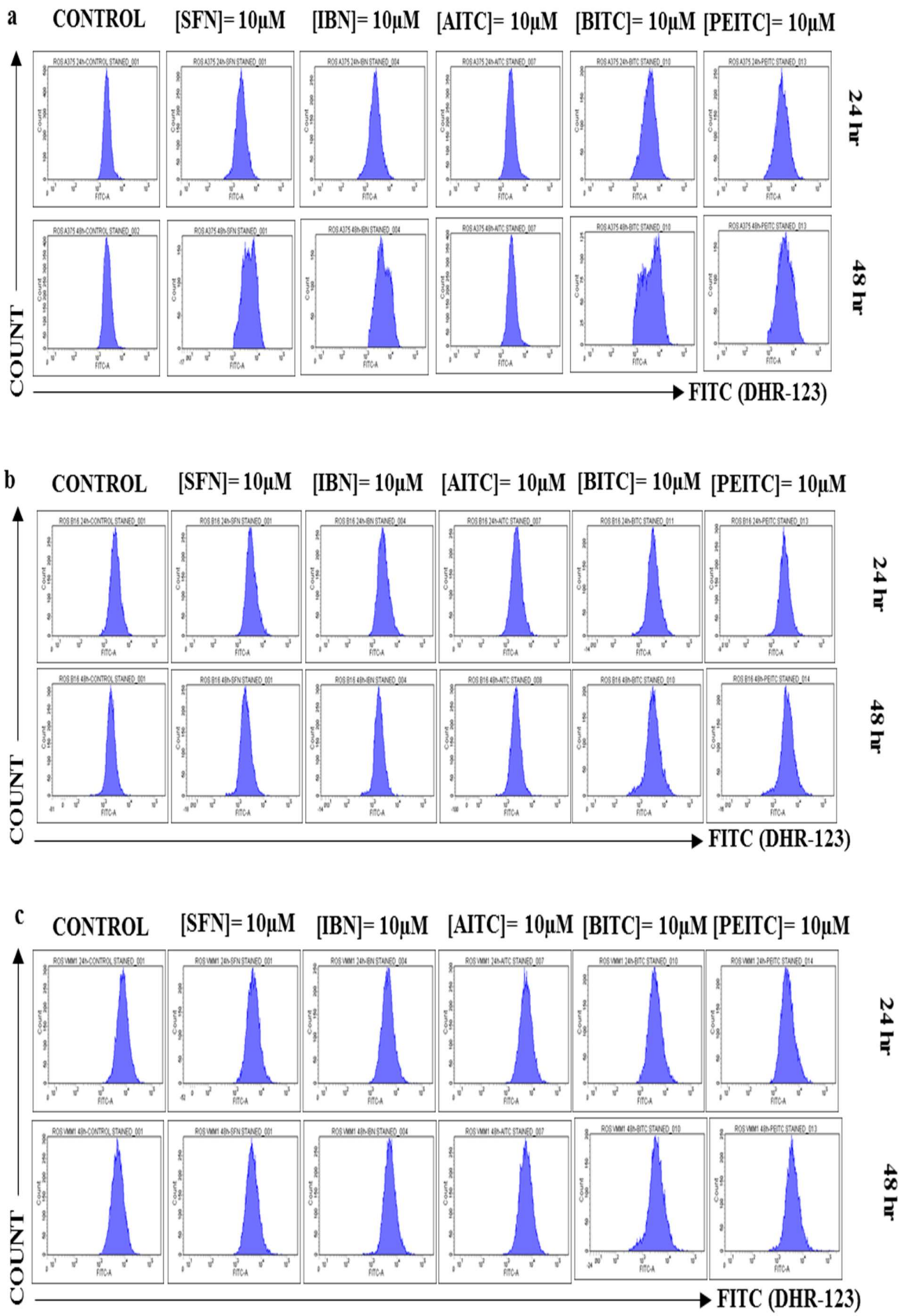
a
CONTROL
[SFN]= 10µM
[IBN]= 10µM
[AITC]= 10µM
[BITC]= 10µM
[PEITC]= 10µM
24 hr
48 hr
COUNT
FITC (DHR-123)
b
CONTROL
[SFN]= 10µM
[IBN]= 10µM
[AITC]= 10µM
[BITC]= 10µM
[PEITC]= 10µM
24 hr
48 hr
COUNT
FITC (DHR-123)
c
CONTROL
[SFN]= 10µM
[IBN]= 10µM
[AITC]= 10µM
[BITC]= 10µM
[PEITC]= 10µM
24 hr
48 hr
COUNT
FITC (DHR-123)

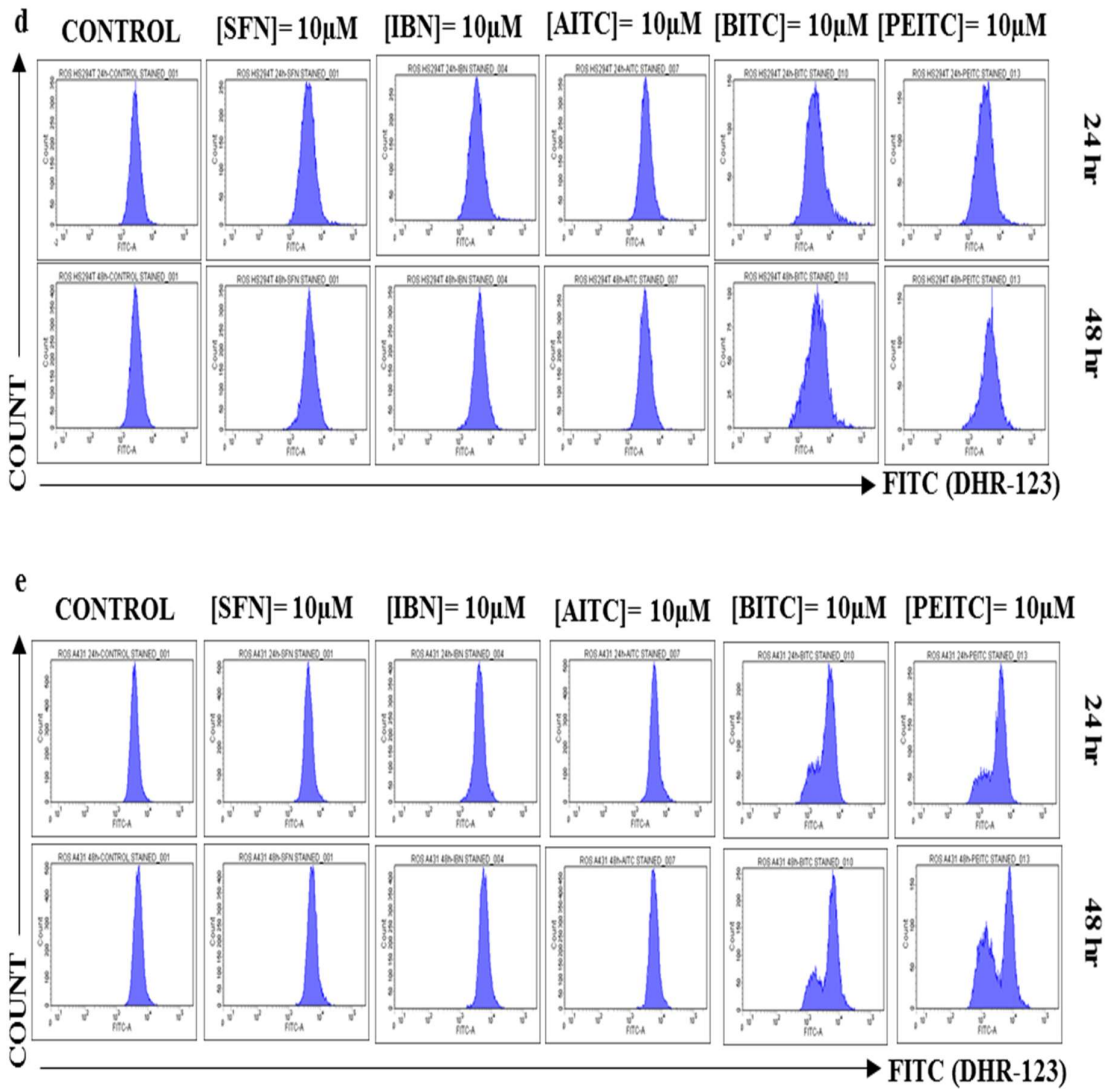
d
CONTROL
[SFN]= 10µM
[IBN]= 10µM
[AITC]= 10µM
[BITC]= 10µM
[PEITC]= 10µM
24 hr
48 hr
COUNT
FITC (DHR-123)
e
CONTROL
[SFN]= 10µM
[IBN]= 10µM
[AITC]= 10µM
[BITC]= 10µM
[PEITC]= 10µM
24 hr
48 hr
COUNT
FITC (DHR-123)

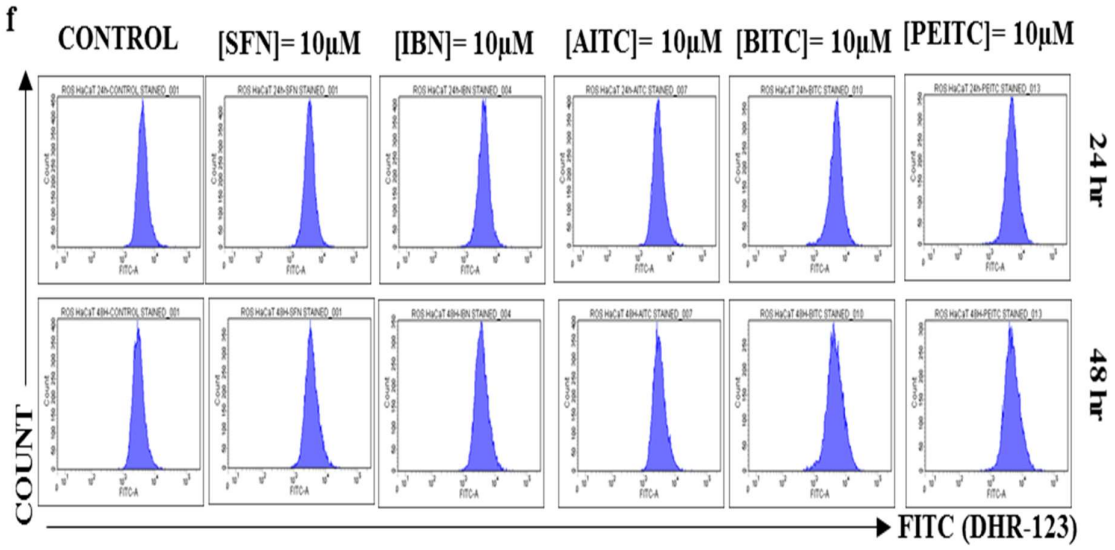

Figure S3: The effect of SFN, IBN, AITC, BITC and PEITC on generation of oxidative stress in an *in vitro* model of malignant melanoma consisting of **a**) human malignant melanoma (A375), **b**) murine malignant melanoma (B16F10), **c**) brain-derived human metastatic melanoma (VMM1), **d**) lymph node-derived human metastatic melanoma (Hs294T), **e**) non-melanoma human epidermoid carcinoma (A431) and **f**) human immortalized keratinocytes (HaCaT) cell lines. All cells were seeded in 100 mm dishes and next day were exposed to 10 µM of each ITC (separately) for 24 and 48 hrs. ROS induction levels were determined by using a DHR-123 fluorescent probe and the oxidative stress response was measured in FITC region and compared to the respective untreated control.

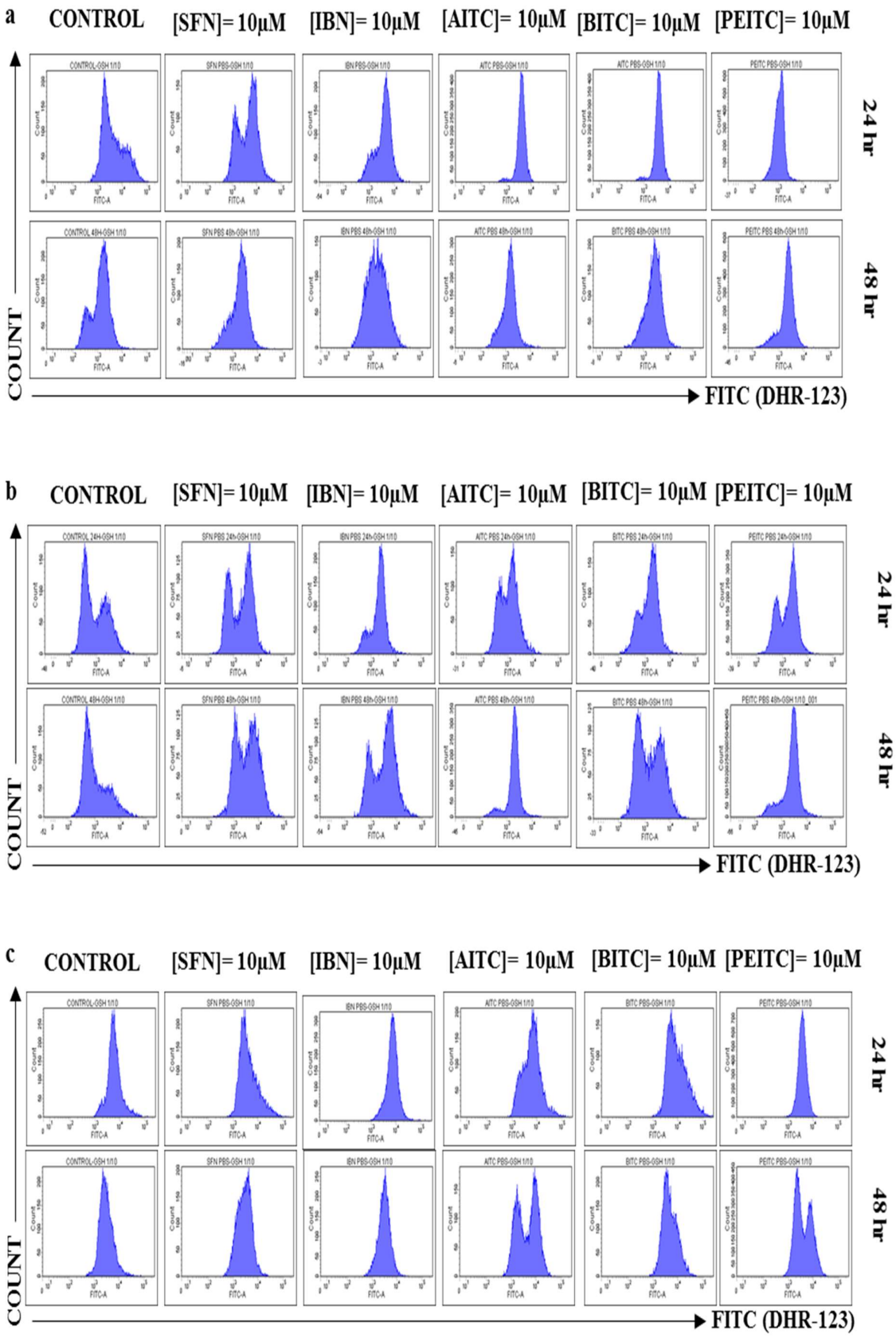
a
CONTROL
[SFN]= 10µM
[IBN]= 10µM
[AITC]= 10µM
[BITC]= 10µM
[PEITC]= 10µM
24 hr
48 hr
COUNT
FITC (DHR-123)
b
CONTROL
[SFN]= 10µM
[IBN]= 10µM
[AITC]= 10µM
[BITC]= 10µM
[PEITC]= 10µM
24 hr
48 hr
COUNT
FITC (DHR-123)
c
CONTROL
[SFN]= 10µM
[IBN]= 10µM
[AITC]= 10µM
[BITC]= 10µM
[PEITC]= 10µM
24 hr
48 hr
COUNT
FITC (DHR-123)

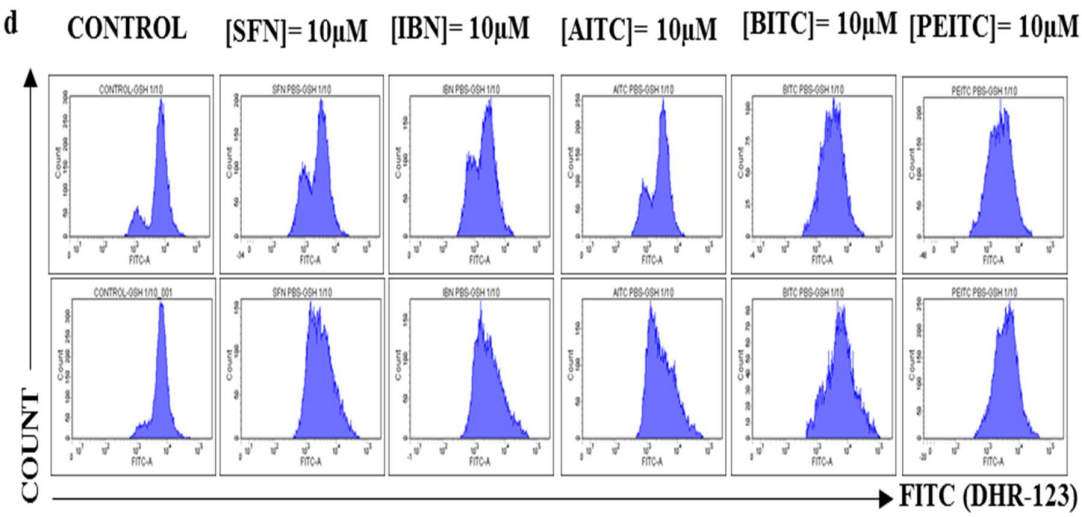
d
CONTROL
[SFN]= 10µM
[IBN]= 10µM
[AITC]= 10µM
[BITC]= 10µM
[PEITC]= 10µM
24 hr
48 hr
COUNT
FITC (DHR-123)

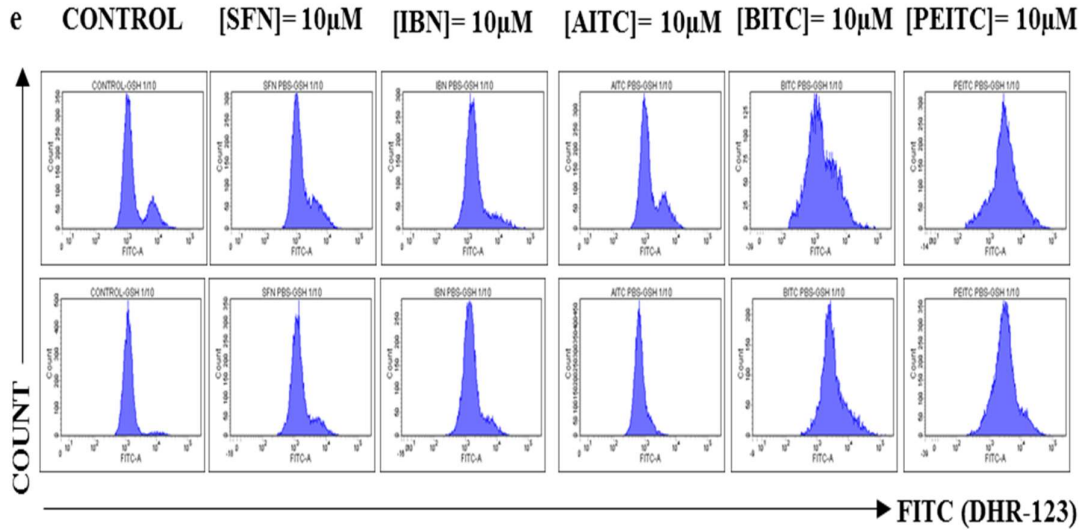
e
CONTROL
[SFN]= 10µM
[IBN]= 10µM
[AITC]= 10µM
[BITC]= 10µM
[PEITC]= 10µM
24 hr
48 hr
COUNT
FITC (DHR-123)

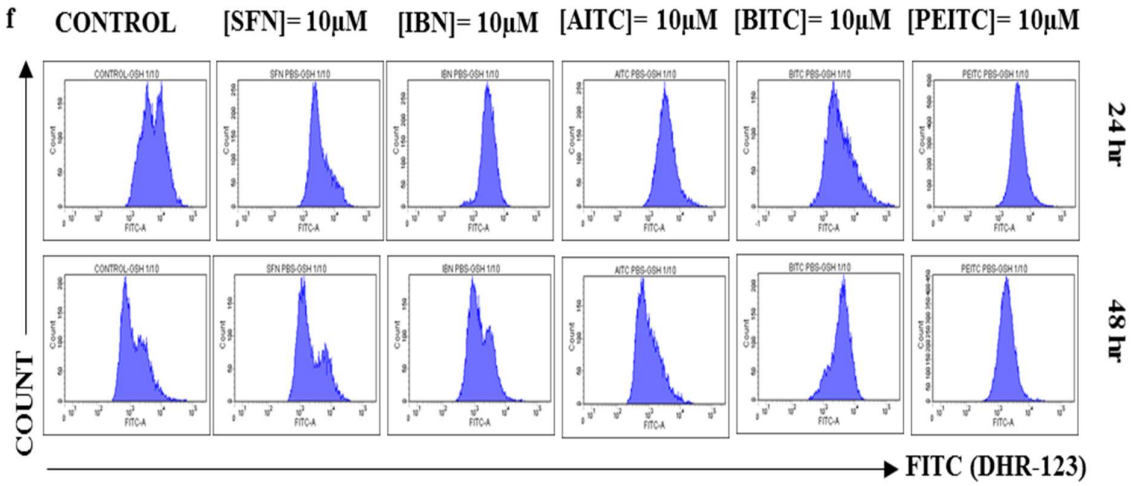

Figure S4: The effect of SFN, IBN, AITC, BITC and PEITC on GSH levels in an *in vitro* model of malignant melanoma consisting of **a**) human malignant melanoma (A375), **b**) murine malignant melanoma (B16F10), **c**) brain-derived human metastatic melanoma (VMM1), **d**) lymph node-derived human metastatic melanoma (Hs294T), **e**) non-melanoma human epidermoid carcinoma (A431) and **f**) human immortalized keratinocytes (HaCaT) cell lines. All cells were seeded in 100 mm dishes and next day were exposed to 10 µM of each ITC (separately) for 24 and 48 hrs. Relative levels of GSH were determined using the Thiol Tracker fluorescent probe. The GSH levels were measured in the FITC region compared to the respective untreated control.

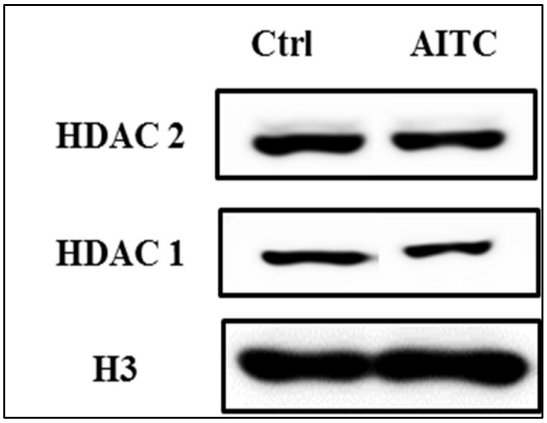

Figure S5: The effect of AITC on protein expression levels of HDAC 1 and HDAC2 in A375 cells exposed to 10 μM of AITC for 48 hrs. Western immunoblotting was used, in nuclear extracts, to determine relevant protein expression levels.

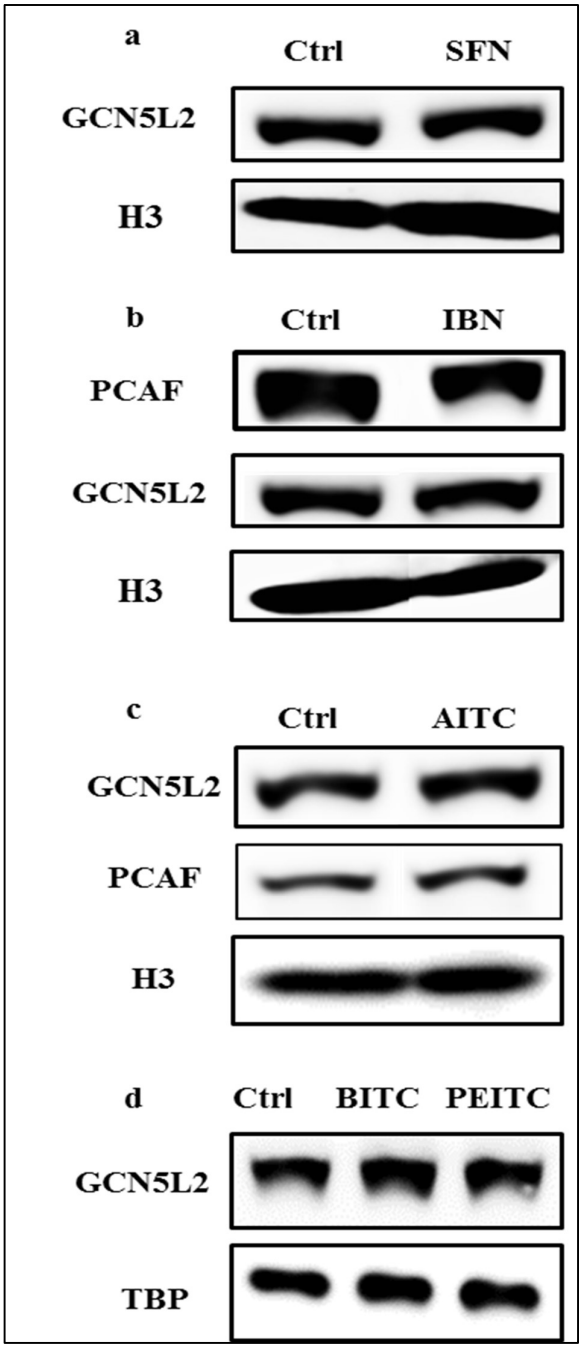

Figure S6: The effect of ITCs on protein expression levels of GCN5L2 and PCAF in A375 cells exposed to 10 μM of **a**) SFN, **b**) IBN, **c**) AITC, **d**) BITC and PEITC for 48 hrs. Western immunoblotting was used, in nuclear extracts, to determine relevant protein expression levels.

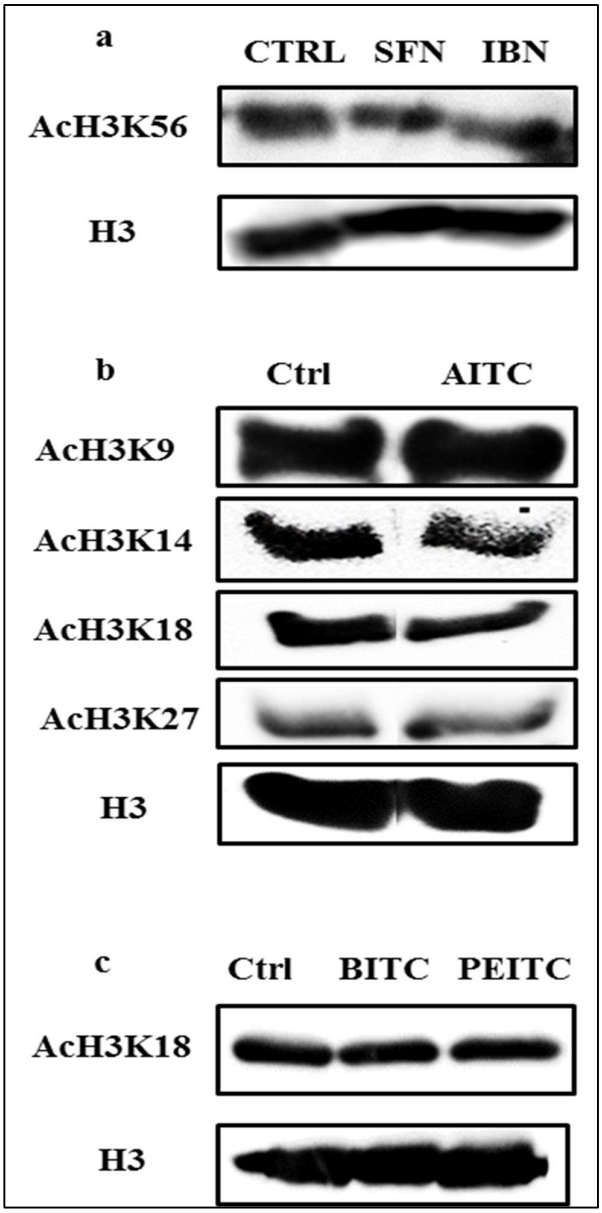

Figure S7: The effect of ITCs on specific H3 lysine acetylation marks in A375 cells exposed to 10 μM of **a**) SFN or IBN, **b**) AITC and **c**) BITC or PEITC for 48 hrs. Western immunoblotting was used, in total histone extracts, in order to evaluate relevant protein expression levels of AcH3K9, AcH3K14, AcH3K18, AcH3K27 and AcH3K56.

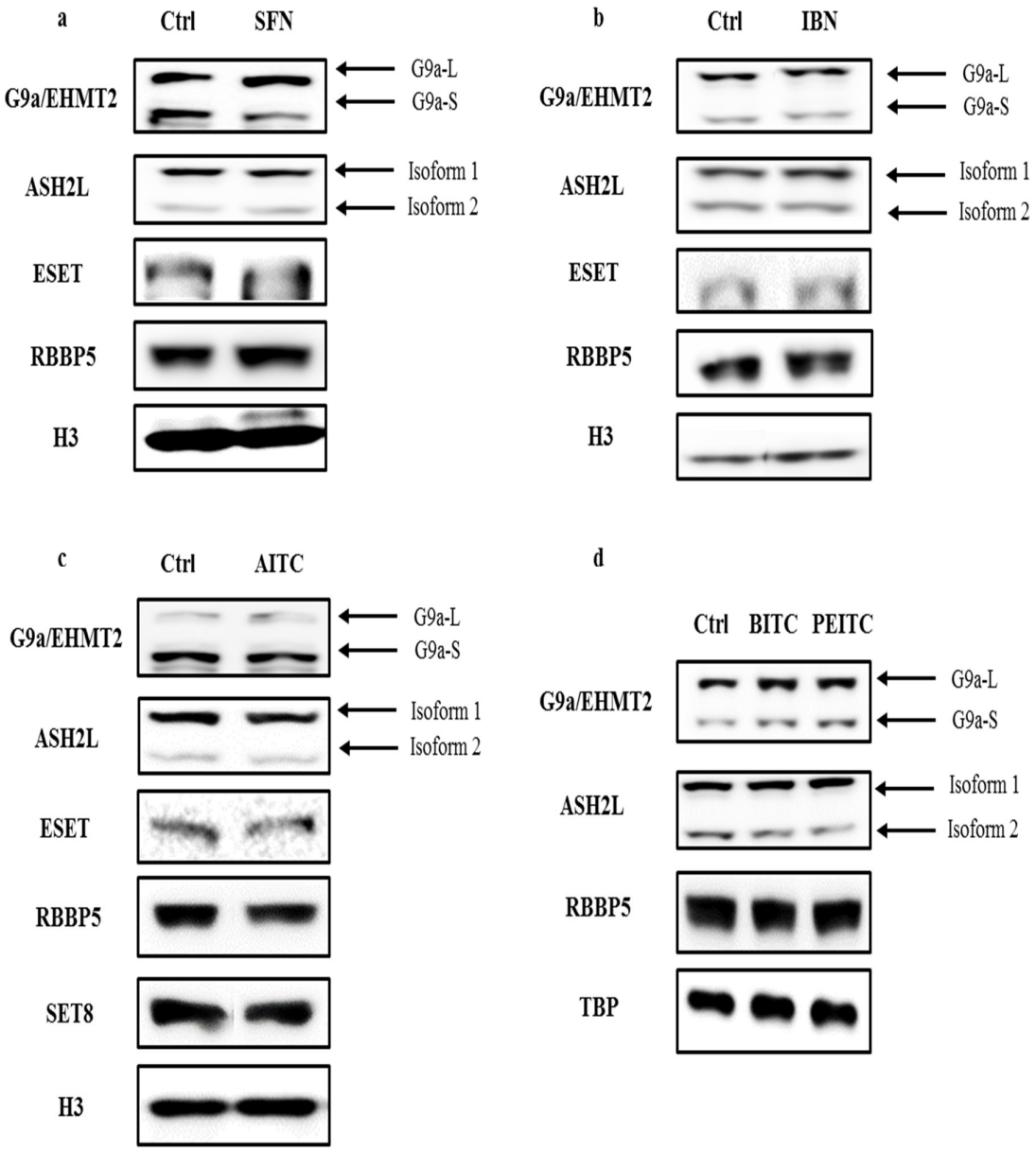

Figure S8: The effect of ITCs on protein expression levels of specific HMTs in A375 cells exposed to 10 μM of **a**) SFN, **b**) IBN, **c**) AITC and **d**) BITC or PEITC for 48 hrs. Western immunoblotting was used in nuclear extracts to determine relevant protein expression levels of G9a/EHMT2, ASH2L, RBBP5, SET8, SET7-9 and ESET.

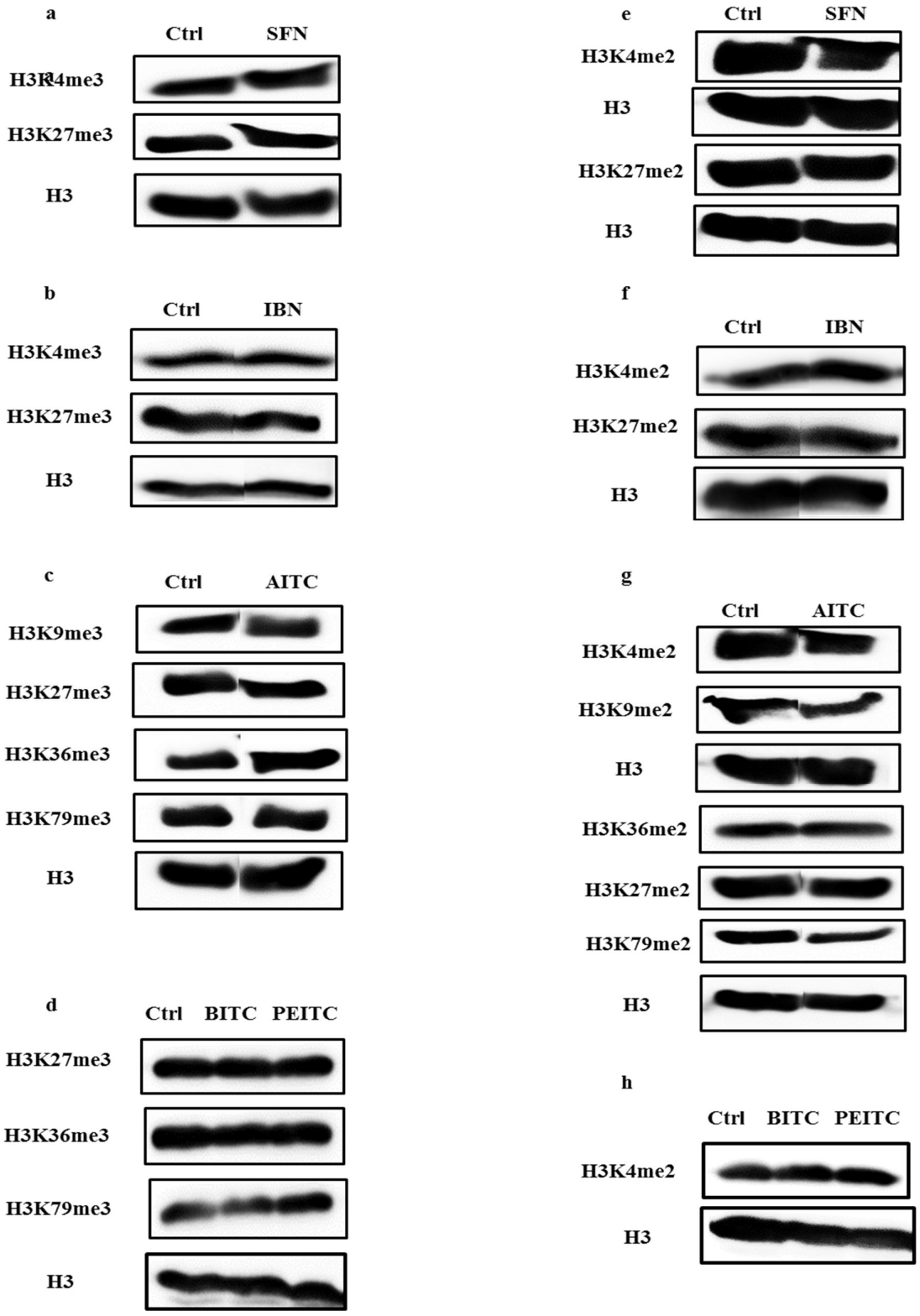

Figure S9: The effect of ITCs on tri- and di-methylation status of specific lysine residues on H3. Western immunoblotting was used, in total histone extracts, of A375 cells exposed to 10 μM of SFN (**a**,**e**), IBN, (**b**,**f**), AITC, (**c**,**g**) and BITC or PEITC (**d**,**h**) for 48hrs to assess relevant protein expression levels of H3K4me3, H3K27me3, H3K9me3, H3K36me3, H3K79me3, H3K4me2, H3K27me2, H3K9me2, H3K36me2 and H3K79me2.